THE UNIVERSITY OF
WARWICK

University of Warwick institutional repository: http://go.warwick.ac.uk/wrap

A Thesis Submitted for the Degree of PhD at the University of Warwick

http://go.warwick.ac.uk/wrap/36099

This thesis is made available online and is protected by original copyright.

Please scroll down to view the document itself.

Please refer to the repository record for this item for information to help you to cite it. Our policy information is available from the repository home page.

COST MINIMISATION IN MICRO-HYDRO SYSTEMS USING PUMPS-AS-TURBINES

Claudio Alatorre-Frenk

A thesis submitted for the degree of Doctor of Philosophy

Development Technology Unit
Department of Engineering, Faculty of Sciences
University of Warwick

February 1994

A mi amada Karin

TABLE OF CONTENTS

ACKNOWLEDGEMENTS

This research was made possible through a grant of the National University of Mexico (UNAM). Additional contributions were made by the Committee of Vice-Chancellors and Principals of the Universities of the United Kingdom, through the Overseas Research Students Awards Scheme, as well as by my parents, Margit Frenk and Antonio Alatorre. All of these have been greatly appreciated.

In addition, I thank:

- Terry Thomas, for his invaluable supervision.
- SPP Pumps Ltd. and Geoff Lake, for lending a pump for the cavitation tests.
- Arthur Williams, for the fruitful exchange of experiences and information (and for providing his left ear to detect the inception of cavitation!).
- The Engineering technicians, especially Paul Hedley, Stuart Edris, Andrew Leeson, John Matteri, PhilDexter, Len, Dave Thompson and Graham Robinson for their work and enthusiasm in the test-rig.
- John Burton, Adrian Boldy, Tim Jeffery, Peter Giddens, E.W. Thorne, and Prof. Li for their comments and advice, and of course Jacinto Viqueira, Paul Fountain, Peter Glover, Colin Oram, Chris Studman, Harold Pearson, Andy Hawkins, Steve Chandler, Bob Chritoph, Les Robinson and many other people that - I hope - will forgive me for not including their names here.

Lastly, I especially thank my wife Karin for her continual support and patience, as well as Andrea and David for their happiness.

NOMENCLATURE

Remark: the units shown here are those preferred or used by default. Other units are also used when indicated.

Roman letters.

A	m^2	Horizontal area (surface or internal)
A_D	m^2	Cross-section internal area of penstock
A_H	$m^{-5}{\cdot}s^2$	First coefficient of turbine-mode head characteristics (Eq. [68], p. 90)
A_M	$kg{\cdot}m^{-4}$	First coefficient of turbine-mode torque characteristics (Eq. [67], p. 90)
a	m^2	Circumferential area between rotor blades
$Æ$		Economic advantage (Eq. [10], p. 21b)
B	m	Square root of the volute throat area (Eq. [24], p. 59)
B_H	$m^{-2}{\cdot}s^2$	Second coefficient of turbine-mode head characteristics (Eq. [68], p. 90)
B_M	$kg{\cdot}m^{-1}$	Second coefficient of turbine-mode torque characteristics (Eq. [67], p. 90)
b	m	Width of rotor
C	£	Cost (Eq. [9], p. 20)
C'	£	Approximate cost (Eq. [79], p. 101)
C_H	$m{\cdot}s^2$	Third coefficient of turbine-mode head characteristics (Eq. [68], p. 90)
c	$m{\cdot}s^{-1}$	Absolute flow velocity
c_u	$m{\cdot}s^{-1}$	Tangential component of the absolute flow velocity
c_m	$m{\cdot}s^{-1}$	Meridional component of the absolute flow velocity
D	m	Diameter
d		Discount rate (Eq. [4b], p. 18)
E_C	J	Energy generated per cycle (intermittent operation) (Eq. [12], p. 34)
E_T		Elasticity of head characteristics at the turbine BEP (Eq. [69], p. 90)

E_{2T}		'Second' elasticity of head characteristics at the turbine BEP (Eq. [70], p. 91)
e		Used instead of η in graphs
F		Cumulative probability function
f		Density probability function
f		Friction coefficient
g	$m{\cdot}s^{-2}$	Gravitational acceleration
H	m	Turbine head
H_{atm}	m	Atmospheric pressure, as column of water
h	m	Head-loss
K_{FT}	m^{-4}	Hydraulic loss coefficient (Eq. [47], p. 68)
K_{LT}	$m^{3.5}{\cdot}kg^{-1.5}$	Leakage loss coefficient (Eq. [52], p. 70)
K_d	s	Discount factor for instantaneous benefit (Eq. [4b], p. 18)
K'_d		Discount factor for O&M costs
K_e	$£{\cdot}W^{-\Gamma}$	Economic function coefficient (Eq. [1], p. 16)
k	£	Cost coefficient
k'	£	Coefficient of the approximate cost function C'
L	m	Length
M	N·m	Shaft torque
m	N·m	Mechanical losses (Eq. [40], p. 66)
N	years	Lifetime of the scheme (Eq. [4b], p. 18)
n		Number of machines in parallel
P	W	Output power
p	Pa	Pressure (relative to atmospheric)
Q	$m^3{\cdot}s^{-1}$	Turbine flow
q		Relative flow (Eq. [6], p. 19)
r	m	Radius
s		Slip factor
t	s	Time
t_R	s	Running time (intermittent operation) (Eq. [16], p. 36)
t_F	s	Reservoir-filling time (intermittent operation) (Eq. [17], p. 36)
V	m^3	Volume
V	£	Benefit (Eq. [4a], p. 18)
$\dot{V}$	$£{\cdot}s^{-1}$	Instantaneous rate of generating value (Eq. [1], p. 16)
v	$m{\cdot}s^{-1}$	Water velocity (Remark: ν is the Greek *nu*, not a *v*)
X		Variable used in function Λ
Y		Ratio of area between the impeller blades at exit (normal to flow velocity) to the throat area of volute (Eq. [37], p. 65)
z	m	Static head
z_a, z_b, z_c, z_d, z_e	m	Double siphon design margins (intermittent operation)

Greek letters.

α		Volute or diffuser angle (see also subscripts, below)
α^*		Angle of absolute flow velocity
β		Rotor blade angle (see also subscripts, below)
β^*		Angle of relative flow velocity
Γ		Exponent of the economic function: sensitivity of output value to output power (Eq. [1], p. 16)
γ_i		Incidence loss coefficient (Eq. [45], p. 67)
Δ		Difference (see also subscripts, below)
δ		Relative distance between PAT 'classes'
ε		Flow-head elasticity of the system {turbine + penstock} (head is static head): $\varepsilon = \frac{dQ_T}{dz}\frac{\tilde{z}}{\tilde{Q}_T}$
η		Efficiency
Θ		Exponent of the cost function for turbomachinery (Eq. [7], p. 19)
Θ'		Exponent of the approximate cost function C'
θ		Double siphon dimensionless parameter
κ		Bias parameter for the definition of the application range of a PAT 'class'
Λ		Function of the specific speed (Eq. [56], p. 84)
λ	$m^{-3\mu}.s^{\mu}$	Hydrological magnitude parameter (Eq. [2], p. 16)
μ		First hydrological shape parameter (Eq. [2], p. 16)
ν_a		Ratio between eye and tip circumferential areas (Eq. [30], p. 61)
ν_r		Ratio between eye and tip radii (Eq. [30], p. 61)
ξ		Second hydrological shape parameter (Eq. [2], p. 16)
ρ	$kg{\cdot}m^{-3}$	Water density
σ		Thoma cavitation coefficient
τ		Torque coefficient: $\tau = M/(\rho{\cdot}a_2{\cdot}r_2{}^3{\cdot}\omega^2)$
Φ		Normalised available flow: $Q_A/\tilde{Q}_T$
ϕ		Flow coefficient: $\phi = Q/(a_2{\cdot}r_2{\cdot}\omega)$
ψ		Head coefficient: $\psi = gH/(r_2{}^2{\cdot}\omega^2)$
Ω		Dimensionless specific speed: $\Omega = \frac{\omega\sqrt{\hat{Q}_{(\text{per entry})}}}{\left[g\hat{H}_{(\text{per stage})}\right]^{0.75}}$
ω	$rad{\cdot}s^{-1}$	Shaft rotating speed

Subscripts.

A	Available
B	Cavitation noise onset
C	Cycle (intermittent operation)
crit	Critical
D	Penstock (duct), or: required to fill the penstock (intermittent operation)
E	Predicted (estimated) point
F	Friction (hydraulic or mechanical)
H	Hydraulic (efficiency)
I	Ideal point
i	Incidence
L	Leakage
M	Miscellaneous costs
O	Actual operating point, or: operation and maintenance (costs)
P	Pump-mode performance
R	Rotor (= impeller = runner)
S	Storage reservoir
T	Turbine; turbine-mode performance
U	Useful
V	Vapour saturation
W	Swirl (whirl)
S,X,Y,Z	Points of the double siphon
α	Object for economic comparison
β	Reference for economic comparison
Δ	Difference between turbine outlet (or pump inlet) and vapour pressure
0	Turbine outlet / pump inlet
1	Rotor eye
2	Rotor tip
1,2,3,4,5,6	Sections of the double siphon

Diacritics.

-	Average
~	Rated
^	Optimum
⌣	Shock-free entry
ˇ	Swirl-free outlet
`	Shut-off

NOTE: The nomenclature appears in a different way in graphs: the subscripts appear as lower-case letters in the normal position; the efficiency is 'e' instead of η; ω is printed as 'w'; κ as 'kappa' and ε as $\in$. Finally, the diacritics are printed as separate characters (except in the case of $\hat{\eta}$, that is printed ê).

ABSTRACT

The use of reverse-running pumps as turbines (PATs) is a promising technology for small-scale hydropower. This thesis reviews the published knowledge about PATs and deals with some areas of uncertainty that have hampered their dissemination, especially in 'developing' countries. Two options for accommodating seasonal flow variations using PATs are examined and compared with using conventional turbines (that have flow control devices). This has been done using financial parameters, and it is shown that, under typical conditions, PATs are more economic. The various published techniques for predicting the turbine-mode performance of a pump without expensive tests are reviewed; a new heuristic one is developed, and it is shown (using the same financial parameters and a large set of test data in both modes of operation) that the cost of prediction inaccuracy is negligible under typical circumstances. The economics of different ways of accommodating water-hammer are explored. Finally, the results of laboratory tests on a PAT are presented, including cavitation tests, and for the latter a theoretical framework is exposed.

0

INTRODUCTION

For several decades, reverse-running pumps have found various applications as turbines in industrial environments, and more recently they have been successfully used in stand-alone and grid-linked hydropower, especially in developed countries. On account of the much larger size of their market, pumps-as-turbines (PATs) - as well as their spares - are cheaper and more promptly available than conventional turbines, and their maintenance is easier due to the broad availability of spares and know-how. However, there are still many areas of uncertainty that have hampered their dissemination, particularly in the context of 'developing' countries.

Chapter 1 of this document reviews the published knowledge on PATs, including their limits of application and the types of pumps suitable to be used as turbines. Chapter 2 develops an economic methodology for micro-hydro, aimed at comparing technical options in a given economic and hydrological context.

The principal difference between a PAT and a conventional turbine is the former's lack of a flow control device. This is at the same time an advantage - it makes it cheaper, and a disadvantage - it makes it less versatile. The disadvantage has been reduced by the advent of electronic load controllers, that keep the generator torque constant by switching in ballast loads whenever electrical demand drops. Due to their fixed geometry, PATs also require constancy in their drive conditions. Seasonal flow variations have been met either by simply designing the system for the minimum annual flow or by operating several machines in parallel. In Chapter 3 these options are examined, a new one is presented (namely the intermittent operation of a single PAT), and all of them are compared with one another and with conventional turbines using the methodology of Chapter 2. Thus the penalty for using unregulated hydraulic machines is assessed.

Chapter 4 compares two different options to accommodate water-hammer in a scheme with PATs, namely a thick penstock and a thin penstock combined with a mechanical device.

The dissemination of PATs has been hampered by a lack of information. Especially in developing countries, even the pump manufacturers ignore the turbine-mode performance of their pumps. Chapter 5 deals with the prediction of PAT performance when only the pump-mode performance is known: it reviews the published knowledge on this field, presents a new prediction method and evaluates the actual economic cost of the inaccuracy of the prediction.

Finally, Chapter 6 deals with cavitation in PATs (a subject that has not been properly studied before). It presents a theoretical background and the results of laboratory tests made to explore the incidence of cavitation in PATs.

It is hoped that the contributions made here to reduce the areas of uncertainty in PAT knowledge will promote the use of this technology and hence of micro-hydro. The development of small-scale hydropower reduces the emissions of CO_2, SO_2 and NO_X and therefore slightly contributes to the control of the greenhouse effect (as pointed out by De Vries[91]). However, the impact of the availability of energy on rural development makes micro-hydro even more promising for the isolated rural communities of developing countries, where it is in many cases the only feasible inanimate energy source.

1

THE USE OF PUMPS-AS-TURBINES

1.1 Why Use a Pump-as-turbine?

1.1.1 The Inter-changeability of Pumps and Turbines

Pumps-as-turbines' lack of regulating devices is not the only difference between them and conventional turbines: a comparison between a pump-as-turbine (PAT) and an unregulated turbine purpose-made for a similar duty reveals that the former has a larger runner with the curvature of the blades in opposite direction (see Fig. 1).

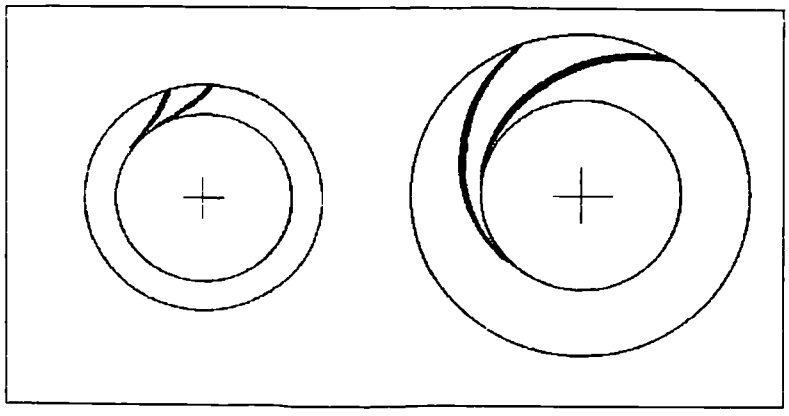

Fig. 1. Comparison between the runner of a Francis turbine and the runner of a PAT, for a similar performance.
Based on a drawing by Meier[62].

The extra cost of the larger runner and the small efficiency loss due to the improper design are largely compensated by the cost reductions derived from its mass production.

The difference in size between a PAT and a turbine of similar duties arises from the need in pump mode to avoid flow separation and diffusion loss. Its decelerating flow

is more difficult to control than the accelerating flow of a turbine, and requires a bigger impeller (between 30% and 40% bigger), with long, gradually diverging channels. The reversed curvature of the PAT blades is due to the need to have a small angle at the outlet in pump-mode for reasons of stability.

A turbine can certainly work as a pump. However, the relatively short channels of a Francis turbine and the big angles of its runner would produce in pump-mode an excessive deceleration and instability. Because of this, pumps can be used as turbines more readily than turbines as pumps, and the purpose-made reversible machines (pump-turbines) for energy storage schemes are much more similar to pumps than to turbines (Chapallaz *et al.*[92], Krivchenko[86], Meier[62], Raabe[81], Sharma[84], Stepanoff[57], Strub[59], Williams[92]).

1.1.2 History

The oldest recorded pump-as-turbine seems to be one installed in Orchard Mesa, USA, in 1926 and that was still working in 1983 (Shafer[83]). It is remarkable how this idea arose in such an early age, before any formal studies of the turbine-mode characteristics of pumps were published.

The early research on the 'four quadrant' characteristics of pumps had in fact a completely different aim, namely the analysis of water-hammer in large pumping stations. The laboratory tests made with this objective led D. Thoma and Clifford Proctor Kittredge to notice incidentally that a reverse-running pump was an efficient turbine (Thoma[31]), and then to hint the possibility of using the same machine as pump and as turbine in storage stations (Kittredge[33]). Later, Sprecher[51] mentioned the possibility of using a pump as a water turbine on its own.

The further development of the technology of pumps-as-turbines, as well as its dissemination, has been inadvertently nurtured by the research on water-hammer in pumping stations and on pump-turbine schemes. This development of a low-cost technology made possible by the indirect benefits derived from R&D on advanced technologies is a pattern that can be observed in many other areas.

Presumably inspired on PATs, there was in 1981 an attempt to use marine bow thrusters as low-head turbines (Huetter & B.[81], Makansi[83]). The 'thrusters' are large diameter shrouded propellers driven by diesel engines to guide tugboats while positioning supertankers in small harbours; they work in both directions. Instead of making studies on a model, it was decided to install a prototype, but the project was a downfall: the turbine produced only one-half of the expected power. After modifying the runner blades and the guide vanes, the efficiency could be improved, but only by 3% (DeLano[84]).

1.2 Limits and Applications of PATs

1.2.1 Size Limits

Some people suggest that the upper limit of application of PATs is established by their market availability 'off the shelf', *i.e.* around 100 kW (Schmiedl[88]) or 250 kW (Engeda & R.[88b]). However, other authors affirm that PATs, even if they have to be manufactured to order, continue to be more economical than conventional turbines up to a much higher threshold: Lawrence[79] mentions 1,5 MW; Garay[80] 2 MW; Grant & B.[84] talk about several MW, with various 500 kW machines in parallel; and Hochreutiner[91] describes a Swiss hydropower station with seven 931 kW PATs in parallel, using "a pump model, cheap and solid, frequently used in South African gold mines and in the Gulf countries".

On the other hand, in some countries with wide availability of locally made cross-flow turbines, and reduced availability of pumps, such as Nepal or Pakistan, the upper limit for application of PATs could be as low as 15 kW, as proposed by Williams[91b], for relatively low specific speeds (see also below).

1.2.2 Specific Speed Limits

Lower Boundary.

The applicability of PATs may be restricted also according to their specific speed. In the low specific speed area, they have to compete with impulse turbines. As can be seen in Fig. 2, below a certain threshold, reaction (Francis) turbines are less efficient than impulse (Pelton) turbines, and the same applies to PATs. This is due to the narrow flow passages characteristic of reaction machines of low specific speed.

In the domain of pumps, where the impulse principle does not work, very low specific speeds can only be achieved by using multistage pumps. Multistage pumps can be used as turbines, but their cost advantage over impulse turbines is offset by ① the high cost of multistage pumps (that are more expensive than single-stage pumps) and ② the low cost of small Pelton, Turgo and cross-flow turbines (that can be fabricated in local workshops).

Moreover, multistage pumps have higher maintenance costs, especially for bearings and seals, than Pelton turbines (Torbin *et al.*[84])

There is no consensus on this issue. Some think that Pelton turbines are unbeatable for $\Omega_T < 0.2$ (Ventrone & N.[82]) and that multistage pumps are too expensive (Acres American[80]), but other people have found these pumps to be cost-effective (Fraser & A.[81], Hergt *et al.*[84], Hochreutiner[91], Semple & W.[84]).

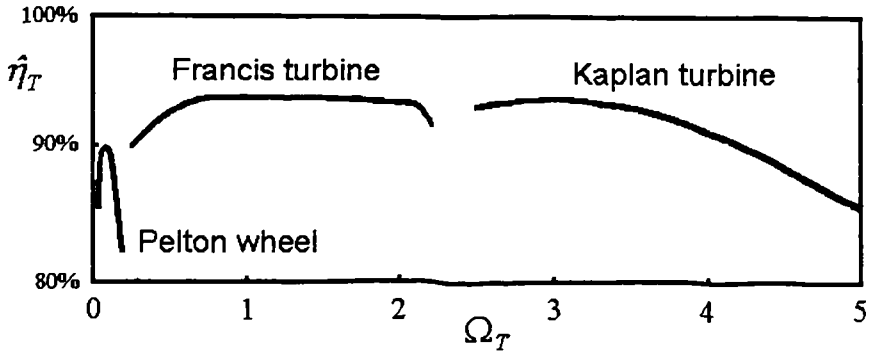

Fig. 2. Relation between specific speed (Ω_T) [1] and efficiency ($\hat{\eta}_T$) [2] of turbines.
Based on Shepherd[65].

Upper Boundary.

At the other end of the specific speed scale, where axial machines have to be used, PATs have also some disadvantages: axial flow PATs are more expensive than other pumps; there is little turbine-mode experimental information available on them; their long shaft (in the case of vertical pumps) may be unreliable (Wong[87]), and the shape of the impeller blades, used to promote stability in pump-mode, has the potential to be counter-productive to turbine stability (Acres American[80]).

Moreover, Ventrone & N.[82] have identified that, unlike other turbines, small axial turbines (with $\Omega_T > 2$) are suitable for standardisation, on account of the possibility to adjust their performance to a range of conditions, just by changing the number and pitch of the blades.

There are some disadvantages that affect all axial machines - turbines and PATs: their proneness to cavitation, their high runaway speed and their low efficiency. The latter is due to the lack of proper guidance of the fluid by the impeller blades, which in turn is due to the shorter blade length and smaller blade lap (Engeda & R.[87]).

For these reasons, and for the specific disadvantages of axial PATs, Fraser & A.[81] proposed the use of several mixed-flow PATs in parallel instead of an axial machine. In the context of the USA, a set of up to five mixed-flow PATs was found to be cheaper than a single conventional hydraulic turbine of comparable capacity. This approach has a

---

1 The notation proposed by Ida *et al.*[90] is adopted here for the dimensionless specific speed, which is defined for both turbine-mode and pump-mode as $\omega \cdot Q^{0.5} \cdot (gH)^{-0.75}$, *i.e.* the metric specific speed divided by 53.

2 Diacritic ^ means the best efficiency point (BEP). Some diacritics will be used throughout this document to represent the different operating points of hydraulic machines, because the use of subscripts would make the notation too clumsy, especially in the following chapters.

very important additional advantage: it permits part-load operation during low-flow seasons (see also p. 28).

Conclusions.

It is not possible to draw a general rule regarding the limits of applicability of PATs according to their specific speed, since they will vary from one country to another, depending on the availability and cost of pumps and turbines.

In countries like Peru or Nepal, where there is expertise in the manufacture of impulse turbines, the lower boundary may be near the $\Omega_T = 0.2$ limit proposed by Ventrone and Navarro. In other countries, this boundary will be shifted to a lower specific speed, especially if multistage pumps are locally available.

Lastly, the standardised axial turbines proposed by Ventrone and Navarro require building up an industrial infrastructure that is unjustifiable in most countries. Under these circumstances, the upper boundary of specific speed is defined only by the availability of pumps, and axial-flow PATs or mixed-flow PATs sets may be the best solutions for low head sites, that have most of the small hydro potential in the world (Kumar & T.[84]).

1.2.3 Maintenance and Silt Resistance

The maintenance of PATs is easier than that of conventional turbines due to the broad availability of spares and know-how. According to the experience of McClaskey & L.[76], the maintenance of a pump is easier when it is used in turbine-mode (*i.e.* as a PAT) than in 'normal' pump-mode! The availability of spares leads to the philosophy of 'repair by replacement', as suggested by Grant & B.[84].

Yedidiah[83] mentions an additional advantage of PATs: their ability to handle abrasive or corrosive liquids in industrial environments. In micro-hydro, this ability may permit a reduction in intake costs, as long as the PAT has adequate seals (Williams[91c]). For instance, Giddens[91] reports a PAT scheme with a perforated stainless steel plate inclined 30° as intake[3], that has worked in New Zealand for one year without any problem: "the intermittent flow of fine material (in this case greywacke, which is quite hard) passing through the cast iron pump casing and impellers at times of flood flow has done no serious damage to the pumps; in fact, it has fettled them!"

1.2.4 Examples of Applications

In addition to free-standing energy generation from rivers, PATs have found a number of other applications:

---

3 For more about intakes see: Dechaumé[91], Giddens[84, 86a], Koonsman & A.[51] and Wiesner[67].

They are used for energy recovery in water supply and sewage systems (Engeda & R.[88b], Mikus[83], Schnitzer[92], Wilson & P.[92]), especially in Germany, where it has been estimated that the energy potential of the water supply systems is 64 MW (Apfelbacher & E.[88]).

They can work together with pumps, to make variable-duty pumping stations more energy-efficient, instead of throttling (Yedidiah[83]): a PAT can be installed in series with the pump, to reduce the head; or in parallel, as a by-pass, to reduce the flow, although Holzenberger & R.[88] showed that a variable speed drive for the pump is usually a better solution in the first case. In pumping stations where a single pump has to deliver water up to different levels, as often happens in irrigation schemes, PATs can be installed in the lower branches (Yedidiah[83]).

In some cases, the actual pumps of irrigation or sewage pumping stations can themselves be used as turbines during a small part of the year (De Vries[91]). One such scheme, a big one with three 4.5 MW pumps, is described by Duncan[82].

PATs can also be used to drive pumps (Laux[80], Naber & H.[87], Schnitzer[85], Shafer[82]). Kasperowski[66] and Priesnitz[87] studied the performance characteristics of these PAT-pump sets.

They have been described as "the ideal drive for the hose-reel in irrigation machines, to retract the sprinkler attached to the end of the hose" (World Pumps[85]).

PATs have found also a number of industrial applications, driving generators or machines; they have a particular advantage over electrical drives in explosive environments (Yedidiah[83]). In the oil-related industries, they can be used in wells (Engeda & R.[88b]), in gas and oil separation plants (Wong[87]), in synthetic ammonia production and in refineries (Engeda & R.[88b], Taylor[83]), especially in those situated on the shore and cooled with sea water (Wong[87]). PATs can handle two-phase flows, present in many of these applications, in which a gas comes out of solution during the expansion, contributing additional energy, although usually at a lower efficiency (Bolliger & G.[84], Daffner & D.[84], Gopalakrishnan[86], Gülich[81], Hamkins *et al.*[89a, 89b], Kamath & S.[82], Kennedy *et al.*[60], Nelik & C.[84], Olson[74], Winks[77]).

Finally, they have found applications in mine-cooling (Torbin *et al.*[84], World Pumps[85]) as well as in reverse osmosis schemes (Engeda & R.[88b], Salaspini[85]) and they have been used to drive heat pumps by means of a magnetic drive (Schnitzer[85]).

1.3 Suitable Pumps

1.3.1 Suitable Pump Categories

Vertical Diffuser versus Horizontal Volute Pumps.

There is a wide range of low to medium specific speed performances that can be met by pumps with two very different constructions: vertical and horizontal shaft. The

former always have a diffuser and are sometimes called vertical turbine pumps; the latter have typically a volute without diffuser vanes.

Vertical pumps are more expensive, but "they differ from horizontal type centrifugal pumps in that the addition of stages is a simple standard option requiring a minimum of parts, no additional bearings or lubrication devices and is virtually unlimited in the number of stage additions" (Fraser & A.[81]). The possibility of using relatively few pump designs to cover a wide range of conditions, including not only the axial-flow domain (by using several machines in parallel; see p. 6), but also the radial-flow range, by using up to 15 stages in series, has made the vertical mixed-flow PATs a widespread option in the United States, because they make possible some degree of standardisation of small hydropower schemes.

As the specific speed of their impellers is near the optimum (about $\Omega_T = 1$), vertical multistage pumps are more efficient than single-stage centrifugal pumps: they are "an optimal compromise between high specific speed axial pumps, which have inherent disadvantages, and the lower specific speed pumps which tend to be much larger, bulkier and with disadvantages of scale". They have a minimum wear surface and simplified bearings (idem).

When used as turbines, vertical pumps can be installed directly above the tail-water channel (Cooper *et al.*[81], Pelton[88]) or with a secondary outlet siphon, to reduce foundation and structure costs (Fraser & A.[81]). Their diffusion ring permits a more efficient and stable operation than would a simple volute (idem) and makes easier the modification of the turbine-mode performance by machining the diffuser (see below, p. 13) (Chapallaz *et al.*[92], Laux[82], Mikus[83]). Lastly, the installation of an induction motor to be used as generator is easier with vertical pumps, as they are usually sold with vertically mounted motors.

However, in the context of developing countries, the low cost of labour and the high cost of capital reduce the relative advantages of vertical mixed-flow pumps. Their high cost makes them suitable only in large-scale construction programs where the cost reductions derived from standardisation play an important role.

Submersible Pumps.

Submersible pumps, available in small sizes, are usually more expensive than other pumps of similar rating; however, their use as turbines avoids the need of a power-house and tail-race channel: the machine can just lie on the river bed, or it can be located inside a pipe leading to the draft tube (Giddens *et al.*[92]; and also: Hellmann & D.[84]). Moreover, pumps of this kind are robust and very resistant to silt (Williams *et al.*[88]), and they can run continuously for long periods without servicing.

There are several types of submersible pumps, but not all are suitable to be used as turbines: only the dry-motor (motor below the pump), jacket-cooled pumps are

recommended (Williams[90]). Some new designs of submersible pumps may be inadequate: for instance, Williams[92] met a pump with a semi-open impeller which runs against a hard rubber coating on the diffuser in order to cut the leakage losses and whose sharp blade edges, when run in reverse, became locked into the rubber, preventing the machine from running.

With a submersible PAT, the use of brakes and flywheels (see p. 49) to avoid damage by load rejection is impossible, and other means have to be employed (Giddens[91]).

Double Suction Pumps.

Shafer[83] mentions that double suction pumps have worked successfully as turbines, and other authors agree in this possibility (Apfelbacher & E.[88], Grant & B.[84]). Schnitzer[92] even suggests that split-casing in-line double-suction pumps are the ideal to be used as turbines.

However, some pumps of this type have had a very low efficiency when operated as turbines (Williams[90, 91c], Yedidiah[83]). The "adverse conditions" (Swanson[53]) of the turbine-mode performance of double-suction pumps could be related with the fixed (pump-mode) inlet vanes (Williams[92]), with the bends, with the split-casing, with the larger wetted surface or with the shaft across the rotor eye (see Anderson[55]). According to Lawrence[79], some double-suction pumps would probably require major casing modifications for acceptable operation as turbines.

Unconventional Pump Designs.

Some unconventional pumps may be inadequate as turbines. For instance, a pump with a cylindrical casing (no volute) had as turbine a very low efficiency, when tested by Williams[91a]. Vortex impellers are also unsuitable (Williams[91c]).

1.3.2 Suitable Components

Seals.

There is very little information on seals for PATs. It seems though that mechanical seals are to be preferred to packed glands, as a clean supply of gland sealing water is unlikely to be available (Giddens[86b]), and because the former require less maintenance and offer less mechanical resistance (Williams[91c]). However, some modern mechanical seals are inadequate, especially those with springs, that will fail with reverse rotation (Chapallaz *et al.*[92], Williams[91c]). (Although a good mechanical seal may cost almost as much as the pump itself.)

Bearings.

Radial hydrodynamic bearings with lubrication grooves in the shell, as well as all axial hydrodynamic bearings are designed for only one direction of rotation, and

therefore pumps with these should not be used in turbine-mode. Radial bearings with circular shell are adequate (Chapallaz *et al.*[92]).

Rubber bearings lubricated with pressurised water have been successfully used in PATs, and their maintenance is very easy (Cooper *et al.*[81], Makansi[83]).

Open versus Closed Impeller.

This is another controversial issue: according to some authors, closed impellers are to be preferred because of their higher efficiency (Acres American[80]), and because "there is no evidence that open impellers (or impellers with few blades and large passages) will handle a large solid content in the turbine mode as favourably as in the pump-mode" (Chapallaz *et al.*[92]).

However, semi-open impellers have other advantages: they are accessible for cleaning, easier and cheaper to manufacture; they have a higher stress limit; and their efficiency does not fall as sharply in turbine-mode as in pump-mode, *i.e.* pumps with semi-open impellers are "better turbines than pumps" (Engeda & R.[87, 89a], and also: Williams[92]).

1.3.3 Checks

The main check to be made in a pump to be used as turbine concerns the impeller thread and other threaded shaft couplings. Some authors recommend fixing them by a locking plate or by set screws, because under certain circumstances the torque can be negative (Chapallaz *et al.*[92], Chappell *et al.*[82], Jyoti Ltd.[n/a], Schnitzer[92], Spangler[88]). Shaft sleeves screwed onto the shaft should also be protected by set screws. Almost all pumps have these screws, but an operator may forget to put them back after tightening sleeves and stuffing boxes (Chapallaz *et al.*[92]).

Some authors recommend checking the bearings and the shaft stress. However, it has been already shown in the literature that both axial and radial loads on the shaft are smaller in turbine-mode than in pump-mode (Santolaria & F.[92], Yang[83], Yedidiah[83]), and the turbine-mode torque is usually within the operating range of the pump (as long as the speed is not higher than the maximum pump speed).

The critical speed is not generally a problem below the maximum speed for the pump, but in multistage pumps with long shafts this should be checked with the manufacturer (Chapallaz *et al.*[92]; and also: Franke *et al.*[89], Garay[90], Mayo & W.[82], Semple & W.[84]). Mikus[83] recommends measuring the vibration *in situ* always, but this would be relevant only in relatively large schemes.

Tognola[60] suggests removing any flow straightener in the pump inlet, since it could be damaged by the outlet swirl in turbine-mode.

Other possible source of problems, especially in large schemes, could be pressure fluctuations, but it has been shown that they are smaller in turbine-mode than in pump-mode. (Vissarionov *et al.*[89]; and also: Martin[n/a]).

1.3.4 Modifications

Although it is usually possible to use pumps as turbines without any alteration, the literature mentions some ways to improve their efficiency, adjust their performance, improve their stability, and increase their durability.

Most of these modifications are not feasible in small schemes, due to the limited ability of the purchaser to communicate with the manufacturers, and to the considerable expense involved in going back to them. In the case of larger schemes, some of the modifications could be viable, either by the manufacturers themselves or after purchase.

Reduction of Impeller Diameter.

The most straightforward modification to a pump, and one that can usually be made after purchase, is turning down the impeller. In turbine-mode, the performance adjustment that can be achieved by reducing the impeller diameter is very limited, as compared to pump-mode (Hergt *et al.*[84], Nicholas[88], Schnitzer[92], Yedidiah[83]): whereas in pump-mode, the head-flow curves are displaced laterally with both impeller and speed changes, turbine-mode characteristics are displaced approximately along the operating curve (Fraser & A.[81], Thorne[79a]), and performance should be altered by using other techniques (Laux[82], Lueneburg & N.[85]).

Some authors propose the reduction of the impeller as a means of fine-tuning the PAT performance (Chapallaz *et al.*[92], Hancock[63] [4], James[83]), but this is required only in very special circumstances, namely when a over-dimensioned PAT is already bought, and it is not possible to change it for another one.

However, there may be another benefit to be gained by trimming the impeller: an increase in the efficiency. This improvement has been repeatedly reported (Diederich[67], Mikus[83], Thorne[90]), although no explanation has been proposed. More research is required to establish in what cases this effect can be obtained.

In tests made by Knapp & D.[42], "cutting the discharge tips of the impeller blades while leaving the shrouds extended lowered the efficiency", but when the whole impeller

---

4 Hancock proposes in fact reducing the impeller to achieve the required pump-mode performance (when using conversion factors to calculate the ideal pump-mode performance for the known turbine-mode requirements), but this does not make sense.

was reduced the efficiency in both modes of operation (pump and turbine) remained equal.

The diameter reduction should be small; because with big reductions, the efficiency may fall more sharply than in pump-mode, due to excessive losses in the volute (Thome[79a]). On the other hand, the trimming has as a secondary effect "a reduction in the head-flow curve", that can be compensated by sharpening and chamfering the tip of the impeller (Mikus[83]) (see below). Finally, Chapallaz *et al.*[92] recommend restricting this technique to specific speeds below $\Omega_T = 0.6$, as above this threshold the whole geometry of the high pressure side of the impeller is affected.

Other Impeller Modifications.

A sharp edge to the blades on the tip of the impeller, that is harmless in pump-mode, may cause in turbine-mode vortices and separation of flow with a subsequent decrease of efficiency (Chapallaz *et al.*[92]). An increase in efficiency of 1 or 2% can be achieved by machining the impeller tip in both radial and tangential planes (Lueneburg & N.[85]). Mikus[83] proposes increasing β_2 by sharpening the tip of the blade and increasing b_2 (the entrance width) by chamfering the side walls; he reports a small change in performance as well as an efficiency improvement. The blade edges can also be under-filed (Chapallaz *et al.*[92], Yedidiah[83]). Finally, Grant & B.[84] mention the possibility of polishing the impeller.

Special Impellers.

The replacement of the pump impeller by a runner designed to have an optimal performance in the turbine mode has been proposed by Acres American[80], Cooper & W.[81] and Nicholas[88].

Modification of Volute or Diffuser Vanes.

"The energy transfer between the fluid and the impeller in pump-mode is mainly established by the shape (angle) of the blades at the impeller outlet. When flow is reversed in turbine-mode, it is the shape of the pump casing (volute) which determines the energy transfer" (Chapallaz *et al.*[92], Hergt *et al.*[84]). Therefore, the best way to adjust the performance of a PAT is to modify the diffuser vanes or the volute (Mayo & W.[82], McClaskey & L.[76]), by increasing the internal diameter of the diffuser (Mikus[83]), by grinding or welding the guide vanes, to change the cross sectional area of the passages and/or angles of the vanes (Chapallaz *et al.*[92]), or, with volute pumps without fixed-vanes, by increasing or reducing the throat (or 'nozzle') area (Laux[82], Lueneburg & N.[85], Nicholas[88], Williams[92]), or by modifying the region of the cut-water (Hergt *et al.*[84]).

Finally, Sánchez[91] reports his experience on using a small conventional pump impeller in a purpose-made wooden casing and bearings, aimed only at reducing costs.

Modifications of Axial Pumps.

In order to ensure a stable performance in turbine-mode (see p. 6), the shape of the impeller blades should be changed (Acres American[80]). The use of a suitable shape, not only for the impeller blades, but also for the diffuser guide vanes, can also increase the efficiency of axial pumps (Mayo & W.[82]). Finally, Acres American recommends the modification of the hub nose cone.

Other Modifications.

Other possible modifications are the replacement of the pump intake pipe or bell intake by a draft tube (Chapallaz *et al.*[92], Chappell *et al.*[82], Cooper[82], Mayo & W.[82], Yang[83]), the modification of labyrinth seals, to make them more sophisticated (Grant & B.[84]), the use of two seals in tandem for industrial applications (Chadha[84]) and the epoxy-coating of the volute and the discharge nozzle (Chappell *et al.*[82]).

2

AN ECONOMIC METHODOLOGY FOR EVALUATING MICRO-HYDRO

For the purpose of comparing technical options, an economic parameter will be required in the following chapters. As the available economic models for micro-hydro assume a constant value per unit of generated energy, as well as a constant efficiency (of the turbine and the penstock), a new micro-hydro economic model will be developed in this chapter, integrating the hydrology and the technical characteristics of the system.

2.1 Benefit

The benefit of the project is determined by the value of the power generated, which is an economic function of the power, which in turn is a technical function of the available flow, and the latter is a random variable with a hydrological probability function.

2.1.1 Economic Function

The economic function is the one that relates the power P_T being generated at any specific time with its instantaneous value $\dot{V}$. In a large electricity grid, this is a linear function whose slope depends on the price of the unit of energy (that can change in some countries according to the season and the time of the day).

In a small rural community, on the other hand, the instantaneous value is in fact a random variable, fluctuating continuously as the appliances are switched on and off. However, it is proposed to assume, that, on average, there is a fixed relation between the generated power and its value.

The value is defined in this case not as the price paid by the consumers, but as the social value of the task performed by the energy, without taking into account how the revenue is distributed between the end users and the suppliers. The relation between power and this use value is clearly non-linear: if a small amount of power is generated, the essential high-value social needs are satisfied, while a higher power satisfies also low-value, non-essential needs.

The mathematical model proposed is a power function whose exponent (Γ) is 1 for a large electricity grid and smaller for an isolated system.

$$\dot{V} = K_e P_T^{\Gamma} \qquad [1]$$

2.1.2 Technical Function

The technical function is the one that relates the available flow Q_A with the power generated P_T. This function varies with the rated flow $\tilde{Q}_T$[1], as well as with the type, size, number and method of operating machines as turbines. (Examples of technical functions are displayed in Fig. 7, p. 25, Fig. 11, p. 27, Fig. 13, p. 29 and Fig. 20, p. 38.) For flows below some minimum (usually non-zero), P_T is zero, and for flows above some maximum, P_T is constant.

2.1.3 Hydrological Function

The hydrological function is a probability function of the available flow Q_A. The cumulative probability function F_{Q_A} of the random variable Q_A is known in hydrology as the flow-duration curve, although by custom flows are plotted against the probability of their being exceeded (and hence the curve assigns a probability one to a null flow and a probability zero to an infinite flow), whereas cumulative probability functions are usually the other way round.

The analysis of typical flow-duration curves shows that, in the range of flows smaller than the average annual flow (the range of interest for micro-hydro), they fit very well (see Fig. 3) in the following mathematical model, written in the standard notation of probability theory...:

$$F_{Q_A} = 1 - \left(1 - e^{\lambda Q_A^{\mu}}\right)^{\xi} \qquad [2]$$

As in most cases $\xi = 1$, we will simplify this model to:

$$F_{Q_A} = e^{\lambda Q_A^{\mu}}$$

μ is a number between –0.8 (small basins) and –3 (large basins).

1 The diacritic ~means 'rated point'.

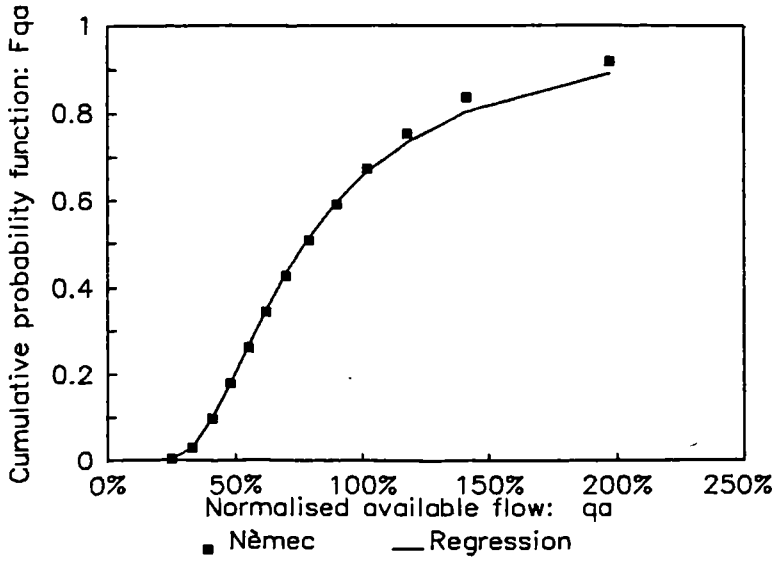

Fig. 3. A flow-duration curve and its fitting mathematical model.

Hydrological data published by Nèmec[72] (region III). $\xi = 1$; $\mu = -1.91$; $\lambda = -0.43$. Regression made by giving to the errors a weight proportional to $(1-F_{QA})$. q_A is defined as in Eq. [6].

Finally, the density probability function f_{QA} is the derivative of the cumulative function:

$$f_{Q_A} = \frac{dF_{Q_A}}{dQ_A} = \frac{d\left(e^{\lambda Q_A^{\mu}}\right)}{dQ_A} \qquad [3]$$

2.1.4 Mathematical Expectation of the Instantaneous Value

The instantaneous rate of generating benefit $\dot{V}$ is a function of a random variable Q_A. (This dependence is in two stages: $Q_A \rightarrow P_T\{Q_A\} \rightarrow \dot{V}\{P_T\}$.) As the probability density function of Q_A is f_{QA}, the average of $\dot{V}$ is a mathematical expectation:

$$E\{\dot{V}(Q_A)\} = \int_0^{\infty} \dot{V}(Q_A) f_{Q_A} dQ_A$$

(As P_T, and therefore $\dot{V}$, is zero for flows below some minimum, an equivalent - and probably clearer - expression would have the minimum flow as the lower limit of integration, as in Eq. 77, p. 101, where $\tilde{Q}_T$ is the minimum flow.)

2.1.5 Present Value of the Benefit

By assuming that the expected yearly benefit will be constant[2] (namely 1 year $\times E\{\dot{V}\}$), we can apply a constant discount factor to establish the present value of the benefit...:

$$V = K_d \, E\{\dot{V}\} = K_d \int_0^\infty \dot{V} \, f_{Q_A} \, dQ_A \qquad [4a]$$

..., where K_d is a function of the discount or interest rate d and the lifetime of the scheme N:

$$K_d = \frac{(1+d)^N - 1}{d(1+d)^N} \cdot 1\text{year} \qquad [4b]$$

Substituting Eq. [1], we get:

$$V = K_d K_e \int_0^\infty P_T^\Gamma \, f_{Q_A} \, dQ_A$$

Finally, from Eq. [3]:

$$V = K_d K_e \int_0^\infty P_T^\Gamma \, d\left(e^{\lambda Q_A^\mu}\right) \qquad [5]$$

2.2 Cost

The cost of a scheme is considered as the sum of the initial investment (*i.e.* turbomachinery, penstock[3], storage reservoir, and miscellaneous items) and the discounted yearly operation and maintenance costs:

$$C = C_T + C_D + C_S + C_M + C_O$$

All these costs are function of the size of the scheme, that is best characterised by the rated flow. In order to handle only dimensionless variables, we define the normalised rated flow $\tilde{q}_T$ as the rated flow $\tilde{Q}_T$ divided by the annual average flow:

---

2 This economic model is aimed at making decisions before the system is built and therefore, unless there are reasons to believe expected flow has a time trend (*e.g.* reduction due to afforestation), the average forecast can be calculated by assuming that every year in the future will be an average year. This assumption is never true in practice, which means that this average forecast may have in some cases a large standard deviation: the occurrence of dry years early on in the project life may profoundly reduce the profitability of the scheme, and *vice-versa*.

3 The penstock is represented by subscript $_D$ (from **duct**), because subscript $_P$ will be used later for pump-mode performance.

$$\tilde{q}_T = \frac{\tilde{Q}_T}{\int_0^\infty Q_A f_{Q_A} dQ_A} \quad [6]$$

2.2.1 Turbomachinery

For a given head, the cost of each PAT or conventional turbine is a power function of its rated flow. If we have n turbines operating in parallel (for the sake of simplicity, we will assume that they are identical to each other), their total cost is:

$$C_T = k_T n \left(\frac{\tilde{q}_T}{n}\right)^\Theta = k_T \tilde{q}_T^\Theta n^{1-\Theta} \quad [7]$$

The exponent Θ varies between 0.55 and 0.7 for PATs.

2.2.2 Penstock

By studying price lists of piping, it is possible to prove that the cost of a given length of pipe is nearly proportional to its cross-section solid area. For a given pressure-rating, the thickness is proportional to the diameter, and then the solid area is proportional to the diameter squared, *i.e.* proportional to the internal area.

From the standard formula for head loss in pipes...

$$h_D = f \frac{L_D}{D_D} . \frac{v_D^2}{2g}$$

...., it is possible to establish the relation between internal area, flow and head loss:

$$A_D = \left(\frac{f L_D \sqrt{\pi}}{4g}\right)^{0.4} h_D^{-0.4} Q_T^{0.8} \quad [8]$$

The head-loss is a function of the efficiency of the penstock:

$$h_D = (1 - \eta_D) z$$

Therefore, the cost of the pipe is:

$$C_D = k_D (1 - \tilde{\eta}_D)^{-0.4} \tilde{q}_T^{0.8}$$

2.2.3 Reservoir

A storage reservoir is required in the case of the intermittent operation of PATs, as explained in p. 30. Its cost is a complex function of its depth, its surface area and its shape. However, we will assume that it is simply a linear function of its volume

($C_S \propto V_S$). The reservoir volume can be related to the penstock volume V_D, which is in turn proportional to the penstock's internal area (for a given length of the penstock). Therefore, from Eq. [8]:

$$C_S = k_S \frac{V_S}{V_D}(1-\tilde{\eta}_D)^{-0.4}\tilde{q}_T^{0.8}$$

2.2.4 The Rest

The cost of the remaining miscellaneous elements (other civil works, and the equipment that uses the energy provided by the turbine shaft) is assumed as a power function of the rated flow. The exponent is close to 1 for the civil works, and close to Θ for the equipment. As the latter is relatively more expensive, we choose Θ (the same exponent as for the turbomachinery).

$$C_M = k_M \tilde{q}_T^{\Theta}$$

2.2.5 Operation and Maintenance

The yearly O&M costs are considered as a fixed proportion k_O of the initial investment. Therefore the present value of the O&M costs is...:

$$C_O = K'_d k_O (C_T + C_D + C_S + C_M)$$

..., where the discount factor K'_d (similar to K_d, Eq. [4b]) is defined as:

$$K'_d = \frac{(1+d)^N - 1}{d(1+d)^N}$$

2.2.6 Present Value of the Cost

Putting all together:

$$C = \left[\left(k_T n^{1-\Theta} + k_M\right)\tilde{q}_T^{\Theta} + \left(k_D + k_S \frac{V_S}{V_D} \right)(1-\tilde{\eta}_D)^{-0.4}\tilde{q}_T^{0.8} \right](1+K'_d k_O) \qquad [9]$$

2.3 Economic Comparison of Two Technical Options

2.3.1 Financial Criterion

Three of the most frequently used financial parameters to evaluate and compare investment projects are the net present value (NPV = V–C), the benefit/cost ratio (BCR = V/C) and the internal rate of return (IRR = d ∋ V–C = 0).

The main difference between the NPV and the other two parameters (BCR and IRR) is that the former compares the net benefits **per site**, whereas the latter compare the net benefits **per unit of capital invested**, regardless of the size of the project.

The NPV is sensitive to the choice of a discount rate, whereas the IRR is not. As for the BCR, its ranking is also unaltered by discount rate, under the conditions assumed in this economic model, namely that:

- the projects have an initial investment followed by a series of constant expected yearly benefits and O&M costs (simple projects),
- all projects being compared have the same lifetime N, and
- all projects have equal O&M factors k_O, relating yearly O&M costs to initial investment.

Under these three conditions, the BCR assigns the same preference rank to the projects being compared as the IRR. However, the ranking according to the NPV disagrees in some cases with the ranking according to the other two parameters. An example is illustrated in Fig. 4a, that compares a (large) project **L** with a (small) project **S**. From the point of view of the IRR (and hence of the BCR), project **S** is preferable, regardless of the discount rate. On the other hand, the ranking according to the NPV depends on the discount rate: a low rate favours project **L** and a high rate favours project **S**.

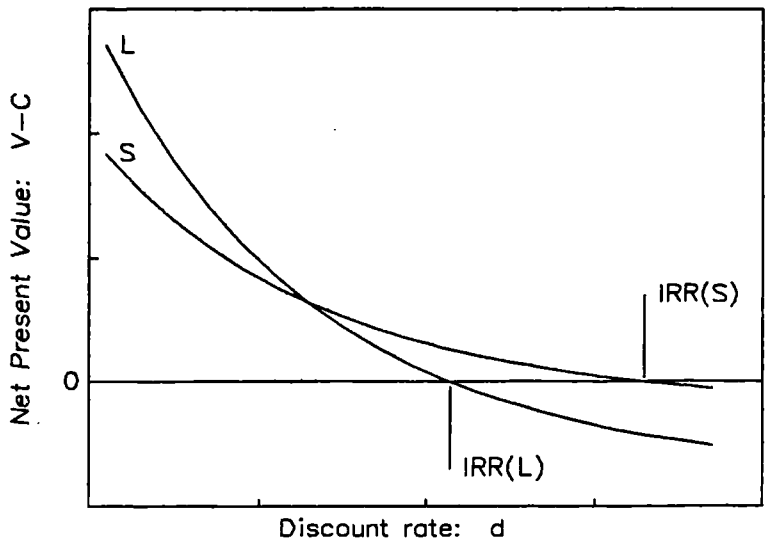

Fig. 4a. The NPV as a function of the discount rate, for projects **L** and **S**.

Since the BCR and the IRR do not provide any information on the **size** of the project, they will tend to favour the smaller projects: "rejection of a project with a lower IRR may come down to rejection of voluminous profits" (Opdam[91]). However, most real

situations in development amongst the rural poor tend to require high discount rates (capital scarcity), at which the three parameters tend to give the same ranking.

The parameter that will be used here for the ranking of the technical options is the BCR, since the use of the NPV would require chosing a discount rate. However, the decision-maker is warned that in many circumstances, especially with low discount rates, the NPV would be preferable (Infante-Villarreal[89]).

Incidentally, the BCR is nearly proportional to the IRR when the lifetime of the projects is relatively long (as in micro-hydro), since the limit of the IRR when $N \to \infty$ is simply the yearly net benefit (yearly benefit minus yearly costs) divided by the initial cost.

2.3.2 Economic Advantage

For our purpose of comparing technical options, we will assume that every scheme is designed by maximising the BCR = V/C (see Fig. 4b), under a given set of hydrological, technical and social conditions.

This of course is very far from the reality. The hydrological probability function of the site, for instance, is seldom based on data taken in a daily basis over a period of at least 15 years. However, we pretend that this assumption does not hamper significantly the achievement of the goal of comparing technical options.

The comparison of two different technical options will be made by calculating the ratio of the respective benefit/cost ratios. This ratio of ratios will be called economic advantage. *i.e*: when comparing the optimum BCRs obtained with options β and α, the economic advantage of β with respect to α is defined (using the German letter *Æ*) as:

$$Æ_{\beta\alpha} = \frac{V_\beta / C_\beta}{V_\alpha / C_\alpha} \qquad [10]$$

This parameter is in fact the optimum BCR that would be obtained with option β if option α produced an optimum BCR equal to one, *i.e.* identical benefit and cost.

As the purpose is just to compare technical options, we do not care about the actual values of the coefficients K_e and K_d (Eq. [5]), that 'disappear' in Eq. [10]. As for the costs, it is relevant only to take into account the proportion of k_T, k_D, k_S, k_M with respect to each other, and k_O and K'_d in Eq. [9] are irrelevant. Therefore, the discount rate d and the lifetime of the scheme N are not applicable. Similarly, the only pertinent hydrological parameter is the shape of the curve, defined by μ, and not its magnitude, defined by λ.

The economic advantage will be used in Chapters 3, 4 and 5 to compare respectively different ways to accommodate flow variations, different techniques for managing

water-hammer and different formulae for predicting the turbine-mode performance of pumps.

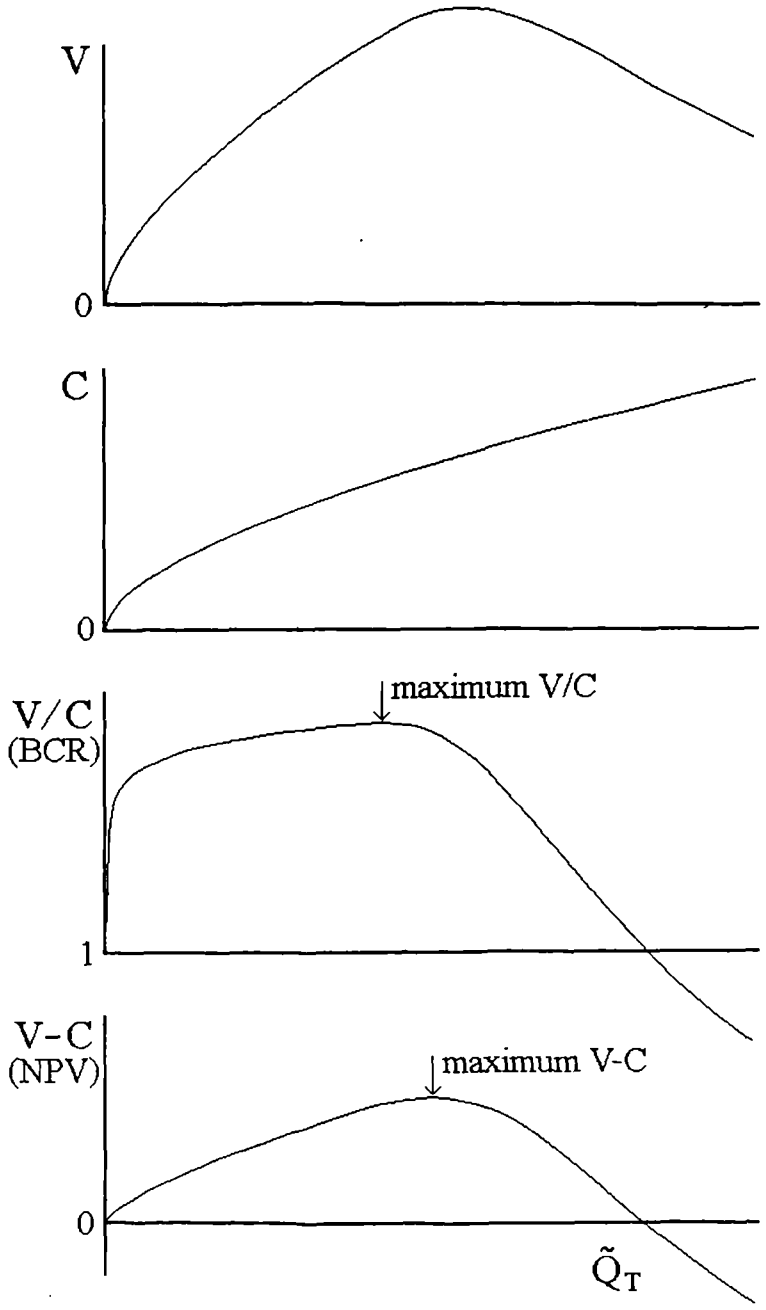

Fig. 4b. Typical shape of the curves for V, C, V/C and $V–C$, in terms of the rated flow $\tilde{Q}_T$ of a micro-hydropower scheme.
Note that maximising the NPV ($V–C$) occurs at a higher value of $\tilde{Q}_T$ than maximising the BCR (V/C), because the NPV tends to favour the larger projects.

3

ACHIEVING FLOW FLEXIBILITY AND ITS ECONOMICS

3.1 Introduction

Conventional turbines have flow-control devices to enable them to meet two kinds of variations in their operating conditions: short term - due to changes in shaft load, and seasonal - due to changes in the available head and flow. PATs, on the other hand, do not have hydraulic controls; on account of this lack, their efficient operation needs constancy of both drive and load conditions.

Among the different possible applications of micro-hydro, neither direct drive of machinery nor grid-linked electricity generation present problems of short-term constancy. This is because either they are constant-load applications or they do not require high efficiency to be maintained over their full range of speed. In stand-alone electricity generation, electronic load controllers or induction generator controllers[1], used instead of traditional mechanical flow controllers, keep the generator torque constant by switching in ballast loads whenever electrical demand drops. The energy provided to ballast loads can be used in a productive way (Kumar & T.[84], Minott & D.[83]), or simply wasted. As most micro-hydro schemes are run-of-the-river (*i.e.* without

1 The recent development of induction generator controllers (Smith *et al.*[90], and also: Giddens *et al.*[82], Shimizu *et al.*[86]), that avoid the need for separately regulating the output voltage and the frequency, facilitates the use of PATs for small-scale free-standing electricity generation: the use of induction generators instead of the conventional synchronous machines permits the use of cheap induction motors as generators and, therefore, of pump-motor sets as turbine-generator sets (Williams *et al.*[89a, 89b]). In addition, with an induction generator, the eventual link of the micro-hydro station with a grid, "the inevitable trend of small hydropower development" (Deng[85]), by removing the load controller and leaving the generator 'floating on the line', is much easier than with a synchronous generator.

storage), this energy would have been 'wasted' anyway, as unused flow, even if a flow controller had been used.

Seasonal flow variations, on the other hand, have been met either by simply designing the system for the minimum annual flow or by operating several machines in parallel. This chapter examines these options and presents a new one, namely the intermittent operation of a single PAT. Finally, using the economic methodology developed in Chapter 2, these techniques will be compared between themselves and with conventional turbines, and the penalty for using unregulated hydraulic machines will be assessed.

3.2 The Performance of Fixed-geometry Turbines

Fig. 5 shows the typical constant-speed performance of a fixed-geometry reaction turbine, such as a pump-as-turbine.

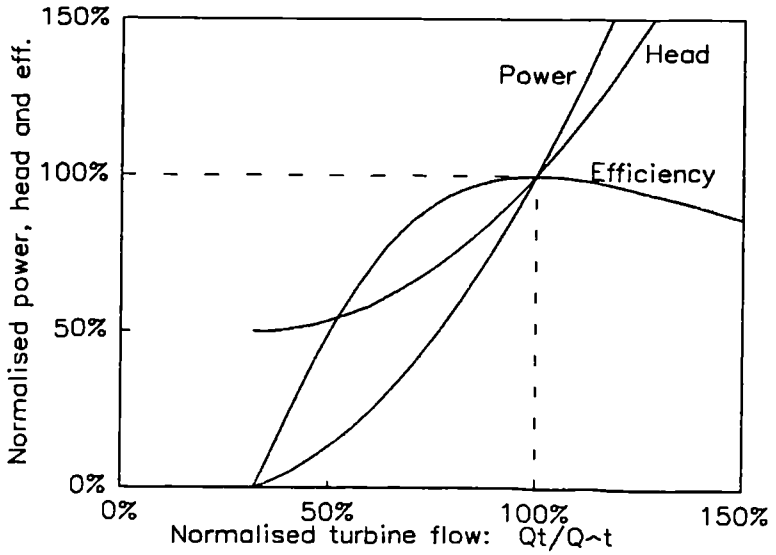

Fig. 5. Typical constant-speed performance of a radial-flow PAT.
Percent of best efficiency point (BEP).

When installed in a typical 'fixed-head' small hydropower scheme[2], the rated or design operating point is defined by the single intersection, in the head-flow plane, of the turbine curve and the penstock curve. For the latter curve, the head is the available head minus the penstock's head-loss, as in Fig. 6. (When we say 'fixed-head' we mean fixed available head; the turbine head can vary.)

2 The operation of PATs under variable-head conditions is discussed by Sheldon[84], James[83] and Apfelbacher & E.[88].

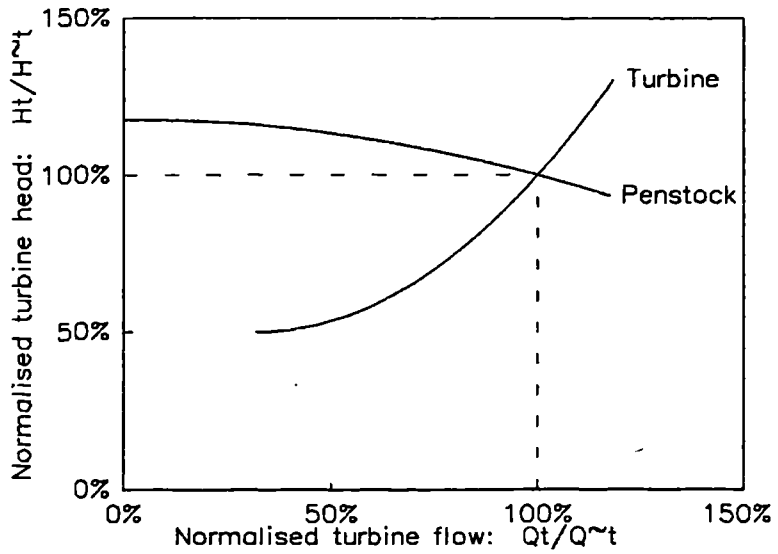

Fig. 6. Penstock and turbine curves.
Percent of rated point (that can be slightly off the BEP).

If the flow available to a PAT falls below the rated flow, the machine can continue to operate, but only if its head is reduced as well, so that its head-flow curve can be followed. In a 'fixed-head' scheme, reducing the turbine head means in fact wasting some of the available head. This waste can take place in a throttling valve[3].

If, on the other hand, the available flow is larger than the rated flow, the excess cannot be used without increasing the head. The resulting flow-power curve is shown in Fig. 7.

Figs. 8 and 9 show how the shape of the flow-power curves changes with different specific speeds and patterns of operation, respectively. The latter demonstrates that there is absolutely no point in changing the speed of the PAT: if it is kept not constant, but proportional to the cubic root of the power, the efficiency of the turbine stays at its maximum, but the turbine head is smaller, and the generated power is in fact lower[4].

---

3 Although throttling increases the cost and complexity of the system, and can cause excessive vibration, as reported by Cooper & W.[81]. If the flow is reduced and the head is not throttled in a valve, the free surface of the water in the penstock descends until the head matches the new operating point of the turbine, and the upper part of the penstock works as a turbulent channel, in which the extra head is dissipated: Williams[92] reports a scheme running smoothly with a partly empty penstock down to a power equal to 25% of the full power, but this could be the exception rather than the rule, because in many cases the entrained air originated in the turbulence in the partially filled section of the penstock can cause operating problems. (Giddens[83, 86a, 86b] designed an air eliminator, but the need to install it in the transition point between channel and full flow reduces its flexibility.)

4 Variable speed operation is only relevant for variable head conditions (Apfelbacher & E.[88], James[83], Levy[90], Sheldon[84]), and not as suggested by, for example, Santolaria & F.[92].

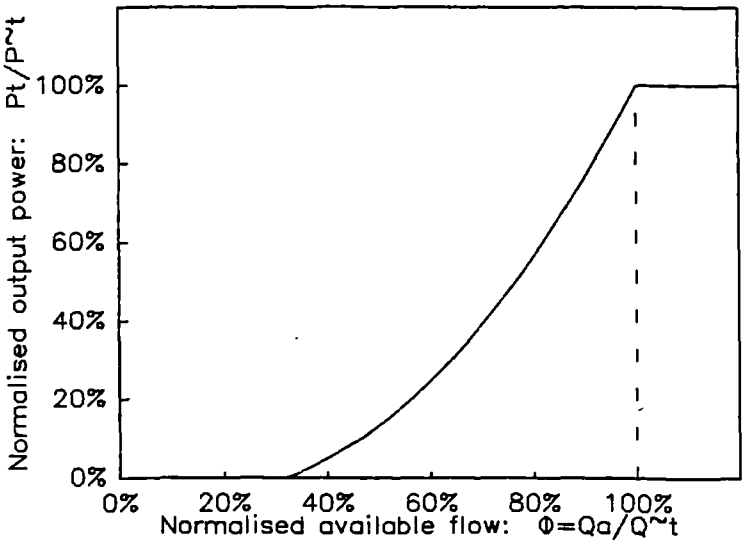

Fig. 7. Typical operating flow-power curve of a PAT.

Constant speed and constant available head; radial-flow PAT. To the left of the rated flow, turbine head is less than available head (some head is wasted); to the right, turbine flow is less than available flow (some flow is wasted). The normalised available flow Φ relates available flow to rated turbine flow: $\Phi = Q_A / \tilde{Q}_T$.

Constant torque operation (when driving a positive-displacement pump, for example) is the worst case (see Fig. 9).

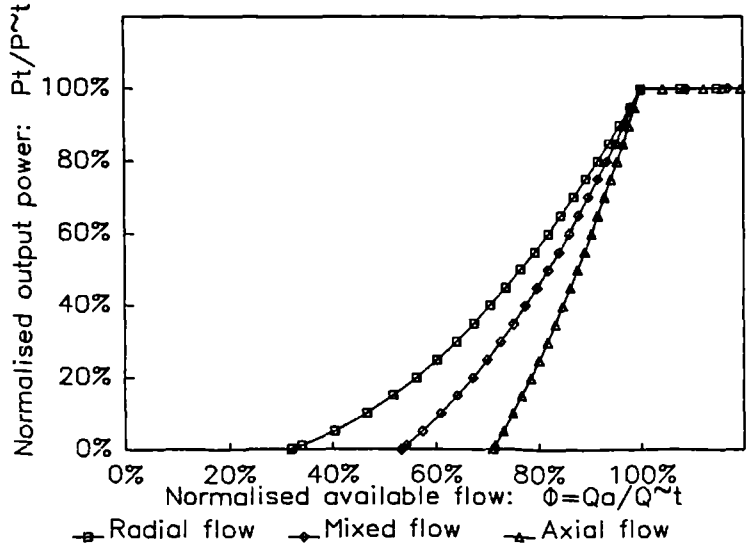

Fig. 8. Flow-power curves for PATs of different specific speeds.

Constant speed and constant available head.

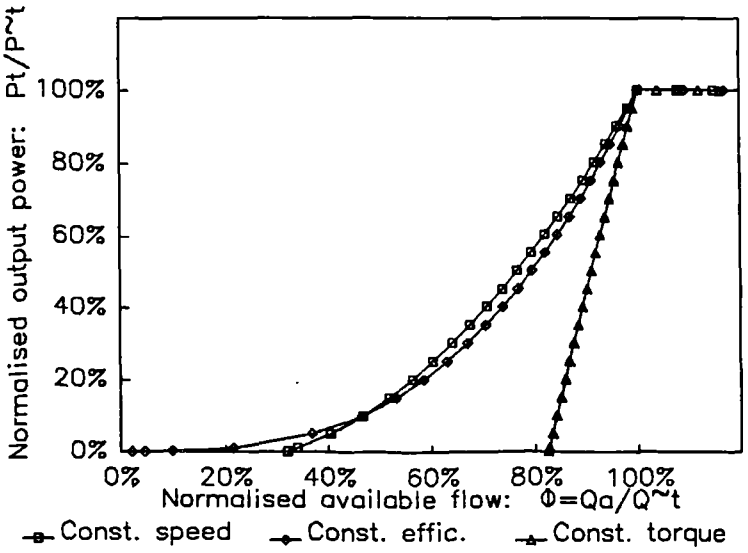

Fig. 9. Flow-power curves for different patterns of operation of a radial-flow PAT.
Constant available head.

Unlike a PAT, a conventional adjustable turbine has hydraulic controls that enable it to have a large (usually infinite) number of head-flow curves, one for each setting of its guide-vanes, runner-blades or spear-valves. The intersection of each of these curves with the penstock curve define the operating locus of the turbine. A well-designed turbine can maintain a high efficiency along a broad range of flows (see Fig. 10).

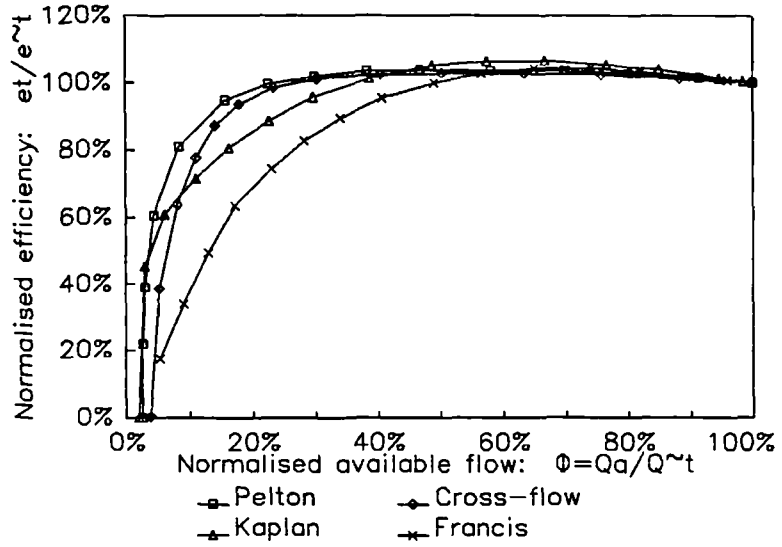

Fig. 10. Typical fixed-head, constant-speed efficiency curves of conventional turbines.
From Engeda & R.[88a]. Note that the rated flow $\tilde{Q}_T$ is usually larger than the best-efficiency flow $\hat{Q}_T$; turbines are designed like this in order to achieve a higher average efficiency.

The efficiency of the machine on its own (Figs. 5 and 10) is a misleading parameter for the comparison of the performance of PATs and conventional turbines. The latter can use all the available head, whereas the former need to waste it when the flow is reduced. A better performance parameter is the actual power generated, taking into account all the head losses, as in Fig. 11. (The ideal parameter would be the **task** performed, because the efficiency of the energy-using devices is often a function of the power, but it is not considered here.)

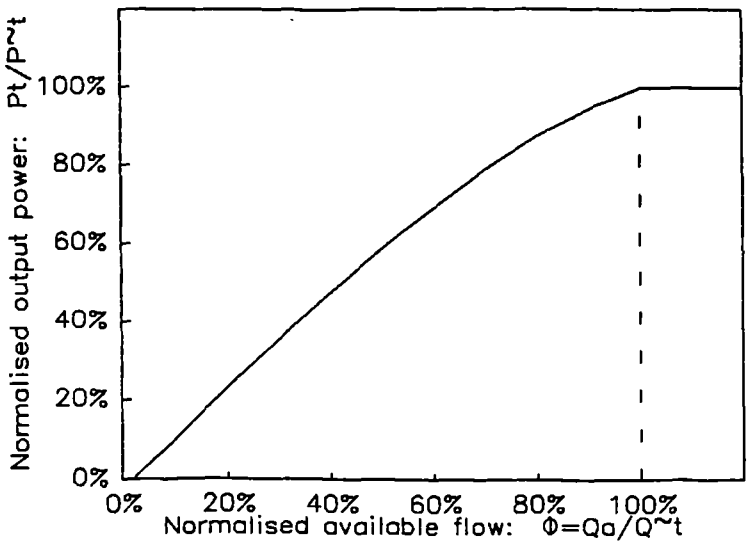

Fig. 11. Flow-power curve for a typical regulated Pelton turbine, under constant available head.

Assuming penstock head loss at full flow = 15%. To the right of the rated (*i.e.* maximum) flow, turbine flow is less than available flow (some flow is wasted).

If we want to compare the efficiency of PATs and conventional turbines, we need to take into account the 'penstock efficiency', *i.e.* the ratio between the turbine head and the available head. Fig. 12 shows the product of turbine efficiency (η_T) and this 'penstock efficiency' (η_D) [5]. The part-load $\eta_D \times \eta_T$ curve of the PAT is much lower than the η_T shown in Fig. 5, on account of the reduction in turbine head. On the contrary, the Pelton $\eta_D \times \eta_T$ curve is in fact a bit higher than η_T in Fig. 10, because the turbine head is actually increased when the flow is reduced (for the reduction in penstock's head-loss).

Fig. 12 displays the main disadvantage of unregulated turbines, namely their poor performance with reduced flow. However, two approaches make possible the operation of schemes with PATs under variable flow conditions, namely the parallel

5 See footnote 2, p. 18.

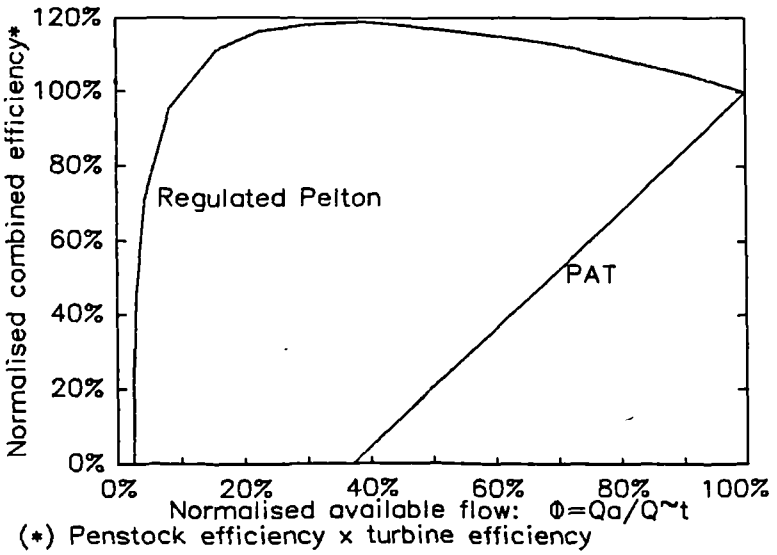

Fig. 12. Combined efficiency ($\eta_D \times \eta_T$) for a radial-flow PAT and a Pelton turbine.

operation (P. O.) of several machines and the intermittent operation (I. O.) of a single machine. They are discussed below.

3.3 Parallel Operation

If two or more PATs are operated in parallel, they can be switched on and off according to the available flow. Parallel operation (P. O.) has proven to be more cost-effective than a single conventional hydraulic turbine of comparable capacity (Spangler[88]): the limit for this advantage is 5 PATs in parallel, according to Fraser & A.[81], or 7, according to Nicholas[88]. Hochreutiner[91] mentions also a Swiss station with 7 PATs in parallel, although it seems that this is simply due to the lack in the market of a pump large enough to meet the requirements of the scheme. Finally, PATs can be installed in parallel with conventional turbines, the fine-tuning being given by the latter (Schnitzer[85]).

The machines can be different or identical to each other (for example, in a two-PAT scheme, the turbines can handle either $^1/_3$ and $^2/_3$ of the full flow, or one half each). The first option increases the energy generation, as it enables more combinations (in this case $^1/_3$, $^2/_3$ and $^3/_3$); the latter restricts the combinations ($^1/_2$ and $^2/_2$), but makes maintenance easier, as the same set of spares can be used in all machines.

Fig. 13 shows the staircase flow-power curve for a P. O. system. Only at the outside corners of the staircase (marked ■ on Fig. 13) is the turbine flow equal to the available flow. At all other points some of the available flow has to be wasted. Just like conventional turbines, P. O. takes advantage of the increase in head (due to fall in

penstock friction loss) when the flow is reduced, as long as the penstock is common. This increase explains, by the way, the uneven size of the steps of Fig. 13.

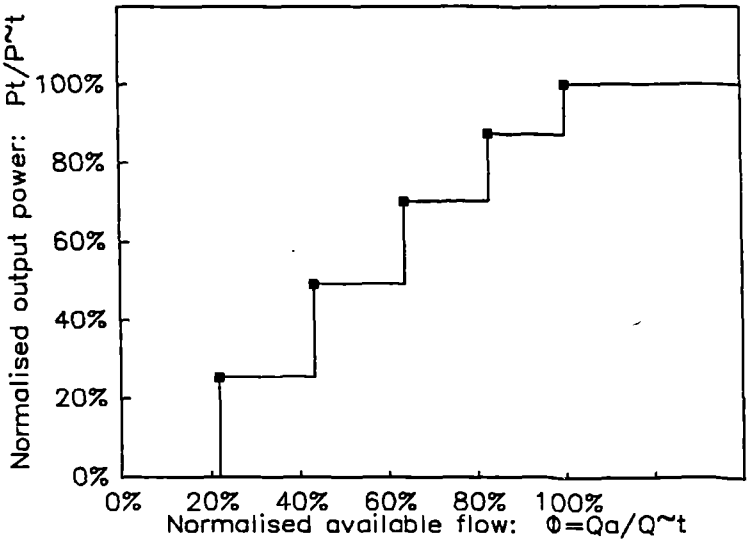

Fig. 13. Flow-power curve for a system with 5 identical PATs operating in parallel, without part-load operation.
Radial flow; constant speed; penstock head-loss at rated flow = 15%.

The performance of P. O. can be slightly improved by enabling the part-load operation of PATs. In Fig. 14, n machines continue to operate with partial head as the flow is reduced (see footnote 3, p. 24), until they generate the same power that $n-1$ machines would generate with full-head. In this moment one is switched off.

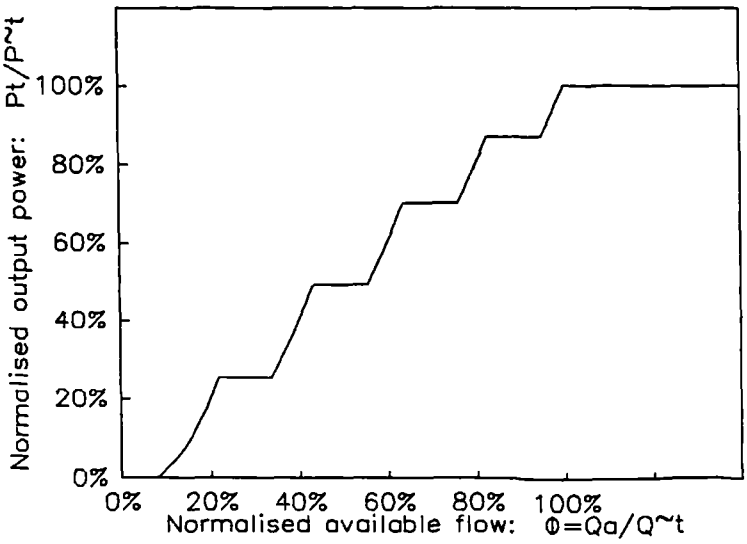

Fig. 14. Flow-power curve for 5 identical PATs with part-load common operation.

A third variant is to throttle just one of them with a valve[6], in order to enable the rest to operate at full head. In this case the power generated is slightly larger (Fig. 15).

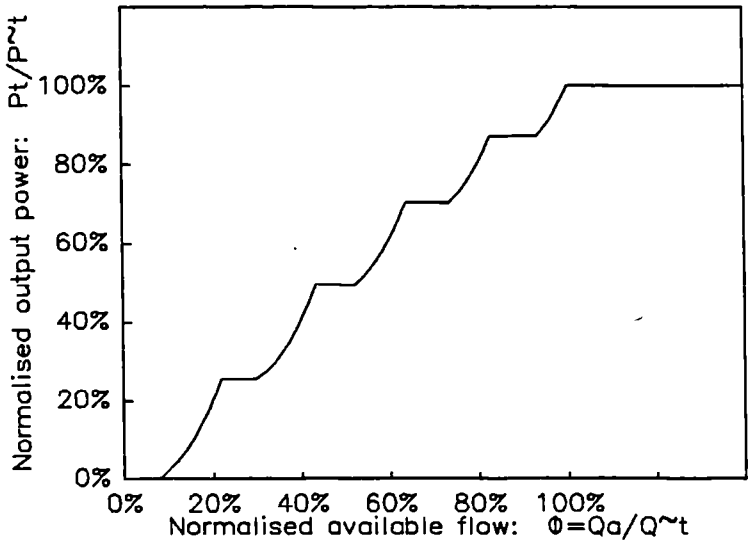

Fig. 15. Flow power curve for 5 identical PATs with part-load operation of only one machine by throttling it.

3.4 Intermittent Operation

3.4.1 Advantages and Disadvantages

Another technique to accommodate flow variations with a fixed geometry turbine is to store water in a reservoir and to release it intermittently, with a pattern either fixed or variable. The former option means usually a daily cycle (*e.g.* to provide continuous energy for lighting during the evening), requiring a relatively large storage, whereas the cycle times of the latter can be much shorter, requiring a smaller reservoir.

It is the variable pattern (mentioned by Schnitzer[92]) that will be analysed here. It means that the reservoir is emptied always as soon as it is full, irrespective of the time of the day, by means of an automatic device such as a siphon.

The reservoir can be located behind a weir or dam, especially when one is already available, but in most cases a forebay outside the river bed will be a better option, to reduce the construction costs[7]. It can act as a silting tank as well.

As compared with parallel operation (P. O.), intermittent operation (I. O.) is more efficient and simpler to operate, because it uses all the available water and its

6 See footnote 3, p. 24..

7 "A dam is a dangerous source of stored energy right where it is not wanted" (Giddens[91]).

operation is automatic. Furthermore, it uses a larger machine, that will usually be more efficient and cheaper than several small machines. Finally, unlike P. O. or a conventional turbine, the I. O. can be simply added to a existing unregulated scheme, in case the dry-season flow turns out to be insufficient.

The main disadvantage of I. O. is that its generation pattern is unsuitable for many end-uses. It can be easily used in grid-linked electricity generation, where it would provide the same kind of erratic power pattern as a wind generator. However, in the context of developing countries, where most micro-hydro schemes are isolated, it can be used only with end-uses such as water-lifting, ice-making, heating and battery-charging, *i.e.* end-uses where an intermediate short-term storage exists between the station and the user - at no extra cost[8]. Lighting is the best example of an end-use that would require an expensive intermediate energy storage (in batteries).

Another disadvantage of I. O. is the thick penstock required to withstand the water-hammer that takes place when the siphon is primed and a column of water rapidly descends the penstock until it is suddenly obstructed by the turbine. This disadvantage can be mitigated by using a valve instead of a siphon.

Moreover, unlike P. O. or a conventional turbine, I. O. does not take advantage of the reduction in penstock head-loss that occurs when the flow is reduced.

Finally, I. O. does not have the following two advantages of P. O.: firstly, the possibility of part-load operation during maintenance, and secondly the possibility of installing some of the PATs at a later stage, to reduce the initial cost.

The options for turning on and off the flow in a I. O. system are a valve and a siphon. The former makes the system more efficient, since the penstock is not emptied in each cycle, but it increases the cost and complexity of the system.

The siphon itself can be either double or simple. Double siphons are more complex and expensive, but more efficient as well, as their priming wastes much less water than simple siphons (see Fig. 16 and Appendix A). Moreover, a double siphon can operate with a very small available flow, whereas the efficiency of a simple siphon drops suddenly to zero when it cannot be primed any more, and acts continuously as a weir instead.

---

8 Kumar & T.[84] mention some end-uses adequate for the dummy loads of an electronic load controller (especially a fermentation unit), that would also be adequate for I. O.

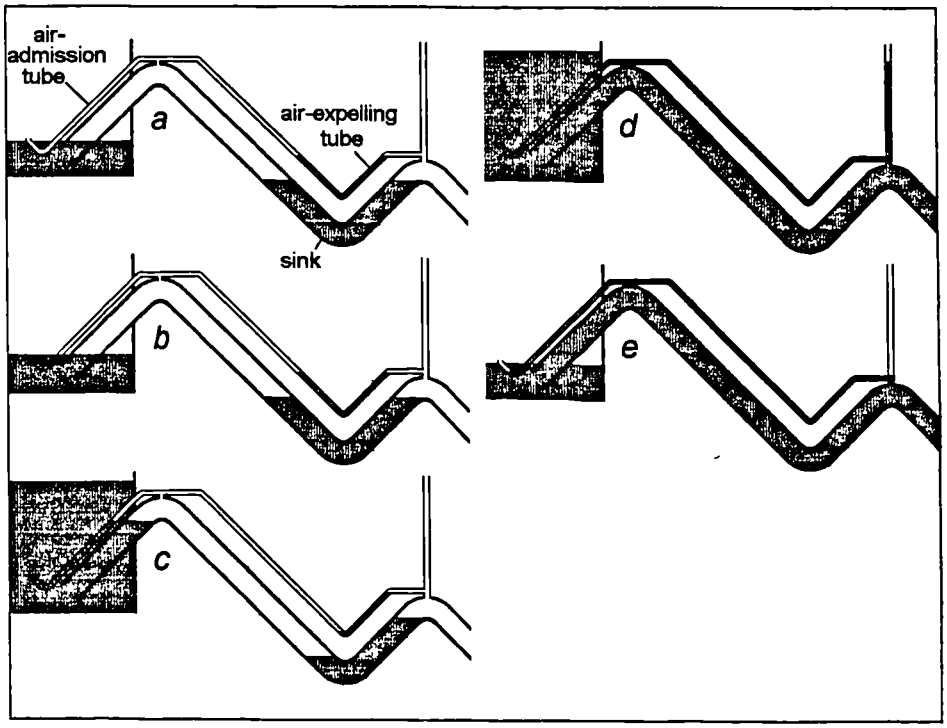

Fig. 16. Principle of operation of double-siphons.

a. The beginning of the cycle: the siphon has just lost its prime and the reservoir starts to fill.

b. A small amount of water enters the air-admission tube when its open end is submerged. From this moment, the air trapped inside the first peak will be compressed.

c. The double siphon just before priming: its first peak is full of compressed air, that is about to be suddenly expelled through the air-expelling tube.

d. The double siphon, just after being primed, begins its running stage.

e. The double siphon just before losing its prime by air coming in through the air-admission tube.

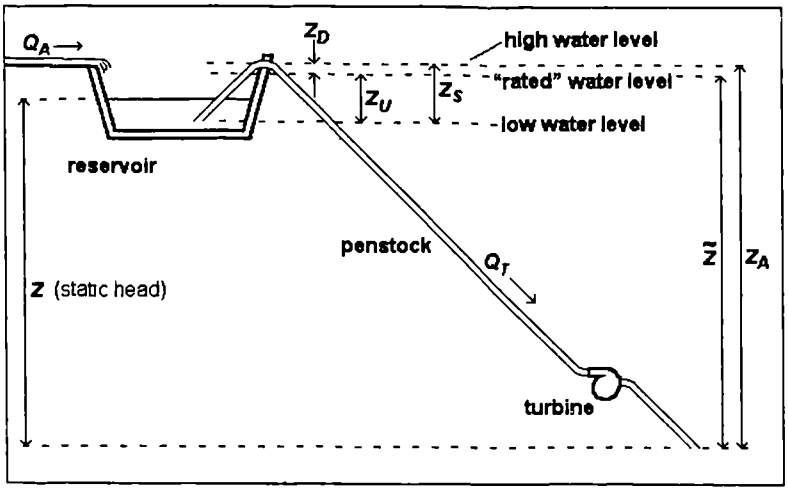

Fig. 17. Schematic layout of an I. O. system.

3.4.2 Performance

The cyclic performance of I. O. is described in Figs. 17 and 18. The turbine flow is a maximum ($\tilde{Q}_T$) when the turbine starts ($z = \tilde{z}$), falling slightly as the head falls, dropping to zero when the head has fallen to $z = \tilde{z} - z_U$ and remaining zero until the reservoir has refilled.

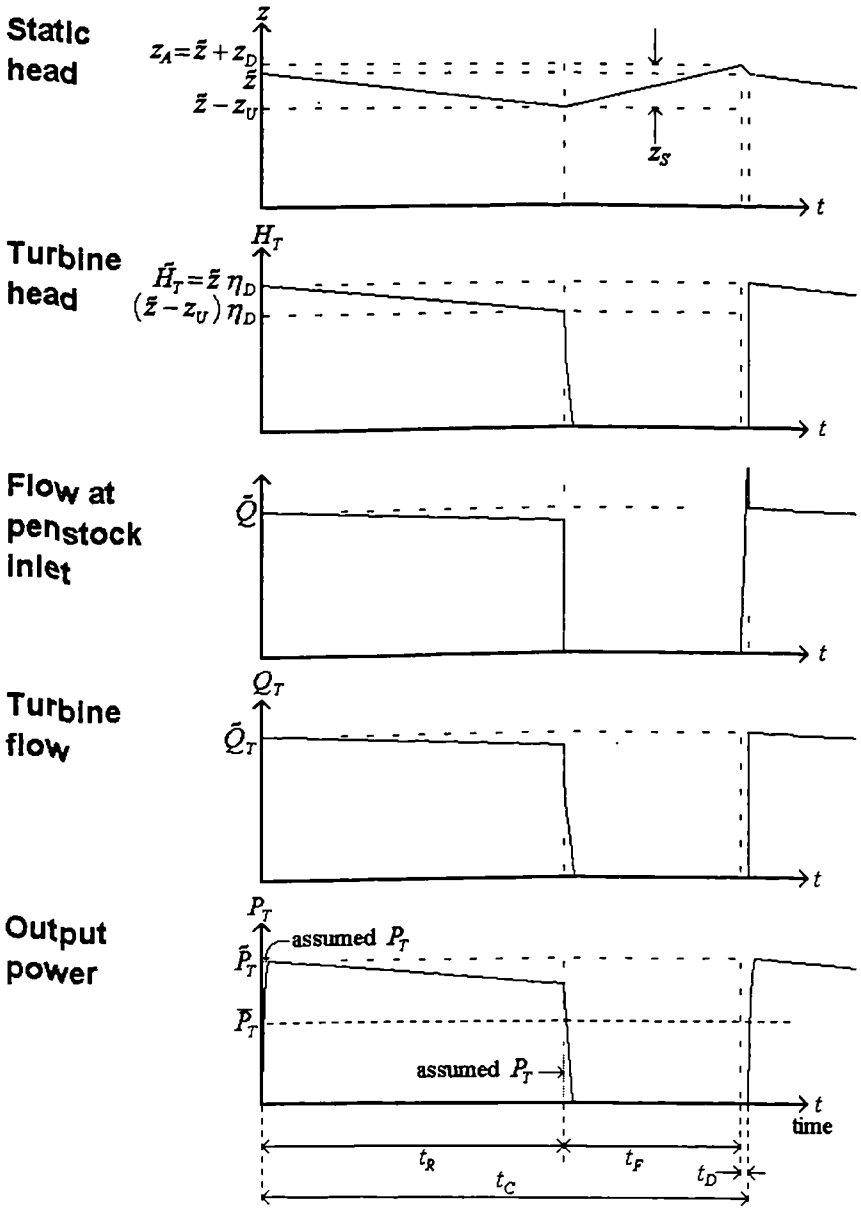

Fig. 18. Intermittent operation performance.
Not to scale.

At the beginning of the running stage, the turbine is accelerated and reaches its full speed and power after a start-up time that depends on the inertia of the system. During the start-up, the efficiencies of both the turbine and the driven machinery are reduced. However, as the inertia of micro-hydro systems is usually insignificant, we can

neglect this mechanical loss. The inertia energy itself can not be considered a start-up loss, because it is recovered in the shut-down.

At the end of the running stage, the penstock is emptied, the head is reduced and the turbine slows down; we then have a head loss and also a mechanical loss, as the efficiencies of the turbine and the driven machinery are diminished. This again depends on the inertia and the characteristics of the system, but we assume that the turbine stops running as soon as the siphon loses its prime (and then we assume that all the water in the penstock is wasted)[9].

At the end of the filling stage, a volume of water required to prime the siphon and fill the penstock is taken from the reservoir before the running stage begins. Even though a single siphon can be primed with a head as little as $^1/_6$ of the diameter (Thomas & A.[89]), this waste can be significant. On the contrary, if a double siphon is used (see p. 31), almost no water is required for the priming, and the only requirement is filling the penstock. (This water is actually used by the turbine, but we can consider it as a stock that will be eventually lost at the end of the cycle; see previous paragraph). The extraction of this volume of water reduces the level of the water in the reservoir by a small depth z_D.

Assuming that the load is constantly adjusted to accept all the varying power produced by the turbine, the average power over a complete cycle (of duration t_C) is...:

$$\overline{P}_T = \frac{E_C}{t_C} \qquad [11]$$

..., where the energy produced per cycle (E_C) is the integral of the power produced during the 'running' part of the cycle:

$$E_C = \int_0^{t_R} P_T\,dt = \rho g \int_0^{t_R} z\,Q_T\,\eta_T\,\eta_D\,dt \qquad [12]$$

During a time step *dt* in the running stage, the change in the volume of the storage reservoir is equal to the volume provided by the river minus the volume taken by the turbine (as the former is smaller than the latter, this number is negative):

$$A_S\,dz = Q_A\,dt - Q_T\,dt$$

9 Refsum & T.[88] made something similar, although with a different purpose (namely cheap turbine tests with an elevated tank instead of a large and expensive feed pump). According to them, "the energy in the water taken to fill the down pipe is most likely to be lost in turbulence". "It was noticed that the filling of the pipe was associated with a fair amount of swirling and, although the pipe filled rapidly, it did so with much less violence than anticipated". Unfortunately, the few results published by them do not permit drawing conclusions applicable to I. O.

$$dt = \frac{A_S}{Q_A - Q_T} dz \qquad [13]$$

Substituting Eq. [13] in Eq. [12], we replace the variable of integration from time to head:

$$E_C = \rho g \int_{\tilde{z}}^{\tilde{z}-z_U} z Q_T \eta_T \eta_D \frac{A_S}{Q_A - Q_T} dz$$

To proceed with the analysis we will make four further assumptions, namely:

① Both penstock efficiency (η_D) and turbine efficiency (η_T) are constant as Q_T and z vary.

② The flow drawn by the turbine varies linearly with the available head.

③ The storage reservoir has a constant surface area A_S.

④ The variations of the available river flow during one cycle are negligible.

Over the small range of variation of the available head met with in a practical scheme (a reservoir with $z_S > 0.1\tilde{z}$ would usually be, not only uneconomic, but also inefficient), the first two assumptions are readily justified. The third is less tenable, as A_S will sometimes vary by a factor of 2 or more during drawn down, especially if the storage is located behind a dam. However, by choosing for A_S a value equal to the reservoir volume variation divided by its height variation, the error due to this third approximation will be small.

From assumptions ① and ③:

$$E_C = \rho g \eta_T \eta_D A_S \int_{\tilde{z}}^{\tilde{z}-z_U} \frac{z Q_T}{Q_A - Q_T} dz \qquad [14]$$

Assumption ② is illustrated in Fig. 19. ε is the dimensionless derivative (*i.e.* 'elasticity') of Q_T with respect to z. It is typically between 0.35 and 0.8, for constant-speed operation (0.05 and 0.9 for constant-torque operation):

$$\frac{(\tilde{Q}_T - Q_T)}{(\tilde{z} - z)} \frac{\tilde{z}}{\tilde{Q}_T} = \text{constant} = \varepsilon$$

$$Q_T = \tilde{Q}_T - \varepsilon \tilde{Q}_T \frac{(\tilde{z} - z)}{\tilde{z}} = \tilde{Q}_T \left(1 - \varepsilon + \frac{\varepsilon z}{\tilde{z}}\right) \qquad [15]$$

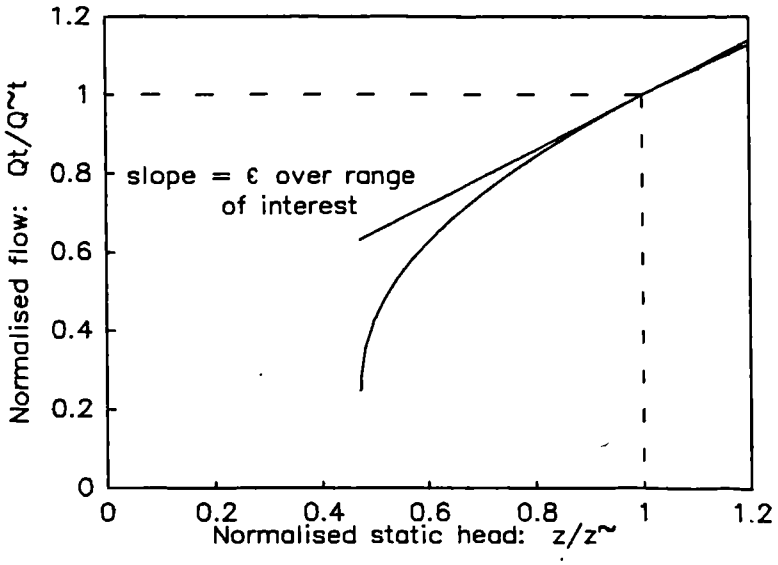

Fig. 19. Actual and assumed relationship between turbine flow and static head.

Substituting in Eq. [14] and using the normalised available flow $\Phi = Q_A/\tilde{Q}_T$:

$$E_C = \rho g\, \eta_T \eta_D A_S \int_{\tilde{z}}^{\tilde{z}-z_U} \frac{z\left(1-\varepsilon+\dfrac{\varepsilon z}{\tilde{z}}\right)}{\Phi-1+\varepsilon-\dfrac{\varepsilon z}{\tilde{z}}}dz$$

$$E_C = \rho g\, \eta_T \eta_D A_S \tilde{z}^2 \left[\left(\frac{\Phi}{\varepsilon}+1\right)\frac{z_U}{\tilde{z}} - \frac{z_U^2}{2\tilde{z}^2} - \left(\frac{\Phi^2}{\varepsilon^2}-\frac{\Phi}{\varepsilon^2}+\frac{\Phi}{\varepsilon}\right)\ln\left|1-\frac{\varepsilon z_U}{(1-\Phi)\tilde{z}}\right|\right]$$

The length of the cycle still remains to be evaluated. From Eqs. [13] and [15], the running time is:

$$t_R = \int_{\tilde{z}}^{\tilde{z}-z_U} \frac{A_S}{\tilde{Q}_T\left(\Phi-1+\varepsilon-\dfrac{\varepsilon z}{\tilde{z}}\right)}dz = \frac{-A_S\tilde{z}}{\varepsilon\tilde{Q}_T}\ln\left|1-\frac{\varepsilon z_U}{(1-\Phi)\tilde{z}}\right| \qquad [16]$$

During the filling stage, the reservoir must be able to store the available river flow:

$$V_S = t_F\, Q_A$$

$$t_F = \frac{V_S}{Q_A} = \frac{A_S z_S}{\Phi \tilde{Q}_T} \qquad [17]$$

(Note that we are using here z_S instead of z_U; see Fig. 17)

Neglecting the time required to prime the siphon (a double one is primed almost instantly) and fill the penstock (*i.e.*: $t_D \approx 0$), the cycle time is simply the addition of the running and the filling times:

$$t_C = t_F + t_R = \frac{A_S \tilde{z}}{\Phi \tilde{Q}_T}\left(\frac{z_S}{\tilde{z}} - \frac{\Phi}{\varepsilon}\ln\left|1 - \frac{\varepsilon z_U}{(1-\Phi)\tilde{z}}\right|\right)$$

Substituting in Eq. [11], the average power is:

$$\overline{P}_T = \rho g \Phi \tilde{Q}_T \tilde{z} \eta_T \eta_D \frac{\left(\frac{\Phi}{\varepsilon}+1\right)\frac{z_U}{\tilde{z}} - \frac{z_U^2}{2\tilde{z}^2} - \left(\frac{\Phi^2}{\varepsilon^2} - \frac{\Phi}{\varepsilon^2} + \frac{\Phi}{\varepsilon}\right)\ln\left|1 - \frac{\varepsilon z_U}{(1-\Phi)\tilde{z}}\right|}{\frac{z_S}{\tilde{z}} - \frac{\Phi}{\varepsilon}\ln\left|1 - \frac{\varepsilon z_U}{(1-\Phi)\tilde{z}}\right|}$$

Or, using the dimensionless coefficients $\theta_S = z_S/\tilde{z}$ and $\theta_U = z_U/\tilde{z}$, as well as the rated power $\tilde{P}_T$:

$$\overline{P}_T = \Phi \tilde{P}_T \frac{\left(\frac{\Phi}{\varepsilon}+1\right)\theta_U - \frac{\theta_U^2}{2} - \left(\frac{\Phi^2}{\varepsilon^2} - \frac{\Phi}{\varepsilon^2} + \frac{\Phi}{\varepsilon}\right)\ln\left|1 - \frac{\varepsilon \theta_U}{1-\Phi}\right|}{\theta_S - \frac{\Phi}{\varepsilon}\ln\left|1 - \frac{\varepsilon \theta_U}{1-\Phi}\right|} \qquad [18]$$

This equation is not valid when the available flow is only slightly smaller than the rated flow, on account of an inherent instability of the intermittent operation of PATs: when the water level of the reservoir drops, the flow through the turbine is slightly reduced; and, if it happens to then match the available flow, the system sticks there, operating continuously.

Substituting in Eq. [15], for $Q_T = Q_A$:

$$Q_A = \Phi \tilde{Q}_T = \tilde{Q}_T\left(1 - \varepsilon + \frac{\varepsilon z}{\tilde{z}}\right) \qquad [19]$$

Therefore the head in this small range is:

$$z = \tilde{z}\left(1 - \frac{1-\Phi}{\varepsilon}\right)$$

And the power is then:

$$P_T = \rho g \Phi \tilde{Q}_T \tilde{z} \eta_T \eta_D \left(1 - \frac{1-\Phi}{\varepsilon}\right) = \Phi \tilde{P}_T \left(1 - \frac{1-\Phi}{\varepsilon}\right) \qquad [20]$$

When the available flow matches the turbine flow with the reservoir empty, *i.e.* just before the siphon loses its prime, we have the critical condition that defines the border between Eqs. [18] and [20], *i.e.* between the intermittent and the continuous operation. Substituting in Eq. [19], for $z = \tilde{z} - z_U$:

$$Q_{A,crit} = \Phi_{crit}\tilde{Q}_T = \tilde{Q}_T\left(1 - \varepsilon + \varepsilon\frac{\tilde{z} - z_U}{\tilde{z}}\right)$$

The critical normalised available flow is then:

$$\Phi_{crit} = 1 - \varepsilon\theta_U$$

Eqs. [18] and [20] constitute the mathematical model of the intermittent operation. The flow-power curve shown in Fig. 20 was constructed by dividing the power by the rated power $\tilde{P}_T$.

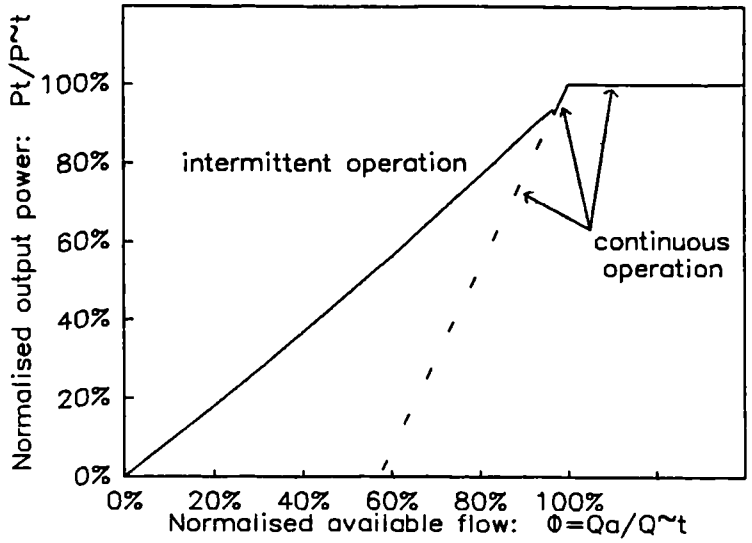

Fig. 20. Flow-power curve for an intermittent operation system.
$\varepsilon = 0.7$; $\theta_U = 0.045$; $\theta_S = 0.05$

This curve shows the unstable performance of I. O. around the critical flow. Between this flow and the rated flow, the (continuous) operation is quite inefficient, on account of the loss of head in the reservoir. Just to the left of the critical flow, the I. O. begins, but most of the time is spent with a low water level, and thus with high reservoir head losses.

3.4.3 Optimum Reservoir Depth

It is interesting to note that, for a given surface area of the reservoir, a given volume of the penstock and a given available flow, there is an optimum depth of the storage (Fig. 21): If it is too shallow, the cycles are too short and too much water is wasted in

each cycle to fill the penstock. On the other hand, the deeper the reservoir the larger the head loss in it (until the critical condition is eventually reached).

The optimum depth is obtained by differentiating the average power:

$$\frac{d\overline{P}_T}{dz_U} = 0 \qquad [21]$$

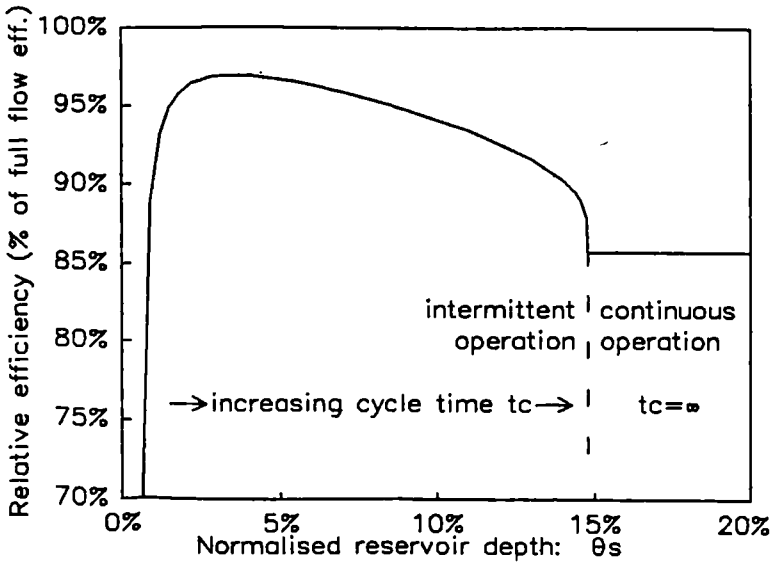

Fig. 21. I. O. efficiency in terms of θ_S.
$\varepsilon = 0.7$; $\Phi = 0.9$; $\theta_D = 0.005$

As Eq. [21] does not have an explicit solution, we can get an approximation by assuming a constant flow:

$$\lim_{\varepsilon \to 0} \overline{P}_T = \Phi \tilde{P}_T \frac{\theta_U - \frac{1}{2}\theta_U^2}{(1-\Phi)\theta_S + \Phi \theta_U}$$

By differentiating this equation we obtain the optimum depth. Using $\theta_D = \theta_S - \theta_U = z_D/\tilde{z}$, we get:

$$\theta_{U,opt} = \sqrt{(1-\Phi)^2 \theta_D^2 + 2(1-\Phi)\theta_D} - (1-\Phi)\theta_D \qquad [22]$$

As the optimum reservoir depth depends on the available flow, ideally, the depth should be continuously adjusted by varying the level at which the siphon loses its prime. Unfortunately, as any siphon requires a minimum depth, it is impossible to avoid the instability of I. O. for relatively large flows, that optimally require a very shallow reservoir (see Fig. 22). Taking into account the cost of building the reservoir, its optimum depth will usually be the minimum, dictated by the siphon, and an

adjustable depth will be a feasible approach only in sites were the reservoir already exists. (Ways to adjust the depth are discussed in Appendix A.)

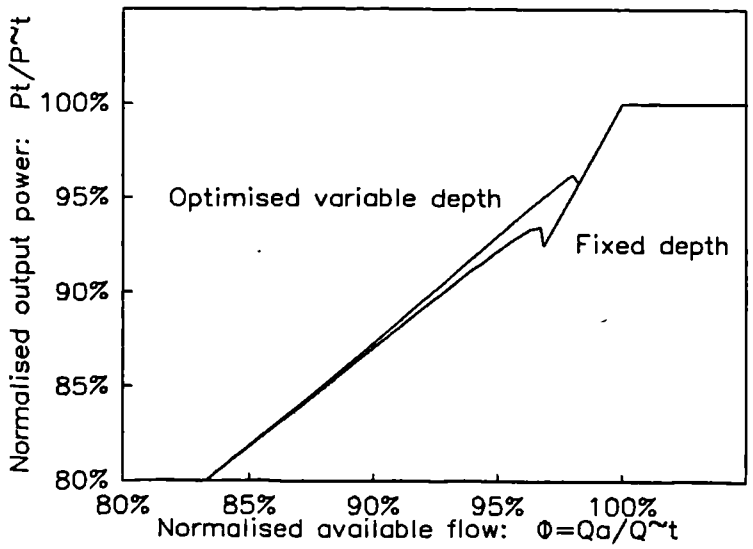

Fig. 22. Comparison of I. O. output power when keeping the reservoir depth fixed [$\theta_S = 0.05$], and when optimising it with a minimum depth [$\theta_S \geq 0.03$].
$\varepsilon = 0.7$; $\theta_D = 0.005$. For smaller flows, both lines are almost identical.

3.5 Economic Comparison of the Methods for Accommodating Reduced Flow

We have identified 5 methods for accommodating flow variations in a system with unregulated turbines, *i.e.* PATs. We will now employ the economic methodology developed in Chapter 2 to assess their relative merits.

As a reference system for this purpose (α in Eq. [10], p. 21b), let us choose an ideal turbine whose efficiency is constant from zero to full flow. (As Fig. 10, p. 26 shows, many conventional turbines are close to this ideal turbine.) Any PAT system is likely to have a lower efficiency at rated flow - and certain to have a lower efficiency at reduced flow. However, its cost is also less, and we are interested in exploring the trade-offs. A PAT operated 'simply' at reduced flow is very inefficient and may compare unfavourably with a very expensive conventional turbine. We are therefore more interested to see how schemes containing PATs operated at reduced flow in the intermittent operation (I. O.) and parallel operation (P. O.) modes compare economically with conventional schemes.

The parallel operation with part-load was calculated assuming that all the machines operate with partial head[10] (Fig. 14, p. 29). This flow-power curve, as well as the one without part-load (Fig. 13), were calculated using a mathematical model described later (Chapter 5, p. 90), for a radial-flow PAT operating at constant speed, assuming that the rated point is the best-efficiency point.

It is assumed that the cost of the turbomachinery includes the extra cost required to withstand or prevent water-hammer and high runaway speeds (this cost is usually higher for PATs than for fully equipped turbines, and higher for I. O. than for P. O.; see Chapter 4), as well as operation and maintenance costs (usually higher for conventional turbines than for PATs).

As the purpose is just to compare technical options, we do not care about the actual values of z_A (the available static head). Assuming that the rated efficiency of PATs $\tilde{\eta}_{T,PAT}$ is the same for P. O. and I. O., its actual value is not important; however, the ratio between it and the efficiency of the conventional turbine will be taken into account.

The comparison was firstly made for a reference hydrological and economic scenario, defined by the following 8 variables:

$\mu =$	−0.8	(a small basin, with very variable flow)
$\Gamma =$	1.0	(a large electricity grid: energy value does not vary with power level)
$\tilde{\eta}_{turbine} / \tilde{\eta}_{PAT} =$	1.05	(the ideal turbine is a bit more efficient than a PAT)
$\Theta =$	0.6	(sensitivity of cost to size)
$k_{T,turbine}/k_{T,PAT} =$	5	(an ideal turbine is 5 times as expensive as a single PAT for similar operating conditions)
$k_{T,PAT}/k_M =$	0.3	(relative cost of turbine to rest of system)
$k_D/k_M =$	0.3	(relative cost of 'unit' penstock to rest of system)
$k_S/k_M =$	0.001	(relative cost of 'unit' storage to rest of system)

The optimum benefit/cost ratio for each technical option in this scenario was calculated by means of a numerical method of optimisation that varies not only the rated flow, but also the rated efficiency of the penstock $\tilde{\eta}_D$ (*i.e.* the relative head-loss), the number of machines (for P. O.) and the area and depth of the reservoir (for I. O.). (The adjustable depth described in Appendix A is not considered here.) The method finds then the peak of the benefit/cost ratio hill (a multi-dimensional hill).

The optimum rated flow ($\tilde{Q}_T$) for an ideal turbine is larger than for PATs, as shown in Fig. 23, that includes the single-PAT option for the sake of completeness. The

10 The small advantage of throttling one PAT when operating several in parallel with part-load (see Fig. 15, p. 30) would be reasonable only if the required valves and control system increased the cost of the scheme by less than 1%, but this is unlikely.

optimum number of machines (n) for P. O. is 3 with part-load and 4 without. The optimum value of $\tilde{\eta}_D$ is always between 12 and 15%. Finally, the optimum size of the reservoir for I. O. is approximately $\theta_U = 0.02$ and $\theta_D = 0.002$ (note that V_S/V_D in Eq. [9] can be substituted by θ_S/θ_D).

A larger rated flow means larger value and cost (Fig. 24), but not necessarily a larger benefit/cost ratio (Fig. 25).

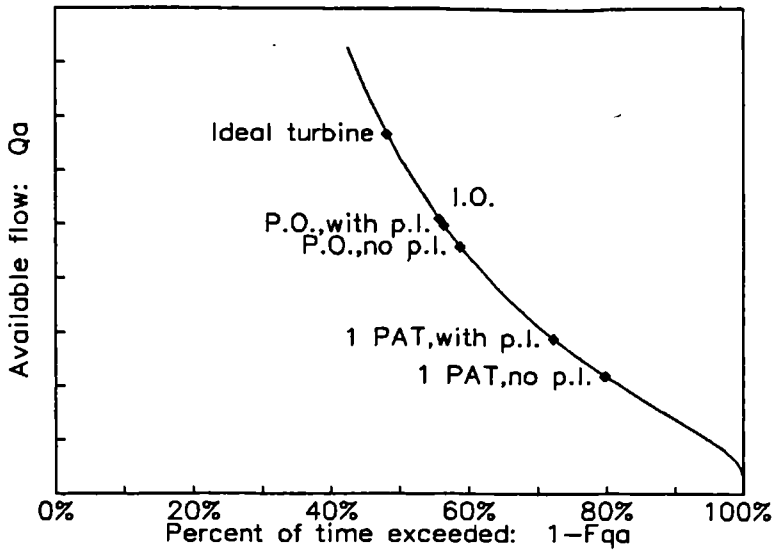

Fig. 23. Flow-duration curve for the reference scenario, showing the optimum rated flows for each technical option.
p.l. means part-load. This curve follows the standard notation of hydrology, instead of the probability theory, *i.e.* it is equal to Fig. 3 turned 90° anti-clockwise.

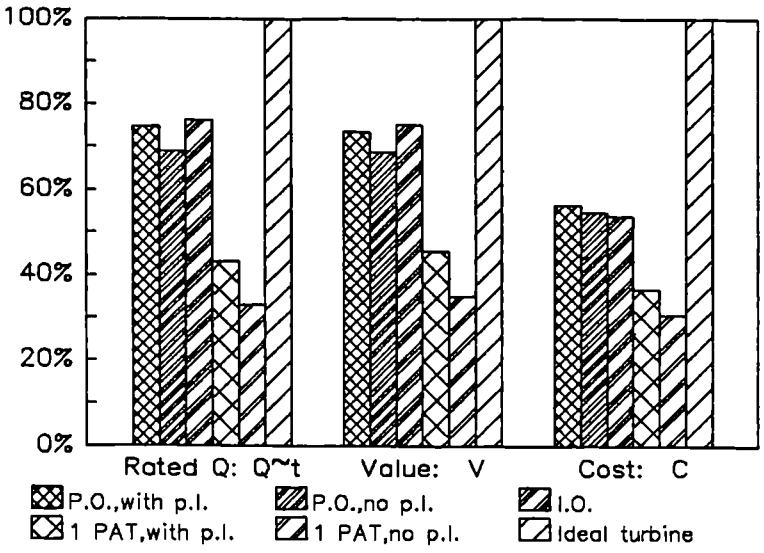

Fig. 24. Rated flow, value and cost for the different technical options, under the reference scenario.

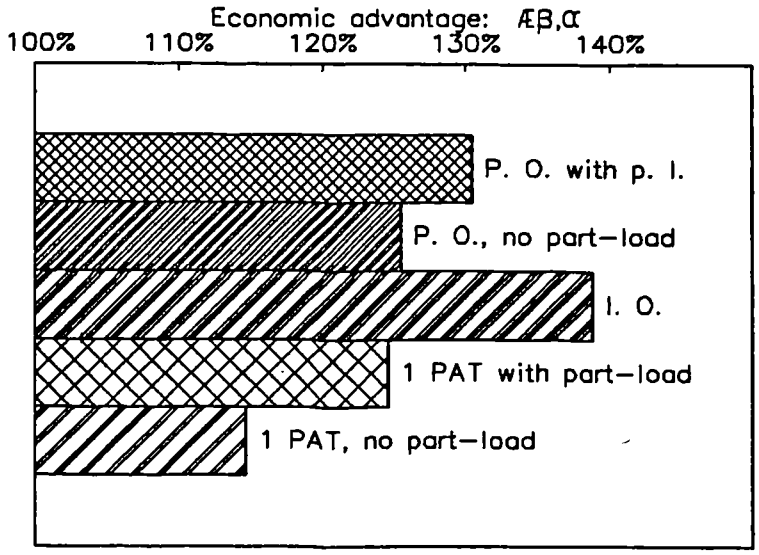

Fig. 25. Economic advantage $Æ_{\beta,\alpha}$ of the different technical options under the reference scenario.
The reference system α (100%) represents an ideal turbine.

Some of the contextual variables were subsequently modified, one in turn, and the same optimisation method described above was used for each point.

Firstly, as the hydrological basin is enlarged, its flow-duration curve is flattened and μ is reduced (*i.e.* its absolute value is increased). A flatter flow-duration curve is obviously advantageous for PATs (Fig. 26).

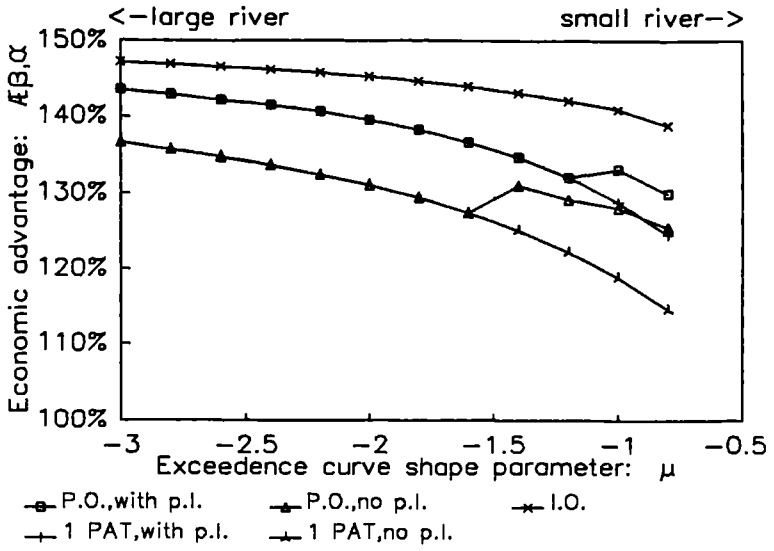

Fig. 26. Economic advantage of the different technical options when varying μ.
The reference system α (100%) represents an ideal turbine. Noteworthily, both P. O. curves join the single-PAT curves to the left of the graph, because the optimum *n* becomes 1 when the flow-duration curve is flattened.

As the energy system becomes smaller, Γ is reduced, and the energy value varies strongly with power (see p. 16). This reduction yields also a relative advantage for PATs (Fig. 27). As Γ is reduced, the optimum size of the scheme is also reduced, and

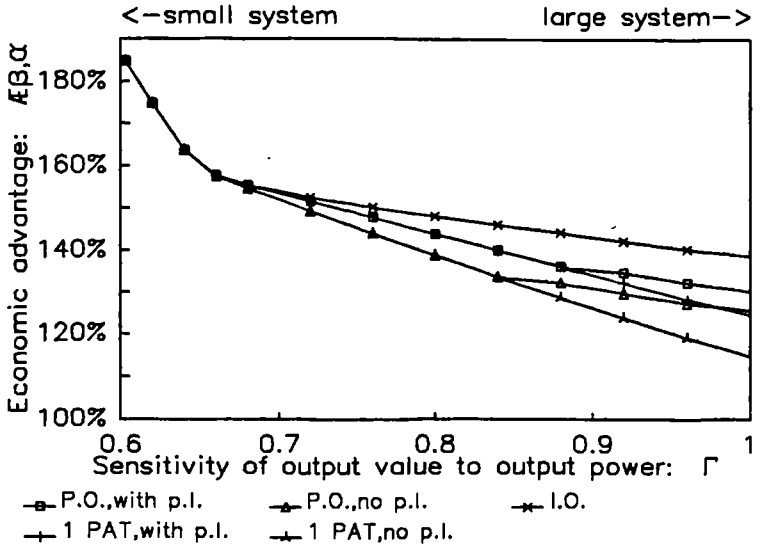

Fig. 27. Economic advantage of the different technical options when varying Γ.

The reference system α (100%) represents an ideal turbine.

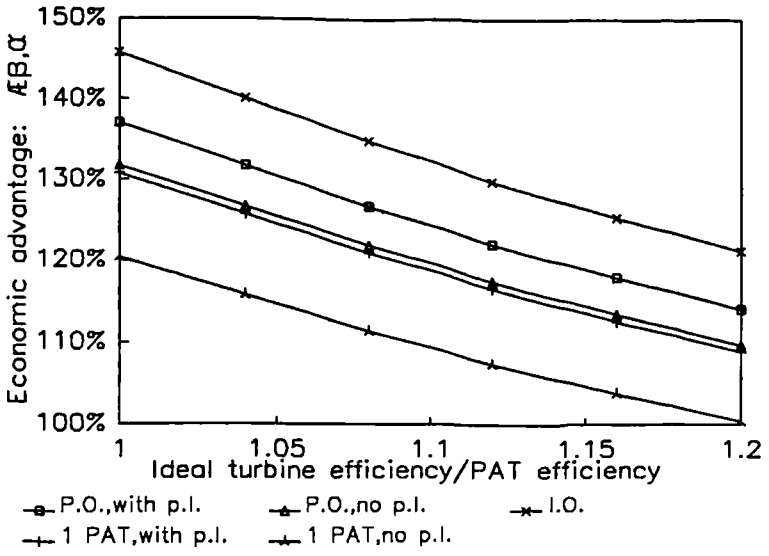

Fig. 28. Economic advantage of the different technical options when varying $\tilde{\eta}_{turbine} / \tilde{\eta}_{PAT}$.

The reference system α (100%) represents an ideal turbine.

becomes infinitely small when Γ approaches Θ [11].

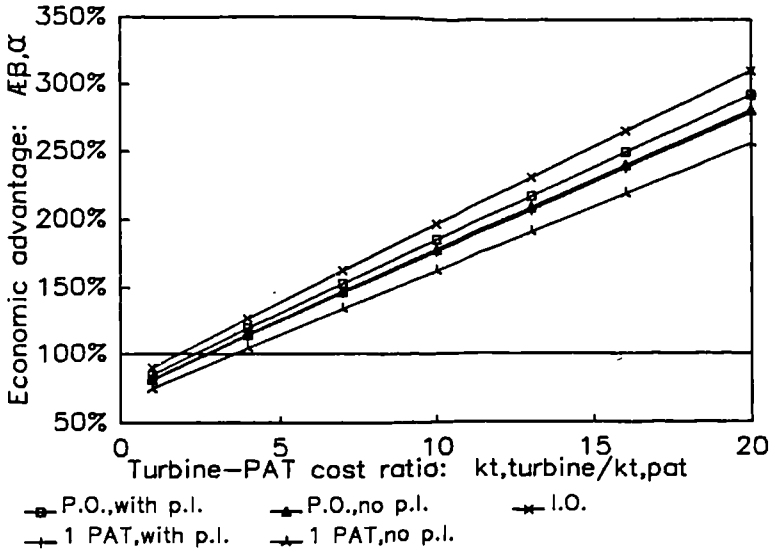

Fig. 29. Economic advantage of the different technical options when varying $k_{T,turbine}/k_{T,PAT}$.
The reference system α (100%) represents an ideal turbine.

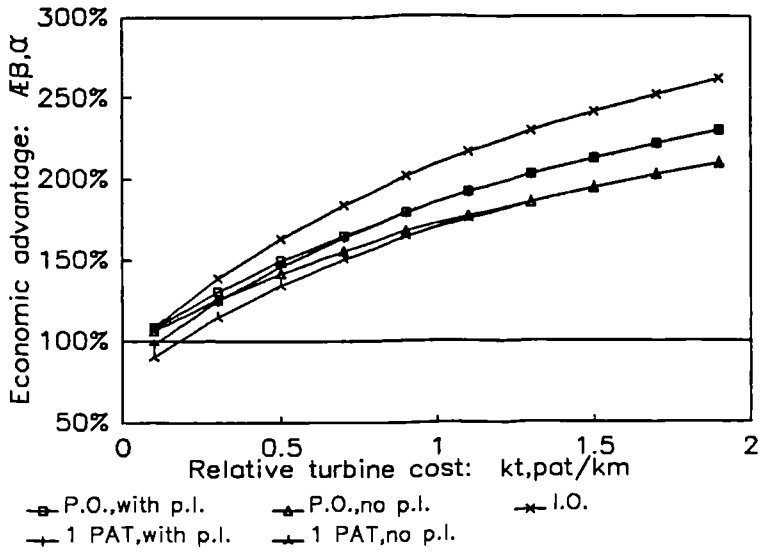

Fig. 30. Economic advantage of the different technical options when varying $k_{T,PAT}/k_M$.
The reference system α (100%) represents an ideal turbine.

11 In order to be able to use values of Γ close to or smaller than Θ, the model would need to be modified in one or more of the following ways:

- To change the cost equation to include a minimum fixed cost.
- To change the power-value equation to include a minimum power (nobody would build a 10 W scheme!).
- To use the net present value (option ①, see p. 20) instead of the benefit/cost ratio (②).

The advantage of the ideal turbine is obviously increased when its efficiency is increased (Fig. 28) or its price reduced (Fig. 29).

In small hydropower, the cost of the turbomachinery relative to the rest is much larger than for large hydropower. As this relative cost is increased, PATs become more desirable (Fig. 30).

Finally, the economic advantage of I. O. is increased when the reservoir is cheaper (Fig. 31).

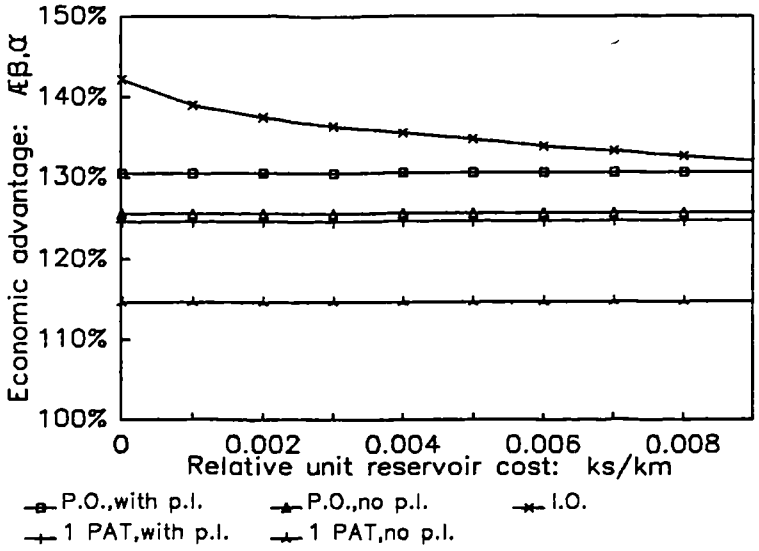

Fig. 31. Economic advantage of the different technical options when varying k_S/k_M.
The reference system α (100%) represents an ideal turbine.

Figs. 25 to 31 (where I. O. is represented by the symbol × and P. O. by the symbols ■ and ▲) indicate that the highest economic advantages come from using intermittent operation (I. O.).

We conclude that I. O. is generally preferable to P. O. (provided the load is compatible with such interrupted power supply). Factors favouring PAT use under varying flows are, in addition to high PAT efficiency and low relative cost:

- a flat flow-duration curve, and
- a small energy system, where the energy value varies strongly with power.

Note that, as mentioned in p. 20, the use of the benefit/cost ratio favours small projects (in this case PATs), in circumstances where the net present value would prefer a larger project. In many cases, the latter is a preferred parameter for project ranking.

4

ACCOMMODATING WATER-HAMMER

4.1 Transients in PAT Systems

In the event of sudden load changes[1], conventional Pelton and Francis turbines have devices to, respectively, deflect or by-pass the flow until the spear-valves or guide-vanes are slowly adjusted, thus avoiding harmful water-hammers as well as excessive speeds. (A flywheel may be required in addition to reduce the speed variations during this process.)

PATs, on the other hand, have no means to avoid flow and speed changes when the load varies suddenly. Even if it is possible to ensure that the normal operating load is kept constant (especially when generating electricity), an electrical or mechanical failure causing the total rejection of the load is usually impossible to prevent[2].

PATs and the rotating equipment driven by them can be designed to withstand the runaway speed, but this involves an additional cost[3], especially with mixed and axial-flow PATs, that can reach very high speeds (see Fig. 32).

On the other hand, the flow is increased or reduced (it is increased for axial-flow PATs and, against what might be expected, reduced for radial-flow machines[4]; see

---

1 A water-hammer may be caused also by the sudden blockage of ① the trash-rack, or even of ② the turbine-inlet (*e.g.* by a log or an otter), but we will assume that an air vent prevents damage caused by ①, and that an adequate trash-rack prevents the occurrence of ②.

2 According to Minott & D.[83], the use of electronic load controllers yields by itself a reduction in penstock costs: he is presumably considering that such devices can be fault-free.

3 This is not the case for the sturdy induction generators, according to Williams[92].

4 According to Terry & J.[42], this is due to the "bucking effect on the head" created by the centrifugal force with high speeds. (In a conventional turbine, with a shorter runner

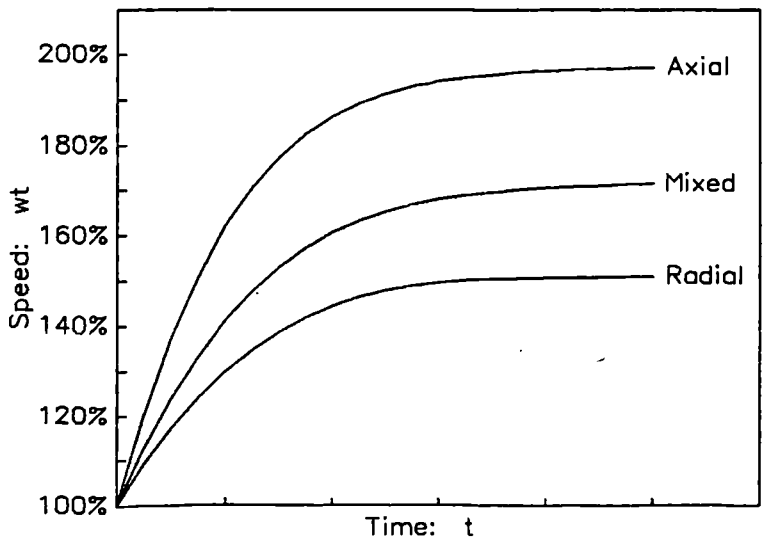

Fig. 32. The change in the speed of PATs in the event of sudden load rejection.

Rated penstock eff. = $\tilde{\eta}_D = 0.85$; simulation made neglecting hydraulic transients, *i.e.* assuming a zero-length penstock, and using the mathematical model of PAT performance described in Chapter 5. The actual runaway speed of radial-flow PATs is often smaller, namely about 130%. A similar graph was published by Strub[59].

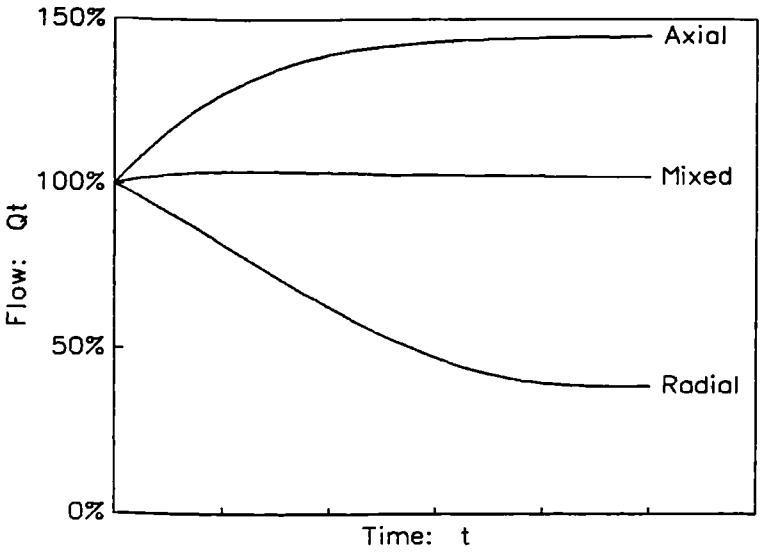

Fig. 33. The change in the flow of PATs in the event of sudden load rejection.

than a PAT, this effect is less important). A similar explanation is proposed by Chapallaz *et al.*[92].

Fig. 33). As the inertia of typical micro-hydro systems is very small, PATs can reach the runaway condition in a very short time in the event of sudden load-rejection, and this abrupt variation of the flow can cause significant pressure surges. A penstock designed to withstand them could have a prohibitive cost, especially taking into account that it is usually the most expensive element of micro-hydro schemes.

From these two reasons arises the need to provide an external means to reduce the speed and the pressure surges in the event of sudden load rejection.

The simplest techniques only damp the pressure surges produced by radial and axial-flow PATs, without reducing their runaway speed (Chapallaz *et al.*[92], Hochreutiner[91], Mikus[83], Schnitzer[92]). They can be used on their own - *e.g.* with radial-flow PATs which have low runaway speed, or in combination with other techniques - *e.g.* with mixed or axial-flow PATs, with runaway speeds too high to tolerate. These simplest techniques are:

- a compressed air tank connected to the penstock, just upstream of the turbine.
- a flywheel on the shaft.
- a valve that is rapidly actuated in order to keep the flow in the penstock constant. With a radial-flow PAT, a small valve in parallel is opened; with an axial-flow PAT, a valve in series is slightly closed. The valve can be a standard servo-valve, a weight-dropping valve or, for a radial-flow machine, a simple pressure-relief valve. (A complex water-actuated valve and membrane system is described by Peicheng *et al.*[89].)

The two techniques that reduce the turbine speed are a valve in series and a brake.

A servo-valve installed upstream or downstream of the turbine can stop the turbine in the event of sudden load rejection. However, as it cannot be closed suddenly without causing excessive pressure surges, either ① the flow must be simultaneously diverted, or ② the valve must be closed slowly. ① requires a changeover with two valves: one in series with the turbine, and one in parallel, to divert the flow. The latter, smaller than the former, causes a head loss similar to the head loss across the turbine. As there is no valve in the market with a linear flow-displacement relation (Giddens[91]), the valves must be actuated in a non-linear way - or very quickly. The changeover must be made before the turbine reaches a dangerous speed (Giddens[86a]). ② must be combined with one or more of the three simple techniques described above in order to damp the pressure surges caused by the abrupt increase or reduction of the flow and/or to prevent excessive speeds while the valve is closing (the second aim is achieved only by a flywheel) (Hochreutiner[91]). Water-actuated servo-valves (Schnitzer[92], Wilson & P.[92]; and also: Chapallaz *et al.*[92]) or pneumatic membrane pinch valves (Fraser & A.[81], Garay[80]) can reduce the costs by taking advantage of the energy of the available water pressure, or from a higher water source.

The second technique is a brake, usually spring-loaded and held open by an electromagnet, that releases it in the event of an electric failure. (The use of cheap car and lorry brakes should be investigated.) According to Etzold *et al.*[88], brakes are much cheaper than valves and flywheels for small schemes. The time delay must usually be smaller than half a second (Apfelbacher & E.[88], Giddens[83]). This technique is especially convenient for radial-flow PATs, whose stall flow is similar to the best-efficiency flow (Fig. 34). With mixed and axial flow PATs, the flow is reduced. The variation of the flow can be smoothed by applying a small torque on the brake, but the torque has to be higher than the stall torque. For this reason, brakes are probably unsuitable for axial-flow PATs, as suggested by Etzold *et al.*[88]. Finally, a brake can be used, not only in emergencies, but also as the **normal** means to stop the turbine (Giddens[91]).

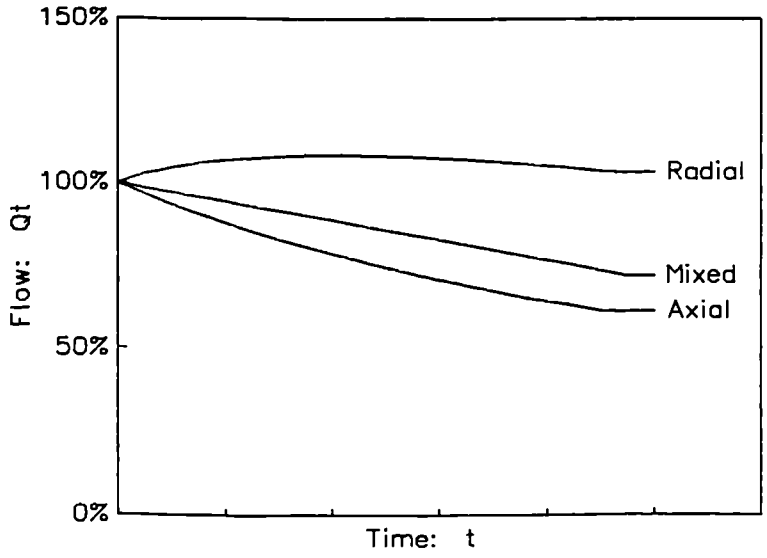

Fig. 34. The change in the flow of PATs when a brake is actuated in the event of sudden load rejection.

The brake torque is twice the normal running torque of the turbine. To be compared with Fig. 33. Axial-flow PATs usually have an unstable performance between the best-efficiency point and the stall point, not reflected in this graph; therefore the flow could change more abruptly with them.

4.2 The Cost of Accommodating Transients

Penstocks usually have a diameter larger than the most economical, in order to ensure low water velocities and thus low pressure surges. However, if they are adequately protected by one of the techniques described above, their diameter can be the most economical (and of course their thickness as well).

The larger the relative cost of the penstock, the larger the savings that can be obtained by protecting it. The savings are also larger in the context of an isolated energy system

(low Γ) than in a large electricity grid, because the economic conditions of the former lead to a smaller penstock, with higher flow velocities. Both conditions (relatively expensive penstock and isolated energy system) are typical of micro-hydro.

The procedure developed in Chapter 2 was used to evaluate the economic advantage of protecting the penstock, by comparing the optimum benefit/cost ratios obtained under the following two conditions:

- Condition α represents a penstock that has been 'oversized' to give low velocities. It is assumed that this condition is satisfied when the penstock head-loss is kept below an arbitrary technical threshold of 10% of the available static head ($\tilde{\eta}_D \geq 0.9$).
- Condition β represents a protected penstock. The technical restriction is eliminated, and the size of the penstock (and therefore $\tilde{\eta}_D$) is the one that optimises the benefit/cost ratio.

The scenario used here is similar to the one used above (p. 41), but with $\Gamma = 0.7$ and $k_D/k_M = 0.5$. Under this scenario, the optimum rated flow for all technical options and both conditions α and β is relatively small, *i.e.* it is available almost all the time, and the optimum number of machines (n) for parallel operation (P. O.) is only 1.

For a single PAT with part-load operation, the economic advantage $Æ_{\beta,\alpha}$ of condition β with respect to condition α is 103.8%. The optimum size of the scheme is in fact a bit larger for condition β than for α: its output value is increased by 7.1%, but the cost by only 3.2%. The penstock costs 46% of the total under condition α, and this percentage is reduced to 40% under condition β.

This economic advantage is similar for one PAT without part-load operation and for I.O., but it is much smaller for the ideal turbine: only 1.3%. This is because the economic conditions of an ideal turbine lead, under condition β, to a larger penstock, not very different from the 'oversized' penstock of condition α: the optimum relative penstock head-loss for the rated flow $(1 - \tilde{\eta}_D)$ is 19% for the single PAT, and only 15% for the ideal turbine.

The two contextual variables Γ and k_D/k_M were subsequently modified, one at a time, and the optimisation method was used for each point and for both conditions α and β.

Connection to a large energy system (large Γ) decreases the advantage of condition β for PATs, but, paradoxically, it has the opposite effect for the ideal turbine (Figs. 35 and 36).

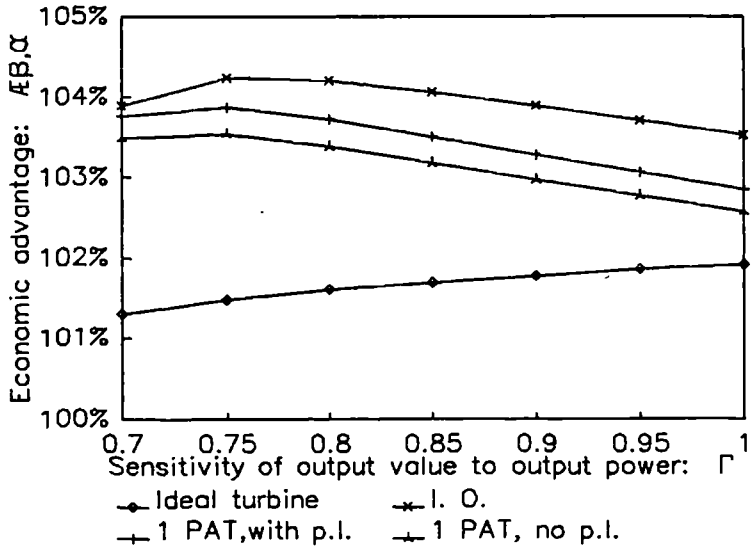

Fig. 35. Economic advantage when Γ is varied.
p.l. means part-load.

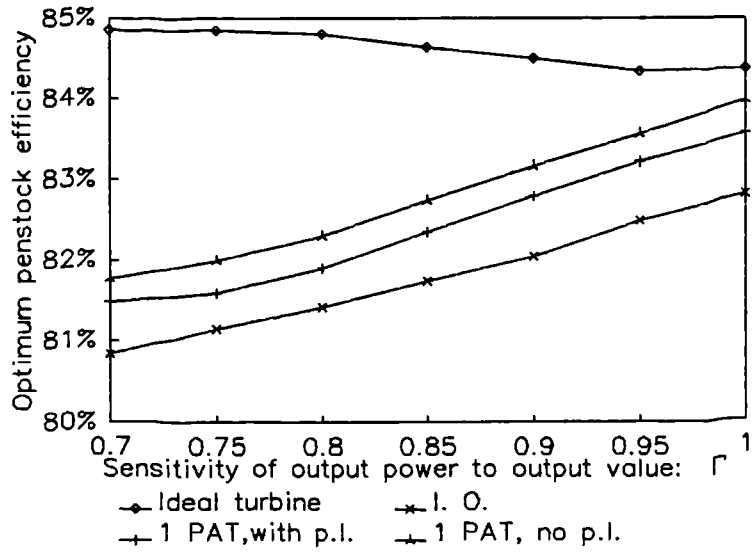

Fig. 36. Optimum value of the rated penstock efficiency $\tilde{\eta}_D$ for condition β, in terms of Γ.

Finally, a penstock that is expensive relative to the rest of the system makes condition β more advantageous, with any technical option (Figs. 37 and 38).

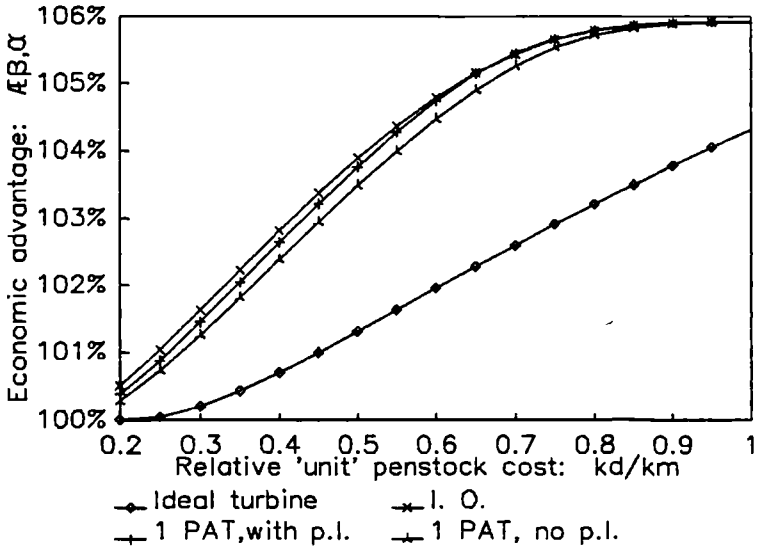

Fig. 37. Economic advantage when k_D/k_M is varied.

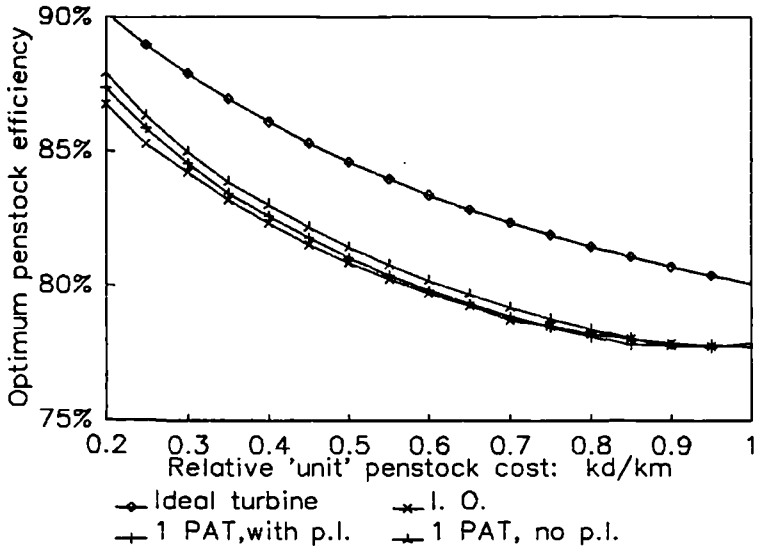

Fig. 38. Optimum value of $\tilde{\eta}_D$ for condition β, in terms of k_D/k_M.

4.3 Conclusion

On account of PAT's lack of a means to avoid flow and speed changes when the shaft load varies suddenly, the options are:

α to stick to a low flow velocity and a large penstock, or

β to provide an external means to protect the penstock[5].

Although option β requires the additional cost of the external device, it permits a substantial reduction in penstock costs: an economic advantage of up to 6% can be obtained by dimensioning the penstock of a PAT scheme with no technical restriction, *i.e.* only according to economic considerations, if it is adequately protected against pressure surges.

In the case of schemes with conventional turbines, due to their higher costs, the optimum penstock size from the economic point of view is larger and therefore the economic advantage of protecting the penstock is reduced.

5 Or any intermediate solution. Giddens[91], for instance, suggests using a brake but also sticking to low penstock velocities.

5

THE PREDICTION OF PAT PERFORMANCE

5.1 The Problem of Selection

The turbine-mode performance of a pump can be established by the users or by the manufacturers, by prediction or by test.

The prediction based on the pump-mode performance is the easiest technique, and the only one that can be easily done by the users; it requires finding out from the pump manufacturers or dealers some basic information about the pump-mode performance, namely the best efficiency head $\hat{H}_P$, flow $\hat{Q}_P$ and efficiency $\hat{\eta}_P$ (for a given speed ω_P), and then doing some calculations. According to some authors, such a technique can be used with reasonable accuracy (Acres American[80], Fraser & A.[81], Garay[90], Sharma[84]), or it may produce small errors that can be corrected by adjusting, after initial field tests, the rotating speed of the turbine - *i.e.* by changing the gear ratio (Chapallaz *et al.*[92]) or the capacitance, when using an induction generator (Smith *et al.*[92]).

According to other authors, the prediction based solely on the pump-mode performance is unreliable, because the manufacture of pumps does not follow a universal standard: two machines with exactly the same best efficiency point as pumps may have different turbine-mode performances, on account of differences in geometrical parameters (Burton & M.[92], Burton & W.[91], Chaudhry[87], Santolaria & F.[92], Strate *et al.*[90], Ventrone & N.[82]). According to Brown & R.[80], the influence of geometry is more obvious with recently-built pumps in the radial flow regime, that exhibit more radical differences in impeller and casing designs. Moreover, Williams[92] notes that, as in many developing countries there are no standards for the accuracy of manufacturers' data, "using this data as the sole basis for predicting the turbine performance of a pump restricts the accuracy of the final result, even if the prediction method itself is highly accurate".

As pump manufacturers never release the geometric data of their pumps, they are the only ones who can use this information in the prediction. The users could open and measure the machine, but, as they usually want to know the performance of several pumps, to find out which one is the best for a particular site, they need to have access to many models - and it is unlikely that any pump dealer will be willing to see his/her pumps disassembled. Although the basic geometric parameters required to calculate the 'theoretical' performance can be easily measured, the accurate determination of the hydraulic, mechanical and volumetric losses involves complex calculations and too many geometric parameters, difficult to measure[1]. Indeed no published method proposes establishing these losses based solely on the geometry; they all use in one way or another the pump-mode peak efficiency $\hat{\eta}_P$ as a datum.

Some pump manufacturers have predicted the turbine-mode performance of their pumps; others have preferred to do laboratory tests, more accurate but more expensive. According to many authors, it is necessary to have recourse to this manufacturers' data, since all simple performance-based prediction techniques are unreliable (Chadha[84], Engeda & R.[88a], Engeda *et al.*[88], Gopalakrishnan[86], Schnitzer[92], Shafer[83]). The performance information provided by the manufacturers may be wrong, especially when they use prediction techniques instead of tests (examples described by Pelton[88] and by Wilson & P.[92]), but then they are responsible for any PAT modification or replacement.

The main problem with these data, whether based on tests or on pump-mode performance and geometry, is that the manufacturers regard the turbine-mode performance information as confidential. In developing countries especially, it is virtually impossible to obtain even from the representatives of the large multinational companies any information on PATs, except for large projects. (Some manufacturers are very reluctant to provide even the pump-mode performance information; however, this secretive behaviour probably hampers the sale of their pumps, and of their PATs as well.) Minott & D.[83] point out that the problem of selection has reduced the use of PATs in small-scale hydropower; "the suppliers of centrifugal pumps should be encouraged to develop and publish tables, graphs, etc., which simplify the design and selection of reverse pump prime movers".

Moreover, the prediction or tests have to be paid by the users, since a pump to be operated as turbine is sold at a higher price than the same machine to be used as pump. In some cases, a small part of this extra price is due to special modifications, but, generally, most of is attributable to the performance information. This information is expensive for the risk involved when obtained by prediction, and, when obtained by test, because the test procedure is relatively complicated and the market for small

1 As suggested by Giddens[86a], the design of micro-hydro schemes should require only "trade skills".

turbines is insignificant as compared with that of 'normal' pumps (Williams[92]). This extra price accounts for 10% of the normal pump's price, according to Dresser Industries[82], Lueneburg & N.[85] and McClaskey & L.[76], but Chapallaz *et al.*[92] detected a much higher over-pricing, of between 30 and 100%.

This chapter reviews the published prediction methods, some based on the geometry and the pump-mode performance and some based solely on the latter. In the first case, a new analysis is presented (to be used as an auxiliary tool for pump manufacturers or for further research), and in the second case, a new prediction method is proposed (aimed at the users and thus avoiding the need to have recourse to the manufacturers' supervision, which is expensive and difficult to get). Finally the economic reliability of the performance-based method is evaluated by means of the economic methodology developed in Chapter 2.

5.2 Prediction Based on Both Geometry and Pump-mode Performance

5.2.1 Theoretical Background

Pump-mode Performance.

Fig. 39 shows the velocity triangles at the inlet and the outlet of a radial pump running in pump-mode. The inlet is assumed to be swirl-free and at the outlet the fluid angle β^*_{2P} is different from the blade angle β_2 on account of the slip, whose parameter is the slip factor s_P. Formulae for the slip factor have been published by Bothmann & R.[83], Friberg *et al.*[88], Wiesner[67] and other authors, in terms of the tip blade angle, the number of blades, and the ratio between tip and eye diameters.

The head transmitted to the fluid by the rotor[2], assuming swirl-free inlet, is given by:

$$g H_{RP} = c_{u2P} u_{2P}$$

(H_{RP} is larger than the actual head H_P developed by the pump, on account of the hydraulic losses.) The corresponding dimensionless head coefficient is:

$$\psi_{RP} = \frac{g H_{RP}}{r_2^2 \omega_P^2} = \frac{c_{u2P} u_{2P}}{r_2^2 \omega_P^2}$$

2 The general term **rotor** (suffix $_R$) is used here to avoid the terms **impeller** and **runner**, specific for pumps and turbines respectively.

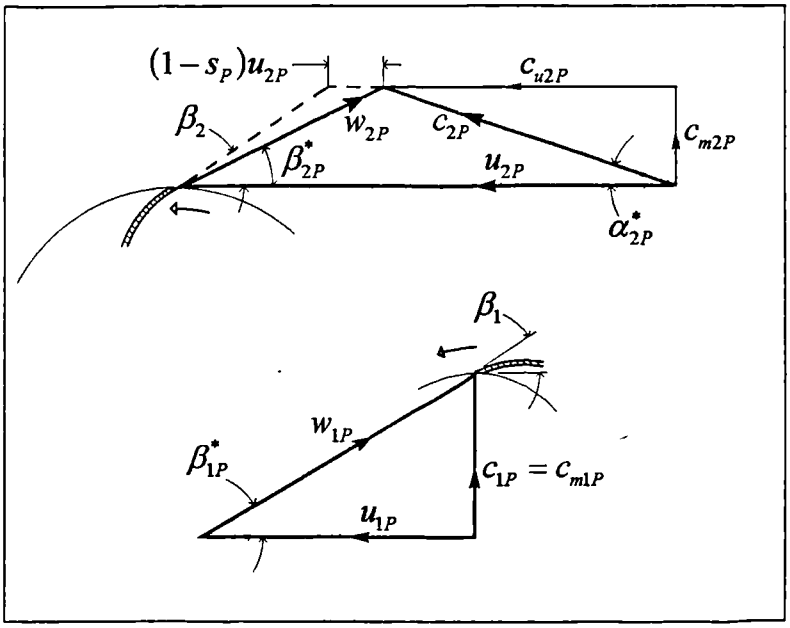

Fig. 39. Velocity triangles in pump-mode.

From the outlet velocity triangle:

$$c_{u2P} = u_{2P} - (1-s_P)u_{2P} - c_{m2P}\cot\beta_2 = s_P u_{2P} - c_{m2P}\cot\beta_2$$

Taking into account that the radial velocity c_{m2P} is equal to the flow Q_{RP} divided by the circumferential tip area a_2, we arrive at...:

$$\psi_{RP} = s_P - \phi_{RP}\cot\beta_2 \qquad [23]$$

..., where the dimensionless flow coefficient ϕ_{RP} is defined as:

$$\phi_{RP} = \frac{Q_{RP}}{a_2 r_2 \omega_P}$$

Eq. [23] is the pump-rotor torque characteristics[3]. (Q_{RP}, the flow that passes through the rotor, is a bit larger than Q_P on account of the leakage flow.)

The head developed by the pump is equal to the head transmitted by the rotor to the liquid, minus the hydraulic losses. These losses are: friction losses, diffusion losses and shock losses.

3 Yedidiah[89] criticizes the use of β_2, because it is referred only to an infinitesimal point. Based on "solidity effects", he proposes taking into account the blade angles along a section of the blade, from the tip of the impeller to an intermediate point between the eye and the tip.

There are two shock losses: The inlet shock loss occurs when $\beta_1 \neq \beta^*_{1P}$, *i.e.* when the angle of the relative flow velocity approaching the eye of the rotor does not match the angle of the rotor blades.

The outlet shock loss occurs when the angle of the absolute flow velocity leaving the rotor does not match the angle of the fixed-vanes - in a pump with diffuser vanes, or the free-vortex flow pattern - in a vane-less volute pump. In order to get a uniform theory for pumps with and without diffuser vanes, we can use the equivalent volute angle, *i.e.* the angle that the absolute flow velocity needs to have at the outlet of the impeller in order to ensure a free-vortex flow pattern without flow disturbances. This equivalent angle is, as deduced by Burton & W.[91] from the paper by Worster[63] about the flow in volutes[4]...:

$$\alpha_2 = \tan^{-1}\left[\frac{B r_2}{a_2}\ln\left(1+\frac{B}{r_2}\right)\right] \qquad [24]$$

..., where B^2 is the volute throat area. Then the shock loss at the outlet of the rotor occurs when $\alpha_2 \neq \alpha^*_{2P}$, and it takes place in the fixed vanes of a diffuser pump or in the cut-water of a vane-less volute pump. The best efficiency point (BEP) usually has a slight outlet shock loss[5], but we can neglect it and assume that:

$$\hat{\alpha}^*_{2P} = \alpha_2$$

From the outlet velocity triangle:

$$\cot \hat{\alpha}^*_{2P} = \frac{\hat{c}_{u2P}}{\hat{c}_{m2P}}$$

Therefore:

$$\hat{\phi}_{RP} = \frac{s_P}{\cot \alpha_2 + \cot \beta_2} \qquad [25]$$

---

4 Eq. [24] is based on the assumption of a square volute. It is somewhat different for 'real' volute shapes (Massey[63]).

5 Many pumps are designed so that, for the same speed, the shock-free entry ($\beta_1 = \beta^*_{1P}$) occurs with a larger flow than the shock-free outlet ($\alpha_2 = \alpha^*_{2P}$), and the BEP is located somewhere in between both points, closer to the second one, since the inlet shock loss is relatively small; "the slight shock loss at the entry in the BEP seems to be compensated by the better performance at higher flows, particularly with regard to cavitation" (Ventrone & N.[82]).

Substituting in Eq. [23], the optimum head coefficient is:

$$\hat{\psi}_{RP} = s_P \left(1 - \frac{1}{\frac{\cot \alpha_2}{\cot \beta_2} + 1} \right) \qquad [26]$$

Turbine-mode Performance.

Fig. 40 shows the velocity triangles at the inlet and the outlet of a radial pump running in turbine-mode. Subscript $_2$ is kept for the tip of the rotor and subscript $_1$ for the eye, as used often in PAT literature for the sake of coherence with pump-mode, although this is against the traditional fluid-mechanics nomenclature, that uses $_1$ for the inlet and $_2$ for the outlet.

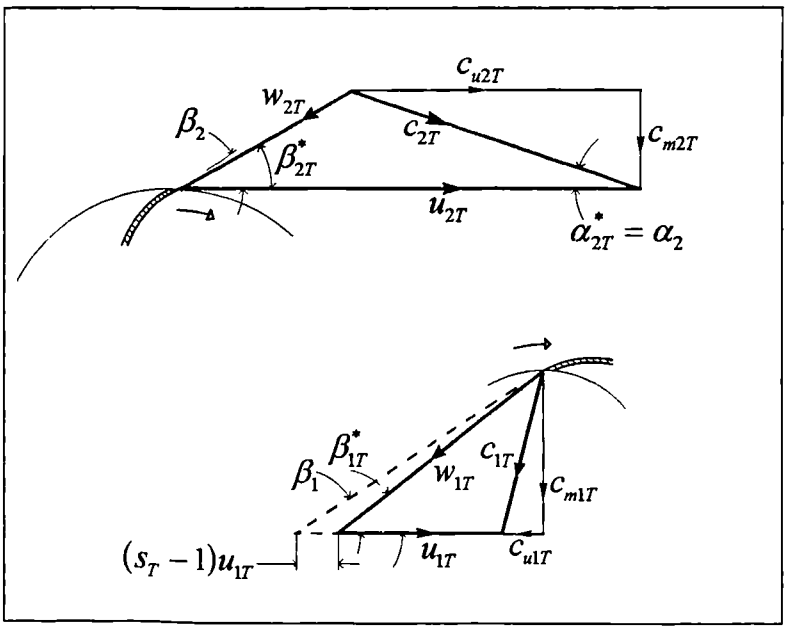

Fig. 40. Velocity triangles in turbine-mode.

The angle of absolute flow velocity at the inlet (α^*_{2T}) is equal to the volute or diffuser angle (α_2), and at the outlet the fluid angle β^*_{1T} is different from the blade angle β_1 on account of the slip, whose parameter is the slip factor s_T.

The turbine-mode outlet slip has not been properly studied. According to Lueneburg & N.[85], the slip-factor is equal in turbine-mode and pump-mode, although this would be odd for the many machines with $\beta_1 \neq \beta_2$. Ventrone & N.[82] state that the same formula used for the pump-mode slip-factor can be used for its turbine-mode counterpart, and that, as the angular deviation of the relative flow velocity between the inlet and the outlet of the rotor is in both modes less than predicted by the one-dimensional theory, the slip has in turbine-mode the opposite direction than in pump-mode, *i.e.* the fluid leaves the

blade with an angle **greater** than the blade angle. Finally, according to Burton & M.[92], Burton & W.[91] and Williams[92], the turbine-mode slip is negligible, since "the blades are much closer together and able to provide good guidance".

Fig. 40 was drawn, following Ventrone & N.[82], with $\beta^*_{1T} > \beta_1$. In order to keep the consistency with pump-mode (where $s_P < 1$), the slip-factor s_T is defined in turbine-mode as larger than the unity, and therefore the slip in the velocity triangle is $(s_T - 1)u_{1T}$, as compared to $(1 - s_P)u_{2P}$ in pump-mode.

It can be seen in Fig. 40 that c_{u1T} and c_{u2T} have opposite directions, as happens in most PATs around their BEPs. To be consistent with the figure, the equation of the head transmitted by the rotor has a **plus** sign:

$$gH_{RT} = c_{u2T}u_{2T} + c_{u1T}u_{1T}$$

The corresponding dimensionless coefficient is:

$$\psi_{RT} = \frac{gH_{RT}}{r_2^2\omega_T^2} = \frac{c_{u2T}u_{2T} + c_{u1T}u_{1T}}{r_2^2\omega_T^2}$$

From the inlet velocity triangle:

$$c_{u2T} = c_{m2T}\cot\alpha_2 \qquad [27]$$

From the outlet velocity triangle:

$$c_{u1T} = c_{m1T}\cot\beta_1 - u_{1T} - (s_T - 1)u_{1T} = c_{m1T}\cot\beta_1 - s_T u_{1T} \qquad [28]$$

Taking into account that...

$$Q_{RT} = c_{m2T}a_2 = c_{m1T}a_1 \qquad [29]$$

..., defining the rotor radius and area ratios as...

$$\nu_r = \frac{r_1}{r_2} \qquad \nu_a = \frac{a_1}{a_2} \qquad [30]$$

..., and the dimensionless turbine-rotor flow coefficient as...

$$\phi_{RT} = \frac{Q_{RT}}{a_2 r_2 \omega_T} \qquad [31]$$

..., we get the turbine-rotor head characteristics, which is a straight line in the ϕ–ψ plane:

$$\psi_{RT} = \left(\cot \alpha_2 + \frac{\nu_r}{\nu_a} \cot \beta_1 \right) \phi_{RT} - s_T \nu_r^2 \qquad [32]$$

The head absorbed by the turbine is equal to the head transmitted by the liquid to the rotor, plus the hydraulic losses: as in pump-mode, there are friction losses and a shock loss at the inlet to the rotor (when $\beta_2 \neq \beta^*_{2T}$), but, instead of an outlet shock loss, there is a swirl loss[6] when $c_{u2T} \neq 0$. The BEP will be located in the operating point where both shock and swirl losses are minimal. As explained by Burton & M.[92], "in a custom built turbine the design can be arranged so that the two conditions of 'shock-free entry' and 'no whirl at exit' occur at approximately one flow: the design condition. In a PAT the two conditions normally happen at different points on the characteristic and the machine's peak turbine performance will be at some intermediate point between these two flow conditions".

The shock-free entry point (diacritic $\breve{}$) occurs when $\beta_2 = \breve{\beta}^*_{2T}$ ∴

$$\breve{\phi}_{RT} = \frac{1}{\cot \alpha_2 + \cot \beta_2} \qquad [33]$$

Substituting in Eq. [32]:

$$\breve{\psi}_{RT} = \frac{\cot \alpha_2 + \nu_r \nu_a^{-1} \cot \beta_1}{\cot \alpha_2 + \cot \beta_2} - s_T \nu_r^2 \qquad [34]$$

The swirl-free point (diacritic $\breve{}$) occurs when $\breve{c}_{u1T} = 0$ ∴

$$\breve{\phi}_{RT} = \frac{s_T \nu_r \nu_a}{\cot \beta_1} \qquad [35]$$

Substituting in Eq. [32]:

$$\breve{\psi}_{RT} = \frac{s_T \nu_r \nu_a \cot \alpha_2}{\cot \beta_1} \qquad [36]$$

6 According to Chapallaz *et al.*[92], "a slight whirl in the suction or draft tube of a PAT (and turbines in general) is favourable especially in view of losses due to the diffusion process (deceleration of flow) at the suction side of a PAT or turbine". However, this effect is not taken into account here.

5.2.2 Published Prediction Methods Using Geometry and Performance

Chapallaz, Eichenberger and Fischer.

The geometric method proposed by Chapallaz *et al.*[92] is the only one based only on the geometry, and not on the pump-mode performance, because it is intended only for those cases where the performance is unavailable (they propose another method, based solely on the performance, to be used when it is available).

This method consists in establishing the pump specific speed Ω_P and the optimum head coefficient $\hat{\psi}_{RP}$ from the pump geometry (namely from r_2/r_1 and b_2/r_2), by using a graph that they reproduce. Then the pump-mode BEP is calculated and their performance-based method is used to obtain the turbine-mode BEP.

Ventrone and Navarro.

According to Ventrone & N.[82], the shock-free entry point is the BEP, although it does not correspond to $\beta^*_{2T} = \beta_2$, but to $\beta^*_{2T} = \beta_2 - i$, where i is an angle that depends on the blade geometry[7]. However, this deviation is likely due not to a boundary-layer effect, as they suggest, but to the swirl loss, that moves the BEP away from the shock-free entry point. If this supposition is true, their procedure to obtain the shock-free point cannot be generalised.

The other difference from the theoretical background developed above is that they multiply a_1 by an obstruction coefficient.

Their method uses the pump-mode performance data in two ways: the volute angle α_2 is obtained from the velocity triangle at the rotor exit for the pump-mode BEP (*i.e.* from Eq. [25]), and the peak efficiencies in both modes are assumed equal ($\hat{\eta}_T = \hat{\eta}_P$).

Unfortunately, they do not explain the procedure used to obtain the obstruction coefficient, the volumetric efficiency and the hydraulic efficiency, necessary to establish the turbine-mode BEP.

Burton and Williams.

The first example of a thorough, analytical prediction of the turbine-mode performance was published by Burton & Williams[91]: The volute performance is established by measuring its throat area, and the different losses by measuring the wall clearance and the leakage path (length and width of the eye clearance). Although the procedure used to calculate the losses is not shown in the example presented by them, it is explained in the PhD thesis published later by Arthur Williams[92]: the mechanical loss is estimated as a factor of the disc friction, calculated according to Stepanoff[57] and the leakage loss is

---

7 Between 4° and 6° for pumps with $27° < \beta_2 < 35°$ and singly-curved blades, and between 0° and 1° for blades with double curvature.

estimated according to Thome[79b]. Finally, both losses are subtracted from the pump-mode input power at the BEP, and the result compared with the hydraulic output power, in order to establish the hydraulic efficiency. ("Accurate calculation of the viscous shear and diffusion is difficult, because it depends on an accurate knowledge of the internal flows in the pump, and the shape of the flow channels".) $\hat{\eta}_P$ is then the only performance datum used by them to determine the turbine performance.

The turbine-mode losses are estimated from the pump-losses without assuming, as Ventrone & N.[82] do, that $\hat{\eta}_T$ and $\hat{\eta}_P$ are always equal: the leakage loss is calculated by taking into account the increase in head, the mechanical power loss is assumed to be proportional to the square of the rotating speed and the hydraulic losses are considered relatively smaller than those in pump-mode[8], "because in turbine-mode the volute represents a converging, rather than a diverging passage, in which the diffusion losses are lower".

Their work is partly based on the paper written by Worster[63], from which they obtained the volute equivalent angle (Eq. [24]). In fact, they use in their equations the right part of Eq. [24] instead of α_2 [9].

Burton and Williams recognise that the exact turbine BEP will be determined by a compromise between running with no whirl at outlet and running with little shock at entry to the impeller blade. However, they suggest designing for a $\check{\phi}_T$ some 10% beyond the shock-free point for two reasons:

① They assume that the shock-free $\check{\phi}_{RT}$ is always larger than the swirl-free $\check{\phi}_{RT}$ [10] (and therefore larger than $\hat{\phi}_{RT}$), and they consider advantageous to design for a rated $\check{\phi}_{RT}$ larger than the optimum. The reason for this consideration is that the efficiency curve is flatter at over-capacity. (See p. 112 for a discussion on the advantage of over-designing.)

② The turbine ϕ_T is larger than the rotor ϕ_{RT}, on account of the leakage loss.

Burton and Mulugeta.

The proposal of Burton & Mulugeta[92] follows the area-ratio theory developed by Anderson[55], who stated that the ratio Y of area between the impeller blades at exit (normal to flow

---

8 Although they wrongly take into account only the volute hydraulic efficiency in the calculation of $\hat{\psi}_{RT} / \hat{\psi}_T$; and they consider the rotor hydraulic loss as a mechanical loss. (The only advantage of calculating separately the rotor and the volute hydraulic efficiencies would be the accurate calculation of the leakage loss, that depends on the pressure difference across the rotor.)

9 Williams[92] applies this equation also to diffuser pumps, but it would probably be more convenient to use in this case the angle of the diffuser vanes.

10 This assumption is not always valid (*e.g.* for some of the pumps described by Williams[92]).

velocity) to the throat area of volute was the single most important factor in explaining the behaviour of the pump[11]. Y is defined by him as:

$$Y = \frac{a_2 \sin\beta_2}{B^2} \qquad [37]$$

Burton and Mulugeta applied Anderson's ideas to turbine-mode operation by analysing the sensitivity of both shock-free entry (Eqs. [33] and [34]) and swirl-free outlet (Eqs. [35] and [36]) points to the following 5 parameters that represent the geometry of the machine: B/b_2, ν_r, β_2, ν_a and Y. (See Eq. [24] for the relation between B and α_2.)

They conclude that the shock-free entry point (but not the swirl-free outlet point) is, like the pump-mode BEP, remarkably independent of all factors except Y [12]. This, together with Burton and Williams' reason ①, leads them to suggest using the shock-free entry point as the design point, by means of two conversion factors - one for the flow and one for the head - relating pump-mode rotor BEP and turbine-mode rotor shock-free entry point. The proposed flow factor is constant (1.26) and the head factor is expressed in terms of Y. (Indeed by dividing Eqs. [33] and [25], we see that the flow factor is simply $1/s_P$.)

In order to use this technique, it is necessary to make judicious estimates of the different losses involved in both modes[13], firstly to translate from the pump-mode machine BEP to the rotor values, and then to translate from the turbine-rotor shock-free entry point to the actual machine operating values.

5.2.3 A New Analysis Using Geometry and Performance

No comprehensive mathematical model of the turbine-mode performance parameters has been proposed so far. The conventional turbine theory is not applicable, since, in the first place, conventional turbines are designed so that the shock-free entry and swirl-free outlet points coincide. The model developed below has still many limitations and therefore it is not proposed as a prediction technique, but just as an

---

11 Yedidiah[83] oddly said that Anderson had used the area-ratio method to determine the turbine-mode performance of a pump from its geometry; "several attempts to correlate this approach with actual test results have ended with rather disappointing results". However, as far as we know, Anderson never used his method in this way.

12 Although it is not usual for the individual factors to vary independently (Worster[63]), a_1/a_2 has an important effect, and so does β_1/β_2 (they assume $\beta_1 = \beta_2$, but most pumps have $\beta_1 \neq \beta_2$).

(Note that there are some misprints in the paper: in Fig. 4 the solid lines should be broken, and *vice versa*; and Eq. 7 corresponds to the swirl-free point.)

13 They also suggest using only the volute efficiency (see footnote 8 above).

auxiliary tool for pump manufacturers or for further research. It is aimed at the numerical calculation of the BEP of radial-flow PATs.

Torque.

The turbine-mode torque dimensionless coefficient τ_T is equal to the rotor torque coefficient minus the mechanical friction losses coefficient:

$$\tau_T = \frac{M_T}{\rho a_2 r_2^3 \omega_T^2} = \tau_{RT} - \tau_{FT} \qquad [38]$$

Firstly, according to Fig. 40, the torque transmitted to the rotor by the liquid is:

$$M_{RT} = \rho Q_{RT} (c_{u2T} r_2 + c_{u1T} r_1)$$

The corresponding dimensionless torque coefficient is:

$$\tau_{RT} = \frac{M_{RT}}{\rho a_2 r_2^3 \omega_T^2} = \frac{Q_{RT} (c_{u2T} r_2 + c_{u1T} r_1)}{a_2 r_2^3 \omega_T^2}$$

From Eqs. [27], [28], [29] and [30], we get the turbine-rotor torque characteristics:

$$\tau_{RT} = \left(\cot \alpha_2 + \frac{\nu_r}{\nu_a} \cot \beta_1 \right) \phi_{RT}^2 - s_T \nu_r^2 \phi_{RT} \qquad [39]$$

... where the flow coefficient is defined in Eq. [31].

Secondly, the friction torque coefficient is defined as...:

$$\tau_{FT} = \frac{m_{FT}}{\rho a_2 r_2^3 \omega_T^2} \qquad [40]$$

..., where m_{FT} is the torque absorbed by the friction losses in the disc, bearings and packing, corresponding to the rotating speed ω_T. As it is not proportional to $\omega_T{}^2$ (one part of it is constant and the rest is approximately proportional to ω_T), the appropriate values of m_{FT} and ω_T should be substituted in this equation, which will then be valid only for the given speed.

By substituting Eqs. [39] and [40] in Eq. [38], the turbine torque coefficient is then:

$$\tau_T = \left(\cot \alpha_2 + \frac{\nu_r}{\nu_a} \cot \beta_1 \right) \phi_{RT}^2 - s_T \nu_r^2 \phi_{RT} - \frac{m_{FT}}{\rho a_2 r_2^3 \omega_T^2} \qquad [41]$$

Head.

The head absorbed by the turbine is equal to the head transmitted by the liquid to the rotor plus all the hydraulic losses: the whirl loss[14], the inlet shock loss and the friction loss. Therefore, the head coefficient is:

$$\psi_T = \frac{gH_T}{r_2^2\omega_T^2} = \psi_{RT} + \psi_{WT} + \psi_{iT} + \psi_{FT} \qquad [42]$$

The first element of Eq. [42] is the head transmitted by the liquid to the rotor (see Eq. [32]), that is:

$$\psi_{RT} = \frac{\tau_{RT}}{\phi_{RT}} = \left(\cot\alpha_2 + \frac{v_r}{v_a}\cot\beta_1\right)\phi_{RT} - s_T v_r^2 \qquad [43]$$

The second element of Eq. [42] is the whirl energy coefficient. The whirl energy is defined as:

$$gh_{WT} = \frac{c_{u1T}^2}{2}$$

Therefore, its dimensionless coefficient is:

$$\psi_{WT} = \frac{gh_{WT}}{r_2^2\omega_T^2} = \frac{c_{u1T}^2}{2r_2^2\omega_T^2}$$

Substituting Eqs. [28], [29] and [30], we arrive to:

$$\psi_{WT} = \left(\frac{\cot^2\beta_1}{2v_a^2}\right)\phi_{RT}^2 + \left(-s_T\frac{v_r}{v_a}\cot\beta_1\right)\phi_{RT} + \left(\frac{s_T^2 v_r^2}{2}\right) \qquad [44]$$

The third element of Eq. [42] is the shock (or 'incidence') loss coefficient. The shock loss is defined by Friberg *et al.*[88] as:

$$gh_{iT} = \frac{w_{2T}^2}{2} 2\gamma_i \sin^2(\beta_2 - \beta_{2T}^*) \qquad [45]$$

..., where γ_i is 2 when the relative flow velocity approaches the concave side of the rotor blade ($\beta_2 > \beta^*_{2T}$), and 4.5 when $\beta_2 < \beta^*_{2T}$[15].

---

14 Unless the machine has fixed guide vanes in the eye of the rotor, the swirl energy is not dissipated anywhere in the turbine, but downstream, and, therefore, strictly speaking, it is not a hydraulic loss of the turbine, but it is considered so here, for the sake of simplicity.

15 According to Anderson[38] and Lueneburg & N.[85] (and apparently also for Ventrone & N.[82]), the shock loss is $v_S^2/2g$, where v_S is the vector difference of the relative velocities before and after the shock. This means that $\gamma_i = 0.5\cdot(\sin\beta_2)^{-2}$. However, Friberg's formula seems more reliable.

Therefore the dimensionless shock loss coefficient is:

$$\psi_{iT} = \frac{g h_{iT}}{r_2^2 \omega_T^2} = \frac{w_{2T}^2}{r_2^2 \omega_T^2} \gamma_i \sin^2\left(\beta_2 - \beta_{2T}^*\right)$$

From the inlet velocity triangle:

$$w_{2T} = \frac{c_{m2T}}{\sin \beta_{2T}^*}$$

Doing some trigonometric transformations, we arrive to:

$$\psi_{iT} = \gamma_i \phi_{RT}^2 \left[\sin^2 \beta_2 \cot^2 \beta_{2T}^* - \sin(2\beta_2) \cot \beta_{2T}^* + \cos^2 \beta_2\right]$$

Again from the velocity triangle:

$$\cot \beta_{2T}^* = \frac{u_{2T}}{c_{m2T}} - \cot \alpha_2 = \frac{1}{\phi_{RT}} - \cot \alpha_2$$

Therefore:

$$\begin{aligned} \psi_{iT} = &\left[\gamma_i \sin^2 \beta_2 \cot^2 \alpha_2 + \gamma_i \sin(2\beta_2) \cot \alpha_2 + \gamma_i \cos^2 \beta_2\right] \phi_{RT}^2 + \ldots \\ &\ldots + \left[-2\gamma_i \sin^2 \beta_2 \cot \alpha_2 - \gamma_i \sin(2\beta_2)\right] \phi_{RT} + \left[\gamma_i \sin^2 \beta_2\right] \end{aligned} \quad [46]$$

Finally, the fourth element of Eq. [42] is the friction loss coefficient. The friction loss in the rotor is proportional to the rotor flow Q_{RT} square, and the friction loss in the casing is proportional to the turbine flow Q_T square. Q_T is a bit larger than Q_{RT} on account of the leakage loss. However, a negligible error is produced by assuming that the friction head loss in the whole turbine is proportional to $Q_{RT}{}^2$:

$$g h_{FT} = K_{FT} Q_{RT}^2 \quad [47]$$

The corresponding coefficient is:

$$\psi_{FT} = \frac{g h_{FT}}{r_2^2 \omega_T^2} = \frac{K_{FT} Q_{RT}^2}{r_2^2 \omega_T^2}$$

$$\psi_{FT} = K_{FT} a_2^2 \phi_{RT}^2 \quad [48]$$

Putting together Eqs. [43], [44], [46] and [48], we get the turbine-mode head characteristics (which is a parabola):

$$\psi_T = \left[\frac{\cot^2\beta_1}{2\,\nu_a^2} + \gamma_i \sin^2\beta_2 \cot^2\alpha_2 + \gamma_i \sin(2\beta_2)\cot\alpha_2 + \gamma_i \cos^2\beta_2 + K_{FT}a_2^2\right]\phi_{RT}^2 + \ldots$$
$$\ldots + \left[\cot\alpha_2 + (1-s_T)\frac{\nu_r}{\nu_a}\cot\beta_1 - 2\gamma_i \sin^2\beta_2 \cot\alpha_2 - \gamma_i \sin(2\beta_2)\right]\phi_{RT} + \ldots \quad [49]$$
$$\ldots + \left[\gamma_i \sin^2\beta_2 - (s_T - \tfrac{1}{2}s_T^2)\,\nu_r^2\right]$$

Flow.

As mentioned above, the turbine flow is the addition of the rotor flow and the leakage flow. Its dimensionless coefficient is:

$$\phi_T = \frac{Q_T}{a_2 r_2 \omega_T} = \phi_{RT} + \phi_{LT} \quad [50]$$

The leakage flow is proportional to the square root of the pressure difference across the rotor. Therefore, its coefficient is:

$$\phi_{LT} = \frac{q_{LT}}{a_2 r_2 \omega_T} = \frac{K_{LT}\sqrt{\Delta p_{RT}}}{a_2 r_2 \omega_T} \quad [51]$$

This pressure difference is proportional to the head absorbed by the rotor plus the shock head-loss plus the friction head-loss in the rotor (assumed as half of the total friction loss) plus the difference in the absolute velocity heads at the eye and the tip of the rotor:

$$\frac{\Delta p_{RT}}{\rho} = gH_{RT} + gh_{iT} + \tfrac{1}{2}gh_{FT} + \frac{c_{1T}^2}{2} - \frac{c_{2T}^2}{2}$$

From the velocity triangles, we have:

$$c_{1T}^2 = c_{u1T}^2 + c_{m1T}^2$$

$$c_{2T}^2 = \frac{c_{m2T}^2}{\sin^2\alpha_2}$$

The pressure difference coefficient, defined as...:

$$\psi_{\Delta p} = \frac{\Delta p_{RT}}{\rho r_2^2 \omega_T^2}$$

... is then equal to:

$$\psi_{\Delta p} = \psi_{RT} + \psi_{iT} + \tfrac{1}{2}\psi_{FT} + \left(\frac{1+\cot^2\beta_1}{2\nu_a^2} - \frac{1}{2\sin^2\alpha_2}\right)\phi_{RT}^2 - s_T\frac{\nu_r}{\nu_a}\cot\beta_1\,\phi_{RT} + \tfrac{1}{2}s_T^2\nu_r^2$$

Substituting in Eq. [51], the leakage coefficient is then:

$$\phi_{LT} = \frac{K_{LT}\sqrt{\rho r_2^2\omega_T^2\psi_{\Delta p}}}{a_2 r_2\omega_T} \qquad [52]$$

Finally, from Eq. [50], the turbine flow coefficient is:

$$\phi_T = \phi_{RT} + \frac{K_{LT}}{a_2}\sqrt{\rho\psi_{\Delta p}} \qquad [53]$$

Efficiency.

The efficiency of the turbine is:

$$\eta_T = \frac{M_T\omega_T}{\rho g H_T Q_T} = \frac{\tau_T}{\psi_T\phi_T}$$

By substituting in it Eqs. [41], [49] and [53], the efficiency is expressed as a complex function of the rotor flow coefficient ϕ_{RT}. $\hat{\phi}_{RT}$ can be obtained numerically with a computer program[16]. The tricky aspect of the prediction lies, as with all geometry-based methods, in the judicious estimation of the losses (*i.e.* m_{FT}, K_{FT} and K_{LT}).

Bobok[75] measured the efficiency $\hat{\eta}_P$ and the hydraulic efficiency $\hat{\eta}_{HP}$ of a set of small pumps. By analysing his data, it can be seen that the latter tends to follow a general trend, function of the flow and the specific speed, whereas the former is much more random: it seems indeed that the volumetric and, especially, the mechanical efficiencies of small pumps are subject to much more variables, difficult to be established by examination of the machine. By fitting Bobok's data in a model similar to the one published by Anderson[77] for the overall pump efficiency $\hat{\eta}_P$ (see Eq. [57], p. 84), the hydraulic efficiency complies closely with the following formula:

$$\hat{\eta}_{HP} = 1 - 0.031\hat{Q}_P^{-0.32} - 0.054(0.0 + \ln\Omega_P)^2 \qquad [54]$$

16 By neglecting the mechanical and leakage losses, it would be possible to write an analytical formula for the ϕ_{RT} corresponding to the optimum (hydraulic) efficiency. However, this value would still be inaccurate. As it is considered here that a geometry-based method can in practice be used only by the pump manufacturers (see p. 56), which are assumed to have computers, there is no point in simplifying the method at the expense of its accuracy.

The approach suggested here is similar to the one proposed by Williams[92] (see p. 64), but the other way round: the hydraulic efficiency is calculated with Eq. [54] and the combined volumetric-mechanical efficiency is calculated by deduction from the pump-mode optimum efficiency obtained by test - in the absence of a more accurate parameter. Finally, the individual share of each one of these two efficiencies (volumetric and mechanical) can be calculated with the equations used by Williams[17].

5.3 Prediction Based on Pump-mode Performance Alone

The users of PATs are unlikely to have access to the geometry of a range of machines, and, in this unlikely event, the measurement and the further calculations required for the prediction are both very complex tasks. Therefore, the data more realistically available to the users are those related with the performance in pump-mode.

In this section the many published methods for predicting turbine-mode performance from pump-mode performance are reviewed. Their accuracy is then visually indicated by comparison with the actual PAT performances of machines for which both pump-mode and turbine-mode test data exist. A formal accuracy evaluation will be made later in § 5.5 (p. 96).

5.3.1 Published Prediction Methods Using Performance Alone

Most published performance-based prediction methods propose factors for converting pump-mode to turbine-mode best-efficiency points: one factor for the head, one for the flow and (sometimes) one for the efficiency, assuming the same speed for both modes. The simplest conversion factors are constant; other factors are functions of either $\hat{\eta}_P$ or Ω_P; the more complex ones are functions of both. (Note that some authors mention conversion factors just as "hypothesized trends", without suggesting that they can be used as proper prediction methods.)

Other methods take into account the shape of the pump-mode characteristics; finally few methods undertake the turbine-mode performance prediction outside the BEP.

Constant Conversion Factors.

Naber & H.[87] propose the following factors (and they imply that $\hat{\eta}_{TE} = \hat{\eta}_P$) [18]:

$$\frac{\hat{Q}_{TE}}{\hat{Q}_P} = 1.3 \qquad \frac{\hat{H}_{TE}}{\hat{H}_P} = 1.35$$

17 Other formulae and graphs for the individual efficiencies of pumps are published by Łazarkiewicz & T.[65], Patel *et al.*[61], Raabe[81] and Thorne[79b].

18 Subscript $_E$ represent the predicted (estimated) conditions. Although it could be omitted here, it is used just for the sake of consistency with the nomenclature required later.

Palgrave[87] in turn suggests that:

$$\frac{\hat{Q}_{TE}}{\hat{Q}_P} = 1.471 \qquad \frac{\hat{H}_{TE}}{\hat{H}_P} = 1.471 \qquad \frac{\hat{\eta}_{TE}}{\hat{\eta}_P} = 1.1$$

Finally, the method of Sánchez[91] is as follows (he does not mention anything about the efficiencies):

$$\frac{\hat{Q}_{TE}}{\hat{Q}_P} = 1.35 \qquad \frac{\hat{H}_{TE}}{\hat{H}_P} = 1.3$$

Conversion Factors in Terms of Efficiency Alone.

Based on an old German doctoral dissertation, Stepanoff[57], states that $\hat{H}_{TE}/\hat{H}_P = (\hat{\eta}_{HT} \cdot \hat{\eta}_{HP})^{-1}$. (This expression seems to assume that there is no slip in any mode and that in turbine-mode the BEP is at the same time swirl-free and shock-free, which is true only in exceptional circumstances.) Assuming similar hydraulic efficiencies in both modes, the former expression is reduced to $\hat{H}_{TE}/\hat{H}_P = \hat{\eta}_{HP}^{-2}$. As for the flows, it is proposed that $\hat{Q}_{TE}/\hat{Q}_P = \hat{\eta}_{HP}^{-1}$. (The only theoretical explanation for this equation would be the assumption that the volumetric efficiency is equal to the square root of the hydraulic efficiency.) The further assumption that $\hat{\eta}_{HP} = \sqrt{\hat{\eta}_P}$ leads Stepanoff (followed by Wong[87]) to propose that:

$$\frac{\hat{Q}_{TE}}{\hat{Q}_P} = \hat{\eta}_P^{-0.5} \qquad \frac{\hat{H}_{TE}}{\hat{H}_P} = \hat{\eta}_P^{-1}$$

A simple method, proposed originally by Childs[62], and mentioned subsequently also by Garay[90], Hancock[63] [19], McClaskey & L.[76] and Thome[79a] [20], is as follows (many of them suggest as well $\hat{\eta}_{TE} = \hat{\eta}_P$):

$$\frac{\hat{Q}_{TE}}{\hat{Q}_P} = \hat{\eta}_P^{-1} \qquad \frac{\hat{H}_{TE}}{\hat{H}_P} = \hat{\eta}_P^{-1}$$

According to Ventrone & N.[82], $\hat{H}_{TE}/\hat{H}_P = \eta_P^{-2}$ and $\hat{P}_{TE}/\hat{P}_P = \eta_P^{-1}$. Therefore, with $\hat{\eta}_{TE} = \hat{\eta}_P$:

---

19 The method proposed by Hancock uses the turbine efficiency instead of the pump efficiency, and is not therefore a proper prediction method. It is intended as a method of finding an appropriate pump from the turbine operating conditions, by assuming a turbine speed and applying these formulae.

20 Who does not propose it as a prediction tool.

$$\frac{\hat{Q}_{TE}}{\hat{Q}_P} = \hat{\eta}_P^{-1} \qquad \frac{\hat{H}_{TE}}{\hat{H}_P} = \hat{\eta}_P^{-2}$$

From Stepanoff's formulae, it is possible to conclude that $\Omega_{TE} = \Omega_P \cdot \sqrt{\hat{\eta}_P}$. Based on this and on the assumption that $\hat{P}_{TE} = \hat{P}_P$ [21], Sharma[84] obtained $\hat{H}_{TE}/\hat{H}_P = \hat{\eta}_P^{-1.6}$ and $\hat{Q}_{TE}/\hat{Q}_P = \hat{\eta}_P^{-0.4}$ (with $\hat{\eta}_{TE} = \hat{\eta}_P$). Williams[90] detected a calculation error in these formulae and corrected them to:

$$\frac{\hat{Q}_{TE}}{\hat{Q}_P} = \hat{\eta}_P^{-0.8} \qquad \frac{\hat{H}_{TE}}{\hat{H}_P} = \hat{\eta}_P^{-1.2}$$

Moreover, Williams[90] suggests multiplying the former formulae by 1.1, on account of the asymmetry of the efficiency curve, as explained above (p. 64). He proposes therefore[22]:

$$\frac{\hat{Q}_{TE}}{\hat{Q}_P} = 1.1\,\hat{\eta}_P^{-0.8} \qquad \frac{\hat{H}_{TE}}{\hat{H}_P} = 1.1\,\hat{\eta}_P^{-1.2}$$

Finally, in their BEng thesis (published in Mexico), Alatorre-Frenk & T.-T.[89] made curve-fitting for a small set of pump and PAT data, and obtained the following formulae (this method is referred to as 'Butu', *i.e.* PAT in Spanish):

$$\frac{\hat{Q}_{TE}}{\hat{Q}_P} = \frac{0.85\,\hat{\eta}_P^5 + 0.385}{2.00\,\hat{\eta}_P^{9.5} + 0.205} \qquad \frac{\hat{H}_{TE}}{\hat{H}_P} = \frac{1}{0.85\,\hat{\eta}_P^5 + 0.385} \qquad \hat{\eta}_{TE} = \hat{\eta}_P - 0.03$$

Conversion Factors In Terms of Specific Speed Alone.

All methods based on the specific speed are empirical, *i.e.* based on test data.

Firstly, Diederich[67] publishes two graphs for the conversion factors, valid for $0.28 \le \Omega_P \le 1.04$, and proposes that $\hat{\eta}_{TE} \ge \hat{\eta}_P$. The graphs follow approximately the following formulae:

$$\frac{\hat{Q}_{TE}}{\hat{Q}_P} = 1.402\,\Omega_P^{-0.171} \qquad \frac{\hat{H}_{TE}}{\hat{H}_P} = 1.556\,\Omega_P^{-0.174}$$

Gopalakrishnan[88] also published two graphs, just to show the "hypothesized trend" - i.e. not to be used in prediction (he also assumes $\hat{\eta}_T = \hat{\eta}_P$). A curve-fitting yielded the following formulae:

---

21 This assumption is wrongly attributed to Karassik *et al.*[76]; it could come from Childs[62].

22 Williams calls this method Sharma's method. We call it Williams' method, to distinguish it from the Sharma's method corrected by Williams but without the 1.1 factors.

$$\frac{\hat{Q}_{TE}}{\hat{Q}_P} = 1.86 - 0.551 \cdot \ln(5\Omega_P) + 0.11\left[\ln(5\Omega_P)\right]^{2.2}$$

$$\frac{\hat{H}_{TE}}{\hat{H}_P} = 2.6 - 9.1 \cdot \ln(5\Omega_P) + 7.96\left[\ln(5\Omega_P)\right]^{1.1}$$

Finally, Grover[82] published three linear graphs valid for $0.2 \leq \Omega_P \leq 1.1$, whose equations, according to Chappell *et al.*[82], are:

$$\frac{\hat{Q}_{TE}}{\hat{Q}_P} = 2.643 - 1.399\Omega_P \qquad \frac{\hat{H}_{TE}}{\hat{H}_P} = 2.693 - 1.212\Omega_P \qquad \frac{\hat{\eta}_{TE}}{\hat{\eta}_P} = 0.893 + 0.0466\Omega_P$$

Conversion Factors in Terms of Both Efficiency and Specific Speed.

Schmiedl[88] was the first to propose a prediction method based on both $\hat{\eta}_P$ and Ω_P: his head and flow conversion factors are expressed in terms of the former, and his efficiency factor in terms of the latter (this method is valid for $0.1 \leq \Omega_P \leq 1.05$):

$$\frac{\hat{Q}_{TE}}{\hat{Q}_P} = -1.378 + 2.455\left(\hat{\eta}_P \hat{\eta}_T\right)^{-0.25}$$

$$\frac{\hat{H}_{TE}}{\hat{H}_P} = -1.516 + 2.369\left(\hat{\eta}_P \hat{\eta}_T\right)^{-0.5}$$

$$\frac{\hat{\eta}_{TE}}{\hat{\eta}_P} = 1.158 - 0.265\Omega_P$$

Chapallaz *et al.*[92] published two graphs based on test data with specific speed as the abscissa and, respectively, a flow and a head conversion factors as the ordinates. A curve-fitting, based on the model proposed by Anderson[77] for $\hat{\eta}_P$ (see Eq. [57], p. 84), was made, and, although the correlation is not excellent (Chapallaz's curves were drawn by hand and do not follow a uniform trend), the equations obtained are the following:

$$\frac{\hat{Q}_{TE}}{\hat{Q}_P} = 1.12\,\hat{\eta}_P^{-0.6}\left[1 + (0.4 + \ln\Omega_P)^2\right]^{0.15}$$

$$\frac{\hat{H}_{TE}}{\hat{H}_P} = 1.1\,\hat{\eta}_P^{-0.8}\left[1 + (0.3 + \ln\Omega_P)^2\right]^{0.3} \qquad [55]$$

$$\hat{\eta}_{TE} = \hat{\eta}_P - 0.03$$

Kittredge's Method.

Kittredge[61] published pump-mode and turbine-mode performance graphs (with head and torque versus flow or speed), normalised to pump BEP, for 4 'model' machines of different specific speeds. He proposed using these data for predicting the turbine-

mode performance of a 'prototype' pump by comparing the shape of the pump-mode performance curves of the 'prototype' pump with those of the 'models' and estimating which one is more alike. (He assumes that two pumps with similar normalised pump-mode characteristics will have similar normalised turbine characteristics.)

The main problem of Kittredge's method is that it expresses turbine head, flow, torque and speed (but not efficiency) in terms of those for the pump, and therefore a 'prototype' with low shaft power in pump-mode (*i.e.* an efficient pump) will also have a low shaft power in turbine-mode (*i.e.* an inefficient PAT). And *vice versa*: if the 'prototype' has a lower $\hat{\eta}_P$ than the 'model', then its turbine-mode efficiency will be higher. In practice, it is more likely that a pump which runs less efficiently than the 'model' when in pump-mode will run also less efficiently than the 'model' in turbine-mode[23]. (Williams[92] describes an example where the calculated turbine efficiency using Kittredge's method is 158%!)

In order to correct this error, $\hat{\eta}_{TE}$ should be adjusted by a factor equal to the square of the ratio of the 'prototype' and the 'model' pump-mode peak efficiencies - as demonstrated by Williams[92] - by correcting the turbine-mode flow or head or shaft power or any combination of them[24]. Fraser & A.[81] wrote a computer program following Kittredge's method that corrects the efficiency by adjusting the flow, whereas Williams[92] distributes the correction among the head (exponent 1.2) and the flow (exponent 0.8) in a computer program modified by him, that was originally written (without efficiency correction) by Acres American[80] (see also Lawrence & P.[81]).

Other Methods.

According to Buse[81] and Spangler[88], both conversion factors are function of the specific speed, and vary between 1.1 and 2.2, but they do not provide any formula.

Bothmann[84] proposed an awkward method for determining, using similarity laws, the turbine-mode performance of a pump when PAT test data are available for another pump, even if it is not similar!

---

23 The same error is made by Stepanoff[57].
Kittredge[76] provides a picturesque justification of his method: "A difficulty with the methods [that establish a relation between the efficiencies in both modes] is the assumption of the correct value of the efficiency. [...] Although the proposed method is more complicated, it avoids a direct assumption of the efficiency, and gives an indication of the approximate efficiency at which the turbine will operate".

24 The methods for calculating water-hammer in large pumping stations use this technique (to express head, flow, torque and speed in terms of those for the pump) to estimate the 'abnormal' behaviour of the pumps in case of failure (in fact, Kittredge inherited this approach from his original experience in this domain). Therefore, they make errors in the turbine quadrant, that could be corrected as described above, or by using a PAT prediction technique for the turbine-mode range. (The water-hammer calculation field should **learn back** from the PAT field; see the reflection of p. 4.)

Brada[82] and Meier[82] published graphs just for the head conversion factor. Meier's paper includes also a power factor graph, but it refers to something like the average power produced in typical storage schemes by pump-turbines in both modes, but not to the BEPs.

Engeda & R.[86] suggest that the ratio $(\hat{H}_{TE}\cdot\hat{Q}_{TE})/(\hat{H}_P\cdot\hat{Q}_P)$ is proportional to $\hat{\eta}_P^{-3}$, but they do not mention what is the share of each individual factor.

Prediction Outside the BEP.

PATs are sometimes designed to operate exactly at their BEP, especially when there is flexibility to decide the rotating speed of the turbine (for example when a belt-drive is used).

However, in many cases a direct-drive is preferable - even if it implies operating the PAT outside its BEP -, because it is more efficient, cheaper and easier to install and to maintain. Moreover, the bearing life (for turbine and generator) is increased (Williams[92] detected serious bearing wear problems in PATs with belt-drive in India and Pakistan). Finally, Smith *et al.*[92] point out that the use of induction generators favours the direct-drive option, firstly because small induction machines with 6 and even 8 poles are available, and secondly because, unlike synchronous generators, their speed can be varied within a small range (see also p. 55).

A PAT with a direct-drive will almost never operate at its BEP, but somewhere near it. However, just few authors undertake the issue of the performance prediction outside the BEP.

Paterson & M.[84] published four-quadrant performance graphs of six representative pumps with different specific speeds. According to them, the shape of the turbine performance curves is a function of Ω_P [25]. "These designs are typical of normal commercial practice. While variations in design features such as area ratio, number of blades, omission of [pump-mode] inlet guide vanes, etc. will have some repercussions in the turbines mode, most modifications also affect the specific speed and, unless they are extreme, should fall inside the data scatter".

Wong[87] describes his method as follows: "To produce an approximate pump turbine [PAT] characteristic for a radial flow impeller first draw the pump characteristic curve and its efficiency curve. Assume the turbine has zero efficiency at about 0.4 of the turbine BEP flow... The turbine efficiency curve can be drawn between BEP and zero efficiency to match the shape of the pump efficiency curve. Assume the zero flow head for the pump turbine to be one third of the shut off head of the pump. The turbine

25 Yedidiah[83] is the only who denies the validity of this statement.

head characteristic can then be drawn between head at turbine BEP and zero flow to reflect the pump characteristic as a mirror image." [!]

Garay[90] does not propose any off-BEP prediction technique, but instead he proposes applying the conversion factors to obtain the required pump from the known turbine performance, and then, "generally, a pump can be converted to a PAT if $\hat{Q}_P$ and $\hat{H}_P$ fall within 20% of the BEP of the pump selected".

The off-BEP 'Butu' prediction method of Alatorre-Frenk & T.-T.[89] (reproduced in Alatorre-Frenk & T.[90]) consists in two formulae: firstly, the slope of the straight torque-speed line in a constant-flow diagram is expressed in terms of Ω_P, and secondly the hydraulic power is defined as a single exponential function of the shaft power (valid for all values of Ω_P).

Chapallaz *et al.*[92] publishes in turn a set of flow-head and flow-efficiency curve shapes, each for a different specific speed. A similar approach is followed by Buse[81] [26].

Finally, some methods for the prediction of four-quadrant performance, that include the turbine performance prediction, are published by Kinno & K.[65] and Thomas[72].

5.3.2 Comparison of Predicted and Actual Performance

Test data in both modes of operation were located in the literature and some unpublished sources for 57 test-PATs. This information, listed in Appendix B, is "random, multi-sourced and in many cases of unspecified accuracy or origin" (Paterson & M.[84]). The data originated in tests performed either for water-hammer analysis or for PAT studies. In addition to the normal measuring errors (at least 3%, according to Mikus[83]), the data have, in some cases, one or more of the following disadvantages:

- The information covers only the range between the runaway point and the BEP, but not between the BEP and the stall point.
- The turbine-mode range of operation is sparsely covered, and the calculation of the BEP required crude interpolations (four-quadrant test-PAT data aimed at water-hammer calculations).
- The quoted speeds in both modes are below-synchronous and, therefore, the doubt arises that the turbine-mode speed may have been wrongly assumed as equal to pump-mode speed (with an induction generator, the turbine-mode speed should be above-synchronous). The doubt is just a doubt because either the data could have been already corrected using the affinity laws, or the test-PAT could have been indeed tested at below-synchronous speed in a test-rig where it was just helping an induction motor to drive a third machine.

26 Although his lines are the wrong way, because they are more steep for low specific speeds.

- It is not explicit that the published turbine-mode data were indeed originated in tests and not in a simple prediction.
- The design of the test-PAT is not 'standard', for one of the following three reasons: pump made just for research purposes; old pump; special 'model' pump with smooth surface finish.
- The basic description of the test-PAT is missing, and therefore the type (and the specific speed) is slightly uncertain (the pump could be double suction or multistage, for instance).
- The PAT head could have been measured without subtracting the outlet velocity head and the draft-tube losses, or: the PAT head was explicitly calculated in this way, but the losses cannot be calculated because the geometry of the draft tube is not described.
- The PAT head could have been measured including the outlet swirl (Paterson & M.[84]).
- The data have different origins for each of the two modes of operation (namely manufacturers' data for pump-mode and published data for turbine-mode)[27].
- The quoted pump-mode BEP is in fact just the rated point, and there is not enough information to check the real BEP.

If all the test-PATs with disadvantages were excluded, there would remain a minuscule sample; moreover, it is impossible to judge what test-PATs are inferior. Therefore, all of them are taken into account.

The majority of the data, presented in graph form, were digitised by means of a scanner and graphics software, and subsequently the BEP in both modes was calculated.

Figs. 41, 42 and 43 show conversion factors from pump-mode to turbine-mode derived from these test data, for flow, head and efficiency (constant speed), as functions of $\hat{\eta}_P$. The functions calculated using some of the published prediction methods (namely those based only on $\hat{\eta}_P$) are superimposed for comparison.

27 Giddens[89] found that the pump-mode efficiencies of several tested machines was 3 or 4% lower than the figures provided by the manufacturers.

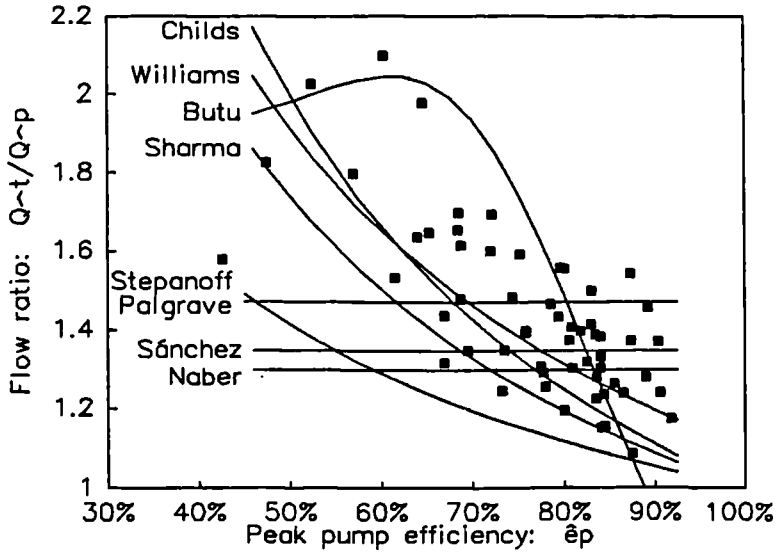

Fig. 41. Test data $\hat{Q}_T/\hat{Q}_P$ (▪) and predicted $\hat{Q}_{TE}/\hat{Q}_P$ (lines), as functions of $\hat{\eta}_P$.

In all graphs, ê stands for $\hat{\eta}$. Ventrone's method coincides here with Childs' method.

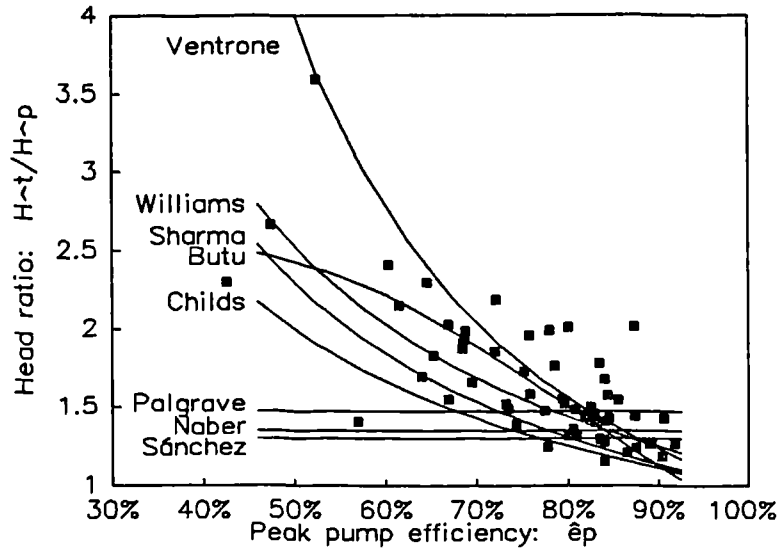

Fig. 42. Test data $\hat{H}_T/\hat{H}_P$ (▪) and predicted $\hat{H}_{TE}/\hat{H}_P$ (lines), as functions of $\hat{\eta}_P$.

Stepanoff's method coincides here with Childs' method.

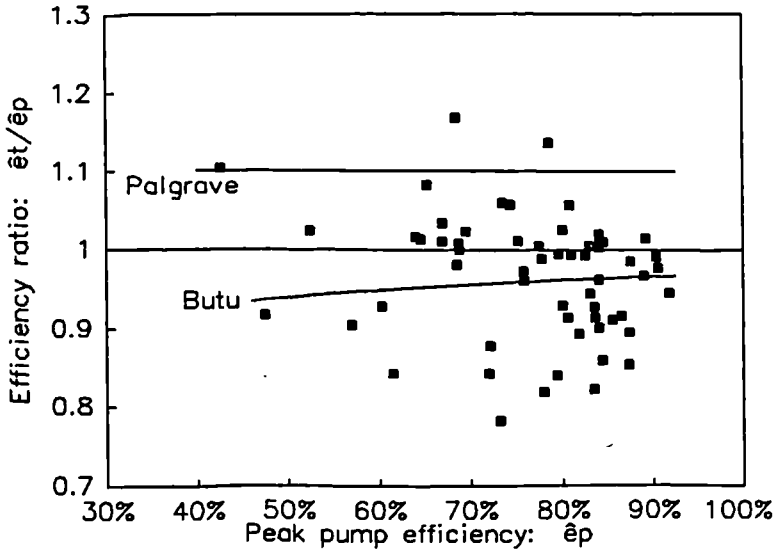

Fig. 43. Test data $\hat{\eta}_T / \hat{\eta}_P$ (▪) and predicted $\hat{\eta}_{TE} / \hat{\eta}_P$ (lines), as functions of $\hat{\eta}_P$.

Most methods propose $\hat{\eta}_T = \hat{\eta}_P$. Chapallaz's method coincides here with the Butu method.

Figs. 44, 45 and 46 show the same test-data ratios, but now as functions of the pump-mode specific speed Ω_P, together with the ratios obtained using prediction methods based only on Ω_P.

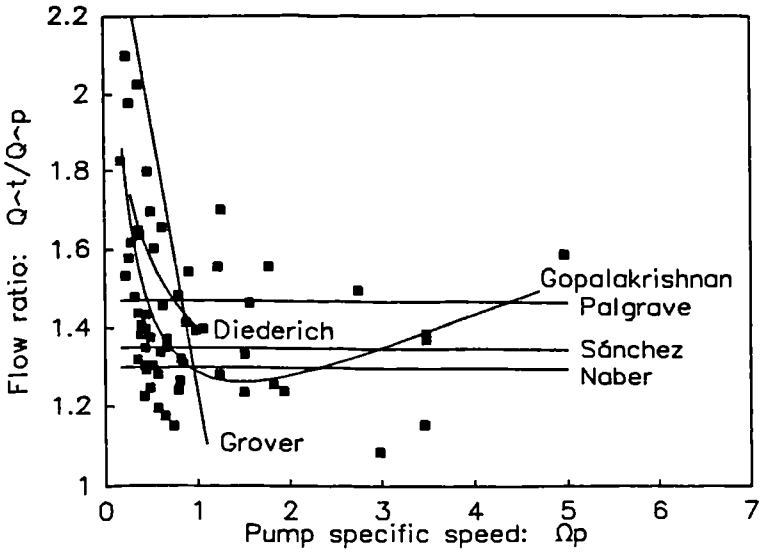

Fig. 44. Test data $\hat{Q}_T/\hat{Q}_P$ (▪) and predicted $\hat{Q}_{TE}/\hat{Q}_P$ (lines), as functions of Ω_P.

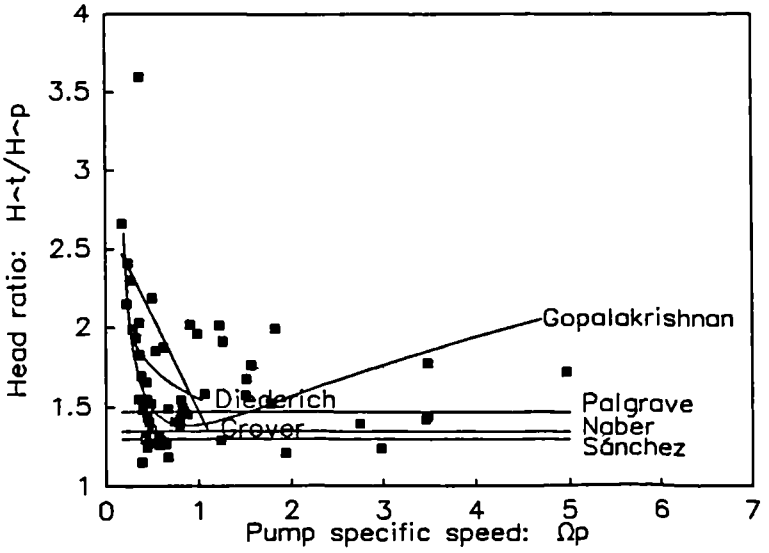

Fig. 45. Test data $\hat{H}_T/\hat{H}_P$ (■) and predicted $\hat{H}_{TE}/\hat{H}_P$ (lines), as functions of Ω_P.

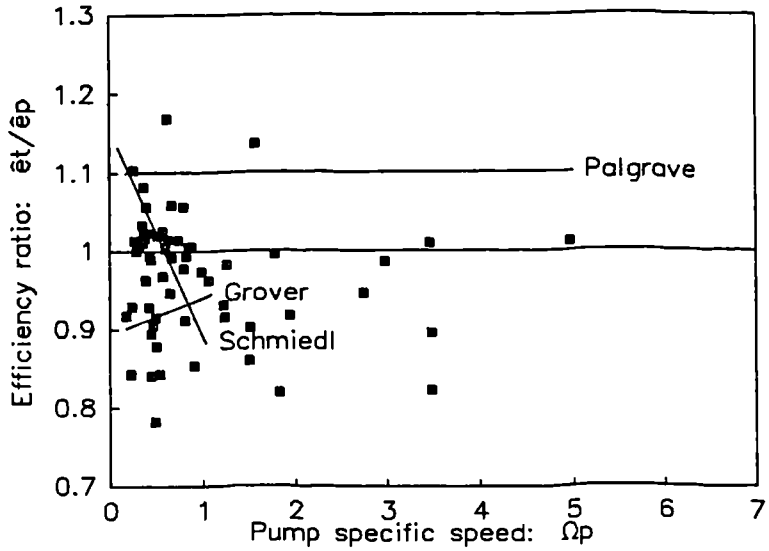

Fig. 46. Test data $\hat{\eta}_T$ / $\hat{\eta}_P$ (■) and predicted $\hat{\eta}_{TE}$ / $\hat{\eta}_P$ (lines), as functions of Ω_P.
Most methods propose $\hat{\eta}_T = \hat{\eta}_P$.

Finally, Figs. 47 and 48 show the test data in the same way as in Figs. 44 and 45, but this time with the $\hat{\eta}_P$ figures for each test-PAT, in order to enable the comparison with the conversion factors proposed by Chapallaz *et al.*[92].

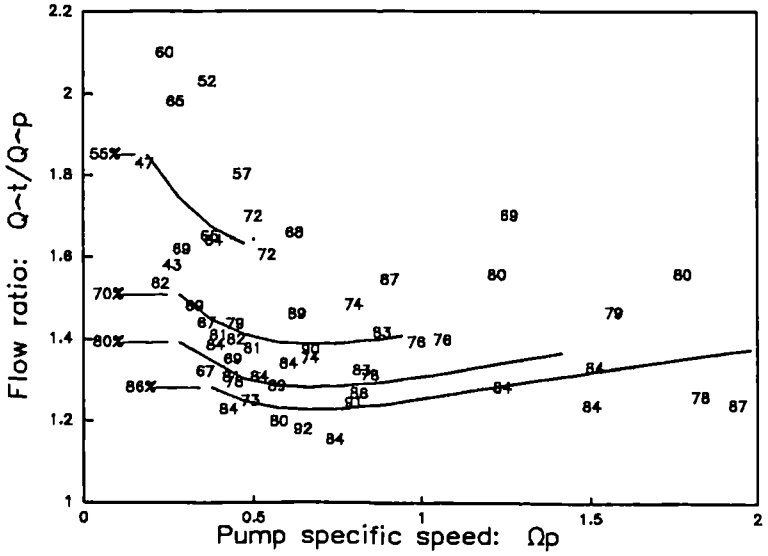

Fig. 47. Test data $\hat{Q}_T/\hat{Q}_P$ (■) and predicted according to Chapallaz $\hat{Q}_{TE}/\hat{Q}_P$ (lines), as functions of Ω_P and $\hat{\eta}_P$.
The figures correspond to $\hat{\eta}_P$ (percent) of each test-PAT. The lines do not match exactly those originally published by Chapallaz *et al*[92], because they were drawn according to the approximate formulae of Eq. [55].

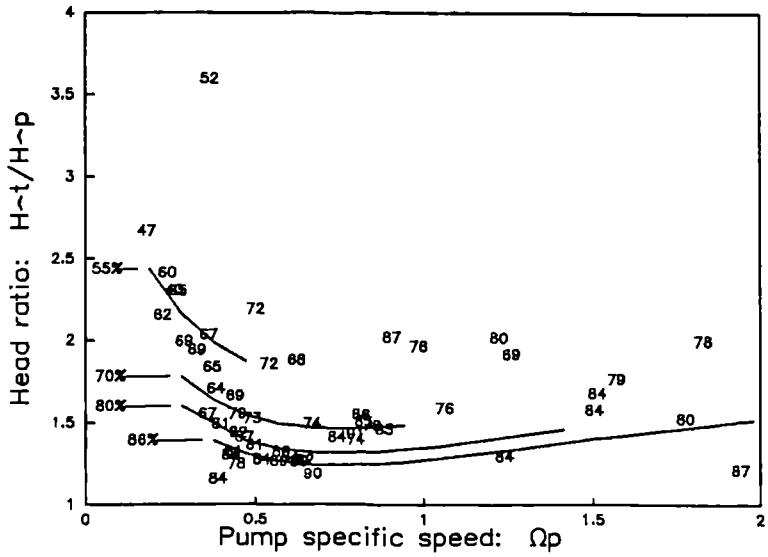

Fig. 48. Test data $\hat{H}_T/\hat{H}_P$ (■) and predicted according to Chapallaz $\hat{H}_{TE}/\hat{H}_P$ (lines), as functions of Ω_P and $\hat{\eta}_P$.
See note of previous Fig.

Figs. 41-48 show that some of the prediction methods are clearly far away from the main trend of the test data. The accuracy of the 'good' methods, on the other hand, can not be judged just by examining the graphs, and it will be evaluated numerically in § 5.5.

5.4 Development of a New Empirical Prediction Method Using Pump-mode Performance (almost) Alone

5.4.1 Introduction

The new heuristic method of forecasting PAT performance described below uses (as Chapallaz *et al.*[92] do) Ω_P and $\hat{\eta}_P$ as parameters, but it takes into account in addition the **type of casing**, a parameter (a geometric parameter, strictly speaking) that is readily available to the users.

Paterson & M.[84] evidenced the difference between volute casing and bowl diffuser casing in mixed flow pumps: In the range of specific speeds where both configurations are available, they have distinct turbine-mode operating characteristics, relative to pump-mode BEP. Therefore, the change of casing type produces a discontinuity in the relation between the specific speed and the performance. In addition, on account of the peculiar features of double-suction pumps in turbine-mode (see p. 10), single-suction and double suction volute pumps are considered separate categories. The single-suction volute-casing category includes multistage and diffuser pumps, under the general description of end-suction pumps.

The new method was obtained using the test data mentioned above and listed in Appendix B, that are more complete and varied than that available to the majority of previous analysts. Furthermore, some of the published prediction methods (notably Chapallaz's) are published in graph form, which hampers their dissemination; it is considered here that formulae are a more convenient form, especially taking into account the world-wide dissemination of electronic calculators.

5.4.2 Prediction of the Turbine-mode BEP

Fundamentals.

The proposed new prediction method for the BEP is based on the following considerations:

The specific speed characterizes - although not perfectly - the geometric parameters (β_1, β_2, α_2, ν_r and ν_a) that define the difference between pump-mode and turbine-mode 'theoretical' performances. On its turn, the efficiency is a parameter of the difference between the 'theoretical' and the real performances in both modes - and the specific speed determines what is the share of the volumetric, hydraulic and mechanical losses (see Stepanoff[57]). Therefore, both are important parameters of the conversion factors between the two modes of operation.

As there is some correlation between the specific speed of a pump and its peak efficiency, both can be used as parameters of each other. This is why both efficiency-

based and specific-speed-based approaches have been proposed in the literature for the calculation of the conversion factors. The problem with both kinds of methods is that there are many other factors involved in the relation between specific speed and efficiency, namely size and design variations.

Although the use of both parameters is still imperfect (as noted above, p. 55, two machines with exactly the same best efficiency point as pumps may have different turbine-mode performances), the accuracy of the prediction could not be improved without increasing tremendously its complexity.

As noted by Chapallaz *et al.*[92] (see Figs. 47 and 48) and by Gopalakrishnan[88] (see Figs. 44 and 45), the conversion factors are not a monotonic function of the specific speed, but rather a firstly (sharply) decreasing and then (slowly) increasing function. This shape can be mathematically modelled by the the following function...:

$$\Lambda = 1 + (X + \ln \Omega_P)^2 \qquad [56]$$

..., which has a minimum value of 1 when $\Omega_P = e^{-X}$.

Incidentally, function Λ is based on the third term (relating Ω_P and $\hat{\eta}_P$) of the formula proposed by Anderson[77] for the pump peak efficiency:

$$\hat{\eta}_P = 0.94 - 0.048 \hat{Q}_P^{-0.32} - 0.055(0.18 + \ln \Omega_P)^2 \qquad [57]$$

Therefore, with the test data divided in the 3 categories mentioned above (namely end-suction, double-suction and bowl pumps), formulae of the type $y_E = a x_1^{\,b} \cdot x_2^{\,c}$ were obtained by making linear regressions with the logarithms of the conversion factors ($\ln y_E$) as dependent variables and the logarithms of both Λ and $\hat{\eta}_P$ as the two independent variables.

A further variable is the X contained in Eq. [56]. In Anderson's formula, $X = 0.18$, because the optimum Ω_P is $e^{-0.18} \approx 0.83$. However, as noted by Hergt *et al.*[90], the optimum specific speed is lower for multistage and "small" pumps (between 0.43 and 0.60 for multistage, and between 0.28 and 0.60 for small pumps). X was optimised 'by hand', *i.e.* by finding the value that minimised the statistical errors of the regressions.

Few test-PATs that are outside the 'main trend' were not taken into account for the regressions. They fall into three classes:

① Small, inefficient, low-specific-speed pumps that, especially on account of their size, have a rather random behaviour in turbine-mode.

② Pumps with very high specific speed, that have a very unstable turbine-mode performance.

③ Pumps with very particular features, such as submersible pumps.

④ Pumps whose data have a doubtful quality.

Of course not all the test PATs of classes ①, ② and ③ were eliminated from the regressions. However, the prediction method should be applied with caution to such pumps.

We regard this non-scientific procedure - discarding points in an arbitrary way - as the cost of using such varied and non-scientific data.

Conversion Factors.

In accordance with the approach described above, formulae for pump-to-turbine conversion factors were derived by curve fitting to the data for each of the 3 categories of pumps.

The following formula was obtained for the head conversion factor, using end-suction pump data:

$$\frac{\hat{H}_{TE}}{\hat{H}_P} = 1.21\,\hat{\eta}_P^{-0.8}\left[1+\left(0.6+\ln\Omega_P\right)^2\right]^{0.3} \qquad [58]$$

The regression was made with 39 test-PATs, which means that it has 34 degrees of freedom. The standard error is 0.1 for the first exponent (–0.8) and 0.07 for the second (0.3), which shows that the correlation is satisfactory. The resulting standard deviation of the relative errors (test factor/calculated factor) is 11.5%.

This three-dimensional regression can be represented in two dimensions by constructing two graphs, one with each independent variable as the abscissa: The correlation in terms of Ω_P, for example, is represented in the following way: the test points are 'displaced' in the direction of the $\hat{\eta}_P$ axis, following the shape of the regression plane, until they reach an arbitrary value of $\hat{\eta}_P$ (e.g. an average value $\overline{\eta}_P$); the ordinate of these 'displaced' test points is then...:

$$\left\{\frac{\hat{H}_T}{\hat{H}_P}\right\}_{\to\overline{\eta}_P} = \frac{\hat{H}_T}{\hat{H}_P}\left(\frac{\overline{\eta}_P}{\hat{\eta}_P}\right)^{-0.8} \qquad [59]$$

And the regression plane is represented by its intersection with the vertical plane $\hat{\eta}_P = \overline{\eta}_P$, *i.e.*:

$$\left\{\frac{\hat{H}_{TE}}{\hat{H}_P}\right\}_{\to\overline{\eta}_P} = 1.21\,\overline{\eta}_P^{-0.8}\left[1+\left(0.6+\ln\Omega_P\right)^2\right]^{0.3} \qquad [60]$$

Fig. 49 shows then the correlation in terms of Ω_P, drawn with this procedure. Two test-PATS were eliminated from the regression: SENU037 [28] (class ①: $\hat{P}_P \approx 200$ W) and WILL047 (class ③: it is the only submersible pump in the sample).

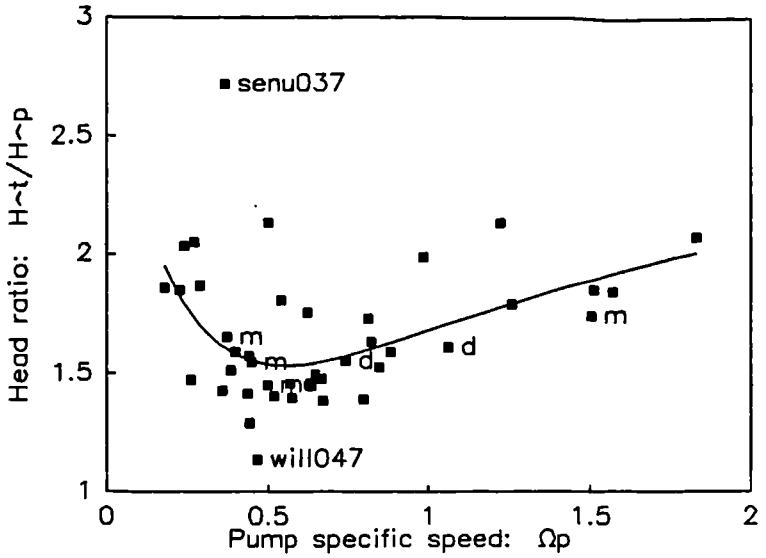

Fig. 49. Correlation of the head conversion factor in terms of Ω_P, for end-suction pumps.

The ■ represent Eq. [59] and the line Eq. [60]. $\bar{\eta}_P$ is 74%. **m** means multistage pump and **d** pump with fixed vanes (diffuser): they follow the same trend as single-stage pumps without fixed vanes.

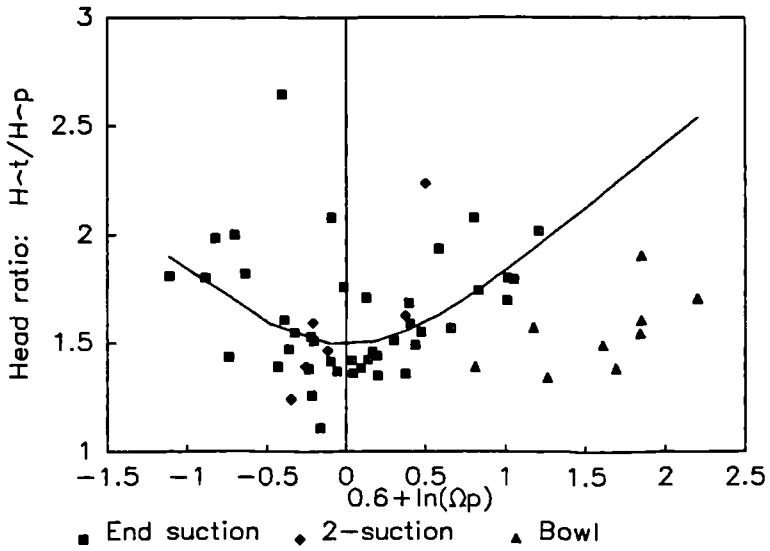

Fig. 50. Correlation of the head conversion factor in terms of Ω_P, for end-suction pumps, showing as well double-suction and bowl pumps.

28 The codes assigned to each PAT with test data are formed with the first four letters of the original author's name followed by three figures corresponding to $100{\cdot}\Omega_P$.

Fig. 50 is similar to Fig. 49, but it shows as well the points corresponding to double suction and bowl pumps: the former do not follow a really distinct trend, but the latter do, and this is even more clear in the case of the efficiency conversion factor (see Fig. 92 in Appendix C).

For the sake of completeness, the correlation in terms of $\hat{\eta}_P$ is shown in Fig. 51, constructed with a procedure similar to the one used for Fig. 49.

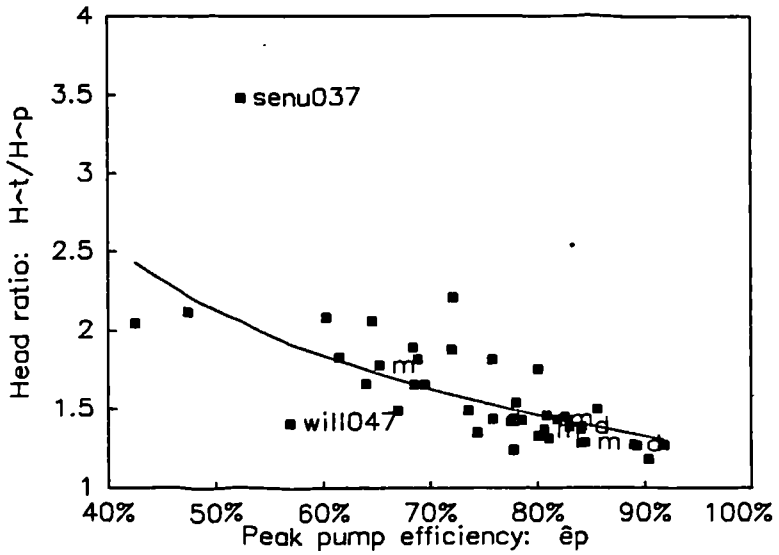

Fig. 51. Correlation of the head conversion factor in terms of $\hat{\eta}_P$, for end-suction pumps. $\overline{\Omega}_P = 0.66$.

The efficiency conversion factor...:

$$\frac{\hat{\eta}_{TE}}{\hat{\eta}_P} = 0.95\,\hat{\eta}_P^{-0.3}\left[1+\left(0.5+\ln\Omega_P\right)^2\right]^{-0.25} \qquad [61]$$

... has a better correlation (5.1% standard deviation of the relative errors), and it was obtained by eliminating three test-PATS: WILL047 (see above), JYOT054 (class ④ [29]) and KENN157, (class ④ [30]). The correlation is represented in Fig. 52.

29 JYOT054 was published in a newsletter of an Indian pump and turbine manufacturer (Jyoti Ltd.[n/a]); its dissidence could be due to a misprint, an extremely unconventional design or to a different casing (*e.g.* it could be a double suction pump).

30 KENN157 was published in an American technical report (Kennedy *et al.*[80]) about two-phase four-quadrant model studies aimed at the calculation of pressure surges in large circulating pumps of nuclear power stations; in this case the dissidence is clearly due to a lack of data: there are very few test points and it was necessary to do a crude interpolation to calculate the BEP.

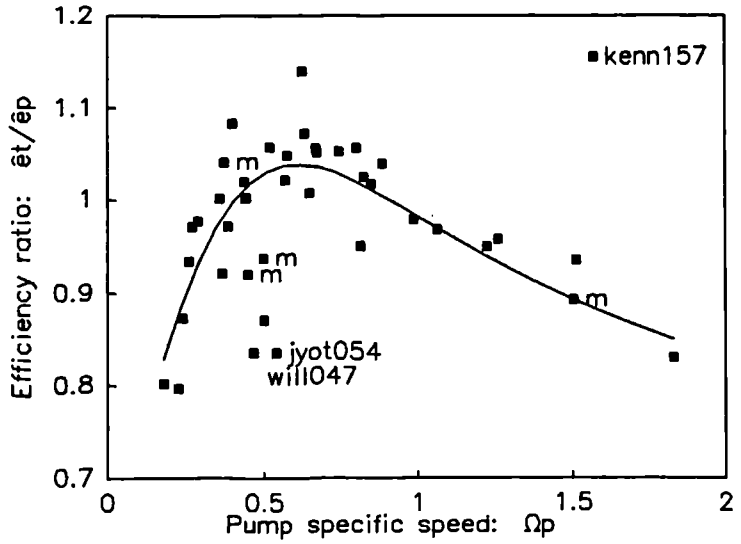

Fig. 52. Correlation of the efficiency conversion factor in terms of Ω_P, for end-suction pumps.
The procedure used to draw the ■ and the line is similar to the one used in Fig. 49.

Note that the efficiencies of two multistage test-PATs (marked **m**) are somewhat below the 'main trend' (although they were all included in the regression). This hints about the need of a separate multistage category. Indeed the geometry of these pumps is completely different: the outlet swirl from one stage is dissipated in a shock loss at the fixed vanes of the next stage. However, there are too few points to be able to formulate a separate formula from them. The only conclusion that can be extracted is the remark that some multistage PATs may have a lower efficiency than predicted.

The last formula for end-suction pumps concerns the flow conversion factor. In this case two facts were observed: firstly, the correlation with Λ is very poor, *i.e.* its coefficient is almost zero, and has a large standard error; secondly, all categories follow a similar trend. Therefore, the following single formula is proposed for **all three categories**:

$$\frac{\hat{Q}_{TE}}{\hat{Q}_P} = 1.21\,\hat{\eta}_P^{-0.6} \qquad [62]$$

The standard deviation of the relative errors is here 10.4%, and the regression has 55 degrees of freedom: all the test PATs were included. Note however the high dispersion, to the left of Fig. 53, of the points corresponding to the following six test PATs: SENU037 (see above), WILL047 (see above), GIDD018 (class ①), WILL026

(class ①), BUSE024 (class ① as well as ④ [31]) and SCHM027 (class ① as well as ③ [32]).

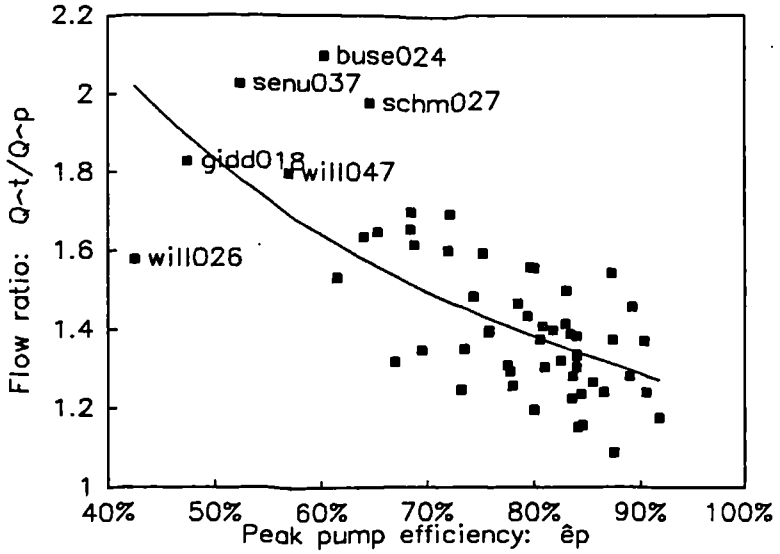

Fig. 53. Correlation of the flow conversion factor in terms of $\hat{\eta}_P$, for all pumps.

The formulae for double-suction pumps shown below (Eqs. [63] and [64]) were obtained with just 3 degrees of freedom (sample size: 7), which arouses serious doubts about their validity. Their correlation is quite good, as would be expected from these degrees of freedom. The large difference between the exponents of these formulae and those of Eqs. [58] and [61] is odd - especially the 1.7 of Eq. [64]. The regression details and figures can be seen in Appendix C.

$$\frac{\hat{H}_{TE}}{\hat{H}_P} = 0.79\,\hat{\eta}_P^{-2.3}\left[1+\left(0.7+\ln\Omega_P\right)^2\right]^{1.9} \qquad [63]$$

$$\frac{\hat{\eta}_{TE}}{\hat{\eta}_P} = 1.31\,\hat{\eta}_P^{1.7}\left[1+\left(0.7+\ln\Omega_P\right)^2\right]^{-0.6} \qquad [64]$$

Finally, the data about high-specific-speed bowl-casing pumps do not follow the shape of function Λ. Therefore, Ω_P was directly used for the head conversion factor (Eq. [65]), while the efficiency conversion factor (Eq. [66]) showed a very poor

31 BUSE024 was published by an author (Buse[81]) who never asserted that the data were indeed obtained in tests; moreover, all the information in the graph is relative to the pump BEP, and it was necessary to calculate the pump and turbine (absolute) efficiencies by deducing them from the head, flow, efficiency and power lines of turbine-mode, that show a lack of consistency.

32 SCHM027 is a non-standard model, whose suction and discharge branches oddly have the same diameter.

correlation with Ω_P - and therefore it is expressed just in terms of $\hat{\eta}_P$. Both regressions excluded one class ③ test-PAT (STIR348: a non-standard pump built just for laboratory purposes). Although the correlations are very good and have more degrees of freedom than the previous correlations (namely 5 and 6 respectively), the sample is still too small (8) to make the formulae qualify to be proposed for design purposes. (See details in Appendix C.)

$$\frac{\hat{H}_{TE}}{\hat{H}_P} = 0.93\,\hat{\eta}_P^{-1.7}\,\Omega_P^{0.1} \qquad [65]$$

$$\frac{\hat{\eta}_{TE}}{\hat{\eta}_P} = 0.88\,\hat{\eta}_P^{-0.5} \qquad [66]$$

5.4.3 Prediction Outside the BEP

Fundamentals.

By neglecting the effect of the mechanical and leakage losses on the **shape** of the characteristics about the BEP[33], the torque characteristic (see Eq. [41]) follows a line close to...:

$$\frac{M_T}{\omega_T^2} \approx A_M\left(\frac{Q_T}{\omega_T}\right)^2 + B_M\left(\frac{Q_T}{\omega_T}\right) \qquad [67]$$

..., and the head characteristics (see Eq. [49]) complies approximately with:

$$\frac{H_T}{\omega_T^2} \approx A_H\left(\frac{Q_T}{\omega_T}\right)^2 + B_H\left(\frac{Q_T}{\omega_T}\right) + C_H \qquad [68]$$

The PAT performance outside the BEP can then be established by finding the value of these five coefficients A_M, B_M, A_H, B_H and C_H. This can be achieved by defining, in addition to the BEP values, just two dimensionless parameters: the 'first' (E_T) and 'second' (E_{2T}) elasticities of the head characteristics at the BEP, defined as:

$$E_T = \frac{\hat{d}\left(\frac{H_T}{\omega_T^2}\right)}{d\left(\frac{Q_T}{\omega_T}\right)} \cdot \frac{\hat{Q}_T\hat{\omega}_T}{\hat{H}_T} \qquad [69]$$

33 In fact it will be shown later (see Fig. 54, p. 93) that PAT test performance follows these two equations along a broad range of conditions.

$$E_{2T} = \frac{\hat{d}^2\left(\frac{H_T}{\omega_T^2}\right)}{d\left(\frac{Q_T}{\omega_T}\right)^2} \cdot \frac{\hat{Q}_T^2}{\hat{H}_T} \qquad [70]$$

(The ^ above the d means: the derivative at the BEP.) Therefore, from Eq. [68]:

$$E_T \approx 2A_H \frac{\hat{Q}_T^2}{\hat{H}_T} + B_H \frac{\hat{Q}_T \hat{\omega}_T}{\hat{H}_T} \qquad [71]$$

$$E_{2T} \approx 2A_H \frac{\hat{Q}_T^2}{\hat{H}_T} \qquad [72]$$

A_H is then, from Eq. [72]:

$$A_H \approx \frac{E_{2T}}{2} \cdot \frac{\hat{H}_T}{\hat{Q}_T^2}$$

B_H is, from Eqs. [71] and [72]:

$$B_H \approx \left(E_T - E_{2T}\right) \frac{\hat{H}_T}{\hat{Q}_T \hat{\omega}_T}$$

and C_H, from Eqs. [68], [71] and [72], is:

$$C_H \approx \left(1 - E_T + \frac{E_{2T}}{2}\right) \frac{\hat{H}_T}{\hat{\omega}_T^2}$$

On the other hand, the efficiency of the turbine is...:

$$\eta_T = \frac{1}{\rho g} \cdot \frac{\left(\frac{M_T}{Q_T \omega_T}\right)}{\left(\frac{H_T}{\omega_T^2}\right)}$$

..., where, from Eq. [67]:

$$\frac{M_T}{Q_T \omega_T} \approx A_M \left(\frac{Q_T}{\omega_T}\right) + B_M \qquad [73]$$

At the BEP, we have:

$$\frac{\hat{d}\eta_T}{d\left(\frac{Q_T}{\omega_T}\right)} = 0$$

Therefore:

$$\frac{\hat{d}\left(\frac{H_T}{\omega_T^2}\right)}{d\left(\frac{Q_T}{\omega_T}\right)}\left(\frac{\hat{M}_T}{\hat{Q}_T\hat{\omega}_T}\right) = \frac{\hat{d}\left(\frac{M_T}{Q_T\omega_T}\right)}{d\left(\frac{Q_T}{\omega_T}\right)}\left(\frac{\hat{H}_T}{\hat{\omega}_T^2}\right)$$

By substituting Eq. [73], differentiating, and then substituting Eq. [69], we arrive to the equation for A_M:

$$A_M \approx E_T \frac{\hat{M}_T}{\hat{Q}_T^2} \qquad [74]$$

And finally, from Eqs. [73] and [74], B_M is:

$$B_M \approx (1 - E_T)\frac{\hat{M}_T}{\hat{Q}_T\hat{\omega}_T}$$

Conversion Factors.

The values of A_M, B_M, A_H, B_H and C_H for each test-PAT were obtained by multiple-variable linear regression, giving to each error a 'weight' proportional to the efficiency (see the introduction to Appendix B). The correlation of the head characteristic is always excellent (except for few axial-flow test-PATs), but, in the case of the torque characteristic, the points close to runaway had almost always to be eliminated: there the effect of the mechanical losses (that is neglected in the model proposed) becomes significant.

A typical example of the regression is shown in Fig. 54. This constant-flow representation of the turbine-mode performance (as proposed by Swiecicki[61] and used by Kittredge[61]) has two advantages over the constant speed representation that has been used so far: firstly, the whole range of turbine-mode performance is covered (the constant speed graph is an incomplete representation, as the stall lies on infinity[34]); and

34 A stall parabola is sometimes included in the head-flow graph, but this still leaves a large gap in the head characteristics, and moreover the stall torque is infrequently mentioned. One example of this is shown in Fig. 54.

secondly, the torque characteristic (neglecting mechanical and leakage losses) is a straight line[35]. Indeed, by rearranging Eqs. [67] and [68], we get:

$$\frac{M_T}{Q_T^2} \approx A_M + B_M\left(\frac{\omega_T}{Q_T}\right)$$

$$\frac{H_T}{Q_T^2} \approx A_H + B_H\left(\frac{\omega_T}{Q_T}\right) + C_H\left(\frac{\omega_T}{Q_T}\right)^2$$

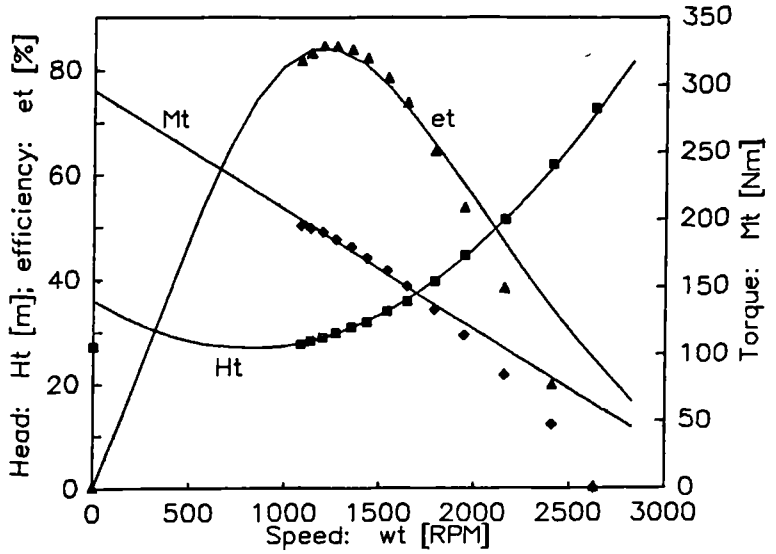

Fig. 54. Example of head and torque characteristics regression.

$Q_T = 0.1$ m^3/s. The ▲, ■ and ♦ correspond to the test-PAT APFE060, and the lines to the regression. The 4 points to the right were eliminated from the regression of the torque characteristics. 'e' means η and 'w' means ω (the rotating speed). Note that ω is usually associated with radians per second, while N or n are used for RPM; however, it does not make sense to use different symbols for the same concept.

E_T and E_{2T} were then obtained from Eqs. [71] and [72] (the BEP was calculated using Eq. [88], Appendix B). The correlation between the latter and the pump-BEP parameters (Ω_P and $\hat{\eta}_P$) showed that: the data scatter is much larger than for the BEP conversion factors; the division between the three categories is apparently not applicable; the correlation with $\hat{\eta}_P$ is very poor; and the points do not clearly follow the shape of function Λ. The formulae obtained for the three categories are then:

35 The traditional constant-speed graphs, and the constant-speed coefficients ϕ, ψ and τ are used in this document for two reasons: firstly, they are the more widely used, and secondly, the speed is the same for the rotor and for the whole machine, which simplifies the theoretical discussions (there is no 'speed loss' but there is a leakage loss, that would complicate the theory of PAT performance if constant-flow coefficients were used).

$$E_{TE} = 0.68 + 1.2\Omega_P^{0.5} \quad [75]$$

$$E_{2TE} = 0.76 + 2.1\Omega_P^{0.5} \quad [76]$$

The correlation of the 'first' elasticity (E_T) is illustrated in Fig. 55. The correlation of the 'second' elasticity (E_{2T}), as illustrated in Fig. 100 (Appendix C), is even worst, but, fortunately, the effect of any error in the calculation of E_{2T} is felt only far away from the BEP. WILL047 was eliminated from the second regression and SWAN496 (class ②) from both.

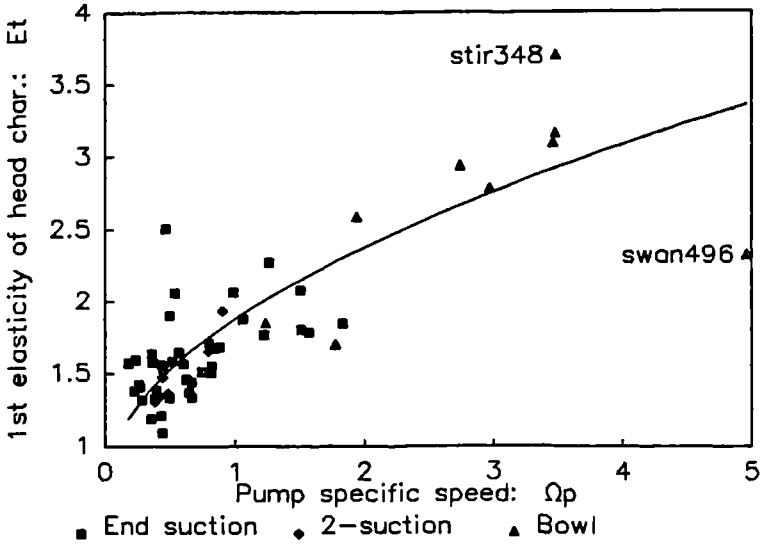

Fig. 55. Correlation of the 'first' elasticity E_T in terms of Ω_P, for all pumps.

5.4.4 Application of the Proposed Method

When a micro-hydro scheme is designed using a PAT, the required turbine performance is known, and the corresponding pump-performance is unknown. However, all prediction methods work the wrong way: they start from the pump-mode performance and end in the turbine-mode performance. This means that the pump selection has to be made on a trial-and-error basis, *i.e.* by predicting the turbine performance of a series of pumps and finding which one is the most appropriate.

This calculation can be easily done by a computer or programmable calculator. However, a more accessible dissemination technique is a graph, that can be, for example, prepared in a head office and then distributed to the field officers of a micro-hydro program.

As mentioned above (p. 76), the application of PATs can be divided in two categories: 'BEP operation' (especially when a belt-drive allows adjustment of the turbine-to-

generator speed ratio) and 'off-BEP operation' (especially with a direct-drive). Correspondingly, two kinds of graphs will be generated[36]:

The first one (Fig. 56) shows only the turbine-mode BEP. One enters the graph with a known figure for $\hat{Q}_T/\sqrt{\hat{H}_T}$, and the graph shows what models are available, with what speeds (ordinate axis $\omega_T/\sqrt{\hat{H}_T}$) and what efficiencies (labels in %). Then one has to decide what speeds are acceptable, and sometimes make a trade-off between inefficient PATs and high - and hence inefficient - gear ratios[37]. Fig. 56 is based upon the published characteristics of some of the pumps made by one manufacturer and covers a very wide range of performances. Such a graph could be constructed for the mix of machines, from different manufacturers, available in some particular country. It could be given higher resolution by restricting the range of machines covered by one graph.

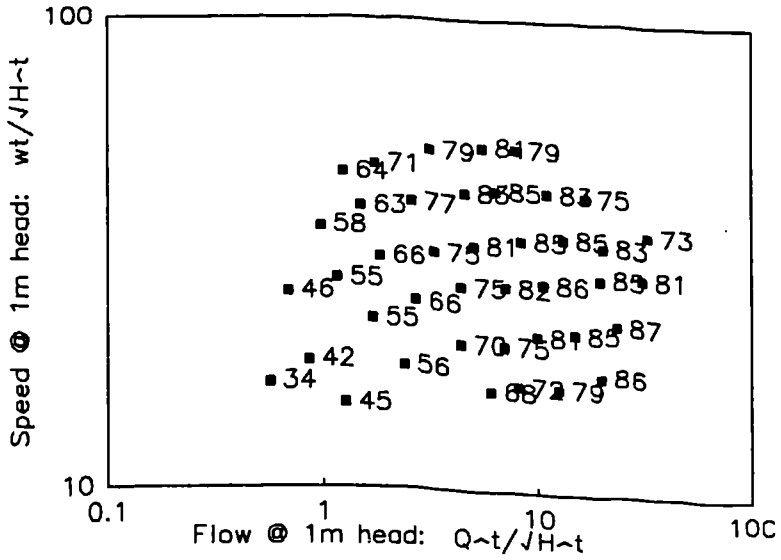

Fig. 56. Predicted BEPs for a series of standard centrifugal pumps.

KSB Etanorm pumps. The pumps that appear at the bottom of the pump catalogue are here at the top. The labels correspond to the percent efficiency. 'w' is ω.

The second graph is aimed at applications where the PAT's torque-speed relationship is given, principally constant-speed applications for electricity generation. In this case, the performance curves are shown on a flow-head coordinate system (Fig. 57).

36 Other application graphs are published by Fraser & A.[81], Schnitzer[92] and Williams[90].

37 Other factors may be taken into account in the selection of the running speed of a PAT: Chapallaz *et al.*[92] recommend a speed "well below" the maximum speed accepted for pump-mode, to avoid problems with the increase in head and power. A fast PAT requires a smaller inertia wheel, as noted by Giddens[91], and is itself smaller and hence cheaper, but its wear is faster, and the bearings and seals have to be replaced more often (Williams[90, 91c]).

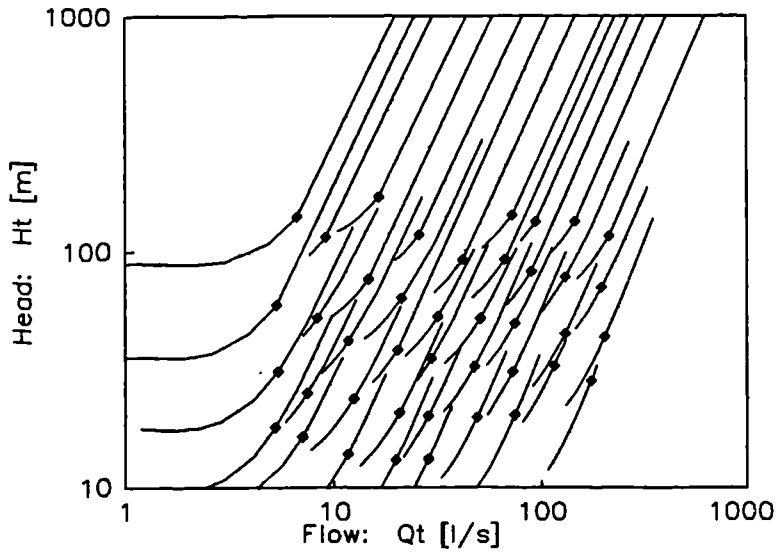

Fig. 57. Predicted off-BEP performance for a series of standard centrifugal pumps.
1850 RPM (*i.e.* 60 Hz., 4-pole induction generator). The ♦ represent the BEPs. The curves would be labelled with the codes of the relevant pumps.

Fig. 57 was built by defining the minimum and maximum operating points as those where the same power can be generated by another machine that uses a smaller flow, or where the efficiency is equal to 70% of the peak efficiency.

5.5 An Economic Evaluation of the Prediction Methods Based on Pump-mode Performance

5.5.1 Published Approaches

The simplest way to evaluate the accuracy of the prediction methods is to compare the predicted and the actual best-efficiency points, using as parameters the predicted/actual ratios for head and flow (as Chapallaz *et al.*[92] do). Fig. 58 illustrates such comparison, using the same test data described above and the new prediction method.

This approach does not take into account the fact that, when installed in real conditions, the PAT will not operate at its actual BEP, but at the intersection between its head-flow characteristics and the system (*i.e.* penstock) curve (see Fig. 6, p. 24). For this reason, Williams[92] considers a prediction as acceptable if the actual BEP is 'above and to the right', or 'below and to the left', but not 'above and to the left', nor 'below and to the right' of the predicted BEP, *i.e.* lie in the first or third quarter of the graph above. As the acceptability limit for the actual BEP, he defines an arbitrary ellipse shown in Fig. 59. (He was inspired by a similar ellipse defined by the British Standard Specification for Acceptance Tests for Pumps.) Moreover, Williams defines a single

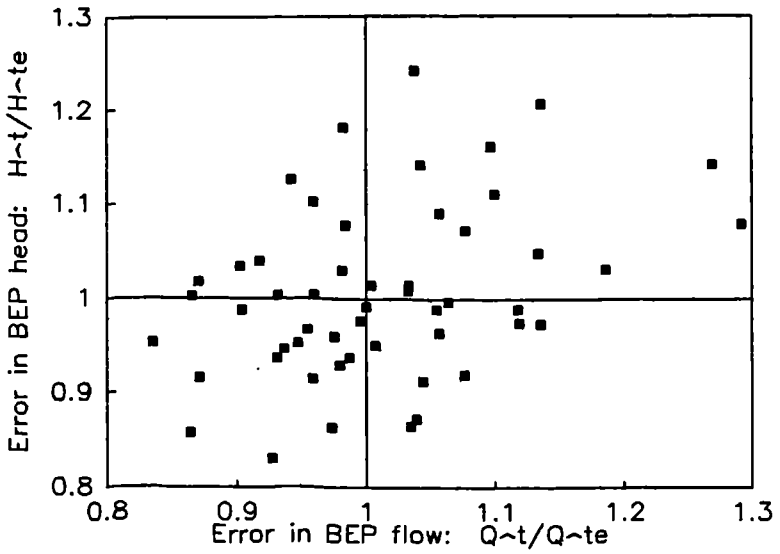

Fig. 58. $\hat{H}_T/\hat{H}_{TE}$ and $\hat{Q}_T/\hat{Q}_{TE}$ for the new prediction method.
Constant speed.

parameter *Cr* for the accuracy of the prediction, that measures the distance (in Fig. 59) between the actual and the predicted BEPs, 'weighted' by the ellipse 'radius' in this direction: it is 0.0 for an absolutely accurate prediction and 1.0 when the actual BEP is exactly on the perimeter of the ellipse (this gives *Cr* an approximately 'error squared' character). By averaging the *Cr*-values associated with each PAT of a set of test data, Williams measures the accuracy of different prediction methods.

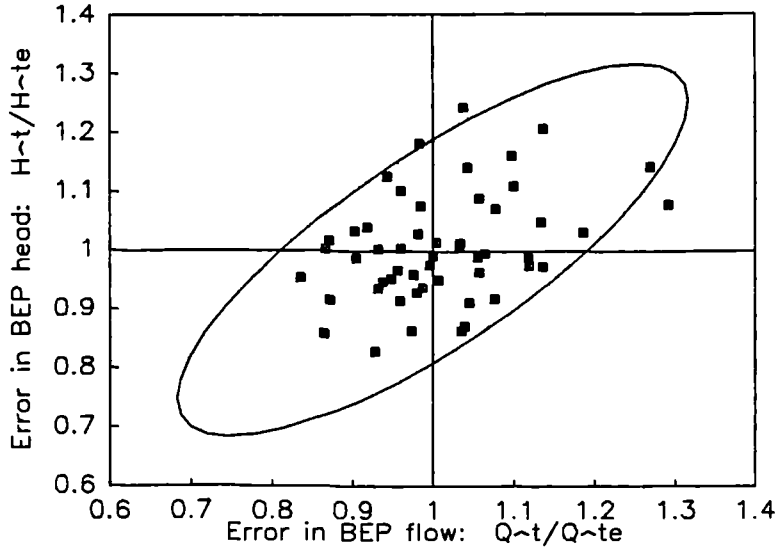

Fig. 59. The points of Fig. 58 and the elliptic limits for acceptable prediction proposed by Williams[92].
The ellipse is defined by the following points: (0.7, 0.7); (1.1, 0.9); (1.3, 1.3); and (0.9, 1.1).

A similar approach was followed by Alatorre-Frenk & Thomas[90]: they compared the predicted point with the actual **operating** point (*i.e.* the intersection between the penstock and the turbine head-flow curves), and they used as parameters the power and the flow. This comparison is illustrated in Fig. 60: in most cases a larger flow is accompanied by a larger power, and *vice versa.* (The procedure to calculate the actual operating point is described in p. 104).

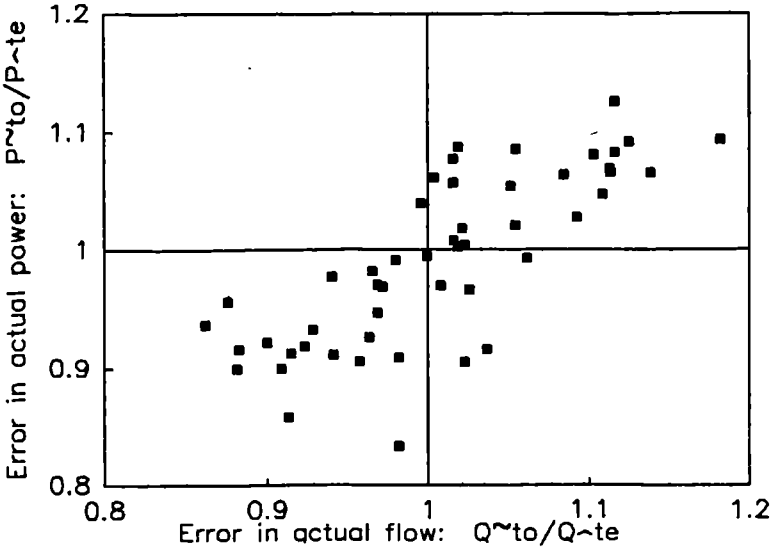

Fig. 60. $\tilde{P}_{TO}/\hat{P}_{TE}$ and $\tilde{Q}_{TO}/\hat{Q}_{TE}$ for the new prediction method.
Constant speed. Subscript $_O$ for actual operating conditions. Two points lie outside the graph: JYOT054, with coordinates (1.01, 0.79), and KENN157, with coordinates (1.07, 1.38) (see footnotes 29 and 30 above).

All these techniques evaluate in one way or another the errors in head, flow and power, but they do not provide an economic measure of the accuracy - or rather the lack of it - of the prediction methods. The economic methodology developed in Chapter 2 will be used here for this purpose.

5.5.2 Evaluation of the BEP Prediction

Introduction.

The trade-off between belt-drive and direct-drive cases was described in p. 76. The accuracy evaluation of the turbine-mode performance will be applied to these two cases in turn.

This section assumes that a belt-drive is used and that, therefore, the PAT is designed to operate exactly at its BEP (this is called assumption zero). The other case is examined in § 5.5.3.

In addition, the following four assumptions will be made here:

① The rated flow of the scheme $\tilde{Q}_T$ is the ideal, *i.e.* the one that optimises the benefit/cost ratio V/C of the scheme.

② The penstock efficiency $\tilde{\eta}_D$ is also the one that optimises the benefit/cost ratio. (Strictly speaking, this assumption implies that there is a continuous range of pipe diameters in the market.)

③ There is a continuous range of available PATs (*i.e.* an infinite number of models in the market).

④ The scheme has a single PAT, with neither part-load nor intermittent operation.

Assumptions ① and ② are hypothetical: in the reality, a micro-hydro design is usually made in a rather arbitrary way, without a careful hydrological and economic investigation. This means that, in the reality, errors in the prediction will sometimes worsen the scheme, and sometimes improve it! The hypothetical assumptions ① and ② represent then the worst case, where any error, positive or negative, worsens the benefit/cost ratio of the scheme.

Fig. 61 shows the predicted (dotted lines) and the actual (continuous lines) curves for the value (V), the cost (C) and the benefit/cost ratio (V/C), according to the proposed model. The three predicted curves may be above or below the actual curves. In this particular case, the predicted V is smaller than the actual V because the predicted peak efficiency $\hat{\eta}_{TE}$ is smaller than the actual $\hat{\eta}_T$, and the predicted C is larger than the actual C because the actual flow is larger than predicted (*i.e.* the actual 'cost per unit flow' is smaller than predicted). Then the predicted V/C is here smaller than the actual.

The actual operating point (**O**) is defined by the intersection of the penstock curve and the head-flow PAT characteristics. On account of the inaccuracy of the prediction, it does not meet assumptions zero, ① nor ②. The operating flow $\tilde{Q}_{TO}$ is different from the predicted $\tilde{Q}_{TE}$ [38], because assumption ① is not met ($\tilde{Q}_{TO}$ is not the ideal), and the operating value (V_O), cost (C_O) and benefit/cost ratio (V_O/C_O) are slightly off the respective actual curves, because assumptions zero and ② are not met (any point in the actual curves is assumed to meet these two assumptions). V_O and C_O may be below or above the corresponding actual curves, depending on the kind of error produced by the prediction, but V_O/C_O will always be below the actual V/C curve.

38 The rated-point diacritic ~ is used here, even though in this particular case the BEP diacritic ^ could be used.

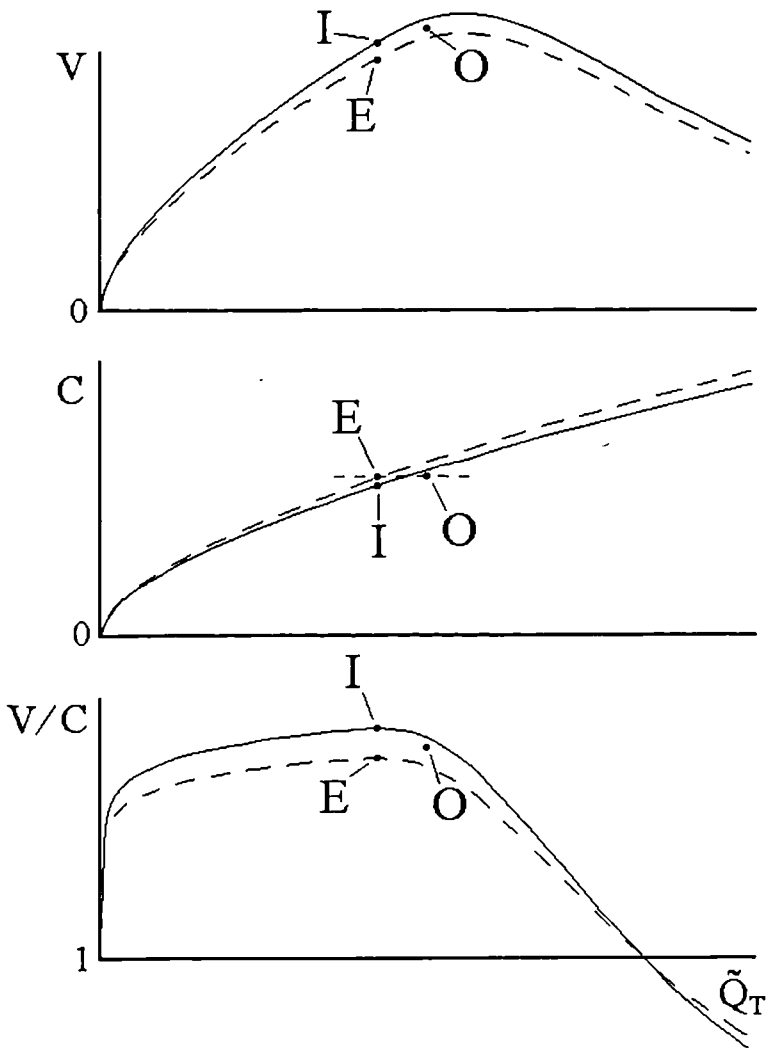

Fig. 61. Example of predicted, operating and ideal values and costs, as functions of rated turbine flow.

The symbols are the same used for the subscripts: **E** = predicted; **O** = operating and **I** = ideal. The dotted lines represent the prediction and the continuous lines the reality (see p. 21c).

In the particular case of Fig. 61, the operating flow $\tilde{Q}_{TO}$ is larger than the predicted $\tilde{Q}_{TE}$, and therefore the penstock is slightly under-dimensioned: C_O is slightly below the actual curve, and V_O as well. Finally, $V_O/C_O > V_E/C_E$, which means that the operating point is 'better' than the predicted one (though worse than the ideal one; see below). However, it does not make sense to talk about 'positive' errors of the prediction: this is why it is irrelevant to compare the operating benefit/cost ratio with the predicted one. (Imagine, for example, a nonsense prediction method that suggests that $\hat{\eta}_{TE} = \hat{\eta}_P/2$; in this case V_O/C_O would always be larger than V_E/C_E!)

On the other hand, the comparison between the operating V_O/C_O and the ideal V_I/C_I that would be obtained by an ideal 100%-accurate prediction method provides a

straightforward measure of the accuracy of the prediction: V_I/C_I is at the peak of the actual V/C curve, and therefore it is always larger than V_O/C_O.

Even though the predicted V/C curve is different from the actual V/C curve, it has its peak at the same $\tilde{Q}_T$ (on account of assumption ③ and because the actual value curve is equal to the predicted value curve multiplied by a **constant**, and the same happens with the cost). This means that the ideal flow $\tilde{Q}_{TI}$ is equal to the predicted $\tilde{Q}_{TE}$.

Assumption ③ (continuous range of available PATs) is also hypothetical. In the reality there would not be continuous curves as in Fig. 61, but a series of dots. In the reality the PAT selection is either wrong or right: the ideal method would select either the same PAT or another one. However, it is assumed that on average the result is correct (a 10% error with a probability of 10% is equal to a 1% error with a probability of 100%). Furthermore, it is assumed that the ideal PAT has the same peak efficiency as the selected PAT. Again this is not true: the efficiency of PATs depends on their specific speed, which means that the ideal PAT would in the reality be sometimes more efficient and sometimes less efficient than the selected PAT, but the end-result is, it is assumed, on average equivalent.

Comparison of Benefit and Cost.

From assumption ④, the power P_T is always equal to the (constant) rated power $\tilde{P}_T$, and therefore we remove it from the integral of Eq. [5], p. 18, to get:

$$V = K_d K_e \left(\rho g \tilde{Q}_T \tilde{z}_A \tilde{\eta}_T \tilde{\eta}_D\right)^{\Gamma} \int_{\tilde{Q}_T}^{\infty} d\left(e^{\lambda Q_A^{\mu}}\right) \qquad [77]$$

Therefore:

$$V = K_d K_e \left(\rho g \tilde{z}_A \tilde{\eta}_T \tilde{\eta}_D\right)^{\Gamma} \tilde{Q}_T^{\Gamma} \left(1 - e^{\lambda \tilde{Q}_T^{\mu}}\right)$$

The relation between the operating and the ideal benefits is then:

$$\frac{V_O}{V_I} = \frac{\left(\tilde{\eta}_{TO} \tilde{\eta}_{DO} \tilde{Q}_{TO}\right)^{\Gamma} \left(1 - e^{\lambda \tilde{Q}_{TO}^{\mu}}\right)}{\left(\tilde{\eta}_{TI} \tilde{\eta}_{DI} \tilde{Q}_{TI}\right)^{\Gamma} \left(1 - e^{\lambda \tilde{Q}_{TI}^{\mu}}\right)} \qquad [78]$$

As for the cost, for the sake of algebraic manipulation, instead of C (Eq. [9], p. 20), a simplified C' will be used:

$$C' = \left[k'_M + k'_D \left(1 - \tilde{\eta}_D\right)^{-0.4}\right] \tilde{q}_T^{\odot'} \left(1 + K'_d k_O\right) \qquad [79]$$

As we will just compare costs, we can further simplify this cost equation by assuming $k'_M = 1$:

$$C' = \left[1 + k'_D\left(1 - \tilde{\eta}_D\right)^{-0.4}\right]\tilde{q}_T^{\Theta'}\left(1 + K'_d k_O\right) \qquad [80]$$

This simplified C' can be made very close to C in the range of interest, namely in the vicinity of the ideal point, by making...:

$$C_I = C'_I \qquad [81]$$

..., and moreover:

$$\frac{d_I C}{d\tilde{q}_T} = \frac{d_I C'}{d\tilde{q}_T} \qquad [82]$$

Substituting in Eq. [80] the ideal and the actual operating costs, we get the following equation:

$$\frac{C'_O}{C_I} = \frac{1 + k'_D\left(1 - \tilde{\eta}_{DO}\right)^{-0.4}}{1 + k'_D\left(1 - \tilde{\eta}_{DI}\right)^{-0.4}}\left(\frac{\tilde{Q}_{TO}}{\tilde{Q}_{TI}}\right)^{\Theta'} \qquad [83]$$

The economic advantage of the actual operating point with respect to the ideal point is, from Eq. [10], p. 21b:

$$Æ_{O,I} = \frac{\left(\frac{V_O}{C'_O}\right)}{\left(\frac{V_I}{C_I}\right)}$$

This is the economic 'advantage' of a prediction method with respect to an ideal 100%-accurate method. (We will continue using the term 'economic advantage' as defined in Chapter 2, although in this case it is always a disadvantage, i.e. $Æ < 1$.)

Taking into account that $\tilde{Q}_{TI} = \tilde{Q}_{TE}$ (hence $\tilde{H}_{TI} = \tilde{H}_{TE}$), that $\tilde{\eta}_{TI} = \hat{\eta}_T$, and that...:

$$\tilde{\eta}_{DO} = \frac{\tilde{H}_{TO}}{z_A} = \frac{\tilde{H}_{TO}}{\tilde{H}_{TI}}\tilde{\eta}_{DI} = \tilde{\eta}_{DI}\frac{\tilde{H}_{TO}}{\tilde{H}_{TE}}$$

..., and substituting Eqs. [78] and [83], we get:

$$Æ_{O.I} = \frac{1 + k'_D\left(1 - \tilde{\eta}_{DI}\right)^{-0.4}}{1 + k'_D\left(1 - \tilde{\eta}_{DI}\frac{\tilde{H}_{TO}}{\tilde{H}_{TE}}\right)^{-0.4}}\left(\frac{\tilde{\eta}_{TO}\tilde{H}_{TO}}{\hat{\eta}_T\tilde{H}_{TE}}\right)^{\Gamma}\left(\frac{\tilde{Q}_{TO}}{\tilde{Q}_{TE}}\right)^{\Gamma-\Theta'}\frac{\left(1 - e^{\lambda\tilde{Q}^{\mu}_{TO}}\right)}{\left(1 - e^{\lambda\tilde{Q}^{\mu}_{TE}}\right)} \qquad [84]$$

This is the proposed formula to evaluate the economic 'advantage' of a prediction method.

Results of the Evaluation.

The accuracy of the prediction methods was evaluated by averaging $Æ_{O,I}$ over all test-PATs (test data in Appendix B). The same reference scenario described in Chapter 3, p. 41 was used. Substituting and differentiating Eqs. [9] and [80] in Eqs. [81] and [82], we get the definition of Θ' and k'_D in terms of the coefficients used in Chapter 3 to establish the reference scenario:

$$\Theta' = \frac{\Theta(k_T + k_M)\tilde{q}_{TI}^{\Theta} + 0.8k_D(1-\tilde{\eta}_{DI})^{-0.4}\tilde{q}_{TI}^{0.8}}{(k_T + k_M)\tilde{q}_{TI}^{\Theta} + k_D(1-\tilde{\eta}_{DI})^{-0.4}\tilde{q}_{TI}^{0.8}}$$

$$k'_D = \frac{(k_T + k_M)\tilde{q}_{TI}^{\Theta-\Theta'} - 1}{(1-\tilde{\eta}_{DI})^{-0.4}} + k_D\tilde{q}_{TI}^{0.8-\Theta'}$$

Finally, assumptions ① and ② have to be met. Assumption ① ($\tilde{Q}_T$ is the ideal)...:

$$\frac{d_I\left(\frac{V}{C'}\right)}{d\tilde{Q}_T} = 0$$

... leads to this implicit equation:

$$\Gamma - \Theta' = \frac{\lambda\mu\tilde{Q}_{TI}^{\mu}}{e^{-\lambda\tilde{Q}_{TI}^{\mu}} - 1}$$

And assumption ② ($\tilde{\eta}_D$ is the ideal)...:

$$\frac{d_I\left(\frac{V}{C'}\right)}{d\tilde{\eta}_D} = 0$$

... leads to another implicit equation:

$$k'_D = \frac{-1}{(1-\tilde{\eta}_{DI})^{-0.4}\left[1 + \frac{-0.4}{\Gamma}\frac{\tilde{\eta}_{DI}}{(1-\tilde{\eta}_{DI})}\right]}$$

The reference scenario is then defined as follows: $\mu = -0.8$, $\Gamma = 1.0$, $\Theta' = 0.66$, $k'_D = 0.27$, $\lambda\tilde{Q}_{TI}{}^{\mu} = -1.52$ and $\tilde{\eta}_{DI} = 0.87$; constant-speed operation.

The following calculation procedure was repeated for each test-PAT: the predicted turbine-mode BEP (point **E**) was calculated from the pump-mode BEP test-data; then it was assumed that this predicted turbine-mode BEP was the optimum solution for a hypothetical site under a given scenario, *i.e.* a site was **simulated** to match the PAT prediction. Using the turbine-mode test-data and the simulated penstock head-flow curve, the actual operating point (**O**) was established[39]. Finally, the economic advantage of the prediction method was calculated with Eq. [84].

Fig. 62 shows for each test-PAT the economic advantage of the new prediction method. Note that the points have a nearly-parabolic envelope. Those located close to the envelope are operating almost at the BEP, even if the flow is not the predicted, whereas those located far below the envelope are operating at a much-lower-than-optimum efficiency.

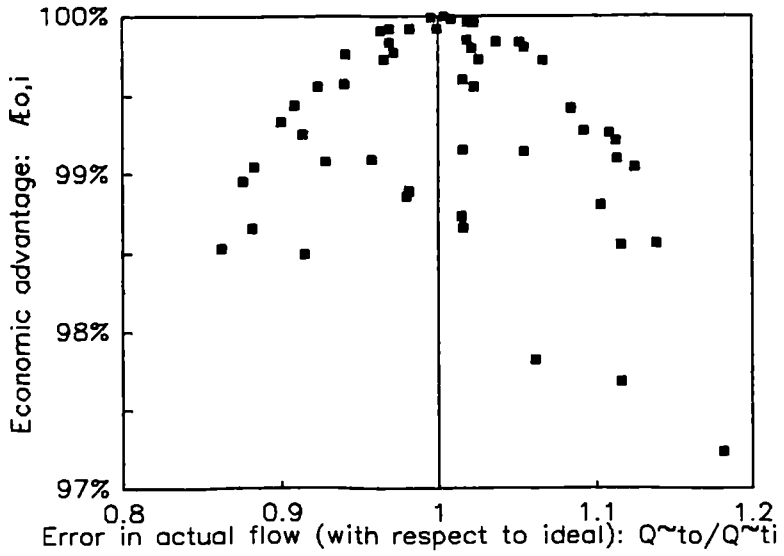

Fig. 62. $Æ_{O,I}$ and $\tilde{Q}_{TO}/\tilde{Q}_{TI}$, for the new prediction method.
Constant speed, reference scenario.

Finally, Figs. 63, 64 and 65 compare the performance-based prediction methods for end-suction, double-suction and bowl PATs respectively. The new method has the highest values of $Æ_{O,I}$, which is not by itself a great achievement, since its accuracy is being measured with the same set of data used for its development.

39 In fact the PAT head characteristics curve was not calculated from the original test data, but from the elasticities E_T and E_{2T}, that were in turn calculated by regression; see p. 92 and Appendix E.

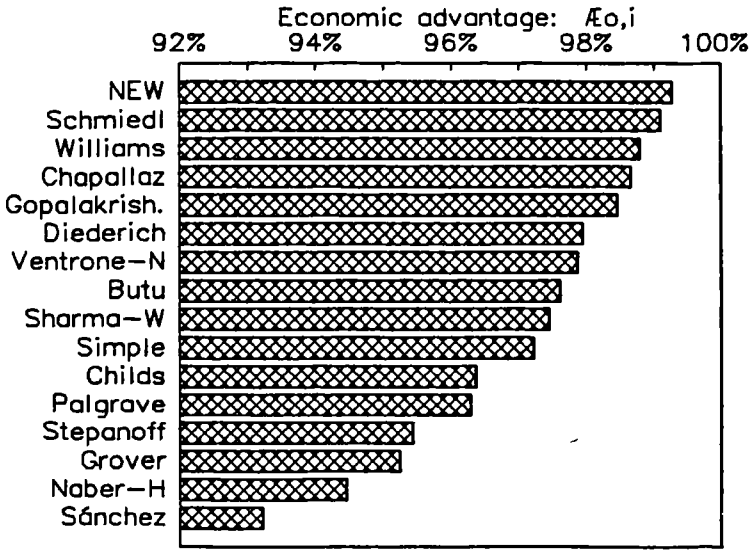

Fig. 63. $Æ_{O,I}$ for end-suction (volute, diffuser and multistage) PATs.

Constant speed, reference scenario. All methods evaluated with 41 test-PATs, except Schmiedl (34), Grover (35) and Diederich (29), that have specific-speed restrictions.

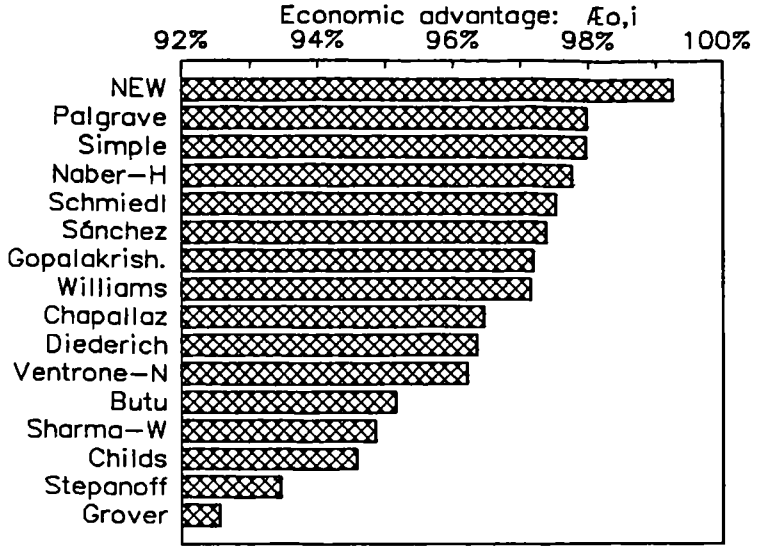

Fig. 64. $Æ_{O,I}$ for double-suction PATs.

Constant speed, reference scenario. All methods evaluated with 7 test-PATs.

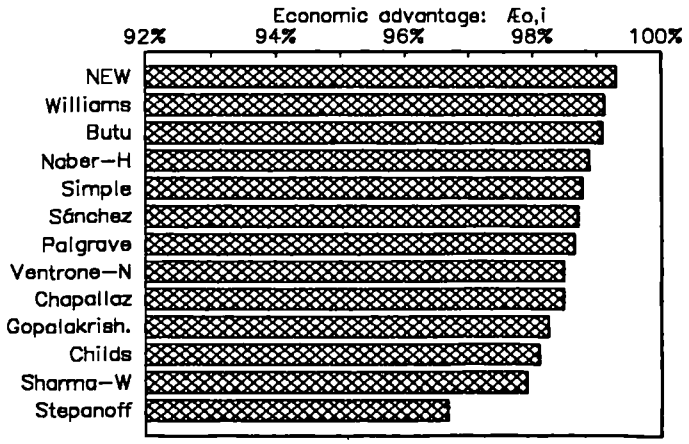

Fig. 65. $Æ_{O,I}$ for bowl-casing PATs.
Constant speed, reference scenario. All methods evaluated with 9 test-PATs.

In addition to the methods described above, a further one, labelled 'simple', is included in the figures: it has a constant flow conversion factor of 1.4, and a constant head conversion factor equal to 1.56; it seems to be slightly better that the other constant-factor prediction methods and is included here just to evaluate the advantage of using a more complex method.

The effect of changes in the reference scenario is as follows: The new method had a $Æ_{O,I} = 99.28\%$ with end-suction pumps, under the reference scenario. This advantage was reduced to 99.20% with constant-efficiency operation and to a low 98.34% with constant-torque operation[40]. $Æ_{O,I}$ increased to 99.43% with $\Gamma = 0.7$ and was slightly reduced to 99.24% with $k'_D = 0.5$.

The cost of the inaccuracy of the prediction methods has three elements, corresponding to the non-compliance of the three assumptions mentioned above. Assumption ②, related to the penstock efficiency $\tilde{\eta}_{DI}$, is the most indirect one; its weight can be measured by making $k'_D \approx 0$ ($\therefore \tilde{\eta}_{DI} \approx 0$), *i.e.*: the penstock is so cheap that it is very, very large, and any increase or reduction in flow has a negligible effect on the head-loss. The result is $Æ_{O,I} = 99.41\%$ with $k'_D \approx 0$, which shows that the indirect effect of the non-compliance of assumption ② is not marginal[41].

Finally, a run was made to evaluate the impact of adjusting the rotating speed of the turbine after initial field tests, in order to achieve BEP performance, as mentioned in p. 55. In this case $Æ_{O,I}$ was increased to 99.66%, *i.e.* the disadvantage was reduced to less than half, which shows that this is a very useful technique, when possible.

---

40 Driving a positive-displacement pump, for example, is a nearly constant-torque operation, as long as the pump head is constant.

41 According to Williams[92], the error in the prediction is higher for high values of $\tilde{\eta}_D$.

5.5.3 Evaluation of the Off-BEP Prediction

Introduction.

This second part of the accuracy evaluation assumes that a direct-drive is used and that, therefore, there is a restriction in the driven end (namely any fixed speed-torque relation, *e.g.* constant or nearly constant speed in the case of electricity generation). The PAT does not necessarily operate at its BEP, and assumption zero (see p. 98) is then eliminated.

Moreover, in order to be consistent with the off-BEP operation, it can not be assumed that there is a continuous range of available PATs. As the complexity of the model would be greatly increased if assumption ③ is eliminated altogether, it will be simply refined by considering a discrete range in $\hat{H}_T$, but a continuous range in $\hat{Q}_T$.

Therefore, this model considers that there is a finite number of PAT 'classes': each 'class' corresponds to a given (optimum) head, and has an infinite number of models, each one for a different (optimum) flow.

It will be assumed that the adjacent PATs (not only within the same class, but also in neighbouring classes) have not only the same efficiency (as assumed above) but also the same relative off-BEP performance. This, again, should not greatly affect the end-result.

The application boundary between one class and the next one is defined by the point where both have the same efficiency, as represented in Fig. 66. (As the model assumes

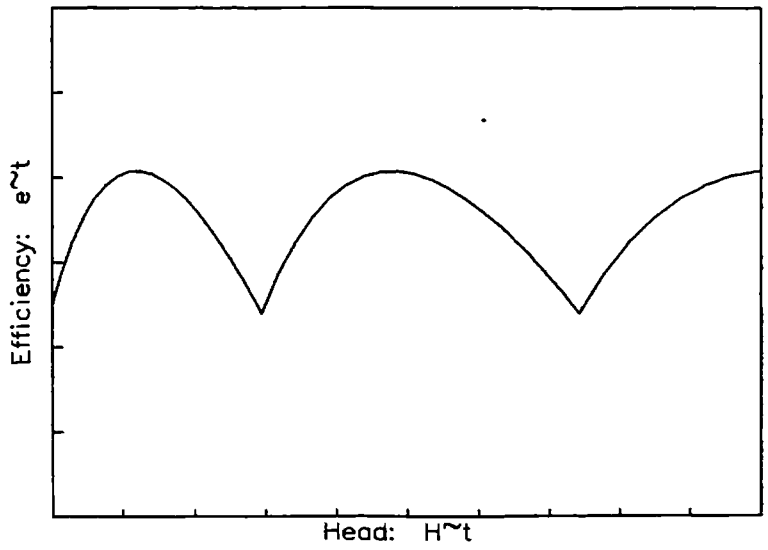

Fig. 66. Typical relation between $\tilde{\eta}_T$ and $\tilde{H}_T$, according to the proposed model.
Three consecutive classes are shown. Constant speed performance.
Prediction made for BUSE024.

that all PATs have the same relative performance, the head-efficiency relation shown in Fig. 66 would be valid for any flow.)

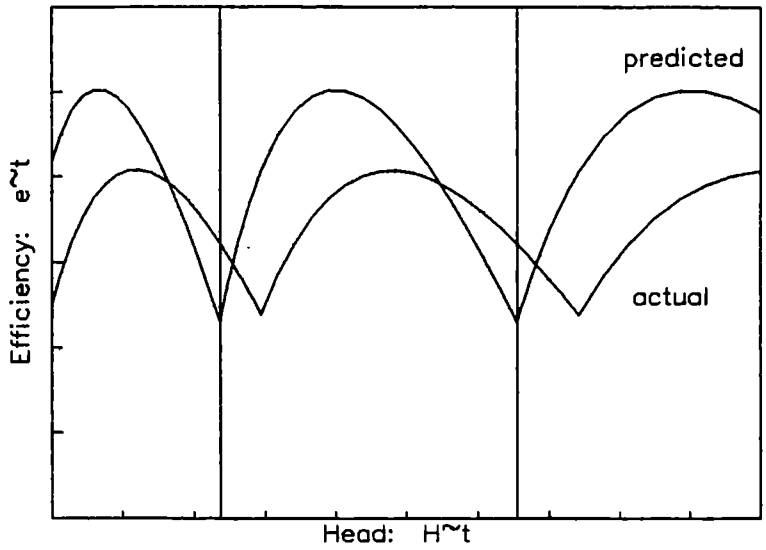

Fig. 67. Typical predicted and actual (ideal) efficiency-head relations.

On account of the prediction errors, the actual efficiency-head relation is different from the predicted (Fig. 67). Therefore, the range of application of a given class (marked by vertical lines in Fig. 67) is divided in two sectors: one where an ideal prediction method would have selected the same PAT (or rather a PAT of the same class), and one where the ideal method would have selected a PAT of a neighbouring class.

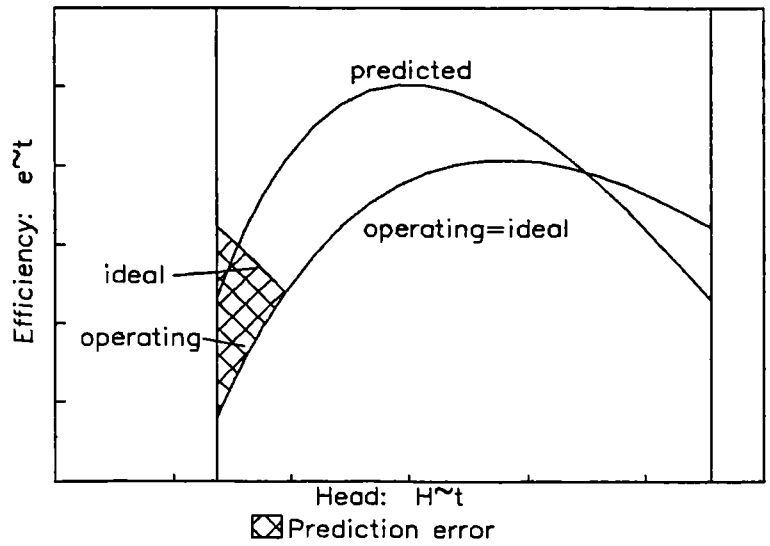

Fig. 68. Typical predicted, operating and ideal efficiencies.

This is illustrated in more detail in Fig. 68: in the small sector were the ideal method would have selected a different class of PATs, the actual operating efficiency is lower than the ideal, and the hatched area represents this error. In the rest of the range both ideal and operating efficiencies are equal (and then the prediction error is very small - only due to the difference between predicted and actual flow).

This model for the off-BEP accuracy evaluation requires one additional variable, to represent the distance between one class and the next one. This variable, called δ, is defined as the ratio between the optimum head for one class and the optimum head for the next (lower) class. Adjacent pumps (with similar flows and different heads) in pump catalogues have head ratios between 1.4 and 1.8. These are then typical values for δ in our model. (δ = 1.5 in Figs. 66, 67 and 68.)

Results of the Evaluation.

The evaluation procedure (repeated for each test-PAT) was as follows: Taking into account the predicted turbine-mode BEP, the predicted performance outside the BEP and an assumed value of δ, the range of application of the simulated PAT class was defined. Then this class was divided into a finite number of steps, each for a different head, and for each step the economic advantage was calculated using Eq. [84]. Finally, all these economic advantages were averaged to get the economic advantage ($Æ_{O,I}$) of the off-BEP prediction.

Fig. 69 shows the economic advantage (in terms of δ) of the new off-BEP prediction method on its own, *i.e.* assuming that the BEP prediction is error-free: the error for

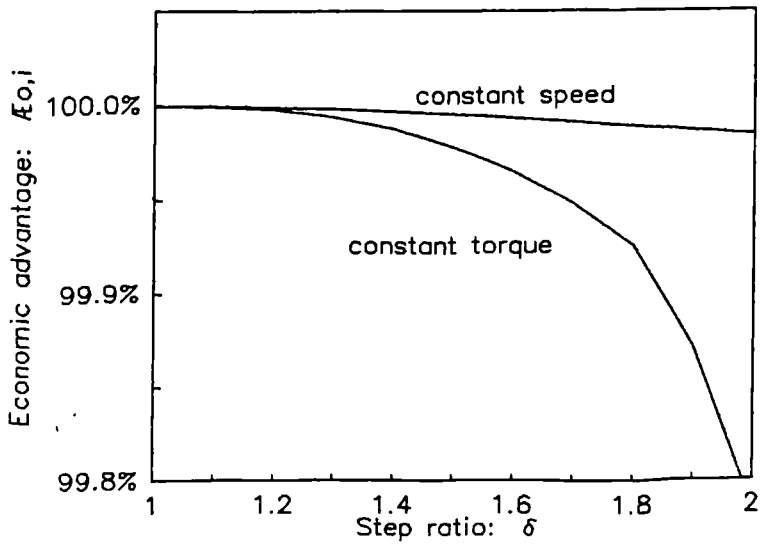

Fig. 69. Economic advantage of the new off-BEP prediction method, in terms of the step ratio δ.

End-suction PATs, reference scenario. Error-free BEP prediction; δ = 1 means no off-BEP operation (and therefore no off-BEP prediction error).

constant-speed operation is negligible ($Æ_{O,I} > 99.98\%$), while constant-torque operation produces a larger (although still minor) error.

The larger error associated with constant-torque operation is due to a sharper fall in efficiency outside the BEP, as illustrated in Fig. 70.

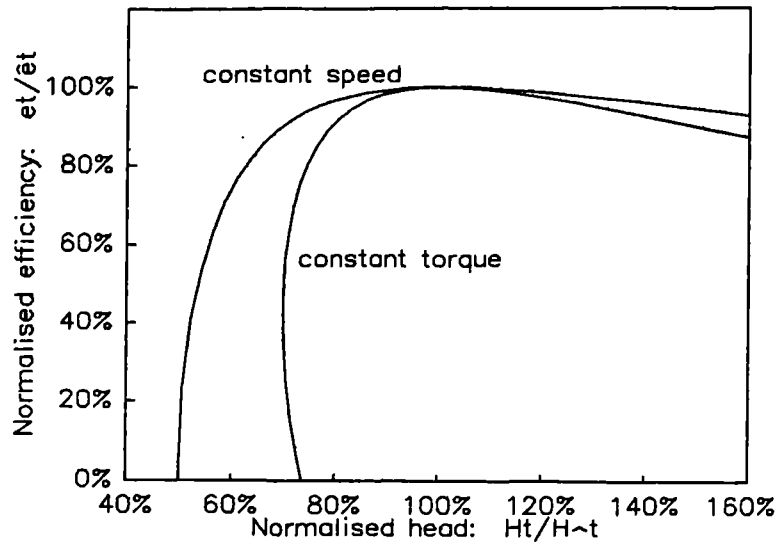

Fig. 70. Typical efficiency-head relations for constant-speed and constant-torque operation.
Graphs drawn using the new prediction method, and assuming $\Omega_P = 0.5$ and $\eta_D = 0$.

Due to the asymmetry of the head-efficiency curves (shown in Fig. 70), when the predicted point is to the 'left' of the BEP, there is a risk of getting too low an actual

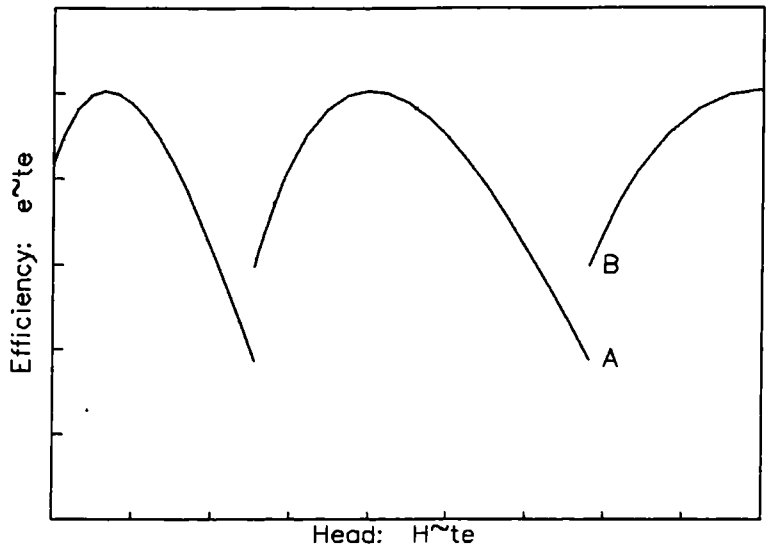

Fig. 71. Biased definition of the application range for a PAT class.
In this case $\kappa < 1$.

operating efficiency $\tilde{\eta}_{TO}$. This risk can be avoided by establishing the range of application of the PAT class with a bias, as illustrated in Fig. 71, *i.e.* by locating the border between classes at the point where the efficiency of the 'lower' class (point A in Fig. 71) is equal to the efficiency of the 'higher' class (point B) multiplied by a bias parameter κ.

When the new off-BEP prediction method is evaluated on its own (as in Fig. 69, assuming that the BEP prediction is error-free), the bias is not applicable (*i.e.* the optimum κ is 1.00 for $1 < \delta < 2$). However, when the whole new prediction method (BEP and off-BEP prediction altogether) is evaluated, the prediction errors are much larger and κ becomes relevant, especially for constant-torque operation, as shown in Fig. 72.

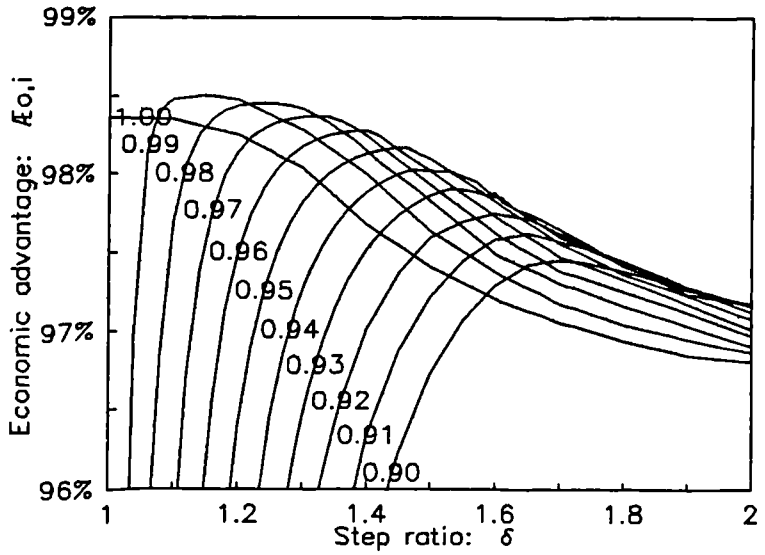

Fig. 72. $Æ_{O,I}$ of the whole new prediction method (BEP and off-BEP), in terms of δ and κ, for constant-torque operation.
End-suction PATs, reference scenario. The lines represent different values of κ.

Thus under constant-torque operation an improvement in economic advantage of the order of 0.7% is achievable by biasing machine selection slightly towards apparently oversize pumps (for $\delta = 1.5$, a typical value, the optimum efficiency bias is 5%). With constant-speed operation however (see Fig. 73), the bias is inapplicable for the usual values of δ, and even for large values its effect is negligible.

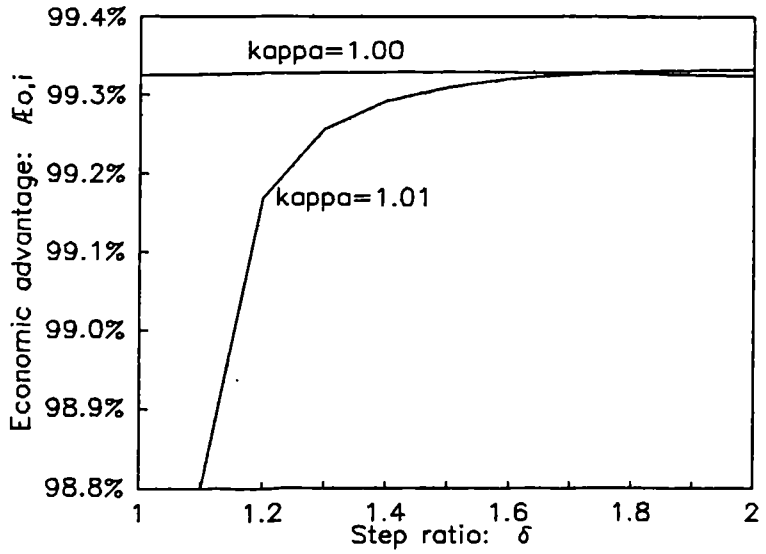

Fig. 73. $Æ_{O,I}$ of the whole new prediction method (off-BEP and BEP), in terms of δ and κ, for constant-speed operation.
End-suction PATs, reference scenario. 'kappa' is κ.

5.5.4 A Note about Over-designing

The class selection bias mentioned above leads to the following question: is a bias applicable also to the pure BEP prediction?, *i.e.*: even when the kind of flexibility provided by a belt-drive is available, is it appropriate to design for a predicted rated point outside the BEP?

In order to answer this question, the economic advantage of designing for a rated point off the BEP was evaluated. In this case, the methodology followed was similar to the one used for the BEP prediction evaluation (*i.e.* with $\delta = 1$), but without assumption zero (see p. 98). The predicted point is not necessarily at the BEP, but the ideal is.

The results of this evaluation (Fig. 74) answer the question: designing for a predicted rated point outside the BEP is not appropriate for constant-speed operation[42], but it may be for other patterns of operation, such as constant-torque. In the case shown in Fig. 74, lower curve, a 0.2% improvement in economic advantage can be achieved by choosing a machine with a head bias of +4%.

---

42 Williams[90] suggested multiplying Sharma's prediction formulae by 1.1 to take into account the asymmetry of the efficiency curve, as mentioned above (p. 73). His method is certainly better than Sharma's, but this is probably because it gives in fact values **closer** to the BEP than Sharma's.

Burton & M.[92] propose a further reason for over-designing, namely the ability to operate the PAT with reduced flow at a "reasonable" efficiency. However, if we take into account the head wasted at reduced flows (see Fig. 7, p. 25), the actual power produced would be in fact lower, except for very small flows.

(The raising trend of σ_{Tcrit} in Fig. 85, p. 128 could be in some cases a further reason against over-designing.)

Note that we are neglecting here the difference in cost between a small and a large PAT, and therefore this conclusion is referred only to the efficiencies of the machines. If we take into account that a smaller machine is cheaper, there could be an economic advantage in over-designing.

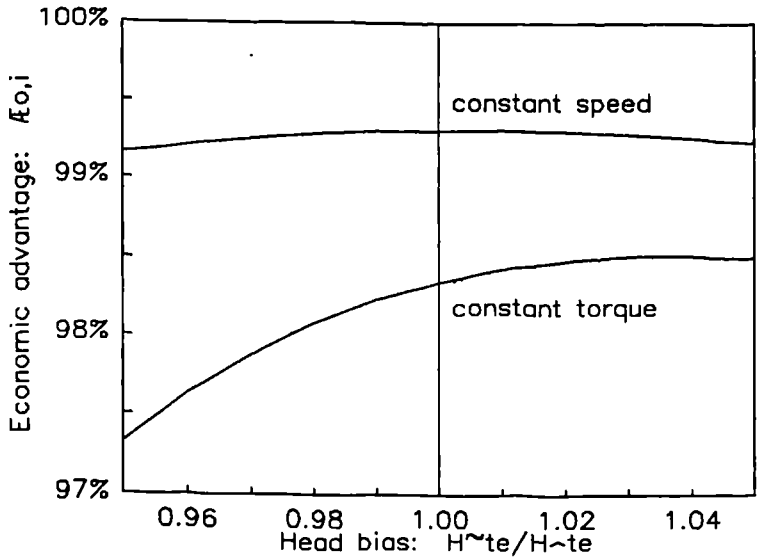

Fig. 74. $Æ_{O,I}$ when the predicted rated point is outside the BEP.
End-suction PATs, reference scenario.

5.6 Discussion

The economic methodology proposed in Chapter 2 was successfully applied to measure the penalty associated with the inaccuracy of the prediction methods[43].

The results of this evaluation show that the new BEP prediction method achieves an economic advantage of about 99.3% (*i.e.* 0.7% less than using an ideal 100%-accurate prediction method), with constant-speed operation, any kind of pump, and under a broad range of economic and hydrological conditions. This is considered acceptable. When the speed of the turbine can be adjusted after initial field tests, the penalty is reduced to about 0.35%. If the PAT has to be designed to operate outside its BEP (because pumps are only available in discrete sizes, with rated head steps of about 150%), the extra cost associated with imperfections in the off-BEP prediction is insignificant for such constant-speed operation.

[43] In this case the use of the net present value (see pp. 20-21b), instead of the benefit-cost ratio would produce a very similar result, since we are not comparing options of different sizes, as we did in Chapters 3 and 4.

Constant torque operation is however less favourable: the benefit/cost ratio is reduced by about 1.7% (compared to using the optimum PAT) for the BEP case, and by more than 2% for the off-BEP case.

Finally, when the pump-performance data required by the new prediction method are not available, simpler methods can be used at the expense of the benefit/cost ratio (more than 2% reduction for the most simple methods). The advantage of using the new PAT selection method developed here (or one of the other recent methods, see Figs. 63-65) is therefore a substantial one in relation to the small increase in system design effort it involves.

An issue that has not been dealt with is the relation between speed and efficiency. The results obtained by Santolaria & F.[92] hint that it is different in both modes of operation (in their tests, the peak efficiency diminished more abruptly in turbine-mode than in pump-mode when the speed was reduced), but the data are clearly too scarce to enable any conclusion to be drawn, and further research is required in this area (more data published by Diederich[67]).

6
EXPERIMENTATION

A PAT test-rig was built in the Department of Engineering of Warwick University using a pump kindly lent by SPP Pumps Ltd., with the primary purpose of establishing the turbine-mode cavitating performance of the machine. The normal (non-cavitating) performance tests are described firstly, and the issue of cavitation is discussed later.

6.1 Pump-as-turbine Tests

6.1.1 Pump Description

The tested PAT is a SPP Unistream 65/16 end-suction pump, with 80 mm (pump-mode inlet) and 65 mm (pump-mode outlet) branches.

The impeller has 6 double-curvature blades, 4 mm thick; their dimensions are shown in Fig. 75a. The circumferential area between rotor blades at the tip of the impeller is then $a_2 = 18\text{mm}\times(174\text{mm}\times\pi - 6\times 4\text{mm}/\sin 33°) = 9046\text{mm}^2$.

The volute throat area, measured according to Fig. 75b, is $B^2 = 3271\text{mm}^2$. The area ratio is then, from Eq. [37] (p. 65), $Y = 9046\times\sin 33°/3271 = 1.51$.

6.1.2 Test-rig Description

An outline of the test-rig is shown in Fig. 76. The PAT is located on a tower about 4.5 m above the feed pump, so as to prevent the latter from cavitating when the former is cavitating.

Instead of the pressurised tanks and vacuum pumps (and degassed water) used in industrial cavitation test-rigs, in this low-cost rig the pressure of the semi-closed circuit PAT-feed-pump is controlled with valves **L2** and **H2**: The highest pressure corresponds to **L2** open and **H2** closed, and then the pressure is reduced by gradually

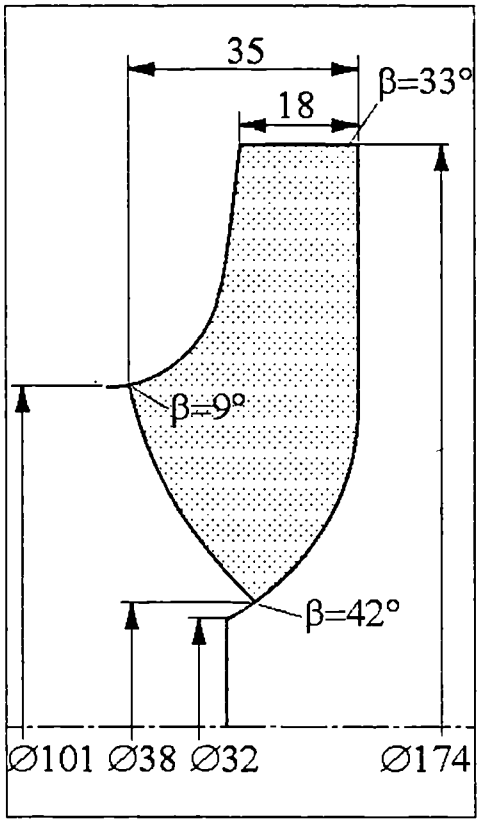

Fig. 75a. Geometry of the pump impeller blades.

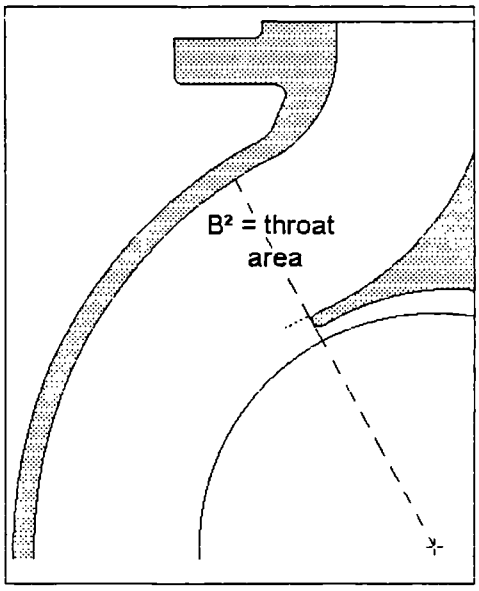

Fig. 75b. Criterion for the measurement of the volute throat area.

opening **H2**. If both valves are just slightly opened, the flow that by-passes the PAT through the upper tank is insignificant as compared with the PAT flow, and the PAT head and flow are kept essentially constant when the opening of **H2** is varied. This method of pressure control is adequate, except when severe cavitation is causing

significant density changes in the hydraulic circuit. Under these latter conditions, circuit instability is manifest and it is not possible to stabilise pressures. As the purpose of the rig was to measure the **onset** of cavitation, this instability was acceptable.

Different operating conditions are obtained by varying the electric load on the dynamometer or by throttling the circuit with valve **T**. Valves **L1** and **H1** are used for similar purposes in non-cavitating tests, and valve **Z** is closed just when the circuit is purged.

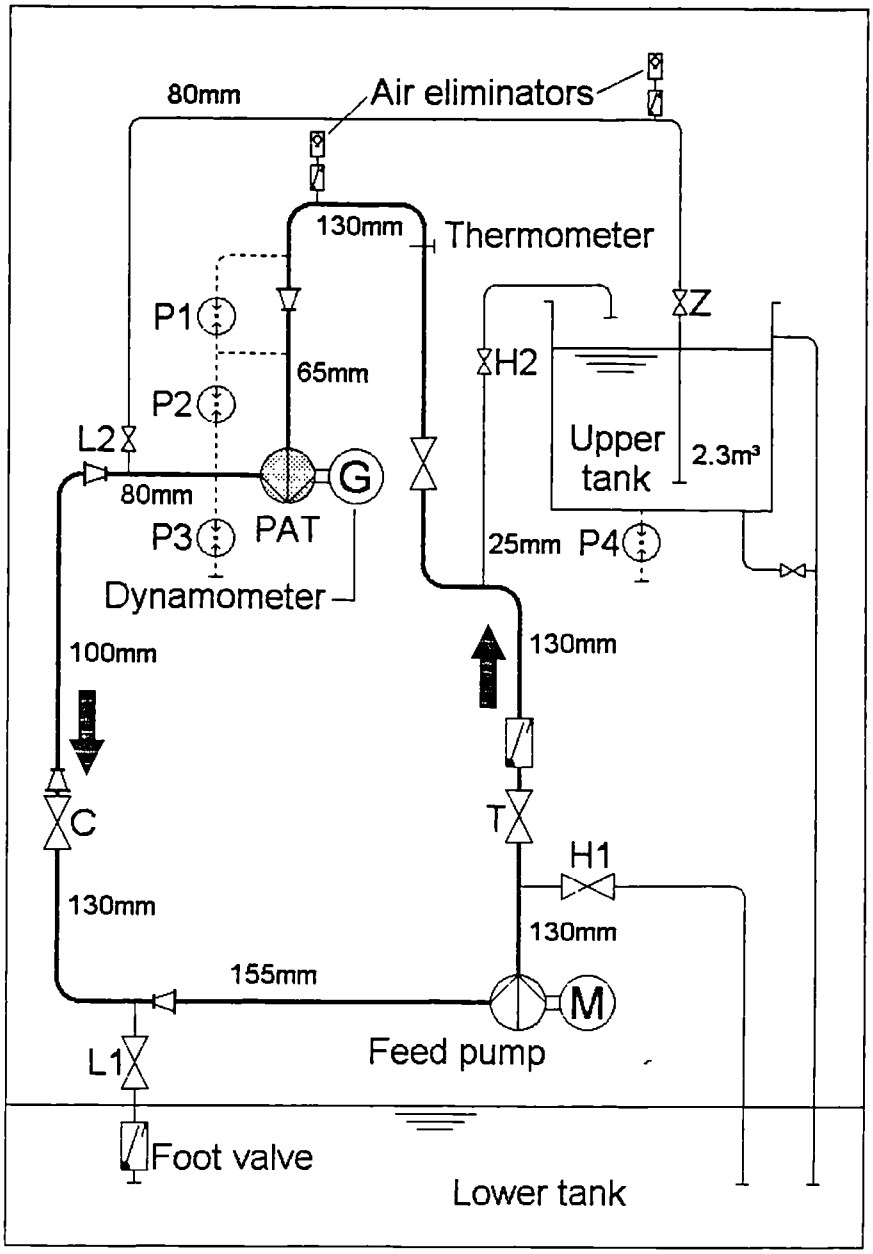

Fig. 76. Cavitation test-rig layout.
Valves designated depending on the branch they are in: the **L**ow-pressure PAT→pump branch or the **H**igh-pressure pump→PAT branch.

All the measurements, except the water temperature, are logged in a portable computer (the processing of data is described with more detail in Appendix D):

① The flow is indirectly determined by measuring with differential pressure transducer **P1** the pressure drop across a reduction. These flow measurements are calibrated by making special calibration tests, that consist in filling the upper tank (by keeping **C** closed and **L2** and **L1** open) and recording the tank volume variation with transducer **P4.**

② The head is established by measuring the pressure drop across the turbine with differential pressure transducer **P2** and taking into account the difference in velocity head between the inlet and the outlet.

③ The outlet pressure of the turbine is measured with pressure transducer **P3.**

④ The speed is measured by software-counting the square-wave cycles produced by a stationary Hall effect device and a magnet mounted on the shaft.

⑤ Finally, the torque is calculated by measuring with a load cell the force of the dynamometer arm (this is a rocking dynamometer with a double-set of bearings).

6.1.3 Pump-mode Performance

Pump-mode tests were not possible in the test-rig, but the manufacturers made 'acceptance' tests before delivery, whose results are shown in Fig. 77. The BEP for a

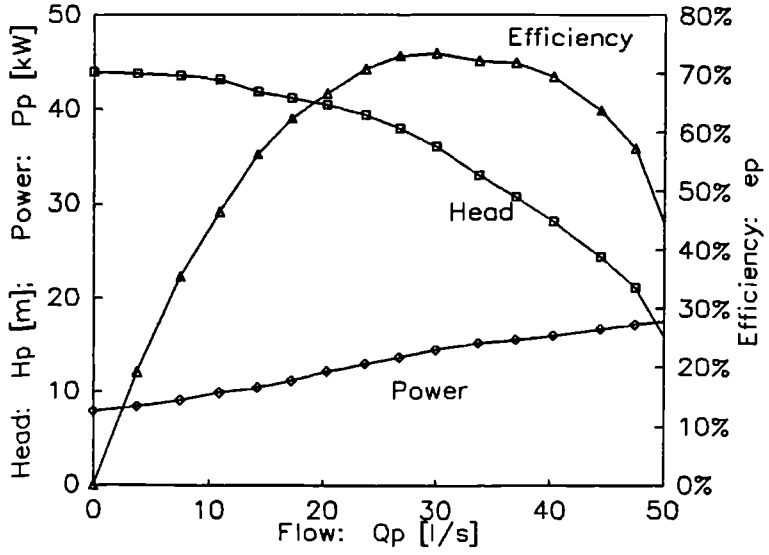

Fig. 77. Pump-mode performance, according to the acceptance tests.
Data corrected to 2950 RPM.

polynomial best-fit based on these test data is: $\hat{Q}_P = 31.29$ l/s; $\hat{H}_P = 35.13$m and $\hat{\eta}_P = 74.0\%$ (at 2950 RPM)[1]. Therefore $\Omega_P = 0.68$.

6.1.4 Turbine-mode Performance

The non-cavitating turbine-mode tests were made in different runs, each one with a given setting of the valves and a varying electric load on the dynamometer. In this way no parameter was kept constant. However, the turbine head was nearly constant: it just varied somewhat because when the flow was reduced the feed-pump head was increased and *vice-versa*. By using the affinity laws we can correct the values obtained to draw a constant-head performance representation; Fig. 78 shows this turbine-mode 'unit-head' performance graph for two different valve settings.

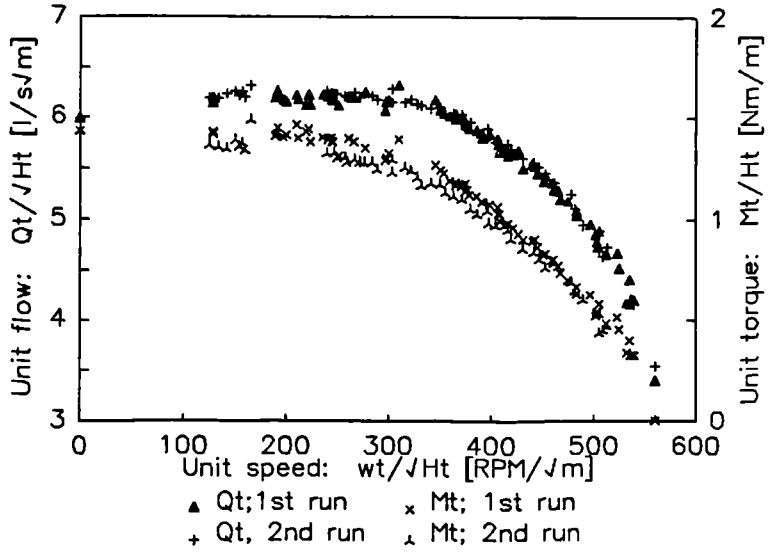

Fig. 78. PAT 'unit-head' performance at $H_T \approx 8.5$ m (1st run) and $H_T \approx 5$ m (2nd run).

(Fig. 78 evinces that the difference in performance between both runs is observed in the torque, but not in the flow, that is uniform. Unfortunately, there are not enough test data to enable any further investigation about the relation between head - and hence speed - and efficiency.)

19 points of the first run were selected as representative of the performance. They are shown in more detail in Fig. 79, and listed under 'ALAT068' in Appendix B.

Using these points and the regression procedure described in Appendix B, the turbine-mode BEP is: $\hat{Q}_T = 17.33$ l/s; $\hat{H}_T = 8.99$ m and $\hat{\eta}_T = 77.9\%$. at 1200 RPM.

---

1 The pump manufacturers provided as well general performance curves for this pump type. According to these curves, $\hat{Q}_P = 31.0$ l/s; $\hat{H}_P = 35.2$ m and $\hat{\eta}_P = 82.5\%$, at 2900 RPM.

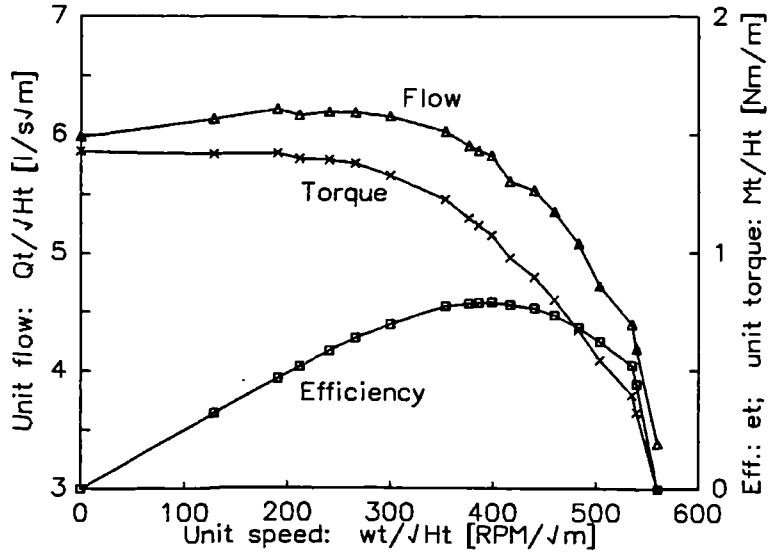

Fig. 79. PAT 'unit-head' performance at $H_T \approx 8.5$ m (selected points).

Finally, Fig. 80 represents a constant-speed graph and Fig. 81 a constant-flow graph, both constructed by correcting the representative points using the affinity laws. Fig. 80 includes as well the stall and runaway parabolas[2].

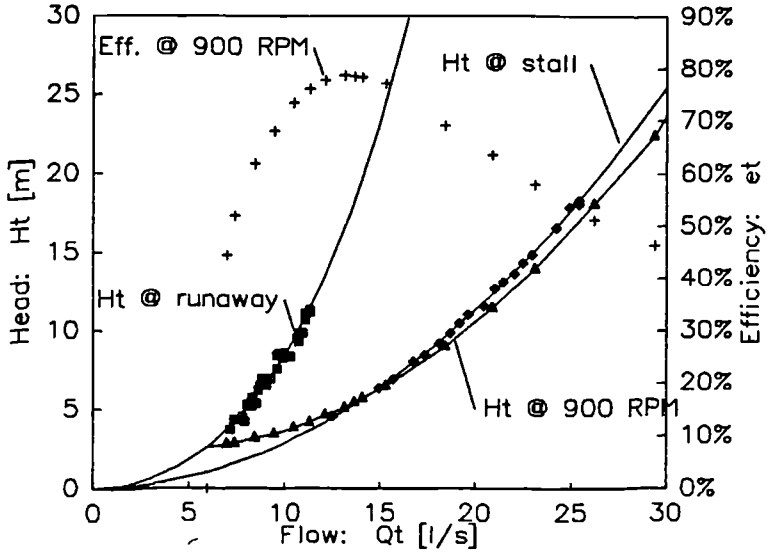

Fig. 80. PAT constant-speed (ω_T = 900 RPM) performance, including stall and runaway parabolas.

2 According to some authors (*e.g.* Diederich[67], Engeda & R.[88a, 88b]), the constant speed head-flow curve always lays between the runaway and the stall parabolas; this is one case where this is not true.

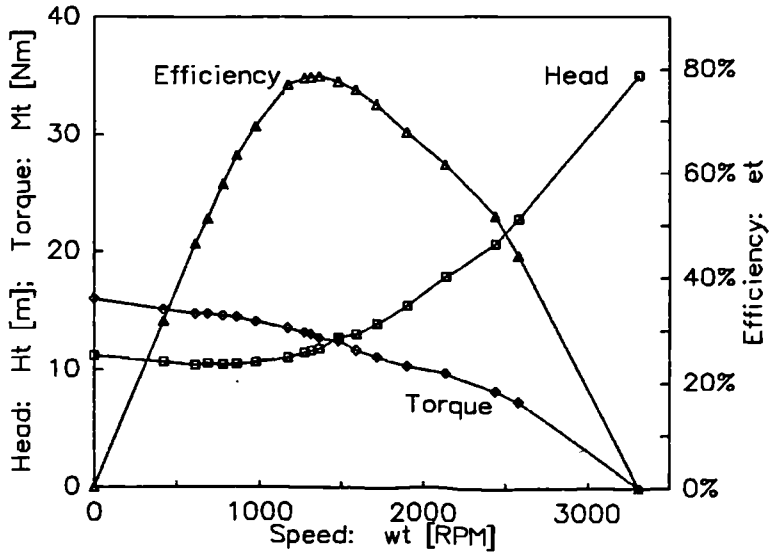

Fig. 81. PAT constant-flow (Q_T = 20l/s) performance.

6.2 Theory of Cavitation

6.2.1 Pumps and Turbines

The phenomenon of cavitation is the formation of vapour pockets or cavities in the interior or on the boundaries of a moving liquid, and their subsequent condensation. Cavitation occurs in turbomachinery when the pressure drops on account of the acceleration of water in the rotor, and of the necessary pressure difference between the two sides of the rotor blades.

The effects of cavitation are hydraulic (low efficiency, due to flow instability) and mechanical (surface damage, noise and vibration). In order to avoid or to reduce them, the available 'net positive suction head' (NPSH) must be larger than the value required by the machine. The available NPSH is the difference between the head corresponding to the vapour saturation pressure and the head at the turbine outlet / pump inlet.

In the case of pumps, the available NPSH ($H_{\Delta PA}$ [3]) is defined as...:

$$gH_{\Delta PA} = \left(\frac{p_0}{\rho} + \frac{v_0^2}{2}\right) - \frac{p_V}{\rho} \qquad [85]$$

3 In Eq. [85], subscript $_0$ represents the pump inlet and subscript $_V$ the vapour pressure. Subscript $_\Delta$ stands for the difference between each other; subscript $_P$ means pump-mode and $_A$ 'available'. $H_{\Delta PA}$ means 'available NPSH in pump-mode'.

..., where the first term represents the specific energy at the inlet of the pump, and the second term the specific energy of the vapour pressure[4]. In Eq. [85] pressures p_0 and p_V are both either absolute or relative.

As for the turbines, the available NPSH (sometimes called net positive exhaust head, NPEH, net positive draft head, NPDH, total available exhaust head, TAEH, *etc.*), is traditionally defined as...:

$$gH_{\Delta TA} = -gz_T - \frac{p_V}{\rho} \qquad [86]$$

..., where z_T is the suction static head, *i.e.* the height of the rotor with respect to the tail-water (positive when the rotor is above the tail-water). In this equation, p_V is relative (to the atmospheric pressure).

The problem with Eq. [86] is that $H_{\Delta TA}$ depends on the head-loss between the turbine and the tail-water, as well as on the amount of velocity-head recovered by the draft tube. These external variables may well follow a standard pattern in large-scale hydro, but not in micro-hydro schemes, which, in the first place, often lack draft tubes. Therefore, the available NPSH ($H_{\Delta TA}$) for micro hydro should be defined in the same way as $H_{\Delta PA}$ in Eq. [85].

Eq. [86] would yield the same value of $H_{\Delta PA}$ as Eq. [85] if the head-loss between the turbine and the tail-water were zero and if the draft tube fully recovered the turbine-outlet velocity head. As these assumptions are never met, the value of $H_{\Delta PA}$ calculated with Eq. [85] will be always larger than that calculated with Eq. [86].

The critical NPSH for pumps ($H_{\Delta Pcrit}$) is usually defined by the point where the head is reduced by 3% due to the cavitation. In the case of turbines, $H_{\Delta Tcrit}$ is defined as the NPSH that produces a change in any performance parameter of 2%.

D. Thoma defined the dimensionless cavitation parameter σ as the ratio between the NPSH and the head absorbed or delivered by the turbine or pump:

$$\sigma = \frac{H_\Delta}{H}$$

4 If the pump inlet is located below the rotor - or more specifically below the area of lowest pressure of the rotor -, the specific energy corresponding to this height difference has to be added to the first term of Eq. [85].

The value of σ_{crit} at the BEP (*i.e.* $\hat{\sigma}_{crit}$) is a function of the specific speed of the machine. In the case of pumps, this function is....:

$$\hat{\sigma}_{Pcrit} = S\,\Omega_P^{(4/3)}$$

...., where S depends on the 'quality' of the machine: about 0.18 for good pumps, 0.24 for average pumps, and 0.40 for bad pumps[5]. As for turbines, the literature does not provide any 'quality measure', and there is somewhat an agreement on the shape of the Ω_T — $\hat{\sigma}_{Tcrit}$ curve (see Fig. 82).

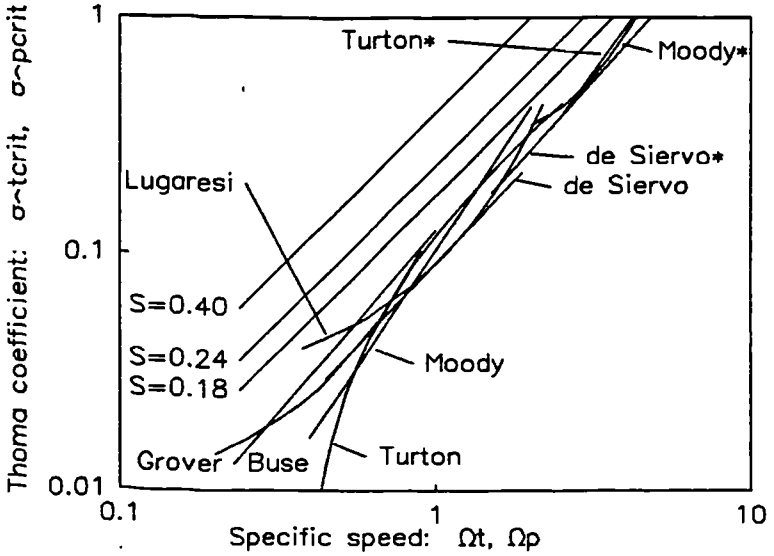

Fig. 82. Relation between Ω and $\hat{\sigma}_{crit}$ for pumps and reaction turbines.

The pump $\hat{\sigma}_{Pcrit}$-values (the three lines on the top) are defined according to Eq. [85]. The turbine curves (defined according to Eq. [86]) are those proposed by Buse[81], de Siervo & d.L.[76,77], Grover[82], Lugaresi & M.[87], Moody (quoted by Mosonyi[57]) and Turton[84]. The curves marked with * are for Kaplan or propeller turbines. Grover proposes his function for PATs, but, as he does not assert that his proposal is based on actual PAT tests, it is assumed that he used conventional turbine data. De Siervo's curves were drawn assuming $\hat{\eta}_T = 0.9$.

This relative uniformity of $\hat{\sigma}_{Tcrit}$ is probably due to the available information being all related to large - and hence good - conventional turbines: small turbines are likely to have larger values of $\hat{\sigma}_{Tcrit}$. However, even good-quality pumps have larger $\hat{\sigma}_{crit}$-

5 For Rúdnev (quoted by Pashkov & D.[77]), S is 0.12...0.14 for very good pumps; 0.20...0.27 for good pumps and 0.32...0.40 for bad pumps. Anderson[55] suggests a value of 0.18 for normal pumps, and 0.12 for special pumps. According to Wislicenus (quoted by Kittredge[76]), S is between 0.16 and 0.26, with an average of 0.24. Stepanoff[57] agrees in the average value of 0.24, but Stelzer[79] prefers 0.27. Finally, Krivchenko[86] says that pumps with inducer ("upstream auger") have values of S as low as 0.025.

values than turbines of similar specific speed (2 or 3 times larger, according to Chapallaz *et al.*[92] and Meier[82]). This is due to the difference in the definition of $\hat{\sigma}_{crit}$, as well as to the difference between both modes of operation of turbomachines:

① On account of cavitation taking place in the low-pressure end of the impeller blades, the danger of cavitation is less severe in turbine-mode than in pump-mode, because in the latter the tips of the blades at the impeller eye constitute a discontinuity that produces separation and vortices downstream, and thus accelerates the development of cavitation, while in the former, the zone of lowest pressure is upstream of this discontinuity (Yedidiah[83]).

② In pump-mode, the cavities originated in the low pressure zone implode downstream (damaging the impeller). In turbine-mode, unless the cavitation is severe, the collapse occurs outside the impeller, without reducing the efficiency (and with a smaller risk of damage) (Mikus[83]).

③ The head loss between the pump inlet and the impeller eye further reduces the pressure in the critical zone, whereas in turbine-mode, the head loss between the eye and the outlet increases it (Wislicenus[47]). (In pump-turbine schemes, the head loss between the machine and the lower reservoir is a further pump-mode handicap.)

Finally, outside the BEP, the NPSH for pumps[6] is approximately...

$$gH_{\Delta Pcrit} \approx S\,\omega_P^{(4/3)} Q_P^{(2/3)} \qquad [87]$$

..., whereas for turbines σ_{Tcrit} is almost constant, and therefore:

$$H_{\Delta Tcrit} \approx \hat{\sigma}_{Tcrit} H_T$$

6.2.2 Pumps-as-turbines

No quantitative studies about turbine-mode cavitation of pumps have been published. The turbine-mode characteristics of a Cornell pump with NPSH appear in a paper by Nicholas[88], but the awkward fact that the NPSH is **exactly** proportional to the head along the whole performance range (*i.e.* constant σ) hints that it was not obtained by tests. Yang[83] mentions a PAT test where the available NPSH ($H_{\Delta TA}$) was smaller than the required NPSH in pump-mode ($H_{\Delta Pcrit}$), but $H_{\Delta Tcrit}$ could not be established. Finally, Priesnitz[87] published a graph with the pressure distribution on the blades, but, as Grein[74]

6 Many authors (especially Anderson, Rúdnev and Wislicenus, see footnote 5 above) propose the use of a 'suction specific speed' instead of σ for pumps. This parameter is similar to the specific speed, but with the NPSH instead of H, and it is approximately constant along the operating range of pumps. The coefficient S proposed here is clearer and Eq. [87] is a simpler way to express the same, we reckon.

points out, "it is not yet possible to predict cavitation satisfactorily on the strength of the pressure distribution". This surprising lack of information may be partly explained by the fact that this is one area that has not received any input from the two fields (see p. 4) that have made major contributions to the knowledge on PATs[7].

Buse[81] and Grover[82] suggest using $\hat{\sigma}_{Tcrit}$-values similar to those of conventional turbines (see their curves in Fig. 82). According to Laux[82], $H_{\Delta Tcrit} = 0.5 \cdot H_{\Delta Pcrit}$, whereas other authors simply say that $H_{\Delta Tcrit} < H_{\Delta Pcrit}$ (Chapallaz *et al.*[92], Lueneburg & N.[85], Schnitzer[92]). However, Chapallaz *et al.* point out that the $\hat{\sigma}_{Tcrit}$-values used for conventional turbines "are valid for relatively large machines with smooth runner surfaces; small pumps usually tend to cavitate earlier". To remain in the safe side and to account for the increase in σ_{Tcrit} due to an operating point located above the BEP (recommended by them for PAT schemes), they propose the use of σ_{Tcrit}-values "at least equal to the values for pumps, if not higher".

6.3 Cavitation Tests

6.3.1 Test Expectations

The hypothesis for the tests is that PATs' σ_{Tcrit}-values should be close to those of conventional turbines, taking into account that the differences between PATs and conventional turbines are small as compared with the radical differences between pump-mode and turbine-mode operation.

According to the manufacturers' data, $\hat{H}_{\Delta Pcrit} = 4.45$ m at 2950 RPM [8]. Therefore, from the BEP data in p. 119, $\hat{\sigma}_{Pcrit} = 0.13$ and $S = 0.21$ (*i.e.* this is an 'average' pump from the point of view of cavitation).

In the (non-cavitating) turbine-mode performance tests it was established that $\Omega_T = 0.57$. The corresponding $\hat{\sigma}_{Tcrit}$ calculated with the curves for conventional turbines (Fig. 82) is between 0.03 and 0.05. However, as we are using Eq. [85] rather than Eq. [86], the expected value of $\hat{\sigma}_{Tcrit}$ is higher. In fact, if we take into account that, under a head $\hat{H}_T = 10$ m, the outlet velocity head of the PAT is $v_0^2/2 = 1.6$ m.

7 Firstly, the research on transients in pump systems is not concerned with the cavitation behaviour of pumps in the 'normal' turbine performance range on account of its short duration during a transient, and only the turbine runaway cavitation is relevant (Borciani & R.[83]). Secondly, pump-turbine research is not concerned with cavitation in turbine-mode, because it is always the pump-mode cavitation that governs the design of energy-storage schemes (*e.g.* Terry & J.[42]).

8 The pump-mode cavitation data appears in the general pump-type performance data mentioned in footnote 1 (p. 119) and not in the 'acceptance' tests. Although the general data is referred to a speed of 2900 RPM, we believe that the figure of 2950 RPM from the acceptance tests is more accurate: given the similitude in $\hat{Q}_P$ and $\hat{H}_P$ between both sources, the 2900 RPM datum seems to mean "using a two-pole induction motor", instead of representing an accurate figure for the speed.

then the **minimum** $\hat{\sigma}_{Tcrit}$ that could be obtained (corresponding to vapour pressure at the outlet) is 0.16.

If, on the other hand, we consider that, in the worst case, the values provided by the literature are referred to turbines with no velocity head recovery in the draft tube (or where the velocity head recovery equals the head loss in the draft tube), then the **maximum** expected $\hat{\sigma}_{Tcrit}$ would be 0.16 plus 0.03...0.05.

We summarise: the expected $\hat{\sigma}_{Tcrit}$ is between 0.16 and 0.21.

6.3.2 Test Results

Fig. 83 shows the shape of the σ_T — η_T curve at the BEP: most points with $\sigma_T > 0.3$ have $\eta_T = 79\% \pm 0.5\%$, the small dispersion being due to the oscillations of the system. In $\sigma_T = 0.25$ there is a distinct increase in efficiency of about 1.5%, that is typical in cavitating turbomachinery[9]. Due to the instability discussed earlier, it was not possible to make readings for lower values of σ_T with this test-rig. Therefore, even though there is no registered efficiency reduction, σ_{Tcrit} is in this case equal to the lowest value of σ_T that was obtained (0.25 in the case of Fig. 83), since any further reduction in σ_T led to evident cavitation. The value of σ_{Tcrit} that would be obtained in a more elaborate cavitation test-rig would certainly be very close.

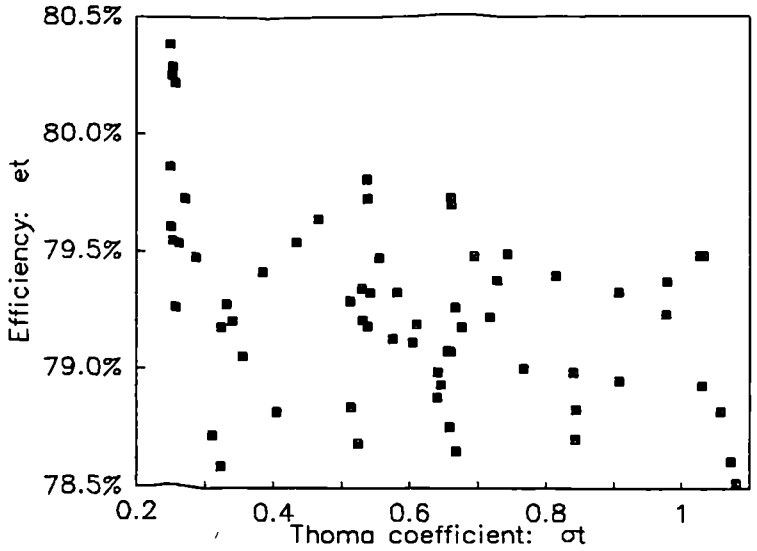

Fig. 83. η_T as a function of σ_T, for the PAT BEP.

9 This increase in efficiency is due to the reduction in the skin friction, by the formation of a thin layer of vapour at the surface of the rotor (Stepanoff[57], Wislicenus[47]). It is not noticeable in the (off-BEP) operating conditions represented by the two leftmost points of Fig. 84 (note: Fig. 84, not Fig. 83).

The value of σ_T corresponding to the onset of cavitation noise (subscript $_B$) was established by listening the noise with the ear next to the piping[10]. This onset always occurred distinctly. In the case of Fig. 83, $\sigma_{TB} = 0.5$.

Fig. 84 shows the σ_{TB} and the critical σ_{Tcrit} obtained for several points around the BEP. The shape of the σ_{TB}-curve is similar to that of pump-mode incipient σ_P (as published by Hergt *et al.*[90] and Karassik[87]), although it is interesting to note that here its minimum value does not coincide with the BEP, but probably with the swirl-free outlet point.

Finally, Fig. 85 represents the expected performance for constant-speed operation, and was obtained (using the affinity-laws) from the same data as Fig. 84.

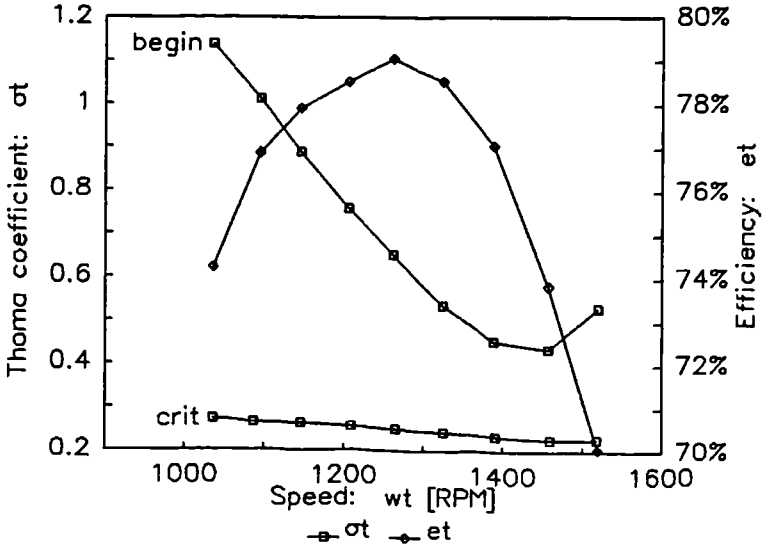

Fig. 84. σ_{TB} (noise-begin), σ_{Tcrit} and η_T as functions of ω_T, for constant-head operation.

The head actually varied somewhat, but the results were affinity-laws-corrected to $H_T = 10$ m.

10 An unfruitful attempt was made to correlate the standard deviation of the PAT-outlet pressure readings with the noise or the cavitating performance. It was incidentally noticed that the relation between the outlet pressure and its standard deviation was (oddly) increasing: the pressure readings became more steady when they were very low.

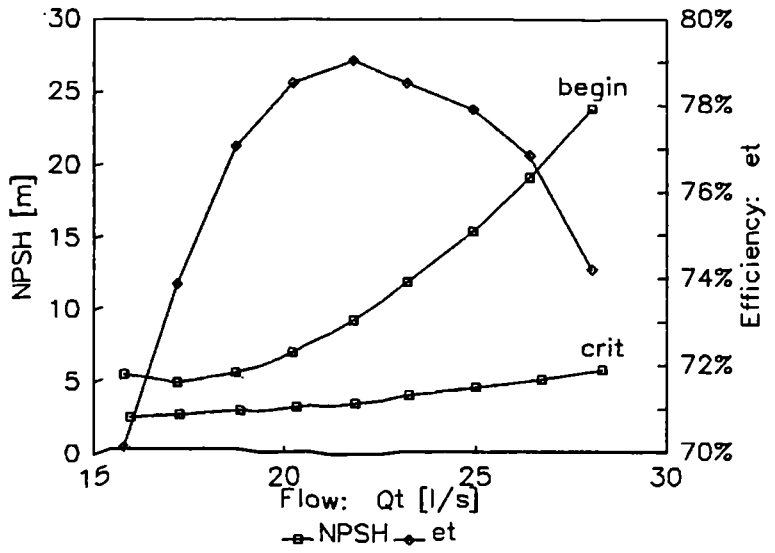

Fig. 85. $H_{\Delta TB}$, $H_{\Delta Tcrit}$ and η_T as functions of Q_T, for constant-speed operation.
ω_T = 1500 RPM.

6.4 Discussion

The value of $\hat{\sigma}_{Tcrit} = 0.25$ obtained in the tests lies outside the expected range (0.16...0.21). This is probably due to the difference (in size and geometry) between this PAT and conventional turbines, as well as to a larger amount of dissolved and entrained air - a critical parameter in cavitation. Although the latter was not measured, it was very likely larger than the quasi-degassed conditions of large hydro, yet smaller than the high-air-content conditions of run-of-the-river micro-hydro. (A high air content promotes cavitation but also dampens its negative effects, as its compressibility reduces the velocity of implosion.)

(Given the value of $\hat{\sigma}_{Tcrit} = 0.25$, this PAT would require an outlet pressure not lower than −82 kPa, when operated at 1500 RPM, with H_T = 14 m. This means that it could be installed 8.4 m above the tail-race. Or 2.1 m above it when operated at a maximum speed of 3700 RPM, with a head of 85 m. These heights would be adequate for most micro-hydro installations.)

According to Karassik[87], there is a high degree of erosion in pumps between the incipient and the critical cavitation (and Gülich & R.[88] found a correlation between noise and erosion). However, due to the differences between both modes of operation (see above, p. 124) the damage in turbine-mode for $\sigma_{TB} < \sigma_{TA} < \sigma_{Tcrit}$, even with noisy operation, should be negligible.

It is hoped that these tests will be a useful basis for further research, to find out if these $\hat{\sigma}_{Tcrit}$ results are a generalised PAT trend, and to verify the validity of the assumption regarding the absence of damage in incipient cavitation.

Meanwhile, it is proposed here to consider that $\hat{\sigma}_{Tcrit}$ is, in general, **twice as large** as $\hat{\sigma}_{Pcrit}$ [11].

11 According to Mikus[83], it is not possible to draw conclusions about turbine-mode cavitation from pump-mode cavitation, but it seems likely that a 'bad' pump (with respect to cavitation) will also be a bad PAT.

7

CONCLUSIONS AND RECOMMENDATIONS FOR FUTURE WORK

7.1 Conclusions

The purpose of this work was to investigate some areas of uncertainty that have inhibited the application of pumps-as-turbines (PATs).

Four problems in particular were addressed, namely the accommodation of seasonal flow variations, water-hammer, the prediction of turbine-mode performance when only the pump-mode performance is known, and finally cavitation in PATs.

In order to evaluate competing solutions to these problems, an economic methodology was developed. This permitted various economic, hydrological and technical parameters to be varied, such as the sensitivity of output energy value to output power and the shape of the exceedence curve.

Using this methodology, both the parallel operation of PATs and their intermittent operation (suitable for some end-uses such as grid-linked electricity generation) were compared with the use of conventional turbines. It was found that, in spite of the lack of flow control devices in PATs, the usually large reduction in cost makes them more economic than conventional machines.

The different technical options for accommodating water-hammer were then compared. It was observed that, given the relatively high cost of the penstock in micro-hydro schemes, it is usually preferable to provide an external device to damp the pressure fluctuations than to use a very thick-walled penstock.

Different methods for forecasting PAT performance have been proposed in the literature; some based on pump-mode performance and some based as well on the geometry of the machine. By means of the economic methodology, the accuracy of the

former methods was evaluated. A new method, based on pump-mode performance and on the type of casing (a datum readily available to the users), was developed and similarly evaluated.

It was found that, under typical conditions, the inaccuracy of the better prediction methods reduces the benefit-to-cost ratio of the scheme by less than 1%. This is considered negligible, given the high cost of turbine-mode laboratory tests which would otherwise be necessary.

Finally, cavitation in PATs, an issue that had not been previously studied, was examined. The results of cavitation tests made in a purpose-made rig showed that cavitation is slightly worse in PATs than in conventional turbines of similar specific speed.

7.2 Recommendations for Future Work

PAT Performance Prediction.

It was mentioned in p. 55 that two pumps with exactly the same pump-mode BEPs can have as PATs different performances. The main parameter that explains this difference is probably the area ratio, *i.e.* the ratio of area between the impeller blades at exit (normal to flow velocity) to the volute throat area. The shape of the pump-mode characteristics is a function of the area-ratio, so that the shut-off head, for example, could be used as an indicator. Although an attempt was already made (see p. 190) to correlate the ratio of shut-off head to BEP head in pump-mode, on one hand, to the pump-to-turbine head and flow conversion factors, on the other, there is still scope for further analytical work, using the data in Appendix B (the shut-off head ratio is included there for this purpose). For example, the turbine-mode efficiency could be predicted more accurately, since a pump with a small area-ratio is bound to have as turbine a low efficiency.

The constant speed performance of radial-flow PATs usually follows closely the stall parabola, as shown in Fig. 80 (p. 120), and the BEP is also very close to it. This is also shown in Fig. 57 (p. 96), where the turbine-mode head-flow characteristics follows from the BEP upwards a straight line in a logarithmic graph. The accurate prediction of the stall parabola could then be very useful[1]. (Moreover, the experimental determination of the stall head-flow parabola is quite easy for pump manufacturers.)

There is a lot of work to be done on multistage, double-suction and bowl-casing PATs. Most of this work is experimental, since there is very little published test data

---

1 Many authors have dealt with runaway (Csemniczky[83], de Siervo & L.[80], Diederich[67], Engeda & R.[88a], Gopalakrishnan & F.[84], Hergt *et al.*[84], Laux[82], Meier[62], Stelzer[79]), but almost nobody with stall (Hergt *et al.*[84], Paterson & M.[84]).

on these kinds of pumps, but the theoretical analysis of their turbine-mode performance could also be rewarding.

Finally, the relationship between speed and efficiency has to be studied, as pointed out in p. 114. This also requires careful laboratory work.

Cavitation.

It would be convenient to do both destructive and non-destructive cavitation tests on more PATs, in order to evaluate the $\hat{\sigma}_{Tcrit}$-values and to formulate a general cavitation theory. (However, the high cost of these tests would make them justifiable only for large pump manufacturers involved in large PAT programs.)

Other issues.

The need for research on the use of cheap car and lorry brakes for PAT stalling was already mentioned in p. 50.

Another issue of interest would be the economic and technical comparison between hydraulic ram pumps and pump-PAT sets, aimed at proposing an application boundary between both technologies.

8

BIBLIOGRAPHY

8.1 References

Acres American[80] Acres American Inc. (1980). *Small Hydroplant Development Program*, USDE.

Alatorre-Frenk & T.[90] Claudio Alatorre-Frenk and Terry H. Thomas (1990). **The Pumps-as-Turbines (PATs) Approach to Small Hydropower**, *First World Renewable Energy Congress "Energy and the Environment into the 1990s" (Reading, UK)*, Pergamon, *5*, 2914-8.

Alatorre-Frenk & T.-T.[89] C. Alatorre-Frenk and Karin Troncoso-Torrez (1989). *Pequeños aprovechamientos hidráulicos para generación de energía. Diseño de una microcentral para Ticuahutipan, Ver.* (BEng Thesis), FI-UNAM, Mexico.

Amblard[79] H. Amblard (1979). **Pump Turbines Operating under High Head**, *Pump Turbine Schemes. Planning, Design and Operation (Niagara Falls)*, ASME, 39-48.

Anderson[38] H.H. Anderson (1938). **Effect of Pump Geometry on Pump Performance**, *Mine Pumps, JI Min. Soc.*, Durham University (Reprinted in Appendix A of: Anderson[86]).

Anderson[55] H.H. Anderson (1955). **Modern Developments in the Use of Large Single-entry Centrifugal Pumps**, *Proceedings of the IMechE, 169*, 141-61.

Anderson[77] H.H. Anderson (1977). **Statistical Records of Pump and Water Turbine Efficiencies**, *Conference 6-9-77*, IMechE, **Paper C172/77**.

Anderson[86] H.H. Anderson (1986). *Submersible Pumps and Their Application*, The Trade and Technical Press.

Apfelbacher & E.[88] Roland Apfelbacher and Frank Etzold (1988). **Energy-saving, Shock-free Throttling With the Aid of a Reverse Running Centrifugal Pump**, *KSB Technische Berichte*, **24e**, 33-41,68.

Ávila-García & G.-C.[86] Patricia Ávila-García and José Francisco Garza-Caligaris (1986). *Bombas utilizadas como turbinas para pequeños aprovechamientos hidráulicos* (Beng thesis), FI-UNAM, Mexico.

Blake[89] L.S. Blake (1989). *Civil Engineer's Reference Book*, Butterworths, London.

Bobok[75] E. Bobok (1975). **Wall Roughness Effects on Loss-Coefficient of Centrifugal Pumps**, *5th Conference on Fluid Machinery (Budapest)*, SSME / STS-HAS, 103-12.

Bolliger & G.[84] Walter Bolliger and Fritz Gajewski (1984). **Energierückgewinnung mit Pumpen im Turbinenbetrieb bei Expansion von gasbeladenen Flüssigkeiten**, *Pumpentagung Karlsruhe*, VDMA, Section C1.

Borciani & R.[83] G.A. Borciani and Giovanni Rossi (1983). **Cavitation-parameter Effects on Francis Turbines and Francis Type Pump-turbines**, *Performance Characteristics of Hydraulic Turbines and Pumps (Boston)*, ASME, 75-82.

Borel & M.[65] L. Borel and M. Mamin (1965). **Transients in a Pump-Turbine Installation**, *International Symposium on Waterhammer in Pumped Storage Project (Chicago)*, ASME, 34-??.

Bothmann[84] Volker Bothmann (1984). **Untersuchung einer Radialpumpe als Turbine**, *Pumpentagung Karlsruhe*, VDMA, Section 1.

Bothmann & R.[83] V. Bothmann and J. Reffstrup (1983). **An Improved Slipfactor Formula**, *7th Conference on Fluid Machinery (Budapest)*, SSME / STS-HAS, 59-68.

Brada[82] Karel Brada (1982). **Hydrodynamische Axialpumpe arbeit als Microturbine**, *Maschinenmarkt (Würzburg)*, *88*, **75**, 1532-5.

Brada & B.[82] K. Brada and Jaroslav Bláha (1982). **Aplizace hydrodynamických čerpadel pro vodní mikroelektrárny** (in Czech), *Energetika*, *32*, **4**, 179-82.

Brown & R.[80] R.J. Brown and D.C. Rogers (1980). **Development of Pump Characteristics from Field Tests**, *Journal of Mechanical Design*, ASME, *102*, **October**, 807-17.

Burgoyne *et al.*[69] D.J. Burgoyne, A.E. Roberts and Z.A. Siddiqi (1969). **The Development of a Large Nuclear Reactor Circulating Pump by Model Testing**, *BPMA Design and Development Conference*, 199ff.

Burton & M.[92] John D. Burton and A.G. Mulugeta (1992). **Running Centrifugal Pumps as Micro-Hydro Turbines: Performance Prediction Using the Area Ratio Method**, *2nd World Renewable Energy Congress "Renewable Energy Technology and the Environment" (Reading, UK)*, Pergamon, *5*, 2839-47.

Burton & W.[91] J.D. Burton and Arthur A. Williams (1991). **Performance Prediction of Pumps as Turbines Using the Area Ratio Method**, *9th Conference on Fluid Machinery (Budapest)*, SSME / STS-HAS.

Buse[81] Fred Buse (1981). **Using Centrifugal Pumps as Hydraulic Turbines**, *Chemical Engineering*, *88*, **2**, 113-7.

Chadha[84] Navneet Chadha (1984). **Use Hydraulic Turbines to Recover Energy**, *Chemical Engineering (NY)*, *91*, **15**, 57-61.

Chapallaz *et al.*[92] Jean Marc Chapallaz, Peter Eichenberger and Gerhard Fischer (1992). *Manual on Pumps Used as Turbines*, GATE / GTZ.

Chappell *et al.*[82] J.R. Chappell, W.W. Hickman and D.S. Seegmiller (1982). *Pumps-as-Turbines Experience Profile*, USDE, Washington, DC.

Chaudhry[87] M. Hanif Chaudhry (1987). *Applied Hydraulic Transients*, Van Nostrand Reinhold Co., NY.

Childs[62] Sheldom M. Childs (1962). **Convert Pumps to Turbines and Recover HP**, *Hydrocarbon Processing & Petroleum Refiner, 41*, **10**, 173-4.

Cooper[82] Paul Cooper (1982). **Performance Tests of a Vertical Circulating Pump in the Turbine Mode**, *2nd Symposium on Small Hydropower Fluid Machinery (Phoenix)*, ASME, 1-12.

Cooper & W.[81] P. Cooper and Richard Worthen (1981). **Feasibility of Using Large Vertical Pumps as Turbines for Small Scale Hydropower: Final Technical Report**, *USDE*.

Cooper *et al.*[81] P. Cooper, M. McCormick and R. Worthen (1981). **Feasibility of Using Large Vertical Pumps as Turbines for Small Scale Hydropower**, *Waterpower' 81 International Conference on Hydropower (Washington)*, USACE / USDE.

Cornell Pump[82] Cornell Pump Company (1982). **Turbine Performance Information of Standard Pumps**, in: Chappell *et al.*[82], D.8.1-17.

Csemniczky[83] J. Csemniczky (1983). **On the Four Quadrant Characteristics of Centrifugal Pumps**, *7th Conference on Fluid Machinery (Budapest)*, SSME / STS-HAS, 165-73.

Curtis[83] E.M. Curtis (1983). **Four Quadrant Characteristics of a Vaned Diffuser, End Suction, Pump**, *6th International Symposium on Hydraulic Transients in Power Stations (Gloucester)*, IAHR.

Daffner & D.[84] Ernst Daffner and Willi Dettinger (1984). **Hydraulische Energierückgewinnung aus Fluids bei hohen Druckgefällen**, *Pumpentagung Karlsruhe*, VDMA, Sektion C1.

de Siervo & d. L.[76] F. de Siervo and F. de Leva (1976). **Modern Trends in Selecting and Designing Francis Turbines**, *IWPDC, 28*, **8**, 28-35.

de Siervo & d. L.[77] F. de Siervo and F. de Leva (1977). **Modern Trends in Selecting and Designing Kaplan Turbines**, *IWPDC, 29*, **12**, 51-8.

De Vries[91] E.T. De Vries (1991). **Dutch Activities on Hydropower**, *Hidroenergia 1991 Conference Proceedings, 2nd International Conference & Exhibition (Nice)*, CEE / ESHA, 532-8.

Dechaumé[91] Jean-Marie Dechaumé (1991). **Les prises d'eau de montagne**, *Hidroenergia 1991 Conference Proceedings, 2nd International Conference & Exhibition (Nice)*, CEE / ESHA, 32-41.

Deng[85] Deng Bingli (1985). **Small Hydro in China: Progress and Prospects**, *IWPDC, 37*, **2**, 15-7.

DeFazio[67] F.G. DeFazio (1967). **Transient Analysis of Variable-Pitch Pump Turbines**, *Journal of Engineering for Power*, ASME, **October**, 547-57.

DeLano[84] A.L. DeLano (1984). **Stone Drop. Ultra Low Head Using a Marine Thruster**, *3rd Symposium on Small Hydropower Fluid Machinery (New Orleans)*, ASME, 35-40.

Diederich[67] Herbert Diederich (1967). **Verwendung von Kreiselpumpen als Turbinen**, *KSB Technische Berichte*, **12**, 30-6.

Donsky[61] Benjamin Donsky (1961). **Complete Pump Characteristics and the Efects of Specific Speeds on Hydraulic Transients**, *Journal of Basic Engineering*, ASME, **December**, 685-96.

Dresser Industries[82] Dresser Industries, Pacific Pump Division (1982). **Power Recovery Turbines**, in: Chappell *et al.*[82], D.1.1-23.

Duncan[82] W.H. Duncan (1982). **Proposed Use of Existing Pumps for Generation During Spring Runoff**, *2nd Symposium on Small Hydropower Fluid Machinery (Phoenix)*, ASME, 53-60.

Engeda & R.[86] Abraham Engeda and M. Rautenberg (1986). **Performance of Centrifugal Pumps as Hydraulic Turbines**, *4th International Symposium on Hydro Power Machinery (Anaheim)*, ASME.

Engeda & R.[87] A. Engeda and M. Rautenberg (1987). **Centrifugal Pumps with Semi-open Impellers of Larger Tip Clearance Used as Power Recovery Hydraulic Turbines**, *IEE Conference on Alternative Energy*, IEE, 174-7.

Engeda & R.[88a] A. Engeda and M. Rautenberg (1988). **Are Pumps Worthwhile Turbines?**, *IWPDC, 40*, **7**, 19-20.

Engeda & R.[88b] A. Engeda and M. Rautenberg (1988). **Comparisons of the Performance of Hydraulic Turbines and Reversible Pumps for Small-Hydro Applications**, *5th International Symposium on Hydro Power Fluid Machinery (Chicago)*, ASME, *FED-68*, 45-50.

Engeda & R.[89a] A. Engeda and M. Rautenberg (1989). **Investigation of Semi-Open Impellers**, *Pumping Machinery (San Diego)*, ASME, *FED-81*, 55-62.

Engeda & R.[89b] A. Engeda and M. Rautenberg (1989). **On the Flow in a Centrifugal Pump Near Shut-off Head With Positive and Negative Flows**, *11th International Conference of the BPMA (Cambridge)*, 1-7.

Engeda *et al.*[88] A. Engeda, W.P. Strate and M. Rautenberg (1988). **Auswahl von Kreiselpumpen als Turbinen**, *Pumpentagung Karlsruhe*, VDMA, *Sec. A6*.

Etzold *et al.*[88] Frank Etzold, W. Petry and W. Böhr (1988). **Dynamische Probleme beim Einsatz einer Kreiselpumpe als Turbine am Beispiel eines Wasserversorgungsnetzes**, *Pumpentagung Karlsruhe*, VDMA, *Sec. A6*.

Franke *et al.*[89] Hans-Joachim Franke, Heinrich Hofmann, Hans-Otto Jeske and Jürgen Schill (1989). **KreiselPumpen und Energierückgewinnungs-Turbinen in der verfahrenstechnischen Hochdrucktechnik**, *Chemie Ingenieur Technik, 61*, **2**, 141-8.

Fraser & A.[81] Fraser and Associates (1981). *Modular Small Hydro Configuration, Report Nyserda 81-16*, NYSERDA, Albany.

Friberg *et al.*[88] M. Friberg, M. Mahieddine, M. Toussaint and M. Frelin (1988). **Prévision des caractéristiques des turbomachines. Application à une pompe centrifuge, un compresseur centrifuge et une turbine centripète**, *Revue Française de Mécanique*, **4**, 55-66.

Garay[90] Paul N. Garay (1990). **Using Pumps as Hydroturbines**, *Hydro Review*, *9*, **5**, 52-61.

Giddens[83] E. Peter Giddens (1983). **An Air Separator**, *Eight Australasian Fluid Mechanics Conference (Newcastle)*, *1*, 2C.1-3.

Giddens[84] E.P. Giddens (1984). **A Self-cleaning Intake for Mountain Streams,** *Conference on Hydraulics in Civil Engineering (Adelaide) (Pub. No. 8417)*, Inst. of Eng. Australia, 44-8.

Giddens[86a] E.P. Giddens (1986). **A Direction for Research in Microhydropower,** *3rd International Symposium on Wave, Tidal, OTEC and Small Scale Hydro Energy (Brighton)*, BHRA, 43-52.

Giddens[86b] E.P. Giddens (1986). **Research in Microhydropower. A New Zealand Viewpoint,** *Renewable Energy Review Journal, 8*, **1**, 17-29.

Giddens[89] E.P. Giddens (1989). *Turbine Tests of KL-ISO Centrifugal Pumps* (unpublished), University of Canterbury, New Zealand.

Giddens[91] E.P. Giddens (1991). *Personal communication.*

Giddens *et al.*[82] E.P. Giddens, W. Spittal and D.B. Watson (1982). **Small Hydro from a Submersible Pump,** *IWPDC, 34*, **12**, 33-5.

Gopalakrishnan[86] S. Gopalakrishnan (1986). **Power Recovery Turbines for the Process Industry,** *3rd International Pump Symposium (Houston)*, Texas A & M University, 3-11.

Grant & B.[84] Angus A. Grant and James M. Bain (1984). **Pump Turbine - The Economic Answer,** *1st International Conference on Small Hydro (Singapore)*, IWPDC.

Grein[74] Herbert Grein (1974). **Cavitation - An Overview,** *Sulzer Research Number.*

Grover[82] Kenneth M. Grover (1982). **Conversion of Pumps to Turbines,** in: Chappell *et al.*[82], B.1.1-14.

Gülich[81] J.F. Gülich (1981). **Energy Recovery from Expansion of Two-phase Mixtures Using Pumps in the Turbine Mode,** *Sulzer Technical Review*, **3**, 87-91.

Gülich & R.[88] J.F. Gülich and A. Rösch (1988). **Cavitation-erosion in Centrifugal Pumps,** *Sulzer Technical Review*, **1**, 28-32.

Hamkins *et al.*[89a] C.P. Hamkins, Hans-Otto Jeske, Roland Apfelbacher and O. Schuster (1989). **Pumps as Energy Recovery Turbines with Two Phase Flow,** *Pumping Machinery (San Diego)*, ASME, *FED-81*, 73-81.

Hamkins *et al.*[89b] C.P. Hamkins, H.-O. Jeske, R. Apfelbacher and O. Schuster (1989). **Performance Testing of Energy Recovery Turbines with Two Phase Flow under Actual Plant Conditions,** *Seminar The Performance Testing of Fluid Machinery (London)*, IMechE, 65-76.

Hancock[63] John W. Hancock (1963). **Centrifugal Pump as Water Turbine,** *Pipe Line News*, **June**, 25-27.

Hellmann & D.[84] Heinz Dieter Hellmann and Reinhard Dechow (1984). **Unterwassermotorpumpe; Konzept mit vielen Anwendungsmöglichkeiten,** *Pumpentagung Karlsruhe*, VDMA, Section A5.

Hergt *et al.*[84] Peter Hergt, Paul Krieger and Stephan Thommes (1984). **Die strömungstechnischen Eigenschaften von Kreiselpumpen im Turbinenbetrieb,** *Pumpentagung Karlsruhe*, VDMA, Section C1.

Hergt *et al.*[90] P. Hergt, A. Nicklas, Heinz-Dieter Hellmann, J. Schill, D. Schmalzriedt, H. Hartmüller and Herbert Diederich (1990). **Status of Boiler Feed Pump Development,** *15th Symposium of the SHMEC "Modern Technology in Hydraulic Energy Production" (Belgrade)*, U3.1-51.

Hidrostal[90] Hidrostal (1990). **Utilización de bombas hidráulicas como turbinas,** in: Tecnología Intermedia[90], 31-45.

Hochreutiner[91] F. Hochreutiner (1991). **Centrale Hydroélectrique de Tannuwald,** *Hidroenergia 1991 Conference Proceedings, 2nd International Conference & Exhibition (Nice)*, CEE / ESHA, 98-104.

Holzenberger & R.[88] Kurt Holzenberger and Ludwig Rau (1988). **Parameters for the Selection of Energy Conserving Control Options for Centrifugal Pumps,** *KSB Technische Berichte*, **24e**, 3-19.

Hornberger & R.[65] R.G. Hornberger and S. Rodríguez (1965). **Hydraulic Transient Studies for Taum Sauk Pumped-Storage Plant,** *International Symposium on Waterhammer in Pumped Storage Project (Chicago)*, ASME, 8-23.

Huetter & B.[81] John J. Huetter and George Balalau (1981). **Design of Low-cost, Ultra-low Head Hydropower Package Based on Marine Thrusters,** *Waterpower '81. International Conference on Hydropower (Washington)*, USACE / USDE, *2*, 1246-61.

Ida *et al.*[90] T. Ida, T. Kubota and H. Tanaka (1990). **Advanced Scale-up Formulae for Performances of Hydro-turbines and Pump-turbines Considering Surface Roughness,** *15th Symposium of the SHMEC "Modern Technology in Hydraulic Energy Production" (Belgrade)*, B4.1-12.

Infante-Villarreal[89] Arturo Infante-Villarreal (1989). *Evaluación financiera de proyectos de inversión*, Norma, Bogota.

James[83] Kenneth R. James (1983). **Pumps that Play Turbines,** *Water / Engineering and Management, 130*, **7**, 32-6.

Jyoti[n/a] Jyoti, Ltd. (n/a). **n/a,** *Jyoti Company Newsletter*, India.

Kamath & S.[82] P.S. Kamath and W.L. Swift (1982). *Two-Phase Performance of Scale Models of a Primary Coolant Pump, NP2578, Final Report*, EPRI.

Karassik[87] Igor J. Karassik (1987). **Understanding Cavitation ... Quo Vadis?,** *10th International Conference of the BPMA (Cambridge)*, 1-7.

Karassik *et al.*[76] I. J. Karassik, William C. Krutzsch, Warren H. Frazer and Joseph P. Messina (1976). *Pump Handbook*, McGraw Hill, USA.

Kasperowski[66] Eugen Kasperowski (1966). **Das Bewässerungspumpwerk TJURUG WEST in Indonesien,** *KSB Technische Berichte*, **11**, 48-9.

Kennedy *et al.*[80] W.G. Kennedy, M.C. Jacob, J.C. Whitehouse, J.D. Fishburn and G.J. Kanupka (1980). *Pump Two-phase Performance Program (NP-1556) (Vols. 2, 5 and 7)*, EPRI.

Kinno & K.[65] Hitoshi Kinno and John F. Kennedy (1965). **Waterhammer Charts for Centrifugal Pump Systems,** *Journal of the Hydraulic Division*, ASCE, *91*, **May**, 247-70.

Kittredge[31] Clifford Proctor Kittredge (1931). **Centrifugal Pumps Operated Under Abnormal Conditions,** *Power, 73*, **June**, 881-4.

Kittredge[33] C.P. Kittredge (1933). **Vorgänge bei Zentrifugalpumpenanlagen nach plötzlichem Ausfallen des Antriebes,** *Mitteilungen des Hydraulischen Instituts der Technischen Hochschule (München), 7,* 53-73.

Kittredge[56] C.P. Kittredge(1956). **Hydraulic Transients in Centrifugal Pump Systems,** *Transactions of the ASME, 78,* **August,** 1307-22.

Kittredge[61] C.P. Kittredge (1961). **Centrifugal Pumps Used as Hydraulic Turbines,** *Transactions of the ASME, 83,* **January,** 74-8.

Kittredge[76] C.P. Kittredge (1976). **Centrifugal Pump Performance,** in: Karassik[76], 2.125-90.

Knapp[37] Robert T. Knapp (1937). **Complete Characteristics of Centrifugal Pumps and their Use in the Prediction of Transient Behavior,** *Transactions of the ASME, 59,* **November,** 683-9.

Knapp[38] R.T. Knapp (1938). (Closure to: Knapp[37]), *Transactions of the ASME, 60,* **November,** 678.

Knapp[41] R.T. Knapp (1941). **Centrifugal-Pump Performance as Affected by Design Features,** *Transactions of the ASME, 63,* **April,** 251-60.

Knapp & D.[42] R.T. Knapp and J.W. Daily (1942). (Discussion to Terry & J.[42]), *Transactions of the ASME, 64,* **November,** 739-42.

Kobori[53] Takeshi Kobori (1953). **Experimental Research on Water Hammer in the Pumping Plant of the Numazawanuma Pumped Storage Power Station** (in Japanese), *Journal of the JSME, 56,* **413 (June),** 479-86.

Kobori[54] T. Kobori (1954). **Experimental Research on Water Hammer in the Pumping Plant of the Numazawanuma Pumped Storage Power Station,** *Hitachi Review,* **February,** 65-74.

Koonsman & A.[51] George L. Koonsman and Maurice L. Albertson (1951). **Design Characteristics of the Vortex-tube Sand Trap,** *IAHR IV Meeting (Bombay),* 317-23.

Kováts[64] André Kováts (1964). *Design and Performance of Centrifugal and Axial Flow Pumps and Compressors,* Pergamon Press, Oxford.

Krivchenko[86] G.I. Krivchenko (1986). *Hydraulic Machines. Turbines and Pumps,* Mir, Moscow.

Kumar & T.[84] Arun Kumar and O.D. Thapar (1984). **Integrated Small Hydro Energy Development,** *Conference "Water for Resource Development",* ASCE, 704-8.

Laux[80] C.H. Laux (1980). **Reversible Multistage Pumps as Energy Recovery Turbines in Oil Supply Systems,** *Sulzer Technical Review, 62,* **2,** 61-5.

Laux[82] C.H. Laux (1982). **Reverse-running Standard Pumps as Energy Recovery Turbines,** *Sulzer Technical Review, 64,* **2,** 23-7.

Lawrence[79] John D. Lawrence (1979). **Small-scale Hydro: the Use of Pumps as Turbines,** *Waterpower '79 (Washington),* USACE / USDE, 108-15.

Lawrence & P.[81] J.D. Lawrence and Leslie Pereira (1981). **Innovative Equipment for Small-scale Hydro Developments,** *Waterpower '81 International Conference on Hydropower (Washington),* USACE / USDE, 2, 1622-38.

Łazarkiewicz & T.[65] Szczepan Łazarkiewicz and Adam Tadeusz Troskolański (1965). *Impeller Pumps*, Pergamon Press.

Levy[90] Dan Levy (1990). **Optimising Electric Power from a Small-scale Hydro-electric Plant**, *Journal of the Institute of Energy, 63*, **456 (September)**, 109-18.

Lewinsky-Kesslitz[87] Heinz Peter Lewinsky-Kesslitz (1987). **Pumpen als Turbinen für Kleinkraftwerke**, *Wasserwirtschaft, 77*, 531-7.

Lobanoff & R.[85] Val S. Lobanoff and Robert R. Ross (1985). *Centrifugal Pumps: Design and Application*, Gulf Publishing Co, Houston.

Lueneburg & N.[85] Rolf Lueneburg and Richard M. Nelson (1985). **Hydraulic Power Recovery Turbines**, in: Lobanoff & R.[85], 245-86.

Lugaresi & M.[87] A. Lugaresi and A. Massa (1987). **Designing Francis Turbines: Trends in the Last Decade**, *IWPDC, 39*, **11**, 23-8.

Maguire[91] D.P. Maguire (1991). *Appropriate Development for Basic Needs. Proceedings of the conference on Appropriate Development for Survival - the Contribution of Technology (ICE, London 1990)*, ICE / Thomas Telford, London.

Makansi[83] Jason Makansi (1983). **Equipment Options Multiply for Small-scale Hydro**, *Power, 27*, **5**, 33-40.

Marquis[83] J.A. Marquis (1983). *Design and Evaluation of Small Water Turbines (DOE/R4/10243-T1)*, USDE.

Martin[83] Chas Samuel Martin (1983). **Representation of Pump Characteristics for Transient Analysis**, *Performance Characteristics of Hydraulic Turbines and Pumps (Boston)*, ASME, 1-13.

Martin[n/a] C.S. Martin (n/a). **Pressure Pulsations of a Small Centrifugal Pump in Four Quadrants**, *???*.

Martin & H.[90] C.S. Martin and Hans-Burkhard Horlacher (1990). **Correlation of Zero Flow, Locked rotor and Runaway Characteristics of Pump-turbines**, *15th Symposium of the SHMEC "Modern Technology in Hydraulic Energy Production" (Belgrade)*, D3.1-11.

Massey[63] B.S. Massey (1963). Communication to: Worster[63].

Mayo & W.[82] Howard A. Mayo Jr. and Warren G. Whippen (1982). **Use of Pumps for Power Generation**, in: Chappell *et al.*[82], D.3.1-81.

McClaskey & L.[76] B.M. McClaskey and J.A. Lundquist (1976). **Hydraulic Power Recovery Turbines**, *Joint Petroleum Mechanical Engineering and Pressure Vessels and Piping Conference (Mexico City)*, 1-11.

Meier[62] W. Meier (1962). **Pompes-turbines**, *Bulletin Escher-Wyss*, **2**, 6-12.

Mikus[83] K. Mikus (1983). **Erfahrungen mit Kreiselpumpenanlagen zur Energie-rückgewinnung aus dem Trinkwassersystem**, *GWF-Wasser/Abwasser, 124*, **4**, 159-63.

Minott & D.[83] Dennis A. Minott and Richard A. Delisser (1983). **Cost Reduction Considerations in Small Hydropower Development**, *Third Workshop on Small Hydro Power (Kuala Lumpur)*, RCTT / UNIDO / REDP / Government of Malaysia.

Miyashiro & K.[69] Hiroshi Miyashiro and Masamichi Kondo (1969). **Model Tests of Pumps for Snake Creek Pumping Plant No. 1, USA**, *Hitachi Review, 18*, **7**, 286-92.

Miyashiro & K.[70] H. Miyashiro and M. Kondo (1970). **Model Tests of Centrifugal Pumps for Santa Inês Pumping Plant, Brazil**, *Hitachi Review, 19*, **11**, 386-94.

Mosonyi[57] Emil Mosonyi (1957). *Water Power Development*, Budapest.

Naber & H.[87] Gerhard Naber and Karl Hausch (1987). **Reversible Pumpturbinen in Trinkwasserfernleitungen**, *Wasserwirtschaft, 77*, **10**, 538-45.

Narayan[79] Divyendu Narayan (1979). **Theoretical and Experimental Studies of Pressure and Speed Rise of a Pump/Turbine During Various Load Rejections with Particular Reference to Fairfield Pumped Storage Facility, South Carolina Electric and Gas Company**, *Pump Turbine Schemes. Planning, Design and Operation (Niagara Falls)*, ASME, 75-94.

Nelik & C.[84] Lev Nelik and Paul Cooper (1984). **Performance of Multi-stage Radial-inflow Hydraulic Power Recovery Turbines**, *ASME paper*, **84-WA/FM-4**.

Nèmec[72] J. Nèmec (1972). *Engineering Hydrology*, McGraw Hill.

Nicholas[88] William G. Nicholas (1988). **Using Pumps as Turbines. Selection and Application**, *Hydro 88. Third International Conference on Small Hydro (Cancún, Mexico)*, IWPDC.

Nyiri[79] A. Nyiri (1979). **On the Theoretical Full Characteristics of Hydraulic Machines**, *6th Conference on Fluid Machinery (Budapest)*, SSME / STS-HAS, 2, 770-9.

Olson[74] D.J. Olson (1974). *Single and Two-Phase Performance Characteristics of the MOD-1 Semiscale Pump under Steady State and Transient Fluid Conditions (ANCR-1165)*, Aerojet Nuclear Company.

Opdam[91] J. Hans M. Opdam (1991). *Basic Economics of Project Appraisal in the Private Sector*, Technology and Development Group, University of Twente.

Palgrave[87] R. Palgrave (1987). **Hydraulic Power Recovery Using Reverse Running Pumps**, *10th International Conference of the BPMA (Cambridge, UK)*, 229-44.

Pashkov & D.[77] N.N. Pashkov and F.M. Dolqachev (1977). *Hidráulica y máquinas hidráulicas*, Mir, Moscow (Spanish translation: 1985).

Patel *et al.*[81] D.P. Patel, R.K. Srivastava and C.S. Shah (1981). **Performance Prediction in Complete Range of Centrifugal Pumps**, *7th Technical Conference of the BPMA "Pumps-The Developing Needs" (York)*, 271-82.

Paterson & M.[84] I.S. Paterson and C. Samuel Martin (1984). **Effect of Specific Speed on Pump Characteristics and Hydraulic Transients in Abnormal Zones of Operation**, *12th Symposium of the SHMEC "Hydraulic Machinery in the Energy Related Industries" (Stirling)*, 151-72.

Peabody[39] R.M. Peabody (1939). **Typical Analysis of Water Hammer in a Pumping Plant of the Colorado River Aqueduct**, *Transactions of the ASME, 61*, **February**, 117-24.

Peabody[40] R.M. Peabody (1940). **Pump Discharge Valves on the Colorado River Aqueduct**, *Transactions of the ASME, 62*, **October**, 555-66.

Peck[51] J.F. Peck (1951). **Investigations Concerning Flow Conditions in a Centrifugal Pump, and the Effect of Blade Loading on Head Slip**, *Proceedings of the IMechE, 164*, 1-30.

Peicheng *et al*[89] Hu Peicheng, Zheng Pusheng and Abdel F. Elkouh (1989). **Relief Valve and Safety Membrane Arrangement in Lieu of Surge Tank**, *Journal of the Energy Division*, ASCE, *115*, **2**, 78-83.

Pejović *et al*[76] S. Pejović, L. Krsmanović, R. Jemcov and P. Cmković (1976). **Unstable Operation of High-head Reversible Pump-turbines**, *8th Symposium of the SHMC (Leningrad)*, 283-95.

Pelton[88] Foster Pelton (1988). *Report on Modular Hydropower Demonstration, Report Nyserda 88-8*, Acres American Corp. / NYSERDA, Albany.

Priesnitz[87] Christoph Priesnitz (1987). **Einsatzmöglichkeiten von rückwärtslaufenden Standardkreiselpumpen als Turbinen zur Energierückgewinnung**, *Information Pumpen und Verdichter*, **1**, 3-12,36.

Raabe[81] Joachim Raabe (1981). **Optimization of Pump Turbines**, *Journal of the Energy Division*, ASCE, *107*, **1**, 41-63.

Refsum & T.[88] A. Refsum and D.C.H. Thompson (1988). **Full-scale Testing of Small Hydro Turbines**, *IWPDC*, *40*, **4**, 52-3.

Salaspini[85] Aldo Salaspini (1985). **Picking Pumps for RO plant**, *World Water*, **October**, 27-9.

Sánchez[91] Teodoro Sánchez (1991). **Small Hydro Systems Using Pump Impellers as Turbines and Local Materials for Casings and Bearings**, in: Maguire[91], 245-8.

Santolaria & F.[92] Carlos Santolaria and Joaquín Fernández (1992). **Small Low-cost Sets Based on Inverse-working Pumps**, *Hydro 92. Fifth International Conference on Small Hydro (New Delhi)*, IWPDC, 182-91.

Schmiedl[88] E. Schmiedl (1988). **Serien-Kreiselpumpen im Turbinenbetrieb**, *Pumpentagung Karlsruhe '88*, VDMA, Section A6.

Schnitzer[85] Valentin Schnitzer (1985). **Neue Perspektiven zur Nutzung kleiner und kleinster Wasserkräfte durch Pumpen in Turbinenbetrieb**, *Wasserwirtschaft*, *75*, **1**, 21-25.

Schnitzer[92] V. Schnitzer (1992). **Water Energy Recovery from Existing Water Supply Systems with Pumps as Turbines (PAT)**, *Hydro 92. Fifth International Conference on Small Hydro (New Delhi)*, IWPDC, 192-202.

Schobinger & T.[79] E. Schobinger and R. Thalmann (1979). **The Two Vevey Multistage Pump-turbines of the Ste.-Helène Power Plant (EDF)**, *Pump Turbine Schemes: Planning, Design and Operation (Niagara Falls)*, ASME, 49-56.

Semple & W.[84] A.J. Semple and W. Wong (1984). **The Application of Hydraulic Power Recovery Turbines in Process Plant**, *Second European Congress on Fluid Machinery for the Oil, Petrochemical and Related Industries (The Hague)*, IMechE, C35.227-34.

Senu[90] Z. Senu (1990). *A Centrifugal Pump as an Inward Flow Turbine* (BEng Mechanical Engineering Project Thesis, unpublished), Nottingham Polytechnic.

Shafer[82] Larry L. Shafer (1982). **Pumps as Power Turbines**, *Mechanical Engineering*, *104*, **11**, 40-3.

Shafer[83] L.L. Shafer (1983). **Practical Applications for Pumps as Hydraulic Turbines for Small Scale Hydropower**, *Waterpower '83 Conference (Tennessee)*, TVA / UT etc., 74-83.

Sharma[84] K.R. Sharma (1984). *Small Hydro Electric Projects. Use of Centrifugal Pumps as Turbines*, Kirloskar Electric Co. Ltd., Bangalore.

Sheldon[84] L.H. Sheldon (1984). **An Analysis of the Applicability and Benefits of Variable Speed Generation for Hydropower**, *3rd Symposium on Small Hydropower Fluid Machinery (New Orleans)*, ASME, 201-8.

Shepherd[65] D.G. Shepherd (1965). *Principles of Turbomachinery*, MacMillan, NY.

Shimizu *et al.*[86] Y. Shimizu, Y. Shimaji, T. Kubota, K. Morimura and S. Nakamura (1986). **Studies on Integration System of Multi-Micro Water Turbine Set in Mountain Stream**, *4th Hydropower Fluid Machinery Conference (Anaheim)*, ASME, *FED-43*, 117-22.

Smith[86] Nigel P.A. Smith (1986). *PhD Laboratory Book No. 4* (unpublished), Nottingham Polytechnic.

Smith *et al.*[90] N.P.A. Smith, A.A. Williams, Andrew Brown, S. Mathema and A.-M. Nakarmi (1990). **Stand-alone Induction Generators for Reliable, Low Cost Micro-hydro Installations**, *First World Renewable Energy Congress "Energy and the Environment into the 1990s" (Reading, UK)*, Pergamon, *5*, 2904-8.

Smith *et al.*[92] N.P.A. Smith, A.A. Williams, Adam B. Harvey, M. Waltham and A.-M. Nakarmi (1992). **Direct Coupled Turbine-Induction Generator Systems for Low-cost Micro-hydro Power**, *2nd World Renewable Energy Congress "Renewable Energy Technology and the Environment" (Reading, UK)*, Pergamon, *5*, 2509-16.

Spangler[88] David Spangler (1988). **Centrifugal Pumps in Reverse - An Alternative to Conventional Turbines**, *Water and Waste Water International*, *3*, **3**, 13-7.

Sprecher[51] J. Sprecher (1951). **The Hydraulic Power Storage Pumps of the Etzel Hydro-electric Power Scheme**, *Sulzer Technical Review*, *33*, **3**, 1-14.

Stelzer[79] Robert S. Stelzer (1979). **Estimating Reversible Pump-turbine Characteristics**, *Pump Turbine Schemes: Planning, Design and Operation (Niagara Falls)*, ASME, 139-49.

Stepanoff[57] Alexey J. Stepanoff (1957). *Centrifugal and Axial Flow Pumps. Theory, Design and Application*, John Wiley & Sons, New York, 2nd ed.

Stirling[83] T.E. Stirling (1983). **Prediction and Measurement of the Four-quadrant Performance of an Axial Flow Pump of Specific Speed 8900**, *Performance Characteristics of Hydraulic Turbines and Pumps (Boston)*, ASME, 41-9.

Strate *et al.*[90] W.-P. Strate, F. Bahm and M. Rautenberg (1990). **Turbine Performance of Centrifugal Pumps Correlated to the Influence of Ring Clearance and Specific Speed**, *15th Symposium of the SHMEC "Modern Technology in Hydraulic Energy Production" (Belgrade)*, S2.1-16.

Strub[59] R.A. Strub (1959). **Investigations and Experiments on Pump-turbines**, *Sulzer Technical Review*, **2**, 87-94.

Swanson[53] W.M. Swanson (1953). **Complete Characteristic Circle Diagrams for Turbomachinery**, *Transactions of the ASME*, *75*, **July**, 819-26.

Swiecicki[61] Ignacy Swiecicki (1961). (Discussion to Donsky[61]), *Journal of Basic Engineering*, ASME, **December**, 697-8.

Taylor[83] I. Taylor (1983). **Some Installed Power Recovery Turbines Found Unusable Due to Missconceptions of Process and Performance,** *Performance Characteristics of Hydraulic Turbines and Pumps (Boston)*, ASME, 107-10.

Tecnología Intermedia[90] Tecnología Intermedia ITDG (1990), *Microcentrales hidroeléctricas. Avances de la tecnología en el Perú. Primer encuentro técnico sobre microcentrales hidroeléctricas*, Lima.

Terry & J.[42] R.V. Terry and F.E. Jaski (1942). **Test Characteristics of a Combined Pump-turbine Model with Wicket Gates,** *Transactions of the ASME, 64*, **November**, 731-44.

Thoma[31] D. Thoma (1931). **Vorgänge beim Ausfallen des Antriebes von Kreiselpumpen,** *Mitteilungen des Hydraulischen Instituts der Technischen Hochschule München, 4*, 102-4.

Thomas[72] G.O. Thomas (1972). **Determination of Pump Characteristics for a Computerized Transient Analysis,** *Proceedings of the 1st International Conference on Pressure Surges (Canterbury)*, BHRA, A3.21-32, A106-18, A123-9.

Thomas & A.[89] A.R. Thomas and P. Ackers (1989). **Hydraulic Structures,** in: Blake[89].

Thorne[79a] E.W. Thorne (1979). **Centrifugal Pumps as Power Recovery Turbines,** *Pumps '79. 6th BPMA Conference (Canterbury)*, 19-28.

Thorne[79b] E.W. Thorne (1979). **Design by the Area Ratio Method,** *Pumps '79. 6th BPMA Conference (Canterbury)*, 89-101.

Thorne[90] E.W. Thorne (1990). *Personal communication, including turbine and pump mode performance information from Worthington-Simpson, UK.*

Tognola[60] S. Tognola (1960). **Further Development of High-head Storage Pumps,** *Escher-Wyss News, 33*, **1-3**, 58-66.

Torbin *et al.*[84] Robert N. Torbin, Steven D. Lautenschlaeger and Edward D. Thimons (1984). *Conference "Water for Resource Development"*, ASCE, 684-8.

Turton[84] R.K. Turton (1984). *Principles of Turbomachinery*, E & FN Spon.

Ventrone & N.[82] Giuseppe Ventrone and Giampaolo Navarro (1982). **Utilizzazione dell'energia idrica su piccola scala: pompa come turbina,** *L'Energia Elettrica, 59*, **3**, 101-6.

Vissarionov *et al.*[89] V.I. Vissarionov, V.V. Elistratov and M.M. Mukhammadiev (1989). **Energy and Hydrodynamic Studies of Turbine Operating Regimes of Large Pumping Stations,** *Hydrotechnical Construction, 23*, **2**, 84-7.

Wiesner[67] F.J. Wiesner (1967). **A Review of Slip Factors for Centrifugal Impellers,** *Journal of Engineering for Power*, ASME, *89*, **4**, 558-72.

Williams[67] H.C. Williams (1967). **Gisborne Waterworks Intake,** *New Zealand Engineering, 22*, **12**, 502-5.

Williams[89] Arthur A. Williams (1989). *Report on the Running of a Flygt BS2102 Submersible Pump as a Stand-Alone Turbine and Induction Generator* (unpublished), Nottingham Polytechnic.

Williams[90] A.A. Williams (1990). **Application of Pumps as Turbines for Microhydro** (unpublished).

Williams[91a] A.A. Williams (1991). *An Introduction to Micro-hydroelectric Demonstration Scheme at Tennant Gill Farm, Malham* (unpublished), Nottingham Polytechnic.

Williams[91b] A.A. Williams (1991). *Overseas Visit Report. Pakistan* (unpublished), Nottingham Polytechnic.

Williams[91c] A.A. Williams (1991). *Pumps as Turbines: A Users' Guide* (draft version), Nottingham Polytechnic.

Williams[92] A.A. Williams (1992). *Pumps as Turbines Used with Induction Generators for Stand-alone Micro-hydroelectric Power Plants* (PhD thesis), Nottingham-Trent University.

Williams *et al*[88] A.A. Williams, M. Keysell, J.M.K. Pratt and Nigel P.A. Smith (1988). **Characteristics of a Submersible Pump Unit for Use as a Stand-alone Micro-hydropower Generator**, *23rd UPEC*, Session A5.

Williams *et al*[89a] A.A. Williams, N.P.A. Smith and S. Mathema (1989). **Application of Appropriate Technology to Small-scale Hydroelectric Power**, *Science, Technology and Development, 7*, **2**, 98-112.

Williams *et al*[89b] A.A. Williams, M. Keysell, J.M.K. Pratt and N.P.A. Smith (1989). **Criteria for the Selection of Induction Motor Driven Pumps for Stand-Alone Hydroelectric Applications**, *24th UPEC*, 297-300.

Wilson & P.[92] Eric Wilson and Rodney Potts (1992). **Hydro Development at Errwood Reservoir Using a Centrifugal Pump as Turbine**, *Hydro 92. Fifth International Conference on Small Hydro (New Delhi)*, IWPDC, 176-81.

Winks[77] R.W. Winks (1977). *One-Third Scale Air-water Pump Program: Test Program and Pump Performance (NP-135)*, EPRI.

Wislicenus[47] George F. Wislicenus (1947). *Fluid Mechanics of Turbomachinery*, Dover, New York.

Wong[87] W. Wong (1987). **The Application of Centrifugal Pumps for Power Generation**, *10th International Conference of the BPMA (Cambridge)*, 205-14.

World Pumps[85] World Pumps (1985). **Centrifugal Pumps Used as Turbines**, *World Pumps*, **April**, 92-3.

Worster[63] R.C. Worster (1963). **The Flow in Volutes and its Effect on Centrifugal Pump Performance**, *Proceedings of the IMechE, 177*, **31**, 843-75.

Yamamoto *et al*[68] Akihisa Yamamoto, Seiji Kamiya and Takashi Watanabe (1968). **High Head and Large Capacity Deriaz Type Reversible Pump Turbine for Takene No. 1 Power Plant**, *Mitsubishi Technical Review*, **September**, 52-62.

Yang[83] C.S. Yang (1983). **Performance of the Vertical Turbine Pumps as Hydraulic Turbines**, *Performance Characteristics of Hydraulic Turbines and Pumps (Boston)*, ASME-FED, 97-102.

Yedidiah[83] S. Yedidiah (1983). **Application of Centrifugal Pumps for Power Recovery Purposes**, *Performance Characteristics of Hydraulic Turbines and Pumps (Boston)*, ASME-FED, 111-9.

Yedidiah[89] S. Yedidiah (1989). **Calculation of Head Developed by a Centrifugal Impeller**, *Joint ASCE/ASME Applied Mechanics, Biomechanics and Fluids Engineering Conference (San Diego)*, **ASME paper 89-FE-9**.

8.2 Additional Bibliography

Alpan, K. (1989). **Suction Reverse Flow in an Axial-Flow Pump,** *3rd Joint ASCE-ASME Mechanics Conference (San Diego).*

Anderson, H.H. (1961). **The Hydraulic Design of Centrifugal Pumps and Water Turbines,** ASME Paper, **61-WA-320.**

Anderson, H.H. (n/a). *Centrifugal Pumps,* The Trade & Technical Press.

Anderson, H.H. and W.G. Crawford (1960). **Submersible Pumping Plant,** *Proceedings of the IEE, 107,* **A,** 127-140,486.

Bohl, W. (1985). *Strömungsmaschinen,* Vogel-Buchverlag, Würzburg.

Boldy, Adrian P. (1976). **Waterhammer Analysis in Hydroelectric Pumped Storage Installations,** *2nd International Conference on Pressure Surges (London),* BHRA, B1.1-14.

Boldy, A.P. and N. Walmsley (1982). **Performance Characteristics of Reversible Pump-turbines,** *11th Symposium of the SHMEC "Operating Problems of Pump Stations and Power Plants" (Amsterdam), 3,* 60.1-9.

Boldy, A.P. and N. Walmsley (1983). **Representation of the Characteristics of Reversible Pump Turbines for Use in Waterhammer Simulations,** *4th International Conference on Pressure Surges (Bath),* BHRA, G1.287-96.

Butler, J. George (1982). *How to Build & Operate your Own Small Hydroelectric Plant,* Tap Books, Pennsylvania.

Cheng, W. (1983). *Reverse Running of a Centrifugal Pump* (BEng Mechanical Engineering Project Thesis, unpublished), Nottingham Polytechnic.

Dach, H. and H.D. Knöpfel(1977). **Specific Operating Conditions Concerning Boiler Circulating Pumps - etc.,** *17 Congress IAHR (Baden-Baden), 5,* C1.

de Siervo, F. and A. Lugaresi (1980). **Moderns Trends in Selecting and Designing Reversible Francis Pump-turbines,** *IWPDC, 32,* **5,** 33-42.

Donsky, Benjamin; Roxanne M. Byrne and Paul E. Bartlett (1979). **Upsurge and Speed-rise Charts Due tu Pump Shutdown,** *Journal of the Hydraulic Division,* ASCE , **105,** 661-74.

Duc, J. (1955). **The Calculation of Water Hammer in Pumping Plant,** *Sulzer Technical Review, 37,* **1,** 22-32.

Engeda, A. and M. Rautenberg (1987). **Comparison of the Relative Effect of Tip Clearance on Centrifugal Impellers,** *Journal of Turbomachinery,* ASME, *109,* **4,** 545-9.

Enkar Ltd. (1982). **Hydroelectric Power Systems,** in: Chappell *et al*[82], D.4.1-4.

Espinoza, Pablo (n/a). *Utilización de bombas centrífugas como turbinas hidráulicas,* CETAL, Chile.

Evans, Frank L.; Olson; Steen-Johnsen; Swearingen and Jenett (1984). **Process Machinery Drives,** *Perry's Chemical Engineers' Handbook,* Mc Graw Hill, USA, 24.37-45.

Fay, A. (1976). **On the High-accuracy Scaling-up for Pumps and Turbines,** *NEL Conference,* **Paper 2.5.**

Franzke, Adolf (1970). **Benefits of Energy-recovery Turbines,** *Chemical Engineering,* **23 February,** 109-12.

Franzke, A. (1975). **Save Energy with Hydraulic Power Recovery Turbines,** *Hydrocarbon Processing, 54,* **3,** 107-10.

Frost, T.H. and E. Nilsen (1991). **Shut-off Head of Centrifugal Pumps and Fans,** *Proceedings of the IMechE, 205,* 217-23.

Fujii, S. (1948). **Pump Characteristics for the Reverse Flow Condition,** *Journal of the JSME, 51,* **359,** 321-4.

Garay, P.N. (1990). *Pump Application Desk Book,* Fairmont Press, Georgia.

Generation Unlimited (1982). **Energy Recovery Systems,** in: Chappell *et al*[82], D.7.1-2.

Gindroz, Bernard; François Avellan and Pierre Henry (1990). **Guidelines for Performing Cavitation Tests**, *15th Symposium of the SHMEC "Modern Technology in Hydraulic Energy Production" (Belgrade)*, H1.1-11.

Gopalakrishnan, S. and R.S. Ferman (1984). **Development of a New Small Hydroturbine**, *3rd Symposium on Small Hydropower Fluid Machinery (New Orleans)*, ASME, 123-9.

Gordon, J.L. (1989). **Submergence Factors for Hydraulic Turbines**, *Journal of the Energy Division*, ASCE, *115*, **2**, 90-107.

Graeser, Jean-Émile (1982). **Petites installations hydrauliques. État actuel et perspectives de développement.** *Ingénieurs et Architectes Suisses*, **23**, 323-8.

Grover, Kenneth M. (1982). **Electronic Load Diversion for Frequency Control**, in: Chappell *et al.*[82], B.1.15-28.

Haroldsen, R.O. and F.B. Simpson (1982). **Micro-hydropower in the United States**, in: Chappell *et al.*[82], B.4.1-?.

Harper, Mike (1982). **The Use of Pumps as Turbines**, in: Chappell *et al.*[82], B.3.1-30.

Hergt, P. and S. Prager (1991). **The Influence of Different Parameters on the Disc Friction Losses of a Centrifugal Pump**, *9th Conference on Fluid Machinery (Budapest)*, SSME / STS-HAS, 172-8.

Hoffmann, Oliver (1975). **Beitrag zur Druckstoßberechnung bei Pumpenausfall**, *Mitteilungen Technische Universität Berlin, 84.*

Horlacher, Hans-Burkhard (1983). **Vier-Quadranten-Kennlinien von Strömungsmaschinen in der Druckstoßberechnung**, *Druckstoßberechnung von Rohrleitungssystemen (Essen)*, Lehrgang im Haus der Technik.

Hothersall, R.J. (1984). **Micro-hydro: Turbine Selection Criteria**, *IWPDC, 36*, **2**, 26-9.

Hulse, C. Russell and Karl W. Seckel (1982). **Hydroelectric Power Generation in a Water System**, in: Chappell *et al.*[82], B.2.1-7.

Ingersoll-Rand (1982). **Ingersoll Rand Hydro-power Packages**, in: Chappell *et al.*[82], D.6.1-8.

Jarrett, D. (1983). **An Adjustable Guide Vane Hydraulic Power Recovery Turbine**, *Performance Characteristics of Hydraulic Turbines and Pumps (Boston)*, ASME, 103-6.

Jenett, E. (1968). **Hydraulic Power Recovery Systems**, *Chemical Engineering*, **8 April**, 159-64.

Lazzaro, Bruno and Giovanni Rossi (1982). **Experimental Analysis of the Main Factors Affecting the Power of a Hydraulic Machine Operating as a Pump at Zero Discharge**, *11th Symposium of the SHMEC "Operating Problems of Pump Stations and Power Plants" (Amsterdam), 3*, 63.1-12.

Macharadze, L.I. and G.I. Kirmelašvili (1972). **Issledovanie turbinnogo režima nizconapornych centrobežnych nasosov**, *Gornaja elektromechanika i rudnicnaja aerologija* (in Russian), *Mecnier[e?]ba.*

Marchal, M.; G. Flesch and P. Suter (1965). **The Calculation of Waterhammer Problems by Means of the Digital Computer**, *International Symposium on Waterhammer in Pumped Storage Project (Chicago)*, ASME.

Marchal, M.; G. Flesch and P. Suter (1968). **Calculating the Waterhammer in Storage Pump Installations with Electronic Digital Computers**, *Sulzer Research Number*, 67-75.

Martin, C.S. (1982). **Transformation of Pump-turbine Characteristics for Hydraulic Transient Analysis**, *11th Symposium of the SHMEC "Operating Problems of Pump Stations and Power Plants" (Amsterdam)*, 2, 30.1-15.

Martin, C.S. (1986). **Transformation of Pump/Turbine Characteristics for Hydraulic Transient Analysis**, *5th International Conference on Pressure Surges (Hannover)*, BHRA, C2.53-60.

Martin, C.S. (1988). **Extrapolation of Pump-turbine Characteristics towards Closed Guide Vane Position**, *14th Symposium of the SHMEC "Progress within Large and High-specific Energy Units" (Trondheim)*, E1.295-304.

Martin, C.S. (n/a). **Representation of Characteristics of Hydraulic Machinery**, *???*.

McClaskey, B.M. and J.A. Lundquist (1976). **Can You Justify Hydraulic Turbines?**, *Hydrocarbon Processing*, *55*, **10**, 163-6.

McKinney, J.D.; C.C. Warnick; B. Bradley; J. Dodds; T.B. McLaughlin; C.L. Miller; G.L. Sommers and B.N. Rinehart (1983). *Microhydropower Handbook*, EG & G Idaho Inc., Idaho Falls.

Meerbaum, M.I. (1977). *One-Third Scale Air-water Pump Program Test: Alternate Pump Performance Data (NP-385)*, EPRI.

Mikus, Klaus (1981). **Energierückgewinnung aus dem Trinkwassersystem mit Serienpumpen**, *GWF-Wasser/Abwasser*, *122*, **2**, 52-6.

Miyashiro, Hiroshi (1967). **Waterhammer Analysis of Pump System**, *Bulletin of the JSME*, *10*, **42**, 952-8.

Mohammad, W.A. and S.P. Hutton (1986). **Improved Monitoring of Air in Water**, *IWPDC*, *38*, **9**, 48-52.

Német, A. (1974). **Mathematical Models of Hydraulic Plants**, *Escher-Wyss News*, **1**, 3-19.

Nishimura-Escobar, Alejandro and Bernardino Villavicencio-Morales (1987). *Comportamiento de una bomba centrífuga operando como turbina* (BEng thesis), Universidad Autónoma Metropolitana-Azcapotzalco, Mexico.

Nyiri, A. (1970). **Determination of the Theoretical Characteristics of Hydraulic Machines, Based on Potential Theory**, *Acta Technica Academiae Scientiarum Hungaricae*, *69*, **3-4**, 243-73.

Paynter, Henry M. (1972). **The Dynamics and Control of Eulerian Turbomachines**, *Journal of Dynamic Systems, Measurement and Control*, ASME, **September**, 198-205.

Paynter, H.M. (1979). **An Algebraic Model of a Pump/Turbine**, *Pump Turbine Schemes. Planning, Design and Operation (Niagara Falls)*, ASME, 113-5.

Pereira, Leslie (1984). *Cost and Design Study of Modular Small Hydro Plants*, Acres American Incorporated/EPRI, Buffalo, New York.

Purcell, J.M. and M.W. Beard (1967). **Applying Hydraulic Turbines to Hydrocracking Operations**, *Oil and Gas Journal*, **20 November**, 202-7.

Roco, M.C. and L.K. Minani (1989). **Effect of Particle Size Distribution and Gravitation on Wear in Centrifugal Pump Casings**, *Joint ASCE/ASME Applied Mechanics, Biomechanics and Fluids Engineering Conference (San Diego)*, **ASME paper 89-FE-8**.

Samani, Zohrab (1991). **Performance Estimation of Closed-coupled Centrifugal Pumps**, *Applied Engineering in Agriculture*, ASAE, *7*, **5**, 563-5.

Schweiger, F. and J. Gregori (1988). **Prediction of Turbine Shaft Torque**, *5th International Symposium on Hydro Power Fluid Machinery (Chicago)*, ASME, 65-70.

Schweiger, F. and J. Gregori (1990). **Analysis of Small Hydro Turbine Design**, *IWPDC*, **Small Hydro Power 1990 (supplement)**, 8-11.

Sebestyén, G.; J. Demény and A. Szabó (1990). **A Determination of the Critical Cavitation Limit in Pumps**, *Cavitation and Multiphase Flow Forum (Toronto)*, ASME, 53-9.

Serkov, V.S.; V.I. Gorin; V.V. Berlin; O.A. Muraviev and B.B. Pospelov (1990). **O Primeneii Nasosnikh Agregratov v Kachestve Energeticheskogo Oborudovaniya Malikh G.E.S.** (in Russian), *Elektr. Stn.*, **March**, 2-7.

Shafer, Larry L. (1982). **Hydraulic-turbine Control is Simple for Small Power Production**, *Power*, *126*, **8**, 77-8.

Shafer, Larry L. (1982). **Small Pump-Turbines to Supplement Grid Capacity**, *IWPDC*, *34*, **12**, 38-40.

Shafer, Larry L. and Alexander Agostinelli (1981). **Hydraulic Pump in Reverse Makes a Good Low-cost Hydroturbine**, *Power*, *125*, **12**, 87-8.

Sharp, R.E.B. (1940). **Cavitation in Hydraulic-turbine Runners**, *Transactions of the ASME*, *62*, **October**, 567.

Sheer, T.J.; R.J. Baasch and M.S. Gibbs (1973). **Computer Analysis of Water Hammer in Pumping Systems**, *The South African Mechanical Engineer, 23*, **7**, 130-51.

Sheppard, R. and J.W. Barnett (1947). **Turbine-shaft Centrifugal Oil Pump Works with Oil-driven Booster Pump**, *Power, 91*, **2**, 64-7.

Smith, N.P.A. and A.A. Williams (1989). **Micro-Hydro Development Work at Nottingham Polytechnic**, *NAWPU Newsletter*, **October**.

Spangler, D. (1984). **Pumps Prove Versatile as Hydraulic Turbines**, *Power Engineering, 88*, **July**, 52-5.

Spangler, D. (n/a). *Pumps as Hydraulic Turbines for Small Scale Hydropower*, Worthington Div., McGraw-Edison Co.

Steel, D.A. (1986). **Hydraulic Energy Recovery by Means of Submersible Generators**, *International Power Generation, 9*, **1**, 27-30.

Stelzer, R.S. and R.N. Walters (1977). *Estimating Reversible Pump-Turbine Characteristics (Engineering Monograph 39)*, USBE, Denver.

Stoffel, B. and P. Hergt (1988). **Zur Problematik der spezifischen Saugzahl als Beurteilungsmaßstab für die Betriebssicherheit einer Kreiselpumpe**, *Pumpentagung Karlsruhe '88*, VDMA, *3*, B8.1-26.

Streeter, Victor L. (1964). **Waterhammer Analysis of Pipelines**, *Journal of the Hydraulics Division*, ASCE, *90*, **HY4**, 151-71.

Suter, P. (1966). **Representation of Pump Characteristics for Calculation of Waterhammer**, *Sulzer Research Number*, 45-8.

Sutton, M. (1967). **Pump Scale Laws as Affected by Individual Component Losses**, *Proceedings of the IMechE, 182*, **3M**, 76-83.

Szary, Marek (1979). **A Method of Calculating the Pump Efficiency Distributions by Means of the Mathematical Model of its Operation**, *6th Conference on Fluid Machinery (Budapest)*, SSME / STS-HAS, 1149-58.

Thanapandi, P. and Rama Prasad (1991). **A Method of Performance Prediction of Centrifugal Pumps During Reverse Flow Operation**, *9th Conference on Fluid Machinery (Budapest)*, SSME / STS-HAS, 467-74.

Thrash, Cecil (1982). **California City Recovers Power from Water System with Pump**, in: Chappell *et al.*[82], D.2.20-5.

Thrash, C. (1982). **Giant Pumps Running Backwards still Saving City Money After 30 Years**, in: Chappell *et al.*[82], D.2.1-14.

Thrash, C. (1982). **New England Farmer Builds Profitable Mini-Power Plant**, in: Chappell *et al.*[82], D.2.15-9.

Thrash, C. (1982). **Pump Acting as Turbine Provides Emergency Lubricating Water Supply**, in: Chappell *et al.*[82], D.2.26-32.

Turbomachinery International (1977). **Hydraulic Power Recovery Turbines**, *Turbomachinery International, 18*, **6**, 48-50.

Vlaming, D.J. (1981). **Method for Estimating the Net Positive Suction Head Required by Centrifugal Pumps**, *ASME Meeting 15-20 November 1981*, **Paper 81-WA/FE-32**, 1-8.

Yamabe, M. (1971). **Hysteresis Characteristics of Francis Pump-turbines when Operated as Turbine**, *Journal of Basic Engineering*, ASME, **March**, 80-4.

Yedidiah, S. (1980). *Centrifugal Pumps Problems and Cures*, PennWell Books, Tulsa, Oklahoma.

Yokoyama, T.; Y. Hishida and K. Niikura (1984). **Some Operating Experience at Off-design Points for Pump/Turbines and Hydraulic Turbines**, *IAHR 12th Symp.*, 604-19.

8.3 List of Abbreviations

ASAE	American Society of Agricultural Engineers
ASCE	American Society of Civil Engineers
ASME	American Society of Mechanical Engineers
BHRA	British Hydraulics Research Association
BPMA	British Pump Manufacturers' Association
CEE	Commission of the European Communities
CETAL	Centro de Estudios en Tecnología Apropiada para Latinoamérica
EPRI	Electric Power Research Institute (USA)
ESHA	European Small Hydro Association
FI-UNAM	Facultad de Ingeniería, Universidad Nacional Autónoma de México (Faculty of Engineering of the National University of Mexico)
GATE	German Appropriate Technology Exchange
GTZ	Deutsche Gesellschaft für Technische Zusammenarbeit
GWF	Das Gas und Wasserfach
IAHR	International Association for Hydraulic Research
ICE	Institution of Civil Engineers (UK)
IEE	Institution of Electrical Engineers (UK)
IMechE	Institution of Mechanical Engineers (UK)
ITDG	Intermediate Technology Development Group (UK)
IWPDC	International Water Power and Dam Construction
JSME	Japan Society of Mechanical Engineers
KSB	Klein, Schanzlin & Becker
NAWPU	National Association of Water Power Users (UK)
NEL	National Engineering Laboratory (UK)
NYSERDA	New York State Energy Research and Development Authority
SHMC	Section on Hydraulic Machinery and Cavitation of the IAHR
SHMEC	Section on Hydraulic Machinery, Equipment and Cavitation of the IAHR
SSME	Scientific Society of Mechanical Engineers (Hungary)
STS-HAS	Section of Technical Sciences of the Hungarian Academy of Sciences
TVA	Tennessee Valley Authority
UNIDO	United Nations Industrial Development Organization
UPEC	Universities' Power Engineering Conference (UK)
USACE	United States Army Corps of Engineers
USBE	United States Bureau of Reclamation
USDE	United States Department of Energy
UT	University of Tennessee
VDMA	Verband Deutscher Maschinen- und Anlagenbau

APPENDIX A.
THE DESIGN OF DOUBLE-SIPHONS

A siphon is one of the means to enable the intermittent operation of pumps-as-turbines. The siphon can be either double or simple. The former is more complex and expensive, but more efficient as well, as its priming wastes much less water than that of the latter (see p. 31).

A diagram of a double siphon was published by Williams[67] (Fig. 86). In fact, the siphon mentioned by him has a different application: it is used to provide an intermittent back-flow through the trash-rack of a micro-hydro scheme, to clean it. (In his case, the storage tank is located above the intake and fed by a hydraulic ram pump.)

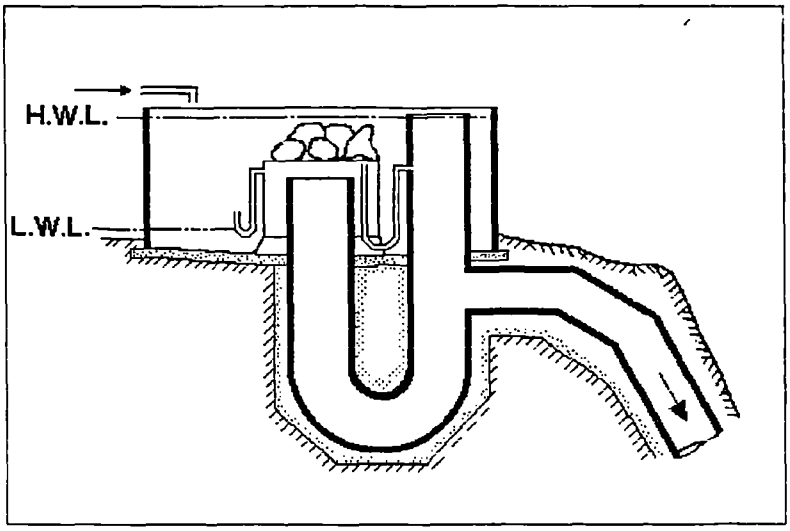

Fig. 86. Double siphon system from Williams[67].
H.W.L and L.W.L. mean high and low water levels.

The alternative design proposed in Fig. 16 (p. 32) seeks to be more appropriate for the conditions of I. O., by minimising head losses and construction costs. Its principle of operation is the same.

Double-siphon Performance.

The design of a double siphon has to observe the following guide-lines (see Fig. 87):

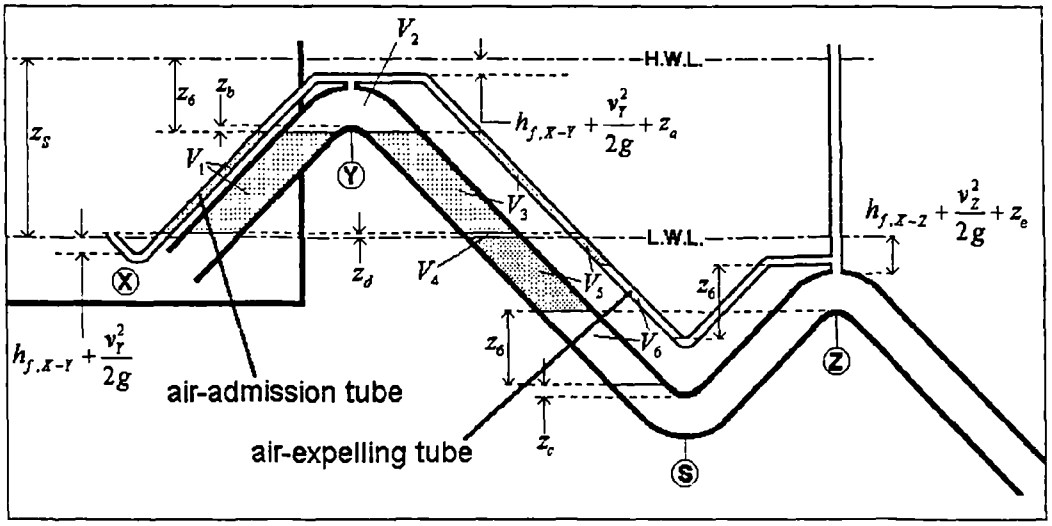

Fig. 87. The geometry of double siphons.

V_6 is the small volume of water that is wasted while the reservoir is filled, *i.e.* between steps *b* and *c* of Fig. 16 - much less than with a simple siphon.

① The top of the first peak of the siphon (**Y**) needs to be below the high water level to ensure appropriate priming. The vertical distance between the high water level and the top of the air-admission tube in the first peak must be equal to the head loss between the reservoir and this point ($h_{fX\text{-}Y}$) plus the velocity head in this point ($v_Y{}^2/2g$) plus a small margin z_a.

② The vertical distance z_6 between the bottom of the air-expelling tube and its open end is equal to the distance mentioned above ($h_{fX\text{-}Y} + [v_Y{}^2/2g] + z_a$) plus the vertical distance between the top of the air-admission tube and the bottom of the pipe plus a small margin z_b. This margin z_b ensures that no water overflows the first peak (**Y**) before the siphon is primed. This overflow would discharge into the sink (**S**), which would in turn overflow the second peak (**Z**), wasting water. (z_6 is the compression head, *i.e.* the height of the column of water that compresses the air trapped inside the first peak of the siphon during the filling stage.)

③ The vertical distance between the ceiling of the sink (**S**) and the floor of the second peak (**Z**) is z_6 plus a small margin z_c (to ensure that the 'trapped' air is expelled through the air-expelling tube and not through the main pipe).

④ The vertical distance between the open-end of the air-admission tube and its bottom is equal to $h_{fX\text{-}Y} + [v_Y{}^2/2g]$ plus a margin z_d (see Fig. 16, *e*).

⑤ The vertical distance between the open-end of the air admission tube and the top of the second peak (**Z**) is equal to the head loss between the reservoir and this point ($h_{fX\text{-}Z}$) plus velocity head ($v_Z{}^2/2g$) plus z_d plus a small margin z_e, in order to ensure that the penstock will remain full even when the water level is the lowest.

⑥ The vertical distance between the high and the low water levels (*i.e.* the reservoir depth z_S) has to be large enough to avoid overflowing the first peak (**Y**) before the siphon is primed: Assuming an isothermal compression of an ideal gas, the product of volume and pressure is equal at the beginning (Fig. 16, *b*) and the end (Fig. 16, *c*) of the process. Expressing the pressure as head of column of water (*i.e.* dividing it by the specific gravity of water), we have:

$$H_{atm}(V_1+V_2+V_3+V_4+V_5)=(H_{atm}+z_6)\cdot(V_2+V_3+V_4+V_5+V_6)$$

Expressing some of the volumes as the product of their vertical heights and their **horizontal** areas:

$$V_1 = A_1(z_S - z_d - z_6)$$
$$V_3 = A_3(z_S - z_d - z_6)$$
$$V_4 = A_3 z_d$$
$$V_6 = A_3 z_6$$

Putting all together we get the minimum value for the 'storage height' z_S (a larger z_S can be obtained by selecting a large value for z_d):

$$z_S = z_6 \frac{H_{atm}A_3 + H_{atm}A_1 + V_2 + V_5 + z_d A_3}{H_{atm}A_1 - z_6 A_3} + z_d$$

⑦ Finally, the vent at the top of the second peak must be higher than the high water level, to avoid spilling water. Moreover, its diameter must be large enough to admit, when the siphon loses its prime, an air flow equal in volume to the turbine rated flow, with a head loss smaller than z_6 (otherwise the water trapped in the sink between both peaks would be sucked).

Alternative Designs.

The intermittent operation (I. O.) of PATs with a siphon penstock has an inherent instability for relatively large flows, described in Chapter 3 (p. 37): if the turbine flow, slightly reduced as the head drops, happens to match the available flow, the system sticks there, operating continuously.

As the station is likely to operate in the unstable range during many days of the year, and as the deeper the reservoir the lower the power in this range, it will be desirable in

many cases to minimise the reservoir depth (z_S). In the case of a double siphon, this can be achieved by increasing the horizontal area (A_1) of the inlet to the first peak (see Fig. 87).

Fig. 88 shows one such double-siphon design, with a large concrete inlet. This design incorporates a trash-rack at the bottom of the inlet, that would be cleaned by a back-flow each time the siphon loses its prime (as suggested by Dechaumé[91], *etc.*).

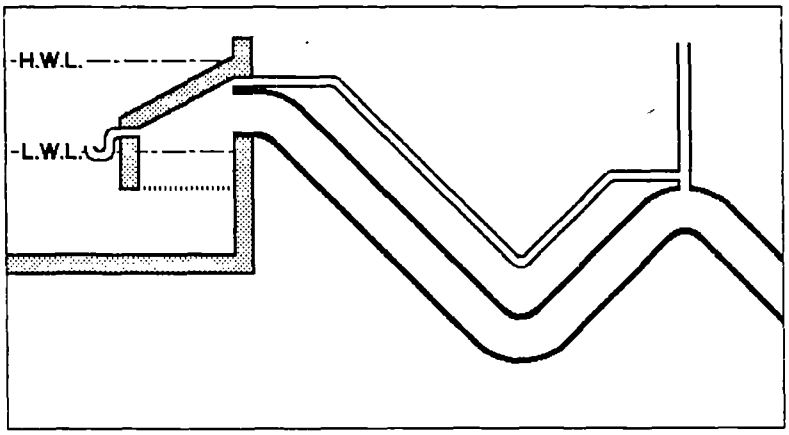

Fig. 88. Double siphon with a large concrete inlet, to reduce the storage depth.

If this depth is too small for the low-flow season, it can be adjusted by increasing z_d. The small amount of extra energy that can be generated in this way hardly justifies building a deeper reservoir. However, if a deep reservoir already exists, it may be desirable to adjust the depth z_S continuously (see p. 39).

This adjustment can be performed by a simple digital control with one input and one output (Fig. 89): the input tells the control whether the station is running or not, preferably by sensing the presence of water in the penstock, and the output actuates a small valve that admits air to the siphon. This air-admission valve must then remain open until the beginning of the running stage.

The proposed control algorithm is as follows: When the control is turned on, it waits until the siphon loses its prime (at the minimum head) and then measures the time required to fill the reservoir. With Eq. [17] (p. 36) it now knows the normalised available flow Φ. Then it calculates the optimum depth with Eq. [22], and the corresponding running time with Eq. [16]. It actuates the air-admission valve at the appropriate moment, and repeats the process from the beginning, except that now the head at which the siphon loses its prime is not the minimum, but the optimum.

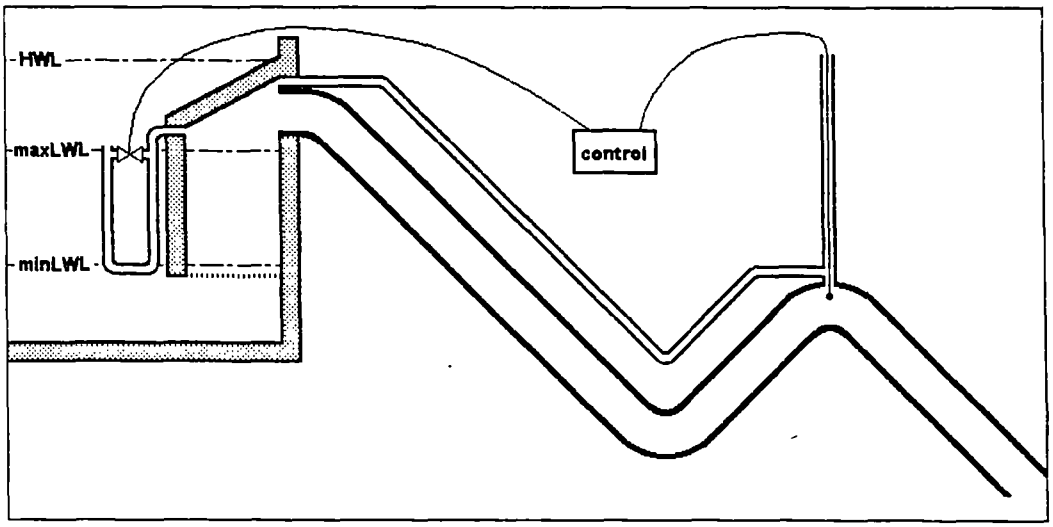

Fig. 89. Automatic adjustment of the reservoir depth of a double siphon with a digital control.

A cheaper option is to install in the siphon several air-admission valves at different heights, and to open or close them manually on a daily or seasonal basis. The design shown in Fig. 90 incorporates two valves: both are closed for low flows; the lower one is opened for medium flows and the upper one is opened for large flows.

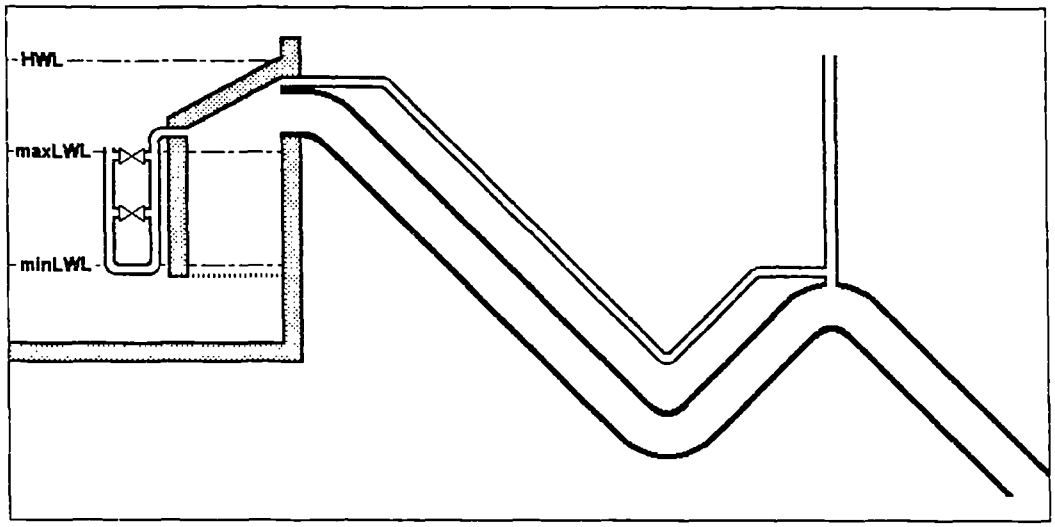

Fig. 90. Manual adjustment of the reservoir depth of a double-siphon.

APPENDIX B
PAT TEST DATA

Introduction

The test data used in Chapter 5 (see p. 77) are fully described here, along with the best efficiency points (BEPs) in both modes of operation. At the end of the Appendix, the unused published test data are also listed.

All the turbine-mode BEPs were calculated by fitting polynomial regressions to the available performance data (see Fig. 54, p. 93), according to the mathematical model of the characteristics defined by Eqs. [67] and [68] (p. 90).

As mentioned in p. 92, these multiple-variable linear regressions were made by weighing the errors for each point with the corresponding efficiency, in order to ensure that the fitting is better in the range of most interest.

Therefore, Eq. [68] is transformed to...:

$$\eta_T = A_H\left(\frac{\eta_T Q_T^2}{H_T}\right) + B_H\left(\frac{\eta_T Q_T \omega_T}{H_T}\right) + C_H\left(\frac{\eta_T \omega_T^2}{H_T}\right)$$

..., and the values of A_H, B_H and C_H are obtained by making a zero-intercept multiple-variable linear regression, with the expressions enclosed in brackets as the three independent variables.

Similarly, A_M and B_M are obtained by transforming Eq. [67] to:

$$\eta_T = A_M\left(\frac{\eta_T Q_T^2}{M_T}\right) + B_M\left(\frac{\eta_T Q_T \omega_T}{M_T}\right)$$

However, this equation can not be applied to runaway, where $M_T = 0$, and therefore it is more convenient to transform it again to:

$$\eta_T = A_M\left(\frac{\omega_T Q_T}{\rho g H_T}\right) + B_M\left(\frac{\omega_T^2}{\rho g H_T}\right)$$

In most cases the actual torque characteristics differ from this model near the runaway, were the mechanical losses (whose effect on the shape of the curve is neglected here; see p. 90) become significant. In these cases the points near the runaway were eliminated from the regressions, in order to ensure a good curve-fitting in the zone of interest (around the BEP). (The points used for the regressions are listed below for each test PAT.)

Finally, by differentiating the efficiency we obtain the following expression to locate the BEP:

$$\frac{\hat{Q}_T}{\hat{\omega}_T} = \sqrt{\frac{B_M^2}{A_M^2} - \frac{B_H B_M}{A_H A_M} + \frac{C_H}{A_H}} - \frac{B_M}{A_M} \qquad [88]$$

The pump-mode BEP was obtained in a similar way, *i.e.* by fitting second-degree polynomials to both the head and the torque characteristics, except in some cases where the pump-mode performance data were either unavailable or too scarce.

Pump-mode shut-off head and power (diacritic ˋ) are also included in the data for future research.

Used Test Data

ALAT068

Category: end-suction/volute (radial flow)
Ω_P 0.683
D_2 174 mm
Data extent: stall↔runaway
Data quality: absolute values
Data presentation: own tests
Nature of the study: PATs
Make: SPP
Type: standard pump (Unistream 65/16)
Original source: author's tests
Other sources:
Pump data from manufacturers.

Performance data:

Q [l/s]	H [m]	ω [RPM]	M [Nm]	η
Pump BEP				
31.29	35.13	2950	47.15	74.0%
Shut-off: $\dot{H}_P/\hat{H}_P = 1.27$; $\dot{P}_P/\hat{P}_P = 0.555$				
Turbine BEP				
17.33	8.99	1200	9.46	77.9%
Regressions: H[1→19]; M[6→15]				
Elasticities: $E_T = 1.44$; $E_{2T} = 2.05$				
Turbine performance (19 points)				
15.00	6.29	0	9.00	0.0%
18.03	8.65	378	12.26	31.8%
18.07	8.46	553	12.00	46.4%
17.99	8.52	618	11.90	51.2%
17.77	8.24	691	11.47	57.9%
17.73	8.23	763	11.34	63.4%
17.86	8.42	871	11.17	69.1%
17.46	8.40	1026	10.31	77.1%
17.29	8.57	1104	9.85	78.3%
17.24	8.64	1134	9.65	78.5%
17.06	8.59	1167	9.24	78.6%
16.64	8.80	1234	8.63	77.8%
16.38	8.76	1302	7.86	76.2%
16.04	9.00	1377	7.20	73.4%
15.87	9.76	1508	6.54	68.1%
14.81	9.86	1581	5.35	61.9%
14.12	10.36	1722	4.13	52.0%
13.61	10.58	1756	3.41	44.4%
11.00	10.58	1823	0.00	0.0%

APFE060

Category: double-suction
Ω_P 0.604
D_2 ≈ 350 mm
Data extent: stall (no M)↔runaway
Data quality: absolute values
Data presentation: constant speed graph
Nature of the study: PATs
Make: KSB
Type: standard pump (RDL 200-340A)
Original source: Apfelbacher & E.[88] and Etzold *et al.*[88]
Other sources:
Turbine data from Franke *et al.*[89]; type and pump data from manufacturers.
Data processing:
$\dot{P}_P$ obtained by extrapolation.

Performance data:

Q [l/s]	H [m]	ω [RPM]	M [Nm]	η
Pump BEP				
90.0	32.50	1450	224.9	84.0%
Shut-off: $\dot{H}_P/\hat{H}_P = 1.28$; $\dot{P}_P/\hat{P}_P = 0.483$				
Turbine BEP				
124.5	44.82	1500	293.6	84.3%
Regressions: H[1→14]; M[1→10]				
Elasticities: $E_T = 1.57$; $E_{2T} = 2.50$				
Turbine performance (14 points)				
111.4	33.81	0	n/a	0.0%
138.5	53.13	1500	374.8	81.6%
132.1	49.26	1500	337.2	83.0%
125.0	45.13	1500	297.3	84.4%
118.1	41.50	1500	257.9	84.3%
111.1	38.13	1500	221.2	83.7%
104.8	35.02	1500	188.0	82.0%
97.2	32.16	1500	152.9	78.3%
91.2	29.82	1500	124.9	73.6%
83.6	27.71	1500	93.0	64.3%
77.0	26.38	1500	67.8	53.5%
69.4	24.79	1500	40.8	38.0%
62.2	23.96	1500	18.2	19.5%
57.0	23.65	1500	0.0	0.0%

BUSE024

Category: end-suction/volute (radial-flow)
Ω_P 0.240 (although this could be Ω_T)
D_2 n/a
Data extent: →runaway
Data quality: only relative values (It is not explicit that the data were actually obtained in tests, and not by prediction.)
Data presentation: constant speed graph
Nature of the study: PATs
Make: Ingersoll-Rand
Type: standard? pump
Original source: Buse[81]
Data processing:
Power curve was used only to calculate $\hat{\eta}_P$.

Performance data:

Q [l/s]	H [m]	ω [RPM]	M [Nm]	η
Pump BEP				
1.000	1.000	401.6	0.387	60.3%
Shut-off: $\dot{H}_P/\hat{H}_P = 1.26$; $\dot{P}_P/\hat{P}_P = 0.440$				
Turbine BEP				
2.100	2.407	401.6	0.660	56.0%
Regressions: $H[1\rightarrow10]$; $M[1\rightarrow8]$				
Elasticities: $E_T = 1.59$; $E_{2T} = 1.89$				
Turbine performance (10 points)				
2.294	2.786	401.6	0.832	55.9%
2.194	2.582	401.6	0.743	56.2%
1.995	2.216	401.6	0.584	56.6%
1.800	1.907	401.6	0.442	55.2%
1.603	1.628	401.6	0.310	51.0%
1.404	1.384	401.6	0.201	44.4%
1.204	1.187	401.6	0.119	35.8%
1.009	1.020	401.6	0.057	23.9%
0.806	0.915	401.6	0.018	10.5%
0.706	0.875	401.6	0.000	0.0%

COOP297

Category: bowl (mixed-flow)
Ω_P 2.97
D_2 686 mm
Data extent: only around the BEP
Data quality: absolute values
Extra data: axial thrust
Data presentation: table
Nature of the study: PATs
Make: Ingersoll-Rand
Type: standard pump
Original source: Cooper & W.[81]
Data processing:
Original head data with draft tube; data modified to take into account the velocity head recovery in it, but not the head-loss, nor the entry head-loss in pump-mode.

Performance data:

Q [l/s]	H [m]	ω [RPM]	M [Nm]	η
Pump BEP				
1539	9.75	700.0	2295	87.5%
Shut-off: $\dot{H}_P/\hat{H}_P = 2.46$; $\dot{P}_P/\hat{P}_P = 1.86$				
Turbine BEP				
1744	13.16	730.0	2541	86.3%
Regressions: $H[1\rightarrow10]$; $M[1\rightarrow10]$				
Elasticities: $E_T = 2.77$; $E_{2T} = 4.09$				
Turbine performance (14 points)				
2136	22.66	731.2	5030	81.1%
2071	20.93	730.4	4591	82.6%
2004	19.40	729.4	4183	83.8%
1984	18.64	729.5	3986	83.9%
1924	17.14	728.3	3595	84.8%
1883	16.32	727.4	3364	85.0%
1810	14.73	726.2	2956	86.0%
1788	14.12	725.2	2802	85.9%
1744	13.22	725.4	2554	85.9%
1652	11.37	725.5	2091	86.2%
1592	9.96	724.2	1746	85.2%
1542	8.81	723.5	1481	84.3%
1529	8.60	723.3	1424	83.6%
1451	7.21	722.2	1096	80.8%

COOP346

Category:	bowl (mixed-flow)
Ω_P	3.46
D_2	686 mm
Data extent:	only around the BEP
Data quality:	absolute values
Extra data:	axial thrust
Data presentation:	table
Nature of the study:	PATs
Make:	Ingersoll-Rand
Type:	standard pump
Original source:	Cooper & W.[81]
Data processing:	See COOP297.

Performance data:

Q [l/s]	H [m]	ω [RPM]	M [Nm]	η
Pump BEP				
1766	8.96	714.0	2456	84.5%
Shut-off data: missing				
Turbine BEP				
2073	13.18	725.0	3011	85.3%
Regressions: $H[3\rightarrow11]$; $M[3\rightarrow11]$				
Elasticities: $E_T = 3.08$; $E_{2T} = 5.39$				
Turbine performance (11 points)				
2242	17.66	729.4	4138	81.4%
2199	16.40	728.2	3826	82.5%
2126	14.34	726.4	3301	84.0%
2033	12.39	726.1	2763	85.0%
1944	10.61	724.4	2261	84.8%
1841	9.05	723.6	1775	82.3%
1799	8.57	723.4	1588	79.6%
1733	7.62	723.1	1299	76.0%
1652	6.38	721.2	904	66.0%
1604	5.81	721.2	700	57.9%
1548	5.21	721.5	531	50.8%

CURT106

Category:	end-suction/volute (radial-flow) (with fixed vanes)
Ω_P	1.06
D_2	177 mm
Data extent:	stall↔runaway
Data quality:	absolute values
Extra data:	outlet swirl, geometry
Data presentation:	constant speed graphs
Nature of the study:	transients in pumps
Make:	CEGB
Type:	model
Original source:	Curtis[83]

Performance data:

Q [l/s]	H [m]	ω [RPM]	M [Nm]	η
Pump BEP				
33.8	12.3	2000	25.6	75.8%
Shut-off: $\dot{H}_P/\hat{H}_P = 1.28$; $\dot{P}_P/\hat{P}_P = 0.540$				
Turbine BEP				
47.3	19.4	2000	31.3	73.0%
Regressions: $H[1\rightarrow18]$; $M[8\rightarrow15]$				
Elasticities: $E_T = 1.88$; $E_{2T} = 2.70$				
Turbine performance (18 points)				
171.5	305.9	2000	625.8	25.5%
151.2	228.8	2000	471.4	29.1%
133.3	176.1	2000	360.2	32.8%
119.4	137.4	2000	279.2	36.4%
104.2	99.9	2000	201.3	41.3%
85.7	66.1	2000	131.9	49.7%
69.6	41.8	2000	82.2	60.3%
63.0	34.4	2000	65.7	64.8%
54.4	25.6	2000	45.8	70.3%
49.3	20.9	2000	35.2	72.9%
45.6	18.0	2000	28.3	73.7%
41.5	15.5	2000	21.8	72.5%
37.5	13.2	2000	15.8	67.8%
33.4	11.0	2000	9.8	57.4%
30.6	9.7	2000	6.7	48.1%
29.3	9.5	2000	5.1	39.1%
26.0	8.1	2000	2.3	23.7%
23.3	7.9	2000	0.0	0.0%

DIED028

Category: end-suction/volute (radial-flow)
Ω_P 0.289
D_2 0.325 m?
Data extent: stall (no M)↔runaway
Data quality: absolute values
Extra data: different diameters
Data presentation: constant speed graphs
Nature of the study: PATs
Make: KSB
Type: standard pump (Etanorm 65-315 or 80-315)
Original source: Diederich[87]
Data processing:
$\dot{P}_P$ obtained by extrapolation.

Performance data:

Q [l/s]	H [m]	ω [RPM]	M [Nm]	η
Pump BEP				
30.62	111.3	3000	154.7	68.8%
Shut-off: $\dot{H}_P/\hat{H}_P = 1.21$; $\dot{P}_P/\hat{P}_P = 0.54$				
Turbine BEP				
49.53	221.2	3000	235.1	68.8%
Regressions: H[1→15]; M[1→10]				
Elasticities: $E_T = 1.32$; $E_{2T} = 2.22$				
Turbine performance (15 points)				
43.44	146.4	0	n/a	0.0%
52.81	243.3	3000	271.5	67.7%
50.05	224.9	3000	241.2	68.7%
47.26	207.2	3000	210.8	68.9%
44.48	192.7	3000	182.0	68.0%
41.69	179.9	3000	155.8	66.6%
38.91	169.6	3000	133.3	64.7%
36.12	160.4	3000	111.7	61.7%
33.40	152.9	3000	90.9	57.0%
30.66	146.6	3000	70.8	50.5%
27.89	140.7	3000	51.7	42.2%
25.08	135.4	3000	33.4	31.5%
22.28	130.6	3000	17.5	19.2%
19.52	126.5	3000	4.1	5.4%
18.56	125.3	3000	0.0	0.0%

DIED037

Category: multistage (6 radial-flow stages)
Ω_P 0.371
D_2 0.180 m?
Data extent: stall (no M)↔runaway
Data quality: absolute values
Extra data: different speeds
Data presentation: constant speed graphs
Nature of the study: PATs
Make: KSB
Type: standard pump (Movi 50/6?)
Original source: Diederich[87]
Data processing:
$\dot{P}_P$ obtained by extrapolation.

Performance data:

Q [l/s]	H [m]	ω [RPM]	M [Nm]	η
Pump BEP				
6.37	16.35	2000	7.47	65.3%
Shut-off: $\dot{H}_P/\hat{H}_P = 1.28$; $\dot{P}_P/\hat{P}_P = 0.47$				
Turbine BEP				
10.51	29.96	2000	10.41	70.6%
Regressions: H[1→15]; M[1→15]				
Elasticities: $E_T = 1.58$; $E_{2T} = 2.18$				
Turbine performance (15 points)				
10.66	29.35	0	n/a	0.0%
11.12	32.72	2000	11.96	70.2%
10.55	30.19	2000	10.51	70.4%
10.01	27.83	2000	9.15	70.2%
9.45	25.54	2000	7.88	69.7%
8.90	23.49	2000	6.74	68.8%
8.34	21.60	2000	5.64	66.9%
7.79	19.86	2000	4.60	63.4%
7.22	18.32	2000	3.61	58.3%
6.68	17.06	2000	2.79	52.3%
6.13	15.85	2000	2.04	44.8%
5.57	14.91	2000	1.40	36.1%
5.01	14.15	2000	0.86	25.8%
4.45	13.60	2000	0.40	14.1%
3.84	13.27	2000	0.00	0.0%

DIED088

Category: end-suction/volute (radial-flow)
Ω_P 0.881
D_2 0.215 m?
Data extent: stall (no M)↔runaway
Data quality: absolute values (is ω_T really 2900 RPM?)
Data presentation: constant speed graphs
Nature of the study: PATs
Make: KSB
Type: standard pump (Etanorm 100-200?) (could be the same as ENGE082 and STRA081)
Original source: Diederich[67]
Data processing:
$\dot{P}_P$ obtained by extrapolation.

Performance data:

Q [l/s]	H [m]	ω [RPM]	M [Nm]	η
Pump BEP				
80.5	45.93	2900	144.0	82.9%
Shut-off: $\dot{H}_P/\hat{H}_P = 1.25$; $\dot{P}_P/\hat{P}_P = 0.61$				
Turbine BEP				
114.0	66.96	2900	205.6	83.4%
Regressions: $H[1\rightarrow16]$; $M[1\rightarrow13]$				
Elasticities: $E_T = 1.68$; $E_{2T} = 2.26$				
Turbine performance (16 points)				
102.0	68.99	0	n/a	0.0%
127.9	82.11	2900	272.4	83.1%
122.4	75.99	2900	250.7	83.5%
116.7	69.70	2900	219.2	83.5%
111.2	64.24	2900	191.7	83.2%
105.6	59.02	2900	166.1	82.5%
100.1	54.18	2900	142.3	81.3%
94.6	49.79	2900	120.8	79.4%
89.0	45.79	2900	100.9	76.7%
83.5	42.29	2900	83.0	72.8%
77.9	38.96	2900	66.2	67.5%
72.3	35.97	2900	50.3	60.0%
66.7	33.19	2900	36.0	50.3%
61.2	30.87	2900	22.8	37.4%
55.8	28.72	2900	10.7	20.7%
51.0	27.01	2900	0.0	0.0%

ENGE057

Category: end-suction/volute (radial-flow)
Ω_P 0.575
D_2 0.262 m?
Data extent: →almost runaway
Data quality: absolute values (is ω_T really 1475 RPM?)
Extra data: different rotor clearances
Data presentation: constant speed graph
Nature of the study: PATs
Make: KSB
Type: standard pump (Etanorm 100-250?)
Original source: Engeda & R.[86]
Other sources:
$\tilde{\eta}_P$ from Engeda & R.[89a], to achieve a better consistency between H_T, η_T and P_T.
ω_P (and also D_2) from manufacturers, to achieve the quoted Ω_P.
Performance data with different clearances in Engeda & R.[87].

Performance data:

Q [l/s]	H [m]	ω [RPM]	M [Nm]	η
Pump BEP				
43.06	21.70	1475	74.15	80.0%
Shut-off: $\dot{H}_P/\hat{H}_P = 1.12$; $\dot{P}_P/\hat{P}_P = 0.462$				
Turbine BEP				
51.48	28.60	1475	76.69	82.1%
Regressions: $H[1\rightarrow6]$; $M[1\rightarrow6]$				
Elasticities: $E_T = 1.64$; $E_{2T} = 3.10$				
Turbine performance (6 points)				
62.25	40.89	1475	129.29	80.0%
55.79	32.41	1475	92.88	80.9%
46.12	24.05	1475	56.03	79.6%
36.16	18.91	1475	27.21	62.7%
28.12	16.17	1475	11.14	38.6%
21.57	14.73	1475	1.39	6.9%

ENGE082

Category: end-suction/volute (radial-flow) (semi-open impeller)
Ω_P 0.821
D_2 219 mm
Data extent: →runaway
Data quality: absolute values
Extra data: different rotor clearances, different speeds, geometry, closed impeller...
(Although it seems that the authors do not consider the closed-impeller data very reliable, since they did not include the corresponding $\hat{\eta}_T$ in the table of Engeda & R.[89a].)
Data presentation: constant speed graphs
Nature of the study: PATs
Make: KSB
Type: modified standard pump (Etanorm 100-200?) (see also DIED088)
Original source: Engeda & R.[86]
Other sources:
Turbine performance from Engeda & R.[89a] (only 1050 RPM data was used, because its extent is broader).
Performance data with different clearances in Engeda & R.[87].

Performance data:

Q [l/s]	H [m]	ω [RPM]	M [Nm]	η
Pump BEP				
43.06	13.50	1475	44.73	82.5%
Shut-off: $\dot{H}_P/\hat{H}_P = 1.12$; $\dot{P}_P/\hat{P}_P = 0.437$				
Turbine BEP				
40.51	10.27	1050	30.42	82.0%
Regressions: $H[1\rightarrow 9]$; $M[1\rightarrow 8]$				
Elasticities: $E_T = 1.56$; $E_{2T} = 1.89$				
Turbine performance (9 points)				
49.26	14.12	1050	49.06	79.1%
44.78	12.10	1050	39.18	81.1%
42.39	11.02	1050	34.08	81.8%
38.02	9.38	1050	26.05	81.9%
34.60	8.19	1050	20.21	80.0%
30.93	6.99	1050	14.57	75.6%
27.55	6.11	1050	10.44	69.6%
23.67	5.36	1050	6.25	55.2%
16.94	4.68	1050	0.00	0.0%

ENGE122

Category: end-suction/volute (radial-flow)
Ω_P 1.22
D_2 185 mm
Data extent: →runaway
Data quality: absolute values
Extra data: different speeds
Data presentation: constant speed graphs
Nature of the study: PATs
Make: KSB
Type: standard pump (Etanorm 100-160?)
Original source: Engeda & R.[86]
Other sources:
Turbine performance from Engeda & R.[88b], because it has absolute values (only 1250 RPM data was used, because it is clearer and its extent broader)
Performance data with different clearances in Engeda & R.[87].

Performance data:

Q [l/s]	H [m]	ω [RPM]	M [Nm]	η
Pump BEP				
41.67	7.78	1475	25.73	80.0%
Shut-off: $\dot{H}_P/\hat{H}_P = 1.25$; $\dot{P}_P/\hat{P}_P = 0.538$				
Turbine BEP				
55.00	11.24	1250	34.44	74.4%
Regressions: $H[1\rightarrow 8]$; $M[1\rightarrow 8]$				
Elasticities: $E_T = 1.77$; $E_{2T} = 2.00$				
Turbine performance (8 points)				
61.50	13.64	1250	45.50	72.4%
54.45	11.13	1250	33.45	73.7%
50.04	9.59	1250	26.32	73.2%
44.65	7.90	1250	18.70	70.8%
41.81	7.11	1250	15.16	68.1%
38.32	6.20	1250	11.30	63.5%
32.90	5.09	1250	6.15	49.0%
26.27	4.01	1250	1.15	14.6%

ENGE151

Category: end-suction/volute (radial-flow) (semi-open impeller)
(According to the authors, a similar $\hat{\eta}_T$ was obtained with a closed impeller.)
Ω_P 1.51
D_2 224 mm
Data extent: →runaway
Data quality: only relative values
Extra data: different clearances
Data presentation: constant speed graphs
Nature of the study: PATs
Make: KSB
Type: modified standard pump (Etanorm 150-200?)
Original source: Engeda & R.[87]
(Only $\lambda = 0.34\%$ was used.)
Other sources:
With the help of Fig. 1 of the original source (that, by the way, uses a definition of ψ 8 times larger than the rest of the paper), and comparing with manufacturers' information, it was possible to determine the type, and hence the pump data.

Performance data:

Q [l/s]	H [m]	ω [RPM]	M [Nm]	η
Pump BEP				
103.6	10.50	1450	83.6	84.0%
Shut-off: $\dot{H}_P/\hat{H}_P = 1.39$; $\dot{P}_P/\hat{P}_P = 0.600$				
Turbine BEP				
138.0	17.62	1450	119.0	75.8%
Regressions: $H[1\rightarrow10]$; $M[1\rightarrow10]$				
Elasticities: $E_T = 1.81$; $E_{2T} = 1.90$				
Turbine performance (10 points)				
133.2	16.59	1450	106.9	74.9%
130.3	15.95	1450	100.5	74.9%
123.1	14.32	1450	83.8	73.6%
118.2	13.33	1450	74.7	73.5%
109.7	11.75	1450	58.9	70.7%
100.9	10.32	1450	45.6	67.8%
94.1	9.23	1450	35.1	62.6%
87.5	8.22	1450	27.0	58.2%
79.6	7.16	1450	16.6	45.1%
68.4	5.75	1450	4.6	18.3%

GIDD018

Category: end-suction/volute (radial-flow)
Ω_P 0.181
D_2 ≈ 200 mm
Data extent: only around the BEP
Data quality: absolute values
Data presentation: table
Nature of the study: PATs
Make: TKL
Type: standard pump (50×32-200)
Original source: Giddens[91]
Data processing:
The tests were made with draft tube and flow straightener, but the head data correspond apparently to the actual H, and therefore no corrections were made.

Performance data:

Q [l/s]	H [m]	ω [RPM]	M [Nm]	η
Pump BEP				
5.51	66.5	3000	24.11	47.4%
Shut-off: $\dot{H}_P/\hat{H}_P = 1.17$; $\dot{P}_P/\hat{P}_P = 0.503$				
Turbine BEP				
10.07	177.1	3000	24.23	43.5%
Regressions: $H[1\rightarrow11]$; $M[1\rightarrow8]$				
Elasticities: $E_T = 1.57$; $E_{2T} = 2.26$				
Turbine performance (11 points)				
10.51	188.9	3000	26.69	43.1%
10.20	181.7	3000	25.10	43.4%
9.79	169.2	3000	22.24	43.0%
9.30	157.4	3000	19.87	43.5%
8.78	146.1	3000	17.35	43.3%
8.48	136.3	3000	15.22	42.2%
8.08	129.6	3000	13.57	41.5%
7.31	116.5	3000	9.83	37.0%
6.61	105.4	3000	6.65	30.6%
6.19	99.1	3000	5.00	26.1%
5.59	92.7	3000	2.62	16.2%

GIDD035

Category:	end-suction/volute (radial-flow)
Ω_P	0.357
D_2	≈ 160 mm
Data extent:	only around the BEP
Data quality:	absolute values
Data presentation:	table
Nature of the study:	PATs
Make:	TKL
Type:	standard pump (65×50-160)
Original source:	Giddens[91]
Data processing:	See GIDD018.

Performance data:

Q [l/s]	H [m]	ω [RPM]	M [Nm]	η
Pump BEP				
10.71	41.76	3000	20.86	66.9%
Shut-off: $\grave{H}_P/\hat{H}_P = 1.20$; $\grave{P}_P/\hat{P}_P = 0.439$				
Turbine BEP				
14.14	64.74	3000	19.77	69.2%
Regressions: $H[1\rightarrow16]$; $M[1\rightarrow13]$				
Elasticities: $E_T = 1.19$; $E_{2T} = 1.48$				
Turbine performance (16 points)				
16.59	80.16	3000	28.31	68.2%
15.80	74.51	3000	24.92	67.8%
15.19	71.04	3000	23.00	68.3%
14.89	68.75	3000	21.73	68.0%
14.49	66.94	3000	20.80	68.7%
13.99	63.77	3000	19.33	69.4%
13.42	59.95	3000	17.36	69.1%
12.60	56.79	3000	15.57	69.7%
11.70	53.12	3000	13.52	69.7%
10.91	49.72	3000	11.10	65.6%
10.11	47.03	3000	9.45	63.7%
9.51	44.66	3000	8.11	61.1%
8.57	41.67	3000	6.16	55.3%
8.01	40.25	3000	4.99	49.6%
7.60	39.42	3000	4.14	44.2%
6.81	36.93	3000	2.39	30.4%

GIDD079

Category:	end-suction/volute (radial-flow)
Ω_P	0.797
D_2	≈ 125 mm
Data extent:	only around the BEP
Data quality:	absolute values
Data presentation:	table
Nature of the study:	PATs
Make:	TKL
Type:	standard pump (80×65-125)
Original source:	Giddens[91]
Data processing:	See GIDD018.

Performance data:

Q [l/s]	H [m]	ω [RPM]	M [Nm]	η
Pump BEP				
19.62	21.43	3000	17.65	74.4%
Shut-off: $\grave{H}_P/\hat{H}_P = 1.27$; $\grave{P}_P/\hat{P}_P = 0.532$				
Turbine BEP				
29.10	29.81	3000	21.28	78.6%
Regressions: $H[1\rightarrow17]$; $M[1\rightarrow14]$				
Elasticities: $E_T = 1.71$; $E_{2T} = 2.91$				
Turbine performance (17 points)				
30.78	33.07	3000	24.91	78.4%
29.68	31.18	3000	22.59	78.2%
29.20	30.00	3000	21.46	78.5%
29.00	29.60	3000	21.04	78.5%
28.51	28.70	3000	20.31	79.5%
27.99	27.79	3000	19.14	78.8%
27.37	26.77	3000	18.10	79.1%
26.99	26.09	3000	17.10	77.8%
25.88	24.68	3000	15.23	76.4%
24.78	23.48	3000	13.57	74.7%
23.87	22.07	3000	11.95	72.7%
22.68	20.58	3000	10.29	70.6%
20.39	18.39	3000	7.20	61.5%
18.80	17.60	3000	5.57	53.9%
17.60	16.50	3000	4.04	44.6%
16.09	15.29	3000	2.17	28.2%
14.81	14.51	3000	0.87	12.9%

HIDR044

Category: end-suction/volute (radial-flow)?
Ω_P 0.442
D_2 0.356 m?
Data extent: only around the BEP
Data quality: absolute values
(The shape of the power curve is very unlikely.)
Extra data: different diameters
Data presentation: constant speed graphs
Nature of the study: PATs
Make: Hidrostal
Type: standard? pump (125-315)
Original source: Hidrostal[90]
Data processing:
$\hat{P}_P$ obtained by extrapolation.

Performance data:

Q [l/s]	H [m]	ω [RPM]	M [Nm]	η
Pump BEP				
84.4	62.90	1800	355.0	77.8%
Shut-off: $\hat{H}_P/\hat{H}_P = 1.10$; $\hat{P}_P/\hat{P}_P = 0.19$				
Turbine BEP				
109.1	78.24	1800	341.6	76.9%
Regressions: $H[1\rightarrow9]$; $M[1\rightarrow9]$				
Elasticities: $E_T = 1.09$; $E_{2T} = 2.21$				
Turbine performance (9 points)				
115.8	83.87	1800	386.9	76.6%
112.3	81.00	1800	364.0	76.9%
108.2	77.32	1800	334.6	76.9%
102.2	72.84	1800	296.0	76.4%
95.9	69.17	1800	260.3	75.5%
89.6	65.80	1800	226.0	73.7%
83.5	63.08	1800	195.0	71.2%
77.7	60.85	1800	167.0	67.9%
73.0	59.24	1800	145.2	64.6%

HIDR177

Category: bowl (mixed-flow)?
Ω_P 1.775
D_2 n/a
Data extent: only around the BEP
Data quality: absolute values
(is ω_T really 1750 RPM??)
Data presentation: constant speed graphs
Nature of the study: PATs
Make: Hidrostal
Type: standard? pump (E8K-HD)
Original source: Hidrostal[90]
Data processing:
Shut-off data obtained by extrapolation.

Performance data:

Q [l/s]	H [m]	ω [RPM]	M [Nm]	η
Pump BEP				
114.4	11.64	1750	89.5	79.6%
Shut-off: $\hat{H}_P/\hat{H}_P = 5.7$; $\hat{P}_P/\hat{P}_P = 1.4$				
Turbine BEP				
178.3	17.71	1750	133.9	79.2%
Regressions: $H[1\rightarrow13]$; $M[1\rightarrow13]$				
Elasticities: $E_T = 1.69$; $E_{2T} = 1.42$				
Turbine performance (13 points)				
190.3	19.92	1750	157.3	77.6%
180.3	17.98	1750	137.1	79.0%
170.8	16.32	1750	118.7	79.6%
160.4	14.77	1750	101.0	79.6%
150.2	13.33	1750	84.3	78.7%
140.4	11.99	1750	68.9	76.4%
130.4	10.59	1750	54.0	73.0%
120.2	9.25	1750	40.5	68.0%
110.0	8.06	1750	28.7	60.4%
100.2	7.00	1750	18.7	49.7%
90.0	5.99	1750	10.4	36.2%
80.3	5.04	1750	4.2	19.4%
74.1	4.55	1750	1.1	5.9%

JYOT054

Category: end-suction/volute (radial-flow)?
Ω_P 0.540
D_2 n/a
Data extent: near the BEP, but without including it
Data quality: absolute values
Data presentation: constant speed graphs
Nature of the study: PATs
Make: Jyoti
Type: standard? pump
Original source: Jyoti Ltd.n/a
(Pump BEP from table, not form graph.)

Performance data:

Q [l/s]	H [m]	ω [RPM]	M [Nm]	η
Pump BEP				
10.67	24.01	3000	11.11	72.0%
Shut-off: $\dot{H}_P/\hat{H}_P$ = n/a; $\dot{P}_P/\hat{P}_P$ = n/a				
Turbine BEP				
17.10	44.52	3000	14.43	60.7%
Regressions: $H[1\rightarrow5]$; $M[1\rightarrow5]$				
Elasticities: $E_T = 2.06$; $E_{2T} = 3.92$				
Turbine performance (5 points)				
16.09	39.13	3000	11.73	59.7%
15.43	36.70	3000	10.75	60.9%
13.80	30.09	3000	6.73	52.0%
12.76	26.73	3000	5.27	49.5%
11.22	23.43	3000	2.75	33.6%

JYOT183

Category: end-suction/volute (mixed-flow)?
Ω_P 1.83
D_2 n/a
Data extent: near the BEP, but without including it
Data quality: absolute values (is ω_T really 1450 RPM??)
Data presentation: constant speed graphs
Nature of the study: PATs
Make: Jyoti
Type: standard? pump
Original source: Jyoti Ltd.n/a
(Pump BEP from table, not form graph.)

Performance data:

Q [l/s]	H [m]	ω [RPM]	M [Nm]	η
Pump BEP				
42.47	4.497	1450	15.82	78.0%
Shut-off: $\dot{H}_P/\hat{H}_P$ = n/a; $\dot{P}_P/\hat{P}_P$ = n/a				
Turbine BEP				
53.39	8.967	1450	19.76	63.9%
Regressions: $H[1\rightarrow9]$; $M[1\rightarrow9]$				
Elasticities: $E_T = 1.85$; $E_{2T} = 3.63$				
Turbine performance (9 points)				
55.55	9.852	1450	23.62	66.8%
53.33	8.934	1450	20.11	65.4%
50.00	7.784	1450	15.94	63.4%
46.67	7.061	1450	12.93	60.8%
43.33	6.471	1450	10.10	55.8%
40.00	5.944	1450	7.75	50.4%
36.67	5.484	1450	5.58	43.0%
33.33	5.011	1450	3.86	35.8%
30.00	4.693	1450	2.30	25.3%

KENN157

Category: end-suction/volute (mixed-flow)
Ω_P 1.57
D_2 n/a
Data extent: stall↔runaway
Data quality: absolute values
Extra data: different air contents
Data presentation: table
Nature of the study: transients in pumps
Make: Combustion Engineering
Type: model (scale 1:5)
Original source: Kennedy *et al.*[80]
(Pump points in p. 4-42; turbine points 394, 396,433,1488 and 1494.)
Other sources:
Shut-off data from Martin[83]
Data processing:
Pump-mode rated point is not the BEP ⇒ pump BEP was calculated.

Performance data:

Q [l/s]	H [m]	ω [RPM]	M [Nm]	η
Pump BEP				
208.9	72.19	4500	399.6	78.5%

Shut-off: $\grave{H}_P/\hat{H}_P = 1.54$; $\grave{P}_P/\hat{P}_P = 0.731$

Turbine BEP				
306.2	127.45	4500	725.0	89.3%

Regressions: $H[1\rightarrow5]$; $M[1\rightarrow5]$
Elasticities: $E_T = 1.78$; $E_{2T} = 1.93$

Turbine performance (5 points)				
114.8	27.34	0	156.2	0.0%
130.3	24.50	2380	106.9	85.2%
111.5	18.82	2250	68.5	78.4%
170.2	45.40	3775	132.0	68.9%
170.0	50.92	4504	84.4	46.9%

KITT038

Category: double-suction
Ω_P 0.388
D_2 505 mm
Data extent: stall↔runaway
Data quality: approximate absolute values
Extra data: geometry
Data presentation: constant flow graph
Nature of the study: transients in pumps
Make: De Laval
Type: old standard pump (L10/8)
Original source: Kittredge[56]
Other sources:
Turbine performance from Kittredge[61], because it is clearer. Runaway tuned with figures from Kittredge[76].
Data processing:
According to a comparative analysis taking into account the information provided by the author about other De Laval pumps, and also according to Brown & R.[80], the specific speed proposed by the author ($N_S = 1500$) corresponds to the whole machine, and therefore it was corrected; this analysis lead also to the approximate calculation of $\hat{H}_P$ and $\hat{Q}_P$.

Performance data:

Q [l/s]	H [m]	ω [RPM]	M [Nm]	η
Pump BEP				
112.0	50.3	1160	541.8	84.0%
Shut-off: $\grave{H}_P/\hat{H}_P = 1.28$; $\grave{P}_P/\hat{P}_P = 0.330$				
Turbine BEP				
112.0	30.3	837	306.6	80.9%
Regressions: $H[1\rightarrow20]$; $M[1\rightarrow17]$				
Elasticities: $E_T = 1.31$; $E_{2T} = 2.57$				
Turbine performance (20 points)				
112.0	39.0	0	392.6	0.0%
112.0	35.0	115	383.0	12.0%
112.0	31.7	233	372.0	26.2%
112.0	29.2	350	361.3	41.4%
112.0	26.5	524	342.7	64.6%
112.0	26.0	580	335.5	71.4%
112.0	27.2	694	325.2	79.1%
112.0	28.4	757	316.9	80.6%
112.0	30.0	818	309.3	80.3%
112.0	31.7	876	301.4	79.5%
112.0	33.4	931	295.2	78.4%
112.0	35.5	989	288.9	76.9%
112.0	37.5	1046	281.8	75.0%
112.0	42.1	1159	269.5	70.7%
112.0	48.8	1272	257.7	64.1%
112.0	66.4	1503	235.0	50.7%
112.0	86.6	1737	205.0	39.2%
112.0	109.3	1965	157.5	27.0%
112.0	135.0	2201	95.0	14.8%
112.0	171.1	2489	0.0	0.0%

KITT074

Category:	end-suction/volute (radial-flow) (with fixed vanes)
Ω_P	0.742
D_2	312 mm
Data extent:	stall↔runaway
Data quality:	absolute values
Extra data:	geometry
Data presentation:	constant speed and constant flow graphs
Nature of the study:	transients in pumps
Make:	Voith
Type:	old standard pump
Original source:	Kittredge[33]

Data processing:
Pump-mode rated point is not the BEP ⇒ BEP calculated with pump performance data.

Performance data:

Q [l/s]	H [m]	ω [RPM]	M [Nm]	η
Pump BEP				
52.53	6.53	700.0	54.6	84.1%
Shut-off: $\grave{H}_P/\hat{H}_P = 1.17$; $\grave{P}_P/\hat{P}_P = 0.385$				
Turbine BEP				
50.00	6.27	578.2	43.3	85.3%
Regressions: $H[1\rightarrow20]$; $M[1\rightarrow20]$				
Elasticities: $E_T = 1.51$; $E_{2T} = 1.98$				
Turbine performance (20 points)				
50.00	6.07	0.0	62.6	0.0%
50.00	5.81	48.7	60.5	10.8%
50.00	5.71	77.0	60.7	17.5%
50.00	5.62	100.3	60.2	22.9%
50.00	5.57	123.6	59.6	28.2%
50.00	5.51	153.2	59.1	35.1%
50.00	5.49	176.5	58.1	39.9%
50.00	5.49	202.2	57.6	45.3%
50.00	5.53	228.0	56.6	49.9%
50.00	5.54	277.0	54.9	58.7%
50.00	5.60	327.2	53.0	66.1%
50.00	5.69	376.1	51.1	72.2%
50.00	5.80	427.5	49.2	77.5%
78.19	13.94	700.0	117.1	80.3%
70.04	11.55	700.0	90.9	84.0%
60.03	9.05	700.0	62.8	86.4%
50.19	6.94	700.0	39.2	84.1%
40.15	5.50	700.0	20.6	69.6%
30.14	4.82	700.0	7.9	40.9%
20.81	4.43	700.0	0.0	0.0%

KNAP044

Category: double-suction
Ω_P 0.446
D_2 n/a
Data extent: stall↔runaway
Data quality: absolute values
Data presentation: Kármán-Knapp diagram
Nature of the study: transients in pumps
Make: Byron Jackson
Type: old standard pump
Original source: Knapp[37]
(Pump data from Figs. 2 and 3, because these graphs are more accurate; turbine performance from Fig. 7; Figs. 4 and 5 yield a very different turbine performance and they were not used because their scale is less clear and they are less consistent: the difference between the 1100 and 3100 RPM data is too far away from the affinity laws!)
Other sources:
Efficiencies from Swanson[53].
Also published by Kittredge[58] in a paper about transients in pumps (it is interesting to note that in a later paper with the PAT approach, Kittredge[61] did not include this data: apparently he considered that mentioning a PAT with $\hat{\eta}_T = \hat{\eta}_P - 12.6\%$ was not a good way to advertise PATs!)

Performance data:

Q [l/s]	H [m]	ω [RPM]	M [Nm]	η
Pump BEP				
17.35	44.74	3100	29.52	79.4%

Shut-off: $\hat{H}_P/\hat{H}_P = 1.29$; $\hat{P}_P/\hat{P}_P = 0.450$

Turbine BEP				
24.91	69.43	3100	34.89	66.8%

Regressions: $H[1\rightarrow 9]$; $M[1\rightarrow 8]$
Elasticities: $E_T = 1.48$; $E_{2T} = 2.15$
Turbine performance (9 points)

16.53	30.48	0	21.92	0.0%
17.15	30.48	366	22.04	16.5%
17.48	30.48	920	20.68	38.1%
17.30	30.48	1346	19.00	51.8%
15.58	28.55	2151	13.56	70.0%
12.91	30.48	2676	6.78	49.3%
14.63	45.72	3416	6.78	37.0%
10.77	30.48	2853	2.71	25.2%
9.43	30.48	2923	0.00	0.0%

KNAP063

Category: end-suction/volute (radial-flow)
Ω_P ≈ 0.630
D_2 ≈ 340 mm
Data extent: stall↔runaway
Data quality: approximate absolute values
Data presentation: Kármán-Knapp diagram
Nature of the study: transients in pumps
Make: Byron Jackson
Type: model? (or old standard pump?)
Original source: Knapp[41]
Data processing:
Ω_P is not explicit for this machine nor for KNAP067; the only explicit datum is that the rated head $\tilde{H}_P$ is 295 ft for both; as they are in group B (designed for a prototype speed of 180 RPM, as compared with 150 RPM of group A), we know that their speed must be in the upper part of the mentioned speed range (2100-2600 RPM), and we assume 2500 RPM. Finally, in order to keep the consistency with this assumed model/prototype ratio, and taking into account a prototype flow of 1600 ft³/s, their rated flow must be around 8.29 ft³/s (that is the value we choose).
The literature on PATs contains several hypothesis concerning the specific speed of both machines: Stepanoff[57] proposed 1850 and 2150 (divide by 2733 to get Ω_P), taking into account that the single-volute pump BEP is well away from the rated point (in the first edition of this book, he had suggested $N_S = 2140$ for both machines , using the rated prototype conditions). So do Lawrence & P.[81] (2000 and 2035). Kinno & K.[65] suppose 2110 and 1500, but this is because they thought that double-volute meant double-suction! There is also a lot of guessing about the diameter of the impeller: 13.25″, according to Lawrence & P.[81], 13″ for Kinno & K.[65]; we simply chose the average between 12.25″ and 14.5″ (the mentioned range).

Performance data:

Q [l/s]	H [m]	ω [RPM]	M [Nm]	η
Pump BEP				
183.2	102.1	2500	784	89.3%

Shut-off: $\grave{H}_P/\hat{H}_P = 1.03$; $\grave{P}_P/\hat{P}_P = 0.524$

Turbine BEP

267.3	128.7	2500	1166	90.5%

Regressions: $H[1\rightarrow20]$; $M[1\rightarrow19]$

Elasticities: $E_T = 1.46$; $E_{2T} = 2.03$

Turbine performance (20 points)

234.9	103.8	0	1282	0.0%
197.1	62.9	497	833	35.7%
199.9	62.9	746	819	51.9%
199.2	62.9	998	777	66.1%
250.2	98.9	1483	1177	75.4%
230.5	89.9	1889	898	87.5%
238.5	98.9	2098	939	89.3%
119.8	27.0	1179	235	91.8%
214.8	89.9	2309	699	89.3%
218.8	98.9	2533	699	87.5%
127.1	36.0	1556	235	85.6%
204.9	98.9	2712	562	80.3%
133.9	45.0	1845	235	77.1%
140.7	54.0	2094	235	69.4%
145.8	62.9	2300	235	63.0%
151.5	71.9	2512	235	58.0%
156.0	80.9	2691	235	53.6%
160.0	89.9	2864	235	50.1%
164.5	98.9	3047	235	47.1%
139.8	89.9	3057	0	0.0%

KNAP064

Category: end-suction/volute (radial-flow)

Ω_P 0.647

D_2 n/a

Data extent: stall↔runaway

Data quality: absolute values

Data presentation: Kármán-Knapp diagram

Nature of the study: transients in pumps

Make: Byron Jackson

Type: model?...

...This test data was published also by Peabody[39]. According to him, it is "based on actual tests of a scale model of one of the pumps for the Colorado River Aqueduct". However, in the next year, Peabody[40] says that the preliminary studies (apparently making reference to his 1939 paper) "were based upon pump characteristics taken from a pump, having a specific speed somewhat near that of the full sized pumps, but not in any sense a scale model". If it is a model, then the prototype would probably be the pumps of the intake pumping plant (see 1940), because they have a similar specific speed, and then the model ratio would be about 1:6

Original source: Knapp[37]

Other sources:

Locked rotor, absolute values and pump BEP from Knapp[38].

Data processing:

The lack of consistency between Fig. 10 (1937) and the left part of Fig. 2 (1938) shows that the rated point used to build the former is not the optimum; this rated point was found by achieving this consistency.

Performance data:

Q [l/s]	H [m]	ω [RPM]	M [Nm]	η
Pump BEP				
210.7	87.42	2133	880	91.8%

Shut-off: $\grave{H}_P/\hat{H}_P = 1.12$; $\grave{P}_P/\hat{P}_P = 0.493$

Turbine BEP

224.6	90.92	1933	858	86.8%

Regressions: $H[1\rightarrow16]$; $M[1\rightarrow13]$

Elasticities: $E_T = 1.38$; $E_{2T} = 2.08$

Turbine performance (16 points)

154.9	40.54	0	577	0.0%
245.0	90.92	1157	1208	67.0%
241.2	90.92	1377	1122	75.3%
236.9	90.92	1563	1035	80.3%
231.9	90.92	1736	949	83.5%
225.6	90.92	1900	863	85.4%
218.4	90.92	2051	776	85.7%
209.6	90.92	2179	690	84.4%
200.4	90.92	2273	604	80.5%
189.1	90.92	2358	518	75.9%
179.2	90.92	2421	431	68.5%
166.2	90.92	2475	345	60.4%
154.6	90.92	2525	258	49.7%
141.6	90.92	2570	172	36.8%
128.3	90.92	2611	86	20.7%
114.1	90.92	2639	0	0.0%

KNAP067

Category: end-suction/volute (radial-flow) (double-volute)

Ω_P ≈ 0.670

D_2 ≈ 340 mm

Data extent: stall↔runaway

Data quality: approximate absolute values

Data presentation: Kármán-Knapp diagram

Nature of the study: transients in pumps

Make: Byron Jackson

Type: old standard? pump (or a model?)

Original source: Knapp[41]

Other sources:

$\hat{\eta}_P$ from Knapp & D.[42].

Data processing:

The same pump-mode rated point as for KNAP063, but a different BEP.

Performance data:

Q [l/s]	H [m]	ω [RPM]	M [Nm]	η
Pump BEP				
195.5	98.1	2500	794.8	90.4%

Shut-off: $\grave{H}_P/\hat{H}_P = 0.999$; $\grave{P}_P/\hat{P}_P = 0.409$

Turbine BEP

268.3	116.2	2500	1045.8	89.6%

Regressions: $H[1\rightarrow19]$; $M[1\rightarrow18]$

Elasticities: $E_T = 1.34$; $E_{2T} = 1.95$

Turbine performance (19 points)

234.8	75.6	0	1010.2	0.0%
156.8	32.4	252	439.3	23.3%
159.3	33.2	497	439.3	44.1%
161.3	34.6	746	439.3	62.7%
242.3	80.9	1400	948.2	72.3%
236.6	80.9	1663	876.7	81.3%
231.9	80.9	1832	823.2	85.8%
228.2	80.9	1961	780.6	88.6%
216.2	80.9	2253	658.9	90.6%
211.0	80.9	2343	604.2	88.6%
181.0	62.9	2115	439.3	87.1%
182.6	66.2	2213	439.3	85.8%
185.1	71.9	2346	439.3	82.7%
187.6	80.9	2533	439.3	78.3%
191.2	89.9	2688	439.3	73.4%
194.3	98.9	2854	439.3	69.7%
197.3	107.9	2998	439.3	66.1%
150.3	80.9	2691	219.6	51.9%
110.9	80.9	2903	0.0	0.0%

LAUX039

Category: end-suction/volute (radial-flow)
Ω_P 0.397
D_2 n/a
Data extent: →runaway
Data quality: only relative values
(It is not explicit that the data were actually obtained in tests.)
Extra data: different air contents
Data presentation: constant speed graphs
Nature of the study: PATs
Make: Sulzer
Type: standard? pump (HPH25)
Original source: Laux[80]
Other sources:
Performance data with different air contents in Gülich[81].

Performance data:

Q [l/s]	H [m]	ω [RPM]	M [Nm]	η
Pump BEP				
1.000	1.000	664.4	0.174	80.8%
Shut-off: $\dot{H}_P/\hat{H}_P = 1.13$; $\dot{P}_P/\hat{P}_P = 0.392$				
Turbine BEP				
1.409	1.487	664.4	0.252	85.4%
Regressions: $H[1\rightarrow12]$; $M[1\rightarrow10]$				
Elasticities: $E_T = 1.39$; $E_{2T} = 1.73$				
Turbine performance (12 points)				
1.604	1.804	664.4	0.338	82.9%
1.500	1.625	664.4	0.291	84.6%
1.374	1.438	664.4	0.237	85.0%
1.311	1.345	664.4	0.211	85.1%
1.257	1.275	664.4	0.191	84.5%
1.130	1.127	664.4	0.147	81.8%
0.999	0.999	664.4	0.108	76.9%
0.889	0.902	664.4	0.079	70.1%
0.758	0.810	664.4	0.050	57.6%
0.632	0.736	664.4	0.025	38.2%
0.502	0.678	664.4	0.005	10.5%
0.464	0.663	664.4	0.000	0.0%

LUEN043

Category: end-suction/volute (radial-flow)?
Ω_P 0.439
D_2 n/a
Data extent: →runaway
Data quality: only relative values
(It is not explicit that the data were actually obtained in tests.)
Data presentation: constant speed graphs
Nature of the study: PATs
Make: Bingham-Willamette?
Type: standard? pump
Original source: Lueneburg & N.[85]
Data processing:
Lack of consistency between the H_T, η_T and P_T curves ⇒ the latter was discarded because its scale makes it the least accurate (it was used only to calculate $\hat{\eta}_P$).

Performance data:

Q [l/s]	H [m]	ω [RPM]	M [Nm]	η
Pump BEP				
1.000	1.000	734.6	0.183	69.5%
Shut-off: $\dot{H}_P/\hat{H}_P = 1.20$; $\dot{P}_P/\hat{P}_P = 0.406$				
Turbine BEP				
1.349	1.659	734.6	0.203	71.0%
Regressions: $H[1\rightarrow11]$; $M[1\rightarrow9]$				
Elasticities: $E_T = 1.56$; $E_{2T} = 2.52$				
Turbine performance (11 points)				
1.499	1.979	734.6	0.262	69.2%
1.396	1.755	734.6	0.220	70.3%
1.299	1.558	734.6	0.182	70.4%
1.196	1.385	734.6	0.148	69.9%
1.094	1.241	734.6	0.117	67.6%
0.996	1.130	734.6	0.090	63.0%
0.896	1.027	734.6	0.065	55.3%
0.796	0.947	734.6	0.044	45.4%
0.698	0.885	734.6	0.024	30.8%
0.600	0.836	734.6	0.004	5.5%
0.587	0.831	734.6	0.000	0.0%

MEIE056

Category: end-suction/volute (radial-flow) (with fixed vanes)
Ω_P 0.569
D_2 n/a
Data extent: only around the BEP
Data quality: only relative values
(It is not explicit that the data were actually obtained in tests.)
Data presentation: constant speed graphs
Nature of the study: pump-turbines
Make: Escher Wyss
Type: standard? pump (or a model?)
Original source: Meier[82]
Data processing:
$\hat{\eta}_P$ calculated by deduction.

Performance data:

Q [l/s]	H [m]	ω [RPM]	M [Nm]	η
Pump BEP				
1.000	1.000	952.2	0.111	89.0%

Shut-off: $\dot{H}_P/\hat{H}_P = 1.16$; $\dot{P}_P/\hat{P}_P = 0.536$

Turbine BEP				
1.095	0.923	813.8	0.100	86.1%

Regressions: $H[1\rightarrow10]$; $M[1\rightarrow10]$
Elasticities: $E_T = 1.65$; $E_{2T} = 1.90$
Turbine performance (10 points)

1.188	1.059	813.8	0.123	85.0%
1.168	1.027	813.8	0.118	85.4%
1.128	0.969	813.8	0.108	86.0%
1.086	0.910	813.8	0.098	86.4%
1.046	0.858	813.8	0.089	86.3%
1.006	0.805	813.8	0.080	86.1%
0.965	0.755	813.8	0.071	85.1%
0.925	0.706	813.8	0.063	83.7%
0.884	0.662	813.8	0.055	81.7%
0.843	0.619	813.8	0.048	79.2%

MIKU049

Category: multistage (3 radial-flow stages)
Ω_P 0.497
D_2 315 mm
Data extent: stall (no M)↔runaway
Data quality: absolute values (see note about ω_T, below)
Extra data: modifications
Data presentation: constant speed graph
Nature of the study: PATs
Make: KSB
Type: standard pump (DIN 1944, group II; WKL... or WKF...)
Original source: Mikus[83]
Data processing:
Lack of consistency between the H, η and P curves in both modes of operation ⇒ in both cases the latter was discarded. The value of $\omega_T = 1510$ RPM was taken from Fig. 2, but in Fig. 4 (where the turbine performance data comes from) the data may have been affinity-laws-corrected to 1500 RPM, in which case the data below would be slightly wrong. $\dot{P}_P$ obtained by extrapolation.

Performance data:

Q [l/s]	H [m]	ω [RPM]	M [Nm]	η
Pump BEP				
60.06	33.65	1500	156.6	80.6%

Shut-off: $\dot{H}_P/\hat{H}_P = 1.24$; $\dot{P}_P/\hat{P}_P = 0.562$

Turbine BEP				
83.21	46.47	1510	176.7	73.7%

Regressions: $H[1\rightarrow13]$; $M[1\rightarrow12]$
Elasticities: $E_T = 1.34$; $E_{2T} = 1.85$
Turbine performance (13 points)

80.27	36.55	0	n/a	0.0%
92.84	54.36	1510	231.3	73.9%
90.48	52.32	1510	216.9	73.9%
83.22	46.38	1510	174.7	73.0%
75.71	41.09	1510	138.1	71.6%
68.02	36.47	1510	106.4	69.2%
62.79	33.79	1510	88.2	67.0%
57.10	31.31	1510	70.6	63.7%
52.59	29.56	1510	58.3	60.5%
46.58	27.51	1510	43.1	54.3%
40.04	25.76	1510	28.2	44.2%
34.04	24.53	1510	12.8	24.8%
29.17	23.79	1510	0.0	0.0%

MIYA079

Category:	double-suction
Ω_P	0.798
D_2	350 mm
Data extent:	stall↔runaway
Data quality:	absolute values
Extra data:	radial thrust
Data presentation:	Kármán-Knapp diagram
Nature of the study:	transients in pumps
Make:	Hitachi
Type:	model (scale 1:4.11)
Original source:	Miyashiro & K.[70]

Data processing:

The pump-mode rated point (necessary to determine the turbine performance, that is expressed in its terms) is the H_P and the η_P corresponding to $\bar{Q}_P$.

Performance data:

Q [l/s]	H [m]	ω [RPM]	M [Nm]	η
Pump BEP				
297.5	127.6	2940	1335	90.6%
Shut-off: $\dot{H}_P/\hat{H}_P = 1.47$; $\dot{P}_P/\hat{P}_P = 0.827$				
Turbine BEP				
369.4	182.0	2940	1895	88.5%
Regressions: $H[1\rightarrow15]$; $M[1\rightarrow14]$				
Elasticities: $E_T = 1.65$; $E_{2T} = 2.78$				
Turbine performance (15 points)				
282.3	120.6	0	1770	0.0%
301.1	120.6	1355	1644	65.5%
167.6	36.2	1190	411	86.2%
302.5	120.6	2438	1233	88.0%
291.6	120.6	2595	1096	86.4%
270.7	120.6	2919	822	78.5%
202.9	72.4	2339	411	69.9%
251.5	120.6	3147	548	60.7%
222.7	96.5	2830	411	57.8%
229.6	108.5	3029	411	53.3%
236.6	120.6	3210	411	49.4%
250.5	144.7	3589	411	43.5%
217.1	120.6	3282	274	36.7%
195.6	120.6	3346	137	20.8%
184.4	120.6	3381	0	0.0%

MIYA194

Category:	bowl (mixed-flow)
Ω_P	1.94
D_2	409 mm
Data extent:	stall↔runaway
Data quality:	absolute values
Data presentation:	constant head graph
Nature of the study:	transients in pumps
Make:	Hitachi
Type:	model (scale 1:8.2)
Original source:	Miyashiro & K.[69]

Data processing:

Lack of consistency between H_P , η_P and P_P curves ⇒ the latter was discarded because it yields an efficiency curve with a very unlikely shape.

In the turbine performance points there is a big jump between the 7th and the 8th points; unfortunately, it is very difficult to get additional intermediate points, on account of the sharp geometry of the flow-torque curve near runaway in Fig. 10.

Performance data:

Q [l/s]	H [m]	ω [RPM]	M [Nm]	η
Pump BEP				
349.4	19.96	1640	460.1	86.5%
Shut-off: $\dot{H}_P/\hat{H}_P = 1.81$; $\dot{P}_P/\hat{P}_P = 0.923$				
Turbine BEP				
424.4	23.20	1607	455.4	79.4%
Regressions: $H[1\rightarrow8]$; $M[1\rightarrow7]$				
Elasticities: $E_T = 2.58$; $E_{2T} = 4.26$				
Turbine performance (8 points)				
289.6	23.20	0	502.4	0.0%
311.1	23.20	203	529.7	16.0%
334.0	23.20	433	557.1	33.3%
356.9	23.20	693	566.9	50.7%
381.4	23.20	984	560.6	66.6%
402.4	23.20	1270	523.0	76.0%
423.6	23.20	1592	454.1	78.6%
444.7	23.20	2494	0.0	0.0%

MIYA348

Category: bowl (axial-flow)
Ω_P 3.48
D_2 409 mm
Data extent: stall↔runaway
Data quality: absolute values
Data presentation: constant head graph
Nature of the study: transients in pumps
Make: Hitachi
Type: model (scale 1:8.2)
Original source: Miyashiro & K.[69]
Data processing:
Lack of consistency between H_P, η_P and P_P curves ⇒ an average was used.

Performance data:

Q [l/s]	H [m]	ω [RPM]	M [Nm]	η
Pump BEP				
327.6	8.77	1640	187.8	87.4%
Shut-off: $\dot{H}_P/\hat{H}_P = 2.50$; $\dot{P}_P/\hat{P}_P = 1.88$				
Turbine BEP				
413.8	10.70	1507	215.3	78.3%
Regressions: H[4→9]; M[2→9]				
Elasticities: $E_T = 3.15$; $E_{2T} = 4.96$				
Turbine performance (9 points)				
225.4	10.70	0	218.6	0.0%
267.5	10.70	423	215.7	34.1%
311.3	10.70	666	223.0	47.6%
353.0	10.70	913	240.6	62.2%
394.8	10.70	1297	236.4	77.6%
438.5	10.70	1766	188.6	75.8%
482.2	10.70	2192	139.5	63.3%
528.9	10.70	2644	75.0	37.4%
575.6	10.70	3060	0.0	0.0%

NELI044

Category: multistage (2 radial-flow stages)
Ω_P 0.448
D_2 284 mm
Data extent: →almost runaway
Data quality: absolute values
(in this case ω_T is clearly 1750 RPM)
Extra data: geometry
Data presentation: constant speed graph
Nature of the study: PATs
Make: Ingersoll-Rand
Type: standard pump
Original source: Nelik & C.[84]
Data processing:
Pump BEP directly from original source (not calculated).
Lack of consistency between H_T, η_T and P_T curves ⇒ the former was discarded to match the turbine BEP proposed by the authors.
Shut-off data slightly extrapolated.

Performance data:

Q [l/s]	H [m]	ω [RPM]	M [Nm]	η
Pump BEP				
36.10	33.80	1750	79.8	81.8%
Shut-off: $\dot{H}_P/\hat{H}_P = 1.28$; $\dot{P}_P/\hat{P}_P = 0.307$				
Turbine BEP				
50.46	48.47	1750	95.7	73.2%
Regressions: H[1→8]; M[1→8]				
Elasticities: $E_T = 1.54$; $E_{2T} = 2.00$				
Turbine performance (8 points)				
60.10	63.27	1750	143.4	70.5%
55.19	56.19	1750	119.9	72.2%
50.12	48.32	1750	95.2	73.4%
45.21	42.27	1750	75.4	73.8%
40.12	35.38	1750	53.6	70.6%
34.98	29.19	1750	33.5	61.3%
29.99	25.68	1750	19.9	48.3%
25.03	24.59	1750	11.7	35.6%

PECK098

Category: end-suction/volute (radial-flow)
Ω_P 0.984
D_2 273 mm
Data extent: stall↔runaway
Data quality: absolute values
Extra data: geometry
Data presentation: constant head graph
Nature of the study: investigation of flow conditions
Make: Loughborough College
Type: special laboratory pump (impeller 'B')
Original source: Peck[51]

Performance data:

Q [l/s]	H [m]	ω [RPM]	M [Nm]	η
Pump BEP				
52.10	9.15	1199	49.1	75.7%
Shut-off: $\dot{H}_P/\hat{H}_P = 1.50$; $\dot{P}_P/\hat{P}_P = 0.445$				
Turbine BEP				
51.85	9.15	857	38.2	73.8%
Regressions: $H[1\rightarrow13]$; $M[1\rightarrow13]$				
Elasticities: $E_T = 2.06$; $E_{2T} = 3.83$				
Turbine performance (13 points)				
37.74	9.15	0	43.7	0.0%
40.61	9.15	110	44.8	14.3%
43.24	9.15	222	45.7	27.4%
45.53	9.15	330	46.5	39.3%
47.47	9.15	436	46.7	50.1%
49.09	9.15	547	45.9	59.8%
50.26	9.15	654	43.8	66.7%
51.37	9.15	764	40.8	70.8%
51.88	9.15	873	37.5	73.6%
51.98	9.15	986	32.6	72.3%
49.95	9.15	1096	23.9	61.3%
46.23	9.15	1204	12.0	36.7%
40.67	9.15	1290	0.0	0.0%

SANT050

Category: end-suction/volute (radial-flow)
Ω_P 0.500
D_2 200 mm
Data extent: →almost runaway
Data quality: absolute values
Extra data: radial load, different speeds
Data presentation: constant speed graph
Nature of the study: PATs
Make: n/a
Type: standard pump
Original source: Santolaria & F.[92]
Data processing:
$\dot{P}_P$ obtained by extrapolation.

Performance data:

Q [l/s]	H [m]	ω [RPM]	M [Nm]	η
Pump BEP				
19.42	23.12	2000	29.15	72.1%
Shut-off: $\dot{H}_P/\hat{H}_P = 1.16$; $\dot{P}_P/\hat{P}_P = 0.38$				
Turbine BEP				
32.95	50.58	2000	49.47	63.4%
Regressions: $H[1\rightarrow16]$; $M[1\rightarrow12]$				
Elasticities: $E_T = 1.90$; $E_{2T} = 3.18$				
Turbine performance (16 points)				
40.90	78.77	2000	89.41	59.3%
39.38	72.67	2000	81.34	60.7%
37.84	67.30	2000	73.85	61.9%
36.43	61.56	2000	65.93	62.8%
34.87	56.56	2000	58.55	63.4%
33.67	52.31	2000	52.38	63.5%
32.49	49.17	2000	47.55	63.6%
31.34	45.41	2000	41.96	63.0%
29.90	42.41	2000	36.90	62.2%
28.57	38.93	2000	31.84	61.1%
27.19	35.97	2000	26.75	58.4%
25.03	32.43	2000	20.92	55.0%
22.88	29.10	2000	15.58	50.0%
20.25	25.91	2000	10.43	42.4%
17.84	22.72	2000	5.91	31.2%
14.55	20.17	2000	1.40	10.2%

SCHM027

Category: end-suction/volute (radial-flow)
Ω_P 0.271
D_2 ≈ 250 mm
Data extent: →runaway
Data quality: absolute values
Data presentation: constant speed graph
Nature of the study: PATs
Make: Rütschi (?)
Type: commercial pump (NCP8-250) that does not follow ISO standards
Original source: Schmiedl[88]

Data processing:
Pump BEP directly from original source. Runaway point from intersection of H_T and $M_T = 0$ curves (and not from $\eta_T = 0$ and $P_T = 0$ points).

Performance data:

Q [l/s]	H [m]	ω [RPM]	M [Nm]	η
Pump BEP				
8.70	19.90	1450	17.31	64.6%
Shut-off: $\dot{H}_P/\hat{H}_P$ = n/a; $\dot{P}_P/\hat{P}_P$ = n/a				
Turbine BEP				
11.88	21.74	1000	15.82	65.4%
Regressions: H[1→17]; M[1→17]				
Elasticities: E_T = 1.41; E_{2T} = 1.76				
Turbine performance (17 points)				
15.31	31.99	1000	27.76	60.5%
14.80	30.20	1000	25.66	61.3%
14.27	28.76	1000	24.05	62.6%
13.96	27.72	1000	22.88	63.1%
13.48	26.25	1000	21.20	64.0%
12.91	24.58	1000	19.26	64.8%
12.37	23.12	1000	17.49	65.3%
11.78	21.59	1000	15.70	65.9%
11.19	20.25	1000	13.97	65.8%
10.57	18.67	1000	12.03	65.1%
9.80	16.95	1000	9.97	64.1%
8.92	15.27	1000	7.89	61.8%
8.32	14.07	1000	6.41	58.4%
7.53	12.92	1000	4.95	54.3%
6.84	12.14	1000	3.66	47.1%
5.54	11.16	1000	1.85	32.0%
3.73	10.15	1040	0.00	0.0%

SENU037

Category: end-suction/volute (radial flow) (semi-open impeller)
Ω_P 0.366
D_2 101.4 mm
Data extent: only around the BEP
Data quality: absolute values
Data presentation: table
Nature of the study: PATs
Make: Gilkes
Type: standard pump (EM132)
Original source: Senu[90] (experiment No. 3)

Other sources:
Also published by Williams[92].

Performance data:

Q [l/s]	H [m]	ω [RPM]	M [Nm]	η
Pump BEP				
1.382	8.11	2500	0.801	52.4%
Shut-off: $\dot{H}_P/\hat{H}_P$ = 1.22; $\dot{P}_P/\hat{P}_P$ = 0.556				
Turbine BEP				
2.801	29.14	2500	1.640	53.6%
Regressions: H[2→17]; M[2→17]				
Elasticities: E_T = 1.64; E_{2T} = 2.06				
Turbine performance (17 points)				
3.180	35.27	2500	2.178	51.8%
3.000	33.13	2500	1.980	53.2%
2.900	30.99	2500	1.799	53.4%
2.800	29.26	2500	1.667	54.3%
2.700	27.32	2500	1.534	55.5%
2.600	25.38	2500	1.403	56.7%
2.500	24.06	2500	1.221	54.2%
2.400	22.83	2500	1.039	50.6%
2.300	21.51	2500	0.908	49.0%
2.200	20.59	2500	0.809	47.7%
2.100	19.16	2500	0.693	46.0%
2.000	18.25	2500	0.610	44.6%
1.900	16.82	2500	0.511	42.7%
1.800	16.11	2500	0.445	41.0%
1.700	14.88	2500	0.363	38.3%
1.600	14.17	2500	0.297	35.0%
1.500	13.25	2500	0.207	27.8%

SMIT035

Category: double-suction
Ω_P 0.346
D_2 246 mm
Data extent: only around the BEP
Data quality: absolute values
Data presentation: constant speed graph
Nature of the study: PATs
Make: Worthington-Simpson
Type: standard pump (3L2) with reduced impeller
(The results of tests with full-sized impeller made in Nottingham Polytechnic are unreliable, according to Williams.)
Original source: Smith[86] (unpublished)
Other sources:
Reproduced by Williams[92].
Pump data from manufacturers, interpolating impeller sizes.

Performance data:

Q [l/s]	H [m]	ω [RPM]	M [Nm]	η
Pump BEP				
20.00	15.40	1425	27.65	73.2%
Shut-off: $\dot{H}_P/\hat{H}_P = 1.28$; $\dot{P}_P/\hat{P}_P = 0.443$				
Turbine BEP				
25.37	24.24	1450	22.78	57.4%
Regressions: $H[1\rightarrow20]$; $M[1\rightarrow20]$				
Elasticities: $E_T = 1.37$; $E_{2T} = 2.71$				
Turbine performance (20 points)				
26.40	25.90	1450	24.95	56.5%
25.50	24.30	1450	23.01	57.5%
24.60	23.00	1450	21.01	57.5%
23.60	22.10	1450	19.03	56.5%
22.70	21.10	1450	17.54	56.7%
22.30	20.70	1450	16.84	56.5%
21.90	20.50	1450	16.09	55.5%
21.60	20.10	1450	15.42	55.0%
21.30	19.70	1450	14.77	54.5%
20.70	19.20	1450	13.91	54.2%
20.30	18.90	1450	13.26	53.5%
20.00	18.70	1450	12.92	53.5%
19.80	18.50	1450	12.42	52.5%
19.30	18.30	1450	11.75	51.5%
18.70	17.80	1450	10.53	49.0%
17.30	17.10	1450	9.08	47.5%
17.10	16.90	1450	8.68	46.5%
16.70	16.70	1450	8.02	44.5%
16.15	16.60	1450	7.19	41.5%
15.70	16.30	1450	6.53	39.5%

STIR348

Category: bowl (axial-flow)
Ω_P 3.48
D_2 n/a
Data extent: stall↔runaway
Data quality: approximate absolute values
Extra data: different heads, axial thrust, geometry
Data presentation: constant head graphs
Nature of the study: transients in pumps
Make: National Engineering Laboratory
Type: special laboratory pump
Original source: Stirling[83].
Data processing:
Lack of consistency between the H_P, η_P and P_P curves ⇒ the latter was discarded to match the $\hat{\eta}_P$ mentioned by the author (84%).
Absolute values decided in an arbitrary way, taking into account the size of the dynamometer.

Performance data:

Q [l/s]	H [m]	ω [RPM]	M [Nm]	η
Pump BEP				
1408	6.957	665	1653	83.4%
Shut-off: $\dot{H}_P/\hat{H}_P = 2.59$; $\dot{P}_P/\hat{P}_P = 2.16$				
Turbine BEP				
1419	6.526	482	1232	68.6%
Regressions: $H[1\rightarrow14]$; $M[1\rightarrow12]$				
Elasticities: $E_T = 3.69$; $E_{2T} = 6.13$				
Turbine performance (14 points)				
752	6.526	0	1467	0.0%
850	6.526	65	1501	19.0%
964	6.526	137	1526	35.7%
1078	6.526	215	1522	49.8%
1177	6.526	294	1503	61.4%
1284	6.526	379	1381	66.8%
1397	6.526	465	1213	66.2%
1498	6.526	543	1082	64.2%
1600	6.526	618	975	61.7%
1702	6.526	689	870	57.7%
1815	6.526	769	717	49.7%
1934	6.526	845	527	37.8%
2064	6.526	925	294	21.6%
2231	6.526	1020	0	0.0%

STRA022

Category: end-suction/volute (radial-flow)
Ω_P 0.226
D_2 320 mm
Data extent: stall (no M)↔runaway
Data quality: absolute values
Extra data: different ring clearances, different speeds, geometry
Data presentation: constant speed graphs
Nature of the study: PATs
Make: KSB
Type: standard pump (Etanorm 50-315)
Original source: Strate *et al.*[90]
(Only smaller ring clearance was used.)
(Some points from Fig. 4.)
Other sources:
Pump data from manufacturers (the pump type was deduced from the geometry data in p. 5 of the original source).
Data processing:
Slight lack of consistency between the H_T, η_T and P_T curves ⇒ an average was used.

Performance data:

Q [l/s]	H [m]	ω [RPM]	M [Nm]	η
Pump BEP				
12.53	32.30	1450	42.49	61.5%
Shut-off: $\dot{H}_P/\hat{H}_P = 1.11$; $\dot{P}_P/\hat{P}_P = 0.31$				
Turbine BEP				
12.19	27.98	920	18.01	51.9%
Regressions: $H[1\rightarrow10]$; $M[1\rightarrow8]$				
Elasticities: $E_T = 1.38$; $E_{2T} = 1.48$				
Turbine performance (10 points)				
11.20	18.15	0	n/a	0.0%
19.11	56.24	920	48.62	44.4%
16.78	45.30	920	37.37	48.3%
12.98	30.73	920	21.15	52.1%
12.71	30.13	920	20.43	52.4%
12.30	28.38	920	18.62	52.4%
10.24	22.01	920	11.71	51.0%
8.18	17.32	920	6.48	44.9%
6.15	14.23	920	2.18	24.4%
5.12	13.21	920	0.00	0.0%

STRA043

Category: end-suction/volute (radial-flow)
Ω_P 0.434
D_2 334 mm
Data extent: stall (no M)↔runaway
Data quality: absolute values
Extra data: different ring clearances, geometry
Data presentation: constant speed graphs
Nature of the study: PATs
Make: KSB
Type: standard pump (Etanorm 100-315)
Original source: Strate *et al.*[90]
(Only smaller ring clearance was used.)
Other sources:
Pump data from manufacturers (the pump type was deduced from the geometry data in p. 5 of the original source).
Data processing:
Slight lack of consistency between the H_T, η_T and P_T curves ⇒ the latter was discarded.

Performance data:

Q [l/s]	H [m]	ω [RPM]	M [Nm]	η
Pump BEP				
51.39	34.70	1450	142.2	81.0%
Shut-off: $\dot{H}_P/\hat{H}_P = 1.15$; $\dot{P}_P/\hat{P}_P = 0.278$				
Turbine BEP				
69.39	49.01	1500	170.9	80.5%
Regressions: $H[1\rightarrow14]$; $M[1\rightarrow11]$				
Elasticities: $E_T = 1.22$; $E_{2T} = 2.04$				
Turbine performance (14 points)				
78.16	57.42	1500	223.3	79.7%
73.33	52.87	1500	194.3	80.3%
71.63	51.12	1500	183.5	80.3%
69.86	49.37	1500	173.5	80.6%
68.33	47.97	1500	164.9	80.6%
67.39	46.91	1500	158.4	80.3%
66.27	46.22	1500	153.5	80.2%
65.10	45.54	1500	148.0	79.9%
60.08	42.07	1500	124.2	78.7%
49.71	36.22	1500	80.8	71.9%
40.25	32.88	1500	48.4	58.6%
30.14	30.97	1500	17.2	29.6%
24.02	30.05	1500	1.0	2.2%
23.29	30.07	1500	0.0	0.0%

STRA081

Category: end-suction/volute (radial-flow)
Ω_P 0.813
D_2 219 mm
Data extent: stall (no M)↔runaway
Data quality: absolute values
Extra data: different ring clearances, geometry
Data presentation: constant speed graphs
Nature of the study: PATs
Make: KSB
Type: standard pump (Etanorm 100-200?) (see also DIED088)
Original source: Strate *et al.*[90]
(Only smaller ring clearance was used.)
Other sources:
Pump data from manufacturers (the pump type was deduced from the geometry data in p. 5 of the original source).
Data processing:
Slight lack of consistency between the H_T, η_T and P_T curves ⇒ the latter was discarded.

Performance data:

Q [l/s]	H [m]	ω [RPM]	M [Nm]	η
Pump BEP				
42.92	13.35	1450	43.3	85.5%
Shut-off: $\dot{H}_P/\hat{H}_P = 1.21$; $\dot{P}_P/\hat{P}_P = 0.441$				
Turbine BEP				
56.15	22.11	1500	60.4	77.9%
Regressions: $H[1\rightarrow14]$; $M[1\rightarrow13]$				
Elasticities: $E_T = 1.51$; $E_{2T} = 2.07$				
Turbine performance (14 points)				
80.11	40.43	1500	140.3	69.4%
70.18	31.70	1500	103.5	74.5%
60.00	24.77	1500	71.9	77.5%
58.68	23.66	1500	67.5	77.8%
57.55	22.72	1500	63.8	78.1%
56.83	22.48	1500	62.3	78.1%
56.05	22.07	1500	60.1	77.9%
55.05	21.64	1500	57.9	77.9%
54.24	21.12	1500	55.7	77.9%
53.34	20.71	1500	53.5	77.6%
50.06	18.72	1500	44.7	76.4%
43.59	15.47	1500	30.8	73.2%
33.45	12.50	1500	14.0	53.7%
22.63	10.37	1500	0.0	0.0%

STRU051

Category: end-suction/volute (radial-flow)
Ω_P 0.518
D_2 n/a
Data extent: stall↔runaway
Data quality: only relativc values
Data presentation: constant speed and constant head graphs
Nature of the study: pump-turbines
Make: Sulzer
Type: standard pump (a bit old)
Original source: Strub[59]
Data processing:
Lack of consistency between the ψ_P, η_P and λ_P curves ⇒ the latter was discarded because its scale makes it the least accurate.
The stall torque was calculated by extrapolation.

Performance data:

Q [l/s]	H [m]	ω [RPM]	M [Nm]	η
Pump BEP				
1.000	1.000	866.8	0.129	84.0%
Shut-off: $\dot{H}_P/\hat{H}_P = 1.31$; $\dot{P}_P/\hat{P}_P = 0.488$				
Turbine BEP				
1.305	1.274	866.8	0.154	85.6%
Regressions: $H[1\rightarrow17]$; $M[1\rightarrow17]$				
Elasticities: $E_T = 1.58$; $E_{2T} = 2.13$				
Turbine performance (17 points)				
1.155	1.000	0.0	0.176	0.0%
1.169	1.000	84.7	0.176	13.6%
1.180	1.000	170.0	0.176	27.1%
1.194	1.000	254.6	0.171	39.0%
1.202	1.000	339.9	0.169	51.1%
1.211	1.000	424.4	0.165	61.6%
1.214	1.000	510.7	0.157	70.7%
1.210	1.000	595.7	0.150	78.7%
1.669	1.950	866.8	0.283	80.6%
1.495	1.598	866.8	0.216	83.9%
1.319	1.304	866.8	0.159	85.6%
1.230	1.175	866.8	0.134	86.1%
1.142	1.046	866.8	0.110	85.6%
0.967	0.828	866.8	0.069	79.4%
0.791	0.681	866.8	0.036	61.1%
0.617	0.623	866.8	0.012	30.0%
0.499	0.599	866.8	0.000	0.0%

SWAN274

Category: bowl (mixed-flow)
Ω_P 2.74
D_2 210 mm
Data extent: stall↔runaway
Data quality: approximate absolute values
Extra data: geometry
Data presentation: constant flow graph
Nature of the study: transients in pumps
Make: Peerless
Type: old standard pump (10MH)
Original source: Swanson[53]
Other sources:
Efficiencies (and geometry) from Kittredge[61].
Pump BEP (and hence absolute values) from the manufacturers.

Performance data:

Q [l/s]	H [m]	ω [RPM]	M [Nm]	η
Pump BEP				
90.40	5.61	1760	32.50	83.0%
Shut-off: $\dot{H}_P/\hat{H}_P = 2.00$; $\dot{P}_P/\hat{P}_P = 1.37$				
Turbine BEP				
90.40	3.48	1173	19.71	78.5%
Regressions: $H[4\rightarrow10]$; $M[4\rightarrow10]$				
Elasticities: $E_T = 2.93$; $E_{2T} = 4.67$				
Turbine performance (10 points)				
90.40	11.91	0	69.02	0.0%
90.40	10.11	194	57.72	13.1%
90.40	8.13	394	47.09	26.9%
90.40	5.97	593	37.44	44.0%
90.40	4.49	794	30.96	64.7%
90.40	3.91	993	24.93	74.8%
90.40	3.51	1194	19.11	76.7%
90.40	2.97	1394	13.15	72.8%
90.40	2.44	1593	6.36	49.1%
90.40	2.16	1773	0.00	0.0%

SWAN496

Category: bowl (axial-flow)
Ω_P 4.96
D_2 203 mm
Data extent: stall↔runaway
Data quality: approximate absolute values
Data presentation: constant flow graph
Nature of the study: transients in pumps
Make: Peerless
Type: old standard pump (10PL)
Original source: Swanson[53]
Other sources:
Geometry from Kittredge[61].
Pump BEP (and hence absolute values) from the manufacturers.
Data processing:
$\hat{\eta}_P$ is 80% according to Swanson and 77.3% according to the manufacturers; however, the value of 75.2% was chosen to achieve consistency between the relative values of M_T, H_T and η_T.

Performance data:

Q [l/s]	H [m]	ω [RPM]	M [Nm]	η
Pump BEP				
51.73	0.793	970.0	5.263	75.2%
Shut-off: $\dot{H}_P/\hat{H}_P = 2.85$; $\dot{P}_P/\hat{P}_P = 2.01$				
Turbine BEP				
51.73	0.540	609.2	3.266	76.0%
Regressions: $H[7\rightarrow13]$; $M[11\rightarrow14]$				
Elasticities: $E_T = 2.31$; $E_{2T} = 2.86$				
Turbine performance (19 points)				
51.73	0.874	0.0	3.305	0.0%
51.73	0.765	47.5	2.709	3.5%
51.73	0.687	97.0	2.551	7.4%
51.73	0.644	143.9	2.664	12.3%
51.73	0.643	194.3	3.015	18.8%
51.73	0.654	243.1	3.459	26.6%
51.73	0.652	289.7	3.806	34.9%
51.73	0.629	337.2	3.972	43.9%
51.73	0.602	388.5	4.013	53.5%
51.73	0.590	435.3	4.095	62.4%
51.73	0.580	484.2	4.069	70.1%
51.73	0.567	531.3	3.867	74.8%
51.73	0.545	580.7	3.516	77.3%
51.73	0.519	630.3	3.083	77.3%
51.73	0.493	677.6	2.630	74.7%
51.73	0.447	727.4	2.082	69.9%
51.73	0.400	769.0	1.588	63.0%
51.73	0.317	832.7	0.839	45.5%
51.73	0.221	902.9	0.000	0.0%

THOM062

Category: end-suction/volute (radial-flow)
Ω_P 0.622
D_2 n/a
Data extent: stall↔runaway
Data quality: absolute values
Data presentation: constant speed and constant flow graphs (Thoma diagram)
Nature of the study: transients in pumps
Make: n/a
Type: old standard? pump
Original sources: Thoma[31] and Kittredge[31]

Performance data:

Q [l/s]	H [m]	ω [RPM]	M [Nm]	η
Pump BEP				
8.54	4.285	1060	4.729	68.4%

Shut-off: $\dot{H}_P/\hat{H}_P = 1.06$; $\dot{P}_P/\hat{P}_P = 0.288$

Turbine BEP				
14.16	8.043	1060	8.042	79.9%

Regressions: $H[1\rightarrow 8]$; $M[1\rightarrow 8]$
Elasticities: $E_T = 1.46$; $E_{2T} = 2.58$

Turbine performance (8 points)

9.19	3.927	0	4.903	0.0%
9.19	3.273	307	4.346	47.5%
9.19	3.130	540	3.787	76.0%
9.19	3.315	675	3.336	79.0%
9.19	3.859	825	2.969	73.8%
9.74	5.490	1060	3.183	67.4%
5.30	4.062	1060	0.238	12.5%
4.45	3.876	1060	0.000	0.0%

THOM150

Category: multistage (2 radial-flow stages)
Ω_P 1.503
D_2 1372 mm [!?]
Data extent: stall↔runaway
Data quality: absolute values
Data presentation: table, Suter-type
Nature of the study: transients in pumps
Make: Byron-Jackson
Type: standard?? pump (54RXM)
Original source: Thomas[72]
Data processing:
The runaway point was obtained by interpolation.

Performance data:

Q [l/s]	H [m]	ω [RPM]	M [Nm]	η
Pump BEP				
2377	25.88	592.0	11533	84.4%

Shut-off: $\dot{H}_P/\hat{H}_P = 1.52$; $\dot{P}_P/\hat{P}_P = 0.785$

Turbine BEP				
2940	40.75	592.0	13753	72.6%

Regressions: $H[1\rightarrow 9]$; $M[1\rightarrow 9]$
Elasticities: $E_T = 2.08$; $E_{2T} = 3.10$

Turbine performance (9 points)

2170	30.28	0.0	13520	0.0%
2170	28.32	98.7	12489	21.4%
2170	25.80	197.3	11000	41.4%
2170	24.40	296.0	9625	57.5%
2170	22.71	394.7	8021	68.6%
2170	22.15	493.3	6416	70.3%
2170	22.15	592.0	5156	67.8%
1808	18.79	592.0	2062	38.4%
1602	16.49	592.0	0	0.0%

THOR042

Category:	double-suction
Ω_P	0.426
D_2	318 mm
Data extent:	→almost runaway
Data quality:	absolute values
Extra data:	different diameters (only for turbine-mode)
Data presentation:	constant speed graph
Nature of the study:	PATs
Make:	Worthington-Simpson
Type:	standard pump (6L2)
Original source:	Thome[90] (unpublished)

Performance data:

Q [l/s]	H [m]	ω [RPM]	M [Nm]	η
Pump BEP				
38.48	30.19	1480	88.0	83.6%

Shut-off: $\dot{H}_P/\hat{H}_P = 1.21$; $\dot{P}_P/\hat{P}_P = 0.440$

Turbine BEP				
48.15	40.84	1510	94.6	77.6%

Regressions: $H[1\rightarrow6]$; $M[1\rightarrow5]$

Elasticities: $E_T = 1.35$; $E_{2T} = 2.08$

Turbine performance (6 points)

65.28	66.50	1518	190.9	71.3%
58.75	54.60	1514	148.2	74.7%
49.03	41.50	1509	98.1	77.7%
41.67	34.50	1506	67.8	75.9%
27.78	24.90	1502	23.5	54.6%
19.45	22.70	1500	3.2	11.6%

THOR090

Category:	double-suction
Ω_P	0.904
D_2	216 mm
Data extent:	→runaway, but without including the BEP
Data quality:	absolute values
Data presentation:	constant speed graph
Nature of the study:	PATs
Make:	Worthington-Simpson
Type:	standard pump (6L1)
Original source:	Thome[90] (unpublished)

Performance data:

Q [l/s]	H [m]	ω [RPM]	M [Nm]	η
Pump BEP				
40.94	11.59	1485	34.28	87.3%

Shut-off: $\dot{H}_P/\hat{H}_P = 1.11$; $\dot{P}_P/\hat{P}_P = 0.372$

Turbine BEP				
64.90	24.64	1525	73.21	74.6%

Regressions: $H[1\rightarrow15]$; $M[1\rightarrow10]$

Elasticities: $E_T = 1.94$; $E_{2T} = 3.22$

Turbine performance (15 points)

66.67	26.29	1528	81.41	75.8%
63.89	23.94	1524	71.21	75.8%
61.11	21.84	1521	61.50	74.9%
58.34	20.02	1518	52.76	73.2%
55.56	18.48	1515	45.02	71.0%
52.78	17.02	1512	37.53	67.5%
50.00	15.70	1510	30.98	63.7%
47.23	14.49	1508	25.09	59.1%
44.45	13.54	1506	20.35	54.4%
41.67	12.58	1505	15.79	48.4%
38.89	11.85	1504	12.01	41.8%
36.11	11.06	1502	8.53	34.3%
33.34	10.37	1501	5.32	24.7%
30.56	9.69	1500	2.49	13.5%
27.78	9.20	1500	0.00	0.0%

VENT084

Category: end-suction/volute (radial-flow)
Ω_P 0.845
D_2 280 mm
Data extent: only around the BEP
Data quality: absolute values
Extra data: hydraulic efficiency, geometry
Data presentation: constant speed graph
Nature of the study: PATs
Make: n/a
Type: standard pump (ISO class C)
Original source: Ventrone & N.[82]
Data processing:
Pump BEP directly from original source. Lack of consistency between the ψ_T, η_T and Π_T curves $\Rightarrow$ the latter was discarded to match the BEP figures given by the authors.

Performance data:

Q [l/s]	H [m]	ω [RPM]	M [Nm]	η
Pump BEP				
86.1	20.11	1450	144.3	77.5%
Shut-off: $\grave{H}_P/\hat{H}_P = 1.21$; $\grave{P}_P/\hat{P}_P = 0.515$				
Turbine BEP				
120.5	34.00	1550	192.7	77.9%
Regressions: $H[1\rightarrow6]$; $M[1\rightarrow6]$				
Elasticities: $E_T = 1.68$; $E_{2T} = 2.65$				
Turbine performance (6 points)				
138.8	43.61	1550	277.2	75.8%
132.5	40.06	1550	247.1	77.1%
122.0	34.83	1550	200.4	78.1%
117.9	32.85	1550	182.3	77.9%
103.3	26.66	1550	124.8	75.0%
88.7	22.13	1550	79.2	66.8%

WILL026

Category: end-suction/volute (radial flow)
Ω_P 0.261
D_2 134 mm
Data extent: $\rightarrow$runaway
Data quality: absolute values
(Power determined by measuring electric ouput power and correcting with generator efficiency.)
Extra data: different diameters (only in turbine-mode)
Data presentation: constant speed graph
Nature of the study: PATs
Make: Worthington-Simpson
Type: standard pump (25 WB 125)
Original source: Williams[92]
Data processing:
$\grave{P}_P$ obtained by extrapolation.

Performance data:

Q [l/s]	H [m]	ω [RPM]	M [Nm]	η
Pump BEP				
2.226	21.24	2900	3.587	42.6%
Shut-off: $\grave{H}_P/\hat{H}_P = 1.20$; $\grave{P}_P/\hat{P}_P = 0.56$				
Turbine BEP				
3.754	55.86	3100	2.975	47.0%
Regressions: $H[1\rightarrow12]$; $M[1\rightarrow10]$				
Elasticities: $E_T = 1.43$; $E_{2T} = 2.47$				
Turbine performance (12 points)				
3.902	59.42	3100	3.271	46.7%
3.875	58.16	3100	3.159	46.4%
3.795	56.33	3100	3.009	46.6%
3.715	56.11	3100	2.909	46.2%
3.634	53.36	3100	2.789	47.6%
3.501	50.51	3100	2.537	47.5%
3.367	47.99	3100	2.246	46.0%
3.153	44.79	3100	1.988	46.6%
2.913	41.71	3100	1.556	42.4%
2.512	37.25	3100	1.037	36.7%
2.378	35.42	3100	0.753	29.6%
1.951	31.42	3100	0.000	0.0%

WILL047

Category: submersible (radial flow)
Ω_P 0.467
D_2 184 mm
Data extent: only around the BEP
Data quality: absolute values
Data presentation: table
Nature of the study: PATs
Make: Flygt
Type: standard pump (BS2102HT)
Original source: Williams[92]
Other sources:
Original test data kindly provided by Williams.
Data processing:
Data corrected assuming usual values for the slip and the efficiency of the generator.
The flow was established indirectly (by measuring the feed-pump head), but the values are unlikely ⇒ they were slightly corrected.
$\hat{P}_P$ obtained by extrapolation.

Performance data:

Q [l/s]	H [m]	ω [RPM]	M [Nm]	η
Pump BEP				
9.86	25.85	2850	14.72	56.9%
Shut-off: $\dot{H}_P/\hat{H}_P = 1.64$; $\dot{P}_P/\hat{P}_P = 0.70$				
Turbine BEP				
18.68	40.31	3000	12.11	51.5%
Regressions: $H[1\rightarrow8]$; $M[1\rightarrow8]$				
Elasticities: $E_T = 2.51$; $E_{2T} = 9.36$				
Turbine performance (8 points)				
21.60	59.50	3042	19.41	49.1%
20.40	52.00	2952	16.46	48.9%
19.75	48.00	2938	14.88	49.3%
17.40	35.00	2769	10.59	51.4%
16.40	30.50	2746	8.70	51.0%
14.40	24.00	2682	5.62	46.6%
12.90	21.50	2661	3.28	33.6%
12.00	19.50	2562	2.47	28.9%

WILL126

Category: submersible (mixed? flow)
Ω_P 1.26
D_2 140 mm
Data extent: near the BEP, but without including it
Data extent: only around the BEP
Data quality: absolute values
Data presentation: constant speed graph
Nature of the study: PATs
Make: Flygt
Type: standard pump (BS2102MT)
Original source: Williams[89]
Other sources:
Reproduced by Williams[92].
Generator efficiency kindly provided by Williams.
Data processing:
PAT efficiency calculated taking into account the generator efficiency.
Not enough pump-mode performance points to calculate the pump BEP (nor $\hat{P}_P$) ⇒ pump BEP from original source.

Performance data:

Q [l/s]	H [m]	ω [RPM]	M [Nm]	η
Pump BEP				
25.00	12.80	2850	15.35	68.5%
Shut-off: $\dot{H}_P/\hat{H}_P = 2.03$; $\dot{P}_P/\hat{P}_P$ = n/a				
Turbine BEP				
44.79	27.12	3000	25.50	67.2%
Regressions: $H[1\rightarrow13]$; $M[1\rightarrow13]$				
Elasticities: $E_T = 2.27$; $E_{2T} = 3.62$				
Turbine performance (13 points)				
43.00	24.80	3000	22.20	66.7%
42.00	23.43	3000	20.52	66.8%
41.00	22.22	3000	18.91	66.5%
40.00	21.10	3000	17.31	65.7%
39.00	20.00	3000	15.75	64.7%
38.00	18.90	3000	14.19	63.3%
37.00	17.90	3000	12.71	61.5%
36.00	16.93	3000	11.32	59.5%
35.00	16.00	3000	10.01	57.3%
34.00	15.15	3000	8.71	54.2%
33.00	14.30	3000	7.48	50.8%
32.00	13.55	3000	6.39	47.2%
31.00	12.80	3000	5.39	43.5%

YANG123

Category: bowl (mixed-flow)
Ω_P 1.237
D_2 n/a
Data extent: →runaway
Data quality: only relative values
(Draft tube included in turbine-mode, and apparently not in pump-mode.)
Extra data: different exhaust heads
Data presentation: constant speed graph
Nature of the study: PATs
Make: Layne and Bowler?
Type: standard pump
Original source: Yang[83]
Data processing:
$\hat{\eta}_P$ calculated by deduction (from Figs. 8 and 9).
Runaway from Fig. 11.

Performance data:

Q [l/s]	H [m]	ω [RPM]	M [Nm]	η
Pump BEP				
1.000	1.000	2070	0.054	83.6%
Shut-off: $\dot{H}_P/\hat{H}_P$ = 1.53; $\dot{P}_P/\hat{P}_P$ = missing				
Turbine BEP				
1.282	1.293	2070	0.057	76.5%
Regressions: H[4→14]; M[1→13]				
Elasticities: E_T = 1.84; E_{2T} = 3.41				
Turbine performance (14 points)				
1.497	1.702	2070	0.084	73.1%
1.468	1.656	2070	0.082	74.3%
1.445	1.617	2070	0.079	74.9%
1.409	1.546	2070	0.074	75.6%
1.344	1.397	2070	0.065	76.1%
1.301	1.335	2070	0.060	76.5%
1.238	1.227	2070	0.053	77.6%
1.208	1.172	2070	0.050	77.6%
1.097	0.992	2070	0.037	75.3%
1.033	0.904	2070	0.030	71.0%
1.012	0.886	2070	0.028	69.7%
0.922	0.796	2070	0.019	57.2%
0.896	0.787	2070	0.017	54.8%
0.706	0.626	2070	0.000	0.0%

YEDI038

Category: end-suction/volute (radial-flow)
Ω_P 0.382
D_2 ≈ 127 mm
Data extent: →runaway
Data quality: absolute values
(is ω_T really 3550 RPM?)
Extra data: different diameters
(but η_T only for the full size)
Data presentation: constant speed graph
Nature of the study: PATs
Make: Worthington-Simpson
Type: standard pump ($1^1/_2$CH-52)
Original source: Yedidiah[83]

Performance data:

Q [l/s]	H [m]	ω [RPM]	M [Nm]	η
Pump BEP				
6.94	35.1	3500	10.17	64.0%
Shut-off: $\dot{H}_P/\hat{H}_P$ = 1.16; $\dot{P}_P/\hat{P}_P$ = 0.5				
Turbine BEP				
11.53	61.4	3550	12.14	65.0%
Regressions: H[1→6]; M[1→6]				
Elasticities: E_T = 1.33; E_{2T} = 2.03				
Turbine performance (6 points)				
21.67	184.0	3550	50.39	47.9%
18.61	134.2	3550	35.05	53.2%
14.89	89.2	3550	21.56	61.6%
10.59	56.3	3550	10.04	63.9%
8.64	44.4	3550	6.12	60.6%
6.76	38.3	3550	3.17	46.4%

Unused Test Data

No Efficiencies.

Source	Category	Ω_P	Remarks
Brown & R.[80]	end-suction/volute (radial-flow)	0.545	
	bowl (mixed-flow)	1.60	
Csemniczky[83]	double-suction	0.907	
	bowl (axial-flow)	2.55	
	bowl (axial-flow)	3.55	
	bowl (axial-flow)	4.71	
Giddens *et al.*[62]	submersible	0.820	only overall efficiency
Kobori[53]	double-suction (2-stages)	0.570	also in Kobori[54]
Yang[83]	bowl (mixed-flow)	1.088	
	bowl (mixed-flow)	1.103	
	bowl (mixed-flow)	1.110	
	bowl (mixed-flow)	1.129	
	bowl (mixed-flow)	1.325	

Only Turbine-mode.

Source	Category	Ω_T	Remarks
Ávila-García & G.-C..[86]	end-suction/volute	0.187	
	end-suction/volute	0.206	
Brada & B.[82]	bowl (axial-flow)	3.46	also in Brada[82]
Cooper & W.[81]	mixed flow/bowl	?	special impeller
Cornell Pump Co.[82]	end-suction/volute (radial-flow)	0.432	
	end-suction/volute (radial-flow)	0.538	
	end-suction/volute (radial-flow)	0.563	
	end-suction/volute (radial-flow)	0.600	
	end-suction/volute (radial-flow)	0.706	
	end-suction/volute (radial-flow)	0.827	
	end-suction/volute (radial-flow)	0.995	
	end-suction/volute (radial-flow)	1.45	
Hidrostal[90]	end-suction/volute (radial-flow)	0.471	
Lueneburg & N.[85]	end-suction/volute (radial-flow)	0.545	
Marquis[83]	end-suction/volute (radial-flow)	0.589	
Nicholas[88]	end-suction/volute (radial-flow)	0.736	
Priesnitz[87]	end-suction/volute (radial-flow)	0.466	
Semple & W.[84]	multistage (12 radial-flow stages)	0.371	
Taylor[83]	multistage (13 radial-flow stages)	0.269	
Wilson & P.[92]	double-suction	?	no η_T
Yedidiah[83]	multistage (10 radial-flow stages)	0.276	
	end-suction/volute (radial-flow)	0.588	

Pump-turbines.

Sources

Amblard[79]; Borel & M.[65]; Brada[82]; DeFazio[67]; Hornberger & R.[65]; Kováts[64]; Martin & H.[90]; Mayo & W.[82]; Meier[62]; Narayan[79]; Pejović *et al.*[76]; Schobinger & T.[79]; Stelzer[79]; Terry & J.[42]; Vissarionov *et al.*[69]; Yamamoto *et al.*[68]

Turbine-mode without BEP.

Source	Category	Ω_P	Remarks
Brown & R.[80]	?	0.296	
	?	0.483	
	?	0.573	
Burgoyne *et al.*[69]	end-suction/volute (mixed-flow)?	2.12	only runaway and stall
	end-suction/volute (mixed-flow)?	2.16	only runaway and stall
	end-suction/volute (mixed-flow)?	2.20	only runaway and stall
	end-suction/volute (mixed-flow)?	2.28	only runaway and stall
	end-suction/volute (mixed-flow)?	2.32	only runaway and stall
	end-suction/volute (mixed-flow)?	2.96	only runaway and stall
Csemniczky[83]	end-suction/volute (radial-flow)	1.08	only runaway
	bowl (mixed-flow)?	1.72	only runaway
	bowl (mixed-flow)?	1.78	only runaway
	bowl (axial-flow)	2.42	only runaway
	bowl (axial-flow)	2.93	only runaway
Engeda & R.[87]	end-suction/volute (radial-flow)	0.330	
Martin[n/a]	end-suction/volute (radial-flow)	0.361	
Stepanoff[57]	multistage (radial-flow)	0.435	only runaway and stall
	multistage (radial-flow)	0.446	only runaway and stall
	multistage (4 radial-flow stages)	0.470	only runaway
	double-suction	1.28	only runaway and stall
	bowl (axial-flow)	2.45	only runaway and stall
	bowl (axial-flow)	2.63	only runaway and stall
	bowl (axial-flow)	4.94	only runaway and stall
Tognola[60]	double-suction (2-stages)	0.531	

Only BEPs in Both Modes, and without η_T.

Source	Category	Ω_P	Remarks
Schmiedl[88]	end-suction/volute (radial-flow)	0.155	
	end-suction/volute (radial-flow)	0.206	
	end-suction/volute (radial-flow)	0.314	
	end-suction/volute (radial-flow)	0.406	
	end-suction/volute (radial-flow)	0.412	
	end-suction/volute (radial-flow)	0.531	
	end-suction/volute (radial-flow)	0.928	
Yedidiah[83]	end-suction/volute (radial-flow)?	0.323	
	end-suction/volute (radial-flow)?	0.434	
	end-suction/volute (radial-flow)?	0.438	
	end-suction/volute (radial-flow)?	0.450	
	end-suction/volute (radial-flow)?	0.468	
	end-suction/volute (radial-flow)?	0.642	
	end-suction/volute (radial-flow)?	0.842	

Rejected Data.

Source	Category	Ω_P	Remarks
Brown & R.[80]	?	0.417	unreliable
Kamath & S.[82]	end-suction/volute (mixed-flow)	1.537	inadequate data
Olson[74]	end-suction/volute (radial-flow)	0.339	very strange!
Sprecher[51]	multistage (5 radial-flow stages)	0.494	special machine
Williams[92]	end-suction/volute (radial-flow)	0.332	sparse data
Williams *et al.*[68]	submersible (2 stages)	0.367	unreliable torque data
Winks[77]	end-suction/volute (mixed-flow)	1.581	inadequate data
Wong[87]	?	?	no ω, unreliable

APPENDIX C
DEVELOPMENT OF THE NEW PERFORMANCE-BASED PREDICTION METHOD

Previous Attempts

The following attempts were made to correlate the turbine-mode performance with various parameters of the pump-mode performance:

The first attempt used a methodology similar to the described in p. 71 to estimate the hydraulic, volumetric and mechanical efficiencies in pump-mode and tried to find a correlation between the volumetric efficiency and the flow conversion factor, on one hand, and between the hydraulic efficiency and the head conversion factor, on the other.

The second attempt looked at the operation in both modes as segments of a continuum four-quadrant representation, and tried to find some kind of continuity between both segments, *i.e.* a correlation between the shut-off point in pump-mode and the stall point in turbine-mode.

The third attempt followed the assumption that the best parameter to characterize the geometry of the machine is, rather than the specific speed - related just to the BEP -, the shape of the pump-mode characteristics (inspired by Anderson[38, 55]), and tried to find a correlation between the head and torque at pump-mode shut-off (relative to pump BEP values) and the conversion factors.

The fourth attempt used the pump-mode peak efficiency, the specific speed and the pump category as parameters for the conversion factors.

Finally, a fifth attempt tried to find a turbine-mode operating point near the BEP whose location could be established more accurately than the BEP. It was assumed in this case that an accurate head and flow prediction for a point near the BEP could in

many cases be more valuable than a less-accurate BEP prediction, even if this involved a loss of few percent in efficiency.

The most successful of the series is the fourth attempt, described in § 5.4 and below. The formulae obtained by curve-fitting are reproduced here, along with the regression details and the graphs that were not included in § 5.4.

Flow Conversion Factor for All Pumps.

The flow conversion factor is:

$$\frac{\hat{Q}_{TE}}{\hat{Q}_P} = 1.21\,\hat{\eta}_P^{-0.6} \qquad [62]$$

Regression made with 57 points, 55 degrees of freedom. The exponent of $\hat{\eta}_P$ has a standard error of 0.09. The standard deviation of the relative errors is 10.4%. Correlation shown in Fig. 53 (p. 89).

End-suction Pumps.

This category includes volute pumps with or without fixed-vanes, multistage pumps and one submersible pump.

The head conversion factor is:

$$\frac{\hat{H}_{TE}}{\hat{H}_P} = 1.21\,\hat{\eta}_P^{-0.8}\left[1+\left(0.6+\ln\Omega_P\right)^2\right]^{0.3} \qquad [58]$$

Regression made with 39 points, 36 degrees of freedom: `SENU037` and `WILL047` were eliminated. The exponent of $\hat{\eta}_P$ has a standard error of 0.10 and the exponent of Λ (*i.e.* of $[1+(0.6+\ln\Omega_P)^2]$) has a standard error of 0.07. The standard deviation of the relative errors is 11.5%. Correlation shown in Figs. 49 (p. 86) and 51 (p. 87).

The efficiency conversion factor is:

$$\frac{\hat{\eta}_{TE}}{\hat{\eta}_P} = 0.95\,\hat{\eta}_P^{-0.3}\left[1+\left(0.5+\ln\Omega_P\right)^2\right]^{-0.25} \qquad [61]$$

Regression made with 38 points, 34 degrees of freedom: `JYOT054`, `KENN157` and `WILL047` were eliminated. The exponent of $\hat{\eta}_P$ has a standard error of 0.06 and the exponent of Λ has a standard error of 0.04. The standard deviation of the relative errors is 5.1%. Correlation shown in Figs. 52 (p. 88) and 91.

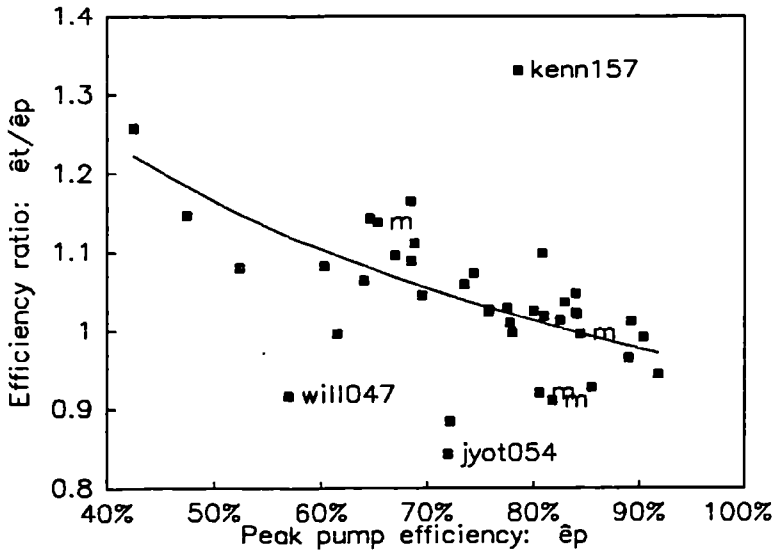

Fig. 91. Correlation of the efficiency conversion factor in terms of $\hat{\eta}_P$, for end-suction pumps.

The procedure used to draw the ■ and the line is similar to the one used in Fig. 49.

Fig. 92 is similar to Fig. 52, but it includes as well the points corresponding to double suction and bowl pumps, just to show how they follow a distinct trend (especially the latter).

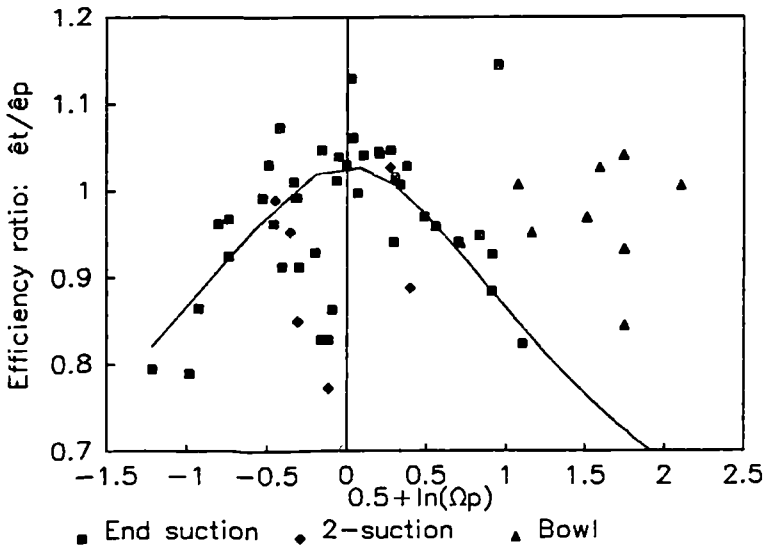

Fig. 92. Correlation of the efficiency conversion factor in terms of Ω_P, for end-suction pumps, including as well double-suction and bowl pumps.

Double-suction Pumps.

The head conversion factor is:

$$\frac{\hat{H}_{TE}}{\hat{H}_P} = 0.79\,\hat{\eta}_P^{-2.3}\left[1+\left(0.7+\ln\Omega_P\right)^2\right]^{1.9} \qquad [63]$$

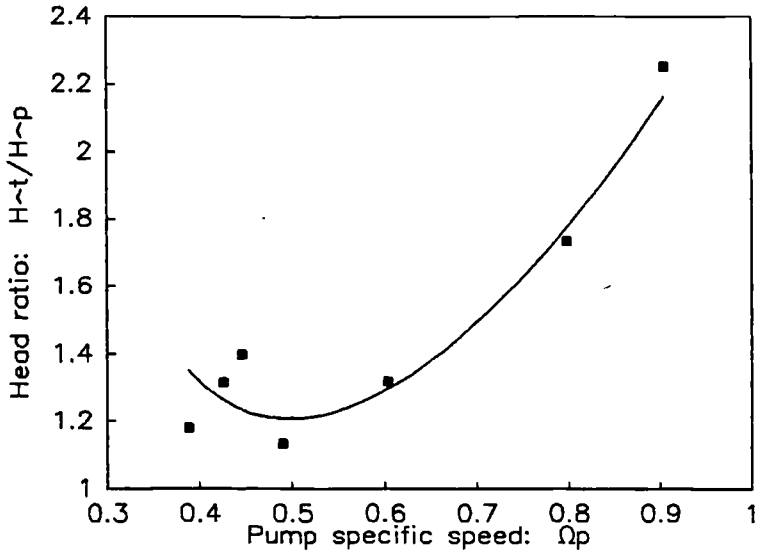

Fig. 93. Correlation of the head conversion factor in terms of Ω_P, for double-suction pumps.
$\overline{\eta}_P = 83\%$.

Regression made with 7 points, 3 degrees of freedom. The exponent of $\hat{\eta}_P$ has a standard error of 0.86 and the exponent of Λ has a standard error of 0.5. The standard deviation of the relative errors is 8.3%. Correlation shown in Figs. 93 and 94.

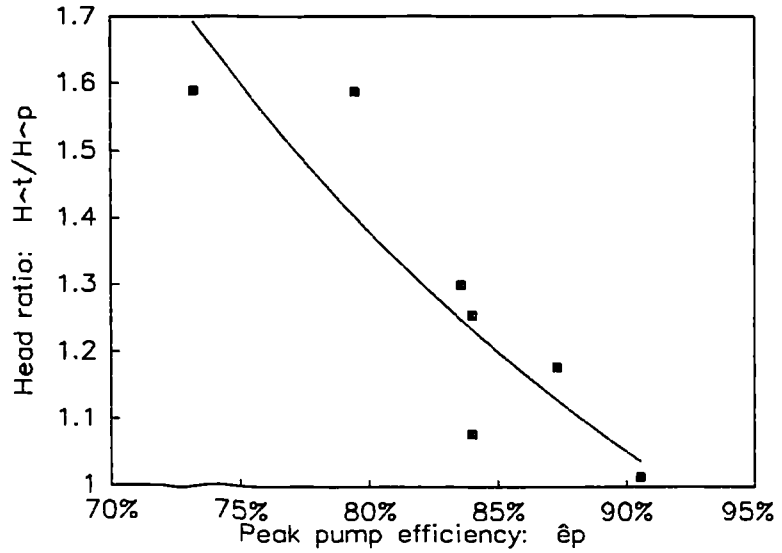

Fig. 94. Correlation of the head conversion factor in terms of $\hat{\eta}_P$, for double-suction pumps.
$\overline{\Omega}_P = 0.58$.

The efficiency conversion factor is:

$$\frac{\hat{\eta}_{TE}}{\hat{\eta}_P} = 1.31\,\hat{\eta}_P^{1.7}\left[1+(0.7+\ln\Omega_P)^2\right]^{-0.6} \qquad [64]$$

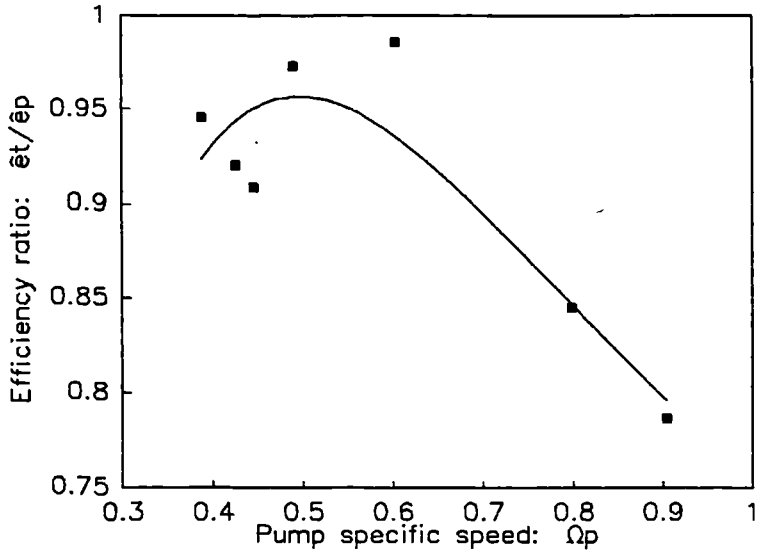

Fig. 95. Correlation of the efficiency conversion factor in terms of Ω_P, for double-suction pumps.
$\overline{\eta}_P = 83\%$.

Regression made with 7 points, 3 degrees of freedom. The exponent of $\hat{\eta}_P$ has a standard error of 0.33 and the exponent of Λ has a standard error of 0.19. The standard deviation of the relative errors is 3.3%. Correlation shown in Figs. 95 and 96.

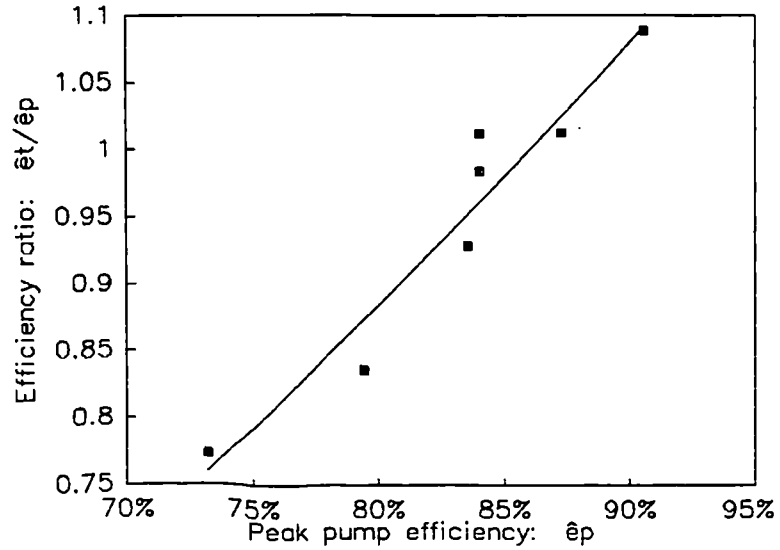

Fig. 96. Correlation of the efficiency conversion factor in terms of $\hat{\eta}_P$, for double-suction pumps.
$\overline{\Omega}_P = 0.58$.

Bowl Pumps.

The head conversion factor is:

$$\frac{\hat{H}_{TE}}{\hat{H}_P} = 0.93\,\hat{\eta}_P^{-1.7}\,\Omega_P^{0.1} \qquad [65]$$

Regression made with 8 points, 5 degrees of freedom: STIR348 was eliminated. The exponent of $\hat{\eta}_P$ has a standard error of 0.4 and the exponent of Ω_P has a standard error of 0.05. The standard deviation of the relative errors is 4.7%. Correlation shown in Figs. 97 and 98.

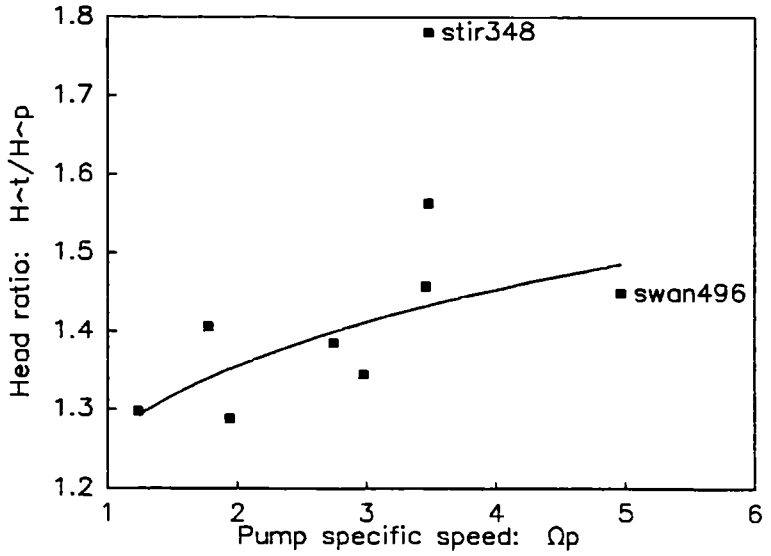

Fig. 97. Correlation of the head conversion factor in terms of Ω_P, for bowl pumps.
$\overline{\eta}_P = 83\%$.

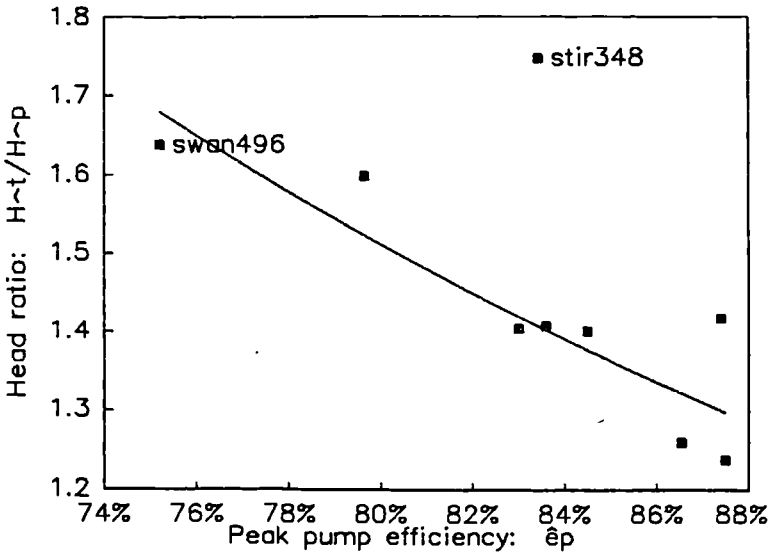

Fig. 98. Correlation of the head conversion factor in terms of $\hat{\eta}_P$, for bowl pumps.
$\overline{\Omega}_P = 2.90$.

The efficiency conversion factor is:

$$\frac{\hat{\eta}_{TE}}{\hat{\eta}_P} = 0.88\ \hat{\eta}_P^{-0.5} \qquad [66]$$

Regression made with 8 points, 6 degrees of freedom: `STIR348` was eliminated. The exponent of $\hat{\eta}_P$ has a standard error of 0.3. The standard deviation of the relative errors is 4.0%. Correlation shown in Fig. 99.

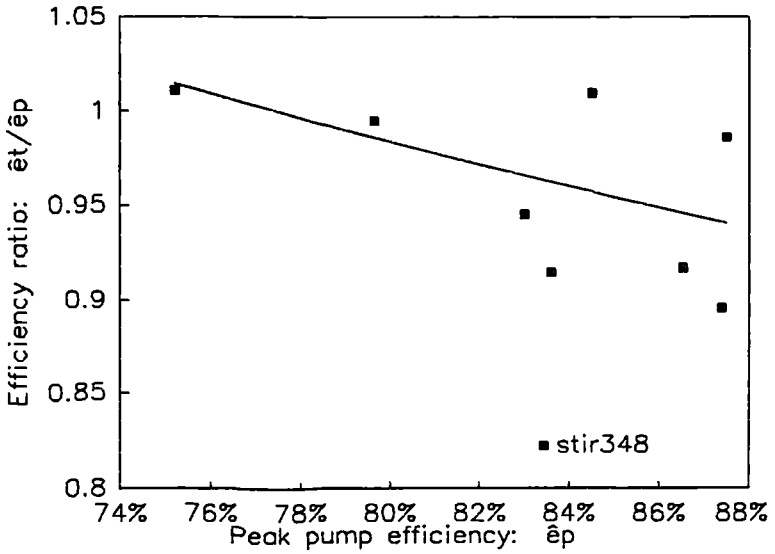

Fig. 99. Correlation of the efficiency conversion factor in terms of $\hat{\eta}_P$, for bowl pumps.

Elasticities for Off-BEP Prediction.

The first elasticity is, for all pumps:

$$E_{TE} = 0.68 + 1.2\Omega_P^{0.5} \quad [75]$$

Regression made with 56 points, 53 degrees of freedom: SWAN496 was eliminated. The coefficient of Ω_P has a standard error of 0.11 . The standard deviation of the relative errors is 16.5% (0.28 absolute standard error). Correlation shown in Fig. 55 (p. 94).

The second elasticity is, for all pumps:

$$E_{2TE} = 0.76 + 2.1\Omega_P^{0.5} \quad [76]$$

Regression made with 58 points, 55 degrees of freedom: SWAN496 and WILL047 (of course) were eliminated. The coefficient of Ω_P has a standard error of 0.25 . The standard deviation of the relative errors is 23.5% (0.67 absolute standard error). Correlation shown in Fig. 100.

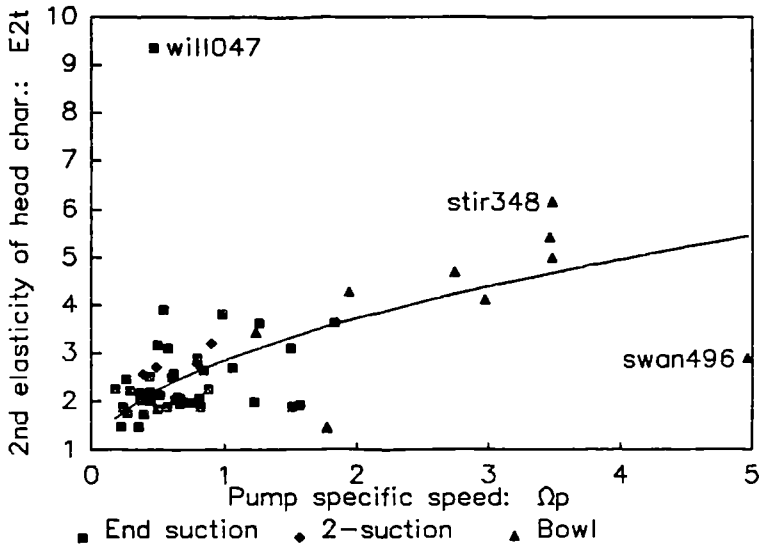

Fig. 100. Correlation of the 'second' elasticity E_{2T} in terms of Ω_P, for all pumps.

APPENDIX D
CAVITATION TEST-DATA PROCESSING

Flow.

The flow was indirectly determined by measuring with a differential pressure transducer the pressure drop across the reduction shown in Fig. 101 ('**a**').

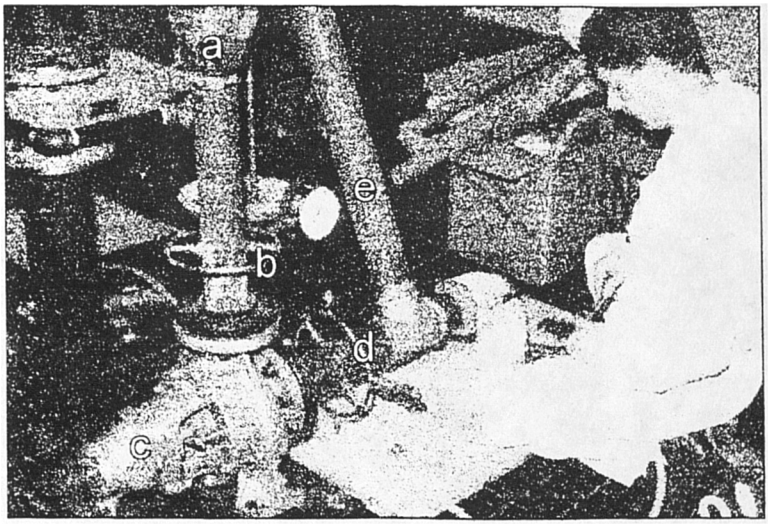

Fig. 101. Paul working on the pressure tappings.
a: reduction used for flow measurements; **b**: PAT-inlet pressure tappings;
c: PAT; **d**: PAT-outlet pressure tappings;
e: pipe used for the calibration of the flow measurements.

The calibration of the flow measurements was made by filling a tank through the pipe marked **e** in Fig. 101.

Head.

The pressure drop across the PAT was measured with a differential pressure transducer ('**g**' in Fig. 102), and the turbine head was calculated taking into account

the difference in velocity heads between the inlet and the outlet of the turbine and the slight head-loss between the turbine flanges and the pressure tappings ('**b**' and '**d**').

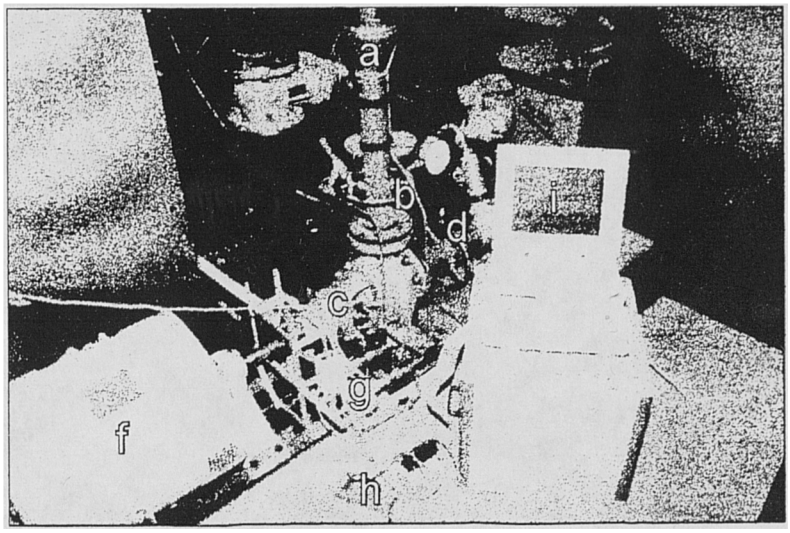

Fig. 102. Panoramic view of the test-rig.
a: reduction used for flow measurements; **b**: PAT-inlet pressure tappings;
c: PAT; **d**: PAT-outlet pressure tappings; **f**: dynamometer;
g: differential pressure transducers; **h**: electronic thermometer;
i: laptop computer.

Torque.

The torque was calculated by measuring with a load cell ('**l**' in Fig. 103) the force of the dynamometer arm ('**j**'). Note the spring link ('**k**') between the dynamometer and

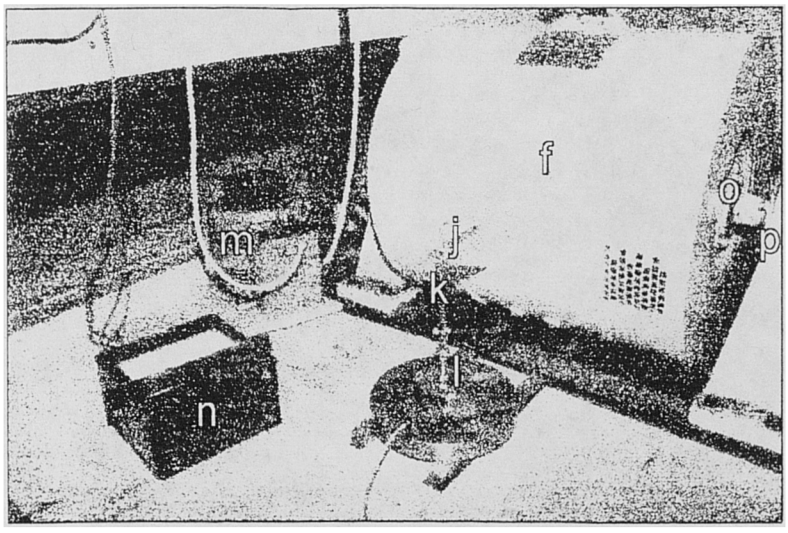

Fig. 103. The dynamometer and the load cell.
f: dynamometer; **j**: dynamometer arm; **k**: spring link; **l**: load cell;
m: power supply for the windings of the dynamometer; **n**: amperometer;
o: rocking bearings; **p**: fixed bearings.

the load cell: it damps the vibrations due to a slight miss-alignment of the dynamometer. Each torque measurement is the average of many readings made during one cycle of the spring vibration - whose frequency is independent of the torque (see Fig. 104).

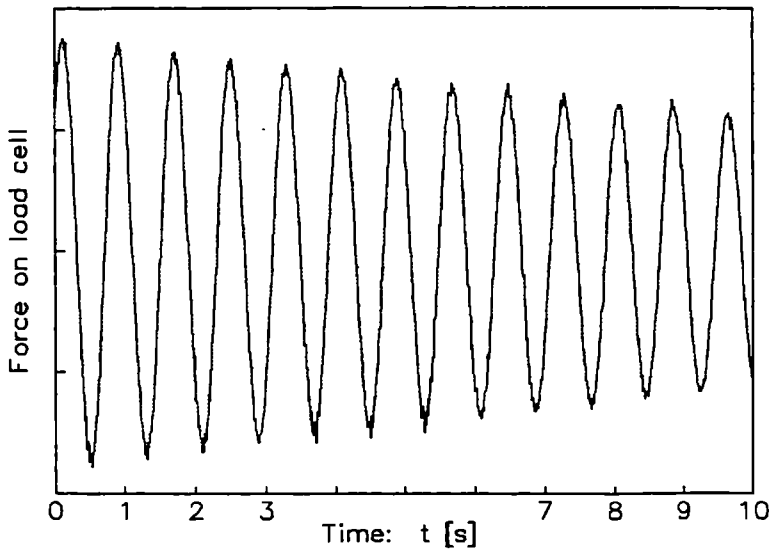

Fig. 104. Spring vibrations registered in the load cell.
The torque readings were made by averaging through one cycle = 0.794 s.

The load cell does not record the friction in the fixed bearings ('**p**' in Fig. 105, middle) nor the ventilation losses inside the dynamometer[1]. The torque absorbed in these two ways is assumed to have two components: one fixed and one proportional to the speed. The values of these components were established by trial-and-error[2] until a reasonable consistency was achieved between the 'normal' performance data and the two extremes of the characteristics (namely stall and runaway, whose obtaining is described below). This consistency is shown in Figs. 78, 79 and 81.

Stall.

The stall measurements mentioned in the previous paragraph were made by connecting with an 'L' bar the shaft coupling and the two eyebolts marked '**q**' in Fig. 105, so that the shaft is locked and the load cell records the stall torque.

Following the recommendation of Strate *et al.*[90], the stall measurements were made in different positions of the rotor. Four positions were used, and for each position the flow and torque were recorded for different values of the head. The lines on the top of

1 Neither does it record the friction in the PAT bearings and packed gland, but this is an **internal** loss of the PAT.

2 The hysteresis torque difference mentioned below could not be used here because it includes as well the friction in the PAT bearing and gland (it is larger).

Fig. 106 are the resulting head-flow parabolas for each one of the four rotor positions labelled **w**, **x**, **y** and **z**. The average parabola is $gH_T = 277000 \cdot Q_T{}^2$ (with Q_T in m^3/s) [3].

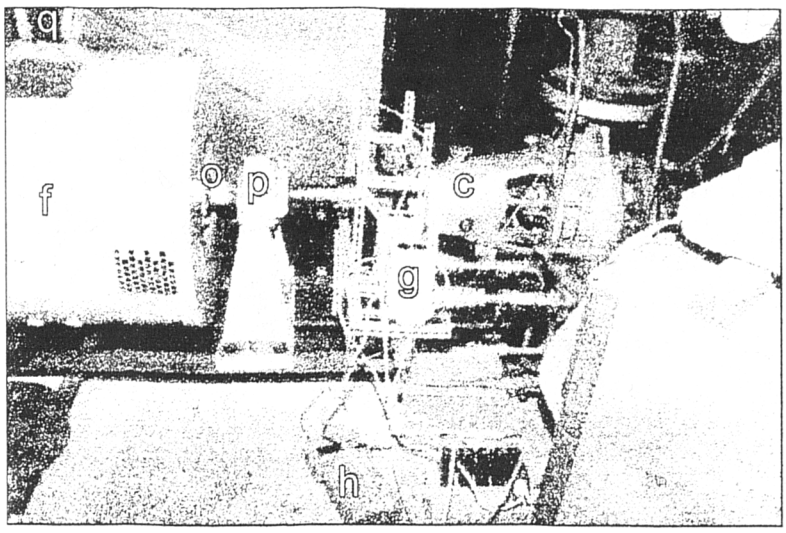

Fig. 105. The dynamometer and the PAT.
c: PAT; **f**: dynamometer; **g**: differential pressure transducers; **h**: electronic thermometer; **o**: rocking bearings; **p**: fixed bearings; **q**: eyebolts.

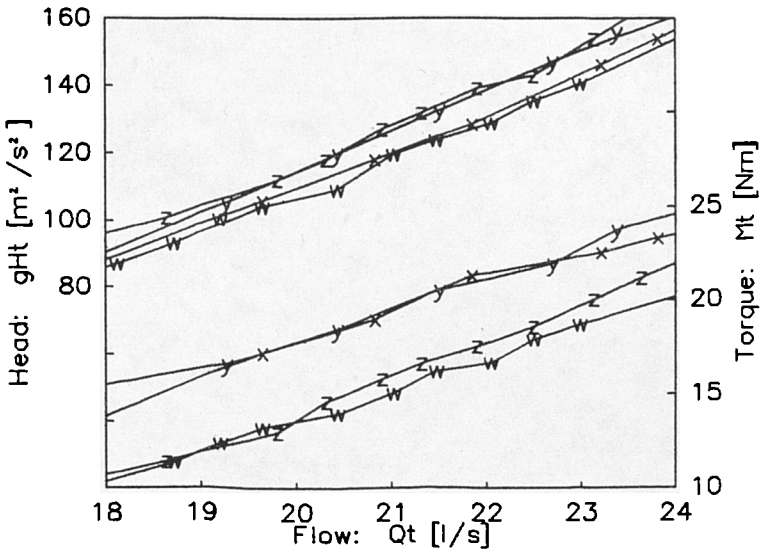

Fig. 106. Stall measurements.

The torque-flow parabolas on the bottom of Fig. 106 follow a different sequence, namely **w-z-x-y**, and there is a large gap between the first and the second pair of lines. This change in sequence and this gap are not related with the rotor position, but with a

3 The stall points in Fig. 80 (p. 120) correspond to those labelled **w** in Fig. 106, slightly adjusted to fit the average parabola (drawn with a line in Fig. 80).

hysteresis effect concerned with the friction in the fixed bearings. Indeed, the readings with positions **x** and **y** were made by reducing the head, while **w** and **z** were made by increasing it. When the head, and hence the torque, is increased, the spring link ('**k**' in Fig. 103) is slightly elongated and the dynamometer slightly rotates, but the friction in the fixed bearings (the two dynamometer bearings + the PAT bearing + the PAT packed gland) is opposed to this movement and it absorbs a small part of the torque produced by the turbine. When the head is reduced, the friction in the bearings has the opposite effect, and the recorded torque is larger that the actual. The average parabola is $M_T = 40000 \cdot Q_T^2$ (with Q_T in m^3/s) (this average was used to draw the stall points in Figs. 78, 79 and 81).

Runaway.

The second points from right to left in both torque and head curves of Figs. 78 and 79 were obtained by removing all the electric load from the dynamometer, but they are still quite far away from the 'true' runaway points (*i.e.* the rightmost points), on account of the bearings friction and ventilation losses in the dynamometer (Only the friction in the rocking bearings ('**o**') is registered by the load cell.).

The 'true' runaway performance was measured by uncoupling the dynamometer. The head-speed curve was found to be parabolic, with a best-fit of $gH_T = 0.002857 \cdot \omega_T^2$ (see Fig. 107). However, in the case of the head-flow curve, shown in Fig. 80, the regression obtained was slightly deviated from the theoretical parabola, *i.e.* $Q_T/\sqrt{(gH_T)} = 0.001305 - 0.02064 \cdot Q_T$ (with Q_T in m^3/s). This deviation is probably due to the effect of the mechanical friction in the PAT bearing and packed gland, that is significant in runaway.

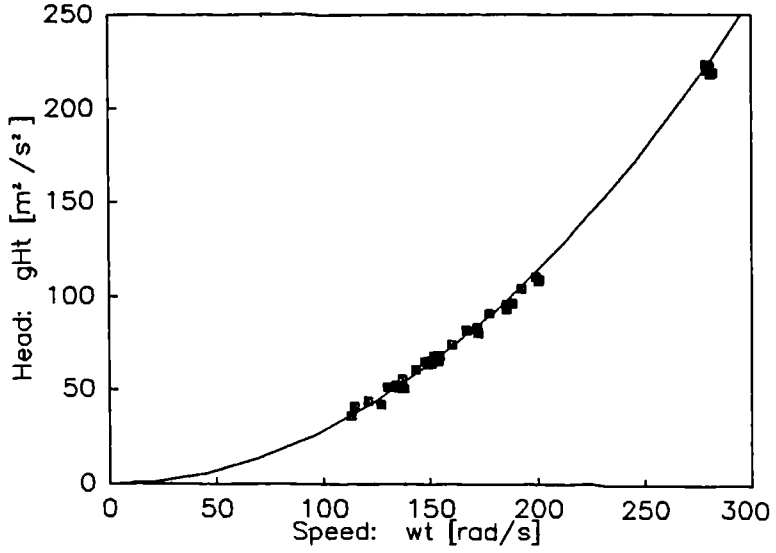

Fig. 107. Relation between ω_T and H_T in runaway.
The line corresponds to the best-fit.